Distribution Agreement

In presenting this thesis or dissertation as a partial fulfillment of the requirements for an advanced degree from Emory University, I hereby grant to Emory University and its agents the non-exclusive license to archive, make accessible, and display my thesis or dissertation in whole or in part in all forms of media, now or hereafter known, including display on the world wide web. I understand that I may select some access restrictions as part of the online submission of this thesis or dissertation. I retain all ownership rights to the copyright of the thesis or dissertation. I also retain the right to use in future works (such as articles or books) all or part of this thesis or dissertation.

_____ _____

Kristen E. Howery Date

Contributions of the Rcs Phosphorelay and $FlhD_4C_2$ to Swarming Behavior in *Proteus mirabilis*

By

Kristen E. Howery

Doctor of Philosophy

Graduate Division of Biological and Biomedical Sciences

Microbiology and Molecular Genetics

_____

Philip N. Rather, Ph.D.
Advisor

_____ _____

Joanna B. Goldberg, Ph.D.
Committee Member

Charles P. Moran, Jr., Ph.D.
Committee Member

_____ _____

Minsu Kim, Ph.D.
Committee Member

William M. Shafer, Ph.D.
Committee Member

_____

David S. Weiss, Ph.D.
Committee Member

Accepted:

_____

Lisa A. Tedesco, Ph.D.
Dean of the James T. Laney School of Graduate Studies

_____

Date

Contributions of the Rcs Phosphorelay and $FlhD_4C_2$ to Swarming Behavior in *Proteus mirabilis*

By

Kristen E. Howery

B.S. Biological Sciences, Georgia State University, 2010

Advisor:

Philip N. Rather, Ph.D

An abstract of

A dissertation submitted to the

Faculty of the James T. Laney School of Graduate Studies of Emory University

in partial fulfillment of the requirements for the degree of

Doctor of Philosophy

In

Graduate Division of Biological and Biomedical Sciences

Microbiology and Molecular Genetics

2016

Contributions of the Rcs Phosphorelay and $FlhD_4C_2$ to Swarming Behavior in *Proteus mirabilis*

By: Kristen E. Howery

Abstract

Proteus mirabilis is a Gram-negative enteric bacterium known for its ability to utilize a specialized form of motility known as swarming. Swarming is the coordinated movement of a bacterial population across a solid or semi-solid surface. Upon surface contact, a subset of the initial population of vegetative, short-rod shaped cells undergoes differentiation into highly flagellated, elongated, and multinucleate swarmer cells. Swarmer cells then move outward from the point of inoculation and migrate for a few hours before de-differentiating back to short, vegetative rods. This work focuses on the role of two transcriptional regulators, RcsB and $FlhD_4C_2$, in the swarming process. The RcsB response regulator directly represses the *flhDC* operon, encoding the master flagellar activator $FlhD_4C_2$. Under conditions non-permissive for swarming, *rcsB* mutants differentiate and form swarmer cells indicating RcsB influences the expression of genes important for differentiation. These RcsB regulated genes were subsequently identified using RNA-Seq. One RcsB-activated locus, the *minCDE* cell division inhibition system, was found to be important for swarmer cell differentiation. Furthermore, RcsB was shown to regulate the expression of genes involved in biofilm formation and virulence. The bifurcation of *P. mirabilis* populations when cells are grown on agar surfaces was also examined. Following the initiation of swarming, only cells at the exterior of a colony were capable of differentiating into swarmer cells while cells in the interior remained short vegetative rods. To understand the mechanism regulating the spatial control of differentiation, expression of the flagellar master operon, *flhDC*, was investigated in single cells. The *flhDC* operon was found to exhibit bistable expression mediated by a positive feedback loop. A previously characterized mutant, SS-P, containing a transposon insertion in the non-coding region 325 bp upstream of *flhDC* transcriptional start site differentiated immediately upon surface contact and maintained swarmer cells throughout colony expansion. Deletion analysis of the region upstream of *flhDC* demonstrated that sequences from -322 to -1000 were required for spatial control of *flhDC* expression within the colony interior. Lastly, using DNA affinity chromatography, proteins bound to the *flhDC* upstream region were identified. The construction of in-frame deletions in the corresponding genes identified novel regulators required for swarmer cell differentiation.

Contributions of the Rcs Phosphorelay and $FlhD_4C_2$ to Swarming Behavior in *Proteus mirabilis*

By

Kristen E. Howery

B.S. Biological Sciences, Georgia State University, 2010

Advisor:

Philip N. Rather, Ph.D

A dissertation submitted to the

Faculty of the James T. Laney School of Graduate Studies of Emory University

In partial fulfillment of the requirements for the degree of

Doctor of Philosophy

In

Graduate Division of Biological and Biomedical Sciences

Microbiology and Molecular Genetics

2016

Acknowledgements

This dissertation would have never been written had it not been for some very special people and certain unexpected events.

First, I would like to thank my advisor, Phil, for his excellent scientific advice, his support, and his patience. When I began working in this lab almost 3 years ago, you not only inherited a green graduate student but one who became unexpectedly pregnant exactly one month after her start date. I will never forget your kindness and poise during that period of my life. Your unwillingness to religuish the high standards you held of me has been crucial to my success.

My thesis committee, Joanna, Charlie, Bill, Minsu, and David, have been fundamental to my growth as a scientist. They have been involved in my work since the beginning – when I was working on biofilm formation in *Streptococccus pneumoniae* – to now as I complete my work on motility in *Proteus mirabilis*. Their advice and ideas at group and individual meetings were essential for my work and well-being.

Minsu and Emrah have been excellent collaborators and some of this work would not exist without them. Bistability was a concept I had not thought about since I was a first-year graduate student, and together we uncovered something amazing.

I cannot express the insurmountable amount of gratitude I have for my family. You instilled me with a fierce will to succeed, empathy for others, and taught me to be a curious combination of optimistic and realistic. You have taken care of me since before I was born and have never asked for anything in return. I love you. To my friends – you have perpetually provided me with laughter, love, and support. You are irreplaceable.

Marin Jean – you saved my life. One day you will know how. Stay kind and graceful, learn all you can, and be true to yourself whatever may come. This work would not exist had you not sprung into existence. You are the apex and the sun and I cannot imagine a world where you are not my daughter.

Thank you.

Table of Contents

Tables and Figures

Chapter 2

Chapter 3

Chapter 4

Chapter 1: Introduction

Proteus mirabilis

Proteus mirabilis is a Gram-negative, dimorphic member of the family *Enterobacteriaceae*. Two trademark characteristics of this bacterium are urease production and its ability to use a multicellular form of motility known as swarming (1). *P. mirabilis* is often isolated from the gastrointestinal tract of humans, but whether it persists in this niche as a commensal or pathogenic organism is unknown. In the urinary tract, *P. mirabilis* is an opportunistic pathogen (2).

P. mirabilis was first isolated from petrified meat in 1885 by Hauser and rightfully named after the sea god Proteus who would change to avoid capture and questioning. *Proteus* earned its name for the morphological metamorphosis it undergoes in order to swarm (3). Swarming motility is central to the biology of this organism and plays a role in its ability to establish infections in humans. As such, this work will focus on swarming motility and mechanisms of its regulation in the human pathogen *P. mirabilis*.

I. Disease

P. mirabilis is an agent of urinary tract infections (UTI) which can lead to pyelonephritis, cystitis, asymptomatic bacteriuria, and urinary stone formation (urolithiasis) (1, 4). These infections can result in bacteremia and urosepsis if left untreated and are common amongst the elderly and immunocompromised populations (5, 6). UTIs caused by *P. mirabilis* can be mediated by translocation of the bacterium from the gastrointestinal tract or by person-to-person transmission. Person-to-person

transmission is especially common in nosocomial infections, as some patients will carry the same strain of *P. mirabilis* in their stool while others have no *P. mirabilis* in their stool (7). This bacterium can also cause otitis media, conjunctivitis, and infections of the skin, nose, and throat (1, 4). Recent studies have shown *P. mirabilis* isolation from 5-20% of Gram-negative bacteremia cases, especially in patients with concurrent UTI. These infections result in a mortality rate as high as 50% in the elderly (8-10).

P. mirabilis causes between 1-10% of all UTIs and up to 44% of catheter associated urinary tract infections (CAUTIs) at a cost of $43-256 million dollars in the United States per year (4, 11). CAUTIs account for 40% of nosocomial infections with the duration of catheterization being the primary risk factor for bacterial infection; most patients catheterized for more than 28 days will develop a CAUTI (12). Up to 77% of CAUTIs are polymicrobial and involve the formation of biofilms. They will frequently contain combinations of *Morganella morganii*, *Escherichia coli*, *Providencia stuartii*, *Klebsiella pneumoniae*, *Pseudomonas aeruginosa*, with *P. mirabilis* being the most common isolate from these infections (4, 12-15). A myriad of factors are utilized by *P. mirabilis* to facilitate (i) entry, (ii) colonization, and (iii) persistence within the urinary tract.

i. Entry to the Urinary Tract

A. Motility

To gain entry to the urinary tract, *P. mirabilis* must utilize a form of motility that allows it to migrate across the catheter surface. The form of motility *P. mirabilis* utilizes for movement over catheters is swarming motility, a population-dependent form of surface migration where highly flagellated and elongated swarmer cells form rafts to

traverse solid surfaces (16, 17). Following contact with a solid surface, such as a catheter, vegetative, short-rod shaped *P. mirabilis* cells undergo a process known as differentiation into highly flagellated, elongated, multinucleate swarmer cells (18). Consolidation is the process by which swarmer cells revert back to vegetative cells following a period of migration (16). Swarming motility is covered in detail later in this chapter.

P. mirabilis adequately swarms across various types of catheter material (17, 19-21), and swarmer cells are found on the surface of biofilms grown on catheters in the presence of artificial urine (12). *P. mirabilis* can also utilize swimming motility, where peritrichously flagellated vegetative cells move independently through aqueous environments. This form of motility cannot be used to migrate across catheter surfaces, but swimming cells can migrate within the aqueous matrix of hydrogel-coated catheters (17, 19). The metabolic status of the cell is important for swarmer cell differentiation, as metabolic intermediates and specific amino acids enhance swarming motility, and mutants in genes required for their catabolism do not swarm (22-24). Interestingly, the amino acids most concentrated in human urine promote the formation of swarmer cells (25-27).

B. Urease and Crystalline Biofilms

Another mechanism to facilitate entry into the urinary tract would be disrupting the flow of urine. For this purpose, *P. mirabilis* encodes a nickel metalloenzyme, urease, which hydrolyzes urea into ammonia and carbon dioxide thus increasing the pH of the environment. An alkaline pH in the urinary tract causes precipitation of calcium and magnesium ions which form crystals of apatite (calcium phosphate) and struvite (magnesium ammonium phosphate) (28). Bacterial adherence to catheters is optimal

under alkaline conditions once crystals have deposited on the surface of the catheter (29). Crystals continue to be integrated into biofilms, and over time this leads to blockage of the catheter lumen (30). Catheter encrustation disrupts urine flow and causes backward flow of urine from the bladder to the kidneys (Vesicoureteral reflux). *P. mirablis* colonization and subsequent disease of the urinary tract can now occur (31, 32).

C. Adherence to Catheters by Fimbriae

Adherence of *P. mirabilis* to catheters must be resilient to overcome the force of urine flow. Several studies have shown that *P. mirabilis* readily adheres to different polymers contained in catheters and adherence is enhanced in the presence of urine or alkaline pH (17, 29, 33). There are 17 putative fimbrial operons in the *P. mirabilis* HI4320 genome (34), more than any other sequenced bacterium, and a few have been implicated in catheter adherence. The Mannose-Resistant *Klebsiella*-like fimbria (MR/K) expressed by *P. mirabilis* is important for attachment to catheters in other urinary tract pathogens (35, 36). As well, the ambient-temperature fimbria (ATF) is optimally expressed at room temperature but not important for colonization of the urinary tract, perhaps implicating it in adherence and persistence outside of the host (37). Supporting this, mutants in ATF proteins are significantly impaired in adherence and migration over catheter surfaces. Lastly, mutants in the major fimbrial subunits of the uroepithelial cell adhesin (UCA), the *P. mirabilis* (PMF), and the mannose-resistant *Proteus*-like (MR/P) fimbriae were also impaired in their ability to colonize catheter surfaces and form biofilms (38).

ii. Colonization of the Urinary Tract

A. Fimbriae

The role of the UCA, PMF and MR/P fimbriae in facilitating entry to the urinary tract requires further examination. However, the contribution of these systems to colonization of the urinary tract has been extensively characterized.

The uroepithelial cell adhesion (UCA) fimbria was first identified in a strain of uropathogenic *P. mirabilis.* UCA was named for its ability to bind the surface of uroepithelial cells, as strains of *P. mirabilis* expressing UCA can bind uroepithelial cells shed from urine (39). Later, an isogenic *ucaA* (the UCA major fimbrial subunit) mutant was constructed and impaired in uroepithelial cell binding and colonization of mouse kidneys (40). UCA is the only fimbria in *P. mirabilis* with known binding targets which are asialo-GM1, asialo-GM2, and lactosyl-ceramide (41). Asialo-GM1 is a glycolipid present on the surface of immune cells including polymorphonuclear leukocytes (PMN) which respond to infections of the urinary tract (42). Currently, no studies have investigated adherence of *P. mirabilis* to PMNs.

Proteus mirabilis fimbria (PMF) was discovered when a degenerate *ucaA* oligonucleotide was used to screen a gene bank of *P. mirabilis* (43). Infection of mice with *P. mirabilis* confers antibodies to PMF, and PMF is essential for infection in a transurethral challenge murine model (44). In a murine model of ascending UTI, a *pmfA* mutant (the PMF major fimbrial subunit) was less efficient in bladder colonization of CBA mice than wild-type in independent and co-challenge experiments (45, 46). The *pmfA* mutant was able to colonize the kidneys unless it was co-challenged (45). Another study evaluated a *pmfA* mutant using a co-challenge hematogenous UTI model in CD-1

mice. Using this model, the *pmfA* mutant was severely outcompeted and less infective than wild-type in the bladder and kidneys (46).

The mannose-resistant *Proteus*-like (MR/P) fimbria is the most extensively characterized fimbrial system in *P. mirabilis*. Multiple mutations in the *mrp* operon reduce the amount of bacteria present in the bladder, kidneys, and urine of mice (47, 48) indicating MR/P is important for *P. mirabilis* colonization of the entire urinary tract. Expression of the MR/P fimbria is governed by phase variation; mutants that are phase-locked for constitutive MR/P expression (MR/P ON) or lack MR/P expression (MR/P OFF) have very different phenotypes. MR/P OFF is outcompeted by wild-type in the bladder, kidneys and urine of mice, while MR/P ON is only outcompeted by wild-type in the bladder 7 days post-infection (49). In colonization of the bladder epithelium, MR/P OFF preferentially colonizes exfoliated cells and the basement membrane of disrupted umbrella cells. MR/P ON colonizes intact epithelium similarly to wild-type, but MR/P ON cells have a slightly elongated phenotype and are heavily fimbriated (50). More than 90% of *P. mirabilis* cells isolated from the urine and bladders of infected mice have the *mrp* promoter in phase ON orientation (49, 51). MR/P fimbriation can be directly visualized in the majority of *P. mirabilis* cells in all parts of the urinary tract (54 to 94%) during infection (50). These studies highlight the importance of the MR/P fimbria in colonization of the urinary tract.

B. Nitrogen Metabolism

Nitrogen metabolism is essential for *P. mirabilis* to establish a UTI based on *in vivo* gene expression and signature-tagged mutagenesis studies. The expression of *gdhA*, encoding glutamate dehydrogenase, is increased during infection for the conversion of

ammonia and α-ketoglutarate to glutamate. Additionally, *gdhA* mutants colonize the urinary tract less efficiently than wild-type *P. mirabilis* during murine infection, and growth of a *gdhA* mutant is inhibited when citrate is present as the sole carbon source. Overall, these data suggest *P. mirabilis* utilizes GdhA to monitor the carbon-nitrogen balance during infection, and this contributes to the pathogenic potential of *P. mirabilis* during colonization (52).

C. Metal Acquisition

Iron scavenging is essential for pathogenic bacteria, as iron is essential for many biological functions, and the urinary tract is an iron-limited environment. Different systems are used to acquire free iron and iron bound in the heme, transferrin, and lactoferrin forms. All of these systems are encoded on the *P. mirabilis* chromosome (34, 53, 54). Ferric iron (Fe^{3+}) is acquired using siderophores which are extracellular chelators that bind and solubilize iron. The siderophore-iron complex is then recognized by a specific outer membrane receptor, TonB, and transported into the cell by the TonB-ExbB-ExbD system. Ferrous iron (Fe^{2+}) uptake is largely mediated by the FeoAB system under anaerobic, iron-limiting conditions. Following uptake, ferrous iron is converted to ferric iron. Lastly, ABC transporters specific for iron can be used for iron acquisition (53). *P. mirabilis* can also use α-keto acids to chelate iron from solutions using the amino acid deaminase Aad, though this mechanism for iron acquisition is less effective than siderophores (55).

The *P. mirabilis* siderophores include the non-ribosomal-peptide synthetase-independent siderophore system, or proteobactin, and a siderophore encoded by the *nrp* operon is homologous to yersinobactin (56). Both systems and a few TonB-dependent

receptors are upregulated during iron limiting conditions (57, 58) and in the murine urinary tract (52). They also are more prevalent in UTI-causing isolates than non-UTI isolates (56). Both siderophores are important for colonization of the murine bladder in a model of ascending UTI, though the *nrp* system is more important for *P. mirabilis* fitness *in vivo* (56). *P. mirabilis* also contains two systems for ferrous iron uptake (*feoAB* and *sitDCBA*) which are upregulated *in vivo* (52). Lastly, an outer membrane heme uptake system was shown to bind heme, generate a humoral response, and is required for murine colonization (59, 60). This system, *hmuR2*, is also upregulated in iron-limiting conditions and *in vivo* (52, 56).

Another metal important for protein and enzyme function is zinc. *P. mirabilis* encodes a zinc uptake system (ZnuABC) which is required for growth when zinc is limited. Both *znuB* and *znuC* are upregulated during ascending murine UTI (52), and ZnuB generates a humoral response (61). A *znuC* mutant is impaired in swimming and swarming motility likely due to the necessity of zinc for a functioning flagellar master regulator, FlhC, which contains a zinc-binding domain (62). This mutant was also impaired during growth in zinc-limiting conditions and in colonization of the murine urinary tract when co-challenged with wild-type but not during independent infection (63). These studies illustrate the importance of metal acquisition for growth and subsequent colonization of the urinary tract.

D. Toxins

Hemolysins are common virulence determinants present in many pathogenic organisms. *P. mirablis* encodes two, *hpmA* and *hpmB*, and the expression of both is associated with swarmer cells (64, 65). Clinical isolates have higher hemolytic activity

than environmental isolates, and *hpmA* mutants are less cytotoxic against human renal cells (2, 66, 67). Hemolysin was once thought to be a factor in bacterial spread to the kidneys leading to pyelonephritis during ascending UTI (68). Surprisingly *hpmA* mutants are not significantly impaired in their ability to colonize the urinary tracts of mice unless flagella are not present (69), and hemolysin expression is not upregulated *in vivo* (52).

Proteus toxic agglutinin (Pta) is a multi-functional outer membrane auto-transporter that mediates *P. mirabilis* cell-to-cell aggregation and contains a catalytically active α-protease domain that lyses uroepithelial cells (58, 70). Inactivation of *pta* results in reduced cytotoxicity and colonization of the murine urinary tract by *P. mirabilis* (70, 71). Interestingly, *hpmA pta* double mutants have reduced pathology compared to each mutation alone, possibly indicating an additive effect of both proteins on uroepithelial cell lysis (71). This could explain why loss of *hpmA* does not significantly affect urinary tract colonization.

iii. Persistence within the Urinary Tract

A. IgA Degrading Protease

Following colonization of the urinary tract, *P. mirabilis* has the ability to persist within the human host despite catheter changes and antibiotic treatment. Evasion of the innate and adaptive immune responses permits survival within the host. One mechanism to evade the mucosal immune response is to degrade host immunoglobulins. *P. mirabilis* employs this tactic through ZapA, a metalloprotease. The *zapA* locus is located in an operon with its own putative ABC transporter (*zapB*, *zapC*, and *zapD*) and a second metalloprotease (*zapE*) (72).

ZapA was identified when immunoglobulin A1 (IgA1), IgA2 and IgG proteolysis was found in the urine of patients suffering from *P. mirabilis* infection (73). In addition to host immunoglobulin proteolysis, ZapA cleaves a range of immune factors found in urine, including cytoskeletal proteins, cell matrix proteins, complement (C1q and C3), and antimicrobial peptides (human beta-defensin 1 and LL-37) (74). Mutants in *zapA* have a reduced capacity to colonize the bladders and kidneys of mice (75) and establish acute and chronic prostatitis in rats (76). Expression of *zapA* is coordinated with differentiated swarmer cells; a 30-fold increase in *zapA* expression is observed in swarmer cells relative to vegetative cells, and *zapA* expression is highest prior to consolidation phase (65, 75).

B. Host Cell Invasion and Urolithiasis

P. mirabilis has been shown to invade a variety of cell lines, including monkey renal parenchymal cells, human bladder cell lines, human urothelium, and primary human renal cells (67, 69, 77-79). The swarmer cell morphotype is associated with the invasion of uroepithelial cells (77), and hyperswarming strains are more invasive than their wild-type counterparts (79). The expression of virulence factors such as *zapA* and hemolysin is coupled with differentiated swarmer cells likely aiding their increased invasiveness (64, 75). Invasion of host cells is hindered when flagella are immobilized, and flagellar mutants are less invasive than wild-type (69). Moreover, host cell invasion may provide protection against antibiotics for internalized *P. mirabilis* (80).

The formation of urinary stones (urolithiasis) requires the production of urease for the precipitation of calcium and magnesium which results in the formation of crystals (67). *P. mirabilis* has been visualized within urinary stones (81), an environment that

could promote persistence by protecting the bacteria from the immune response. Metabolic changes due to nutrient limiting conditions within the urinary stone may help the bacteria resist antibiotics (68). Recently, it was shown urolithiasis is dependent on MR/P fimbria which promotes aggregation of *P. mirabilis* in the urinary tract. These aggregates form urease-mediated crystals causing an influx of neutrophils which release neutrophil extracellular traps (NETs). NET formation in the urinary tract has been shown to be specific to *P. mirabilis*-mediated infection (82), and NETs could provide material to mediate further aggregation of cells and contribute to urolithiasis (83).

C. Phase Variation

Another mechanism of immune evasion is to alter the expression or composition of antigenic structures recognized by the host. Two large structures found on the *P. mirabilis* outer membrane which generate a humoral response in mice include fimbriae and flagella (61, 84). The MR/P fimbria are phase variable through a mechanism of site-specific inversion. The *mrp* operon, encoding the MR/P fimbria, is transcribed divergently from *mrpI* encoding the recombinase MrpI (85). The *mrp* operon is preceded by a σ^{70} promoter within an invertible repeat which is under MrpI control (85). When the σ^{70} promoter faces the *mrp* operon, the MR/P is phase ON. When the σ^{70} promoter faces *mrpI*, MR/P is phase OFF (51). The *mrp* promoter orientation is fixed in the absence of MrpI suggesting it is the sole recombinase for the operon (51). Another element affecting MR/P expression is the last gene in the *mrp* operon, *mrpJ*, which encodes a transcriptional regulator. MrpJ activates expression of the *mrp* operon promoting MR/P phase ON (86). Additionally, there are 14 paralogs of *mrpJ* in *P. mirabilis*: 10 paralogs are a part of fimbrial operons and 4 *mrpJ* paralogs are orphans (87). It is unknown if any

of the MR/P paralogs or the other fimbrial systems in *P. mirabilis* are phase variable, but altering expression of any of these genes could contribute to fimbrial diversity and subsequent fitness within the host.

The effect of the phase variable *mrp* operon is not limited to MR/P fimbriation as it extends to the repression of motility. Locking MR/P in phase OFF increases swarming motility (50), and artificial overexpression of 12 *mrpJ* paralogs thwarts motility to different degrees, with some paralogs preventing swarmer cell differentiation altogether (87). MrpJ and its paralog UcaJ directly bind upstream of the master flagellar operon, *flhDC*, mediating direct repression (88). The other *mrpJ* paralogs contain a conserved DNA-binding domain, but it is unknown if they can bind *flhDC.* Transcriptome profiling of *P. mirabilis* during urinary tract infection revealed the *mrp* genes are the most highly expressed during early infection (1-3 days) but their expression decreased in later infection (3-7 days). Flagellar genes were the most down-regulated genes in early infection, but in later stages of infection their expression increased (52). Overall, *P. mirabilis* is fervently committed to inversely expressing fimbriae and flagella. Altering the expression of these structures has implications for infection as both are antigenic.

D. Antigenic Variation

P. mirabilis encodes two nearly identical flagellins, *flaA* and *flaB.* A third putative flagellin is encoded elsewhere on the chromosome. Despite the close proximity of the two loci, *flaA* is transcribed monocistronically, and *flaB* transcript is scarce in wild-type cells. FlaA is the major flagellin, as *flaA* mutants are non-motile and do not synthesize flagellin while *flaB* mutants exhibit wild-type motility. Mutants of *flaA* frequently revert to motile cells with a flagellum that is antigenically distinct from wild-type (89). These

mutants have hybrid FlaAB flagellin created by deletions in both loci that place the active *flaA* promoter and the 5'coding region of *flaA* with homologous and previously silent regions of *flaB* (90). Later, it was shown *P. mirabilis* populations are naturally heterogeneous in flagellar composition, with 1.0–1.5% of the population expressing hybrid *flaAB* transcript (91). Flagellin rearrangements confer advantages in different environments; bacteria with hybrid FlaAB flagella are more motile in environments with high salinity and extreme pH, while bacteria with FlaA flagella are more motile in low salt conditions (92). Recovery of swimmer and swarmer cells from the murine urinary tract illustrated different hybrid flagellins are formed during infection. All recovered FlaAB proteins were the result of splicing before the antigenically exposed domain of the flagellin molecule. This would result in exposure of different antigenic sites on the surface of the bacterium (90), and both flagellin proteins are capable of generating a humoral response (61). Overall, the ability of *P. mirabilis* to undergo flagellin rearrangements promotes survival in various environments and may help the bacteria evade the immune response during UTI.

II. Surface Motility

Bacteria colonize and persist on surfaces using different behaviors. Bacterial populations can remain sessile, form aggregates and secrete an exopolysaccharide matrix that leads to the formation of multicellular communities known as biofilms (93, 94). Alternatively, bacteria can become motile and disseminate from the initial point of contact to discover new and perhaps more favorable environments. Various forms of motility are utilized by different bacteria to colonize surfaces. Some forms of motility do

not require the presence of flagella (twitching, gliding, and sliding) while others do (swimming and swarming) (95).

A. Flagella-Independent Motility

The use of type-IV pili (T4P) is responsible for a form of motility known as twitching which is used by a variety of bacteria including *Pseudomonas aeruginosa* and *Neisseria gonorrhoeae* (96). The length of T4P is dynamic, and they can be found at one or both cell poles. T4P extend by polymerization and retract by depolymerization. The rapid extension and retraction of T4P is the underlying mechanism for twitching motility; it allows for forward and backward movement of cells and colony expansion up to 1 μm/s (44, 97, 98). The jerky motion associated with this form of motility is the result of groups of twitching cells making contact then rapidly realigning. Twitching motility can result in outward expansion of colonies under nutrient rich conditions. In contrast, other bacteria utilizing twitching motility under nutrient-limiting conditions will form fruiting bodies as cells come together (96).

Gliding is a mysterious form of motility where the long axis of the cell propels bacteria across surfaces in the absence of a visible organelle. It has been observed in organisms from the cyanobacteria and *Cytophaga-Flavobacterium* groups and in *Myxococcus xanthus*, where it is known as adventurous motility (99). Colony edges of gliding bacteria appear similar to swarming or twitching bacteria, but the mechanism for gliding is currently unknown. Cells may use secreted polysaccharides for propulsion (100). Alternatively, proteins in the cytoplasm act may act as a motor to induce movement of cell surface adhesions (101) or cells may contract fibrils in the cell wall for mobility (102).

Sliding is the passive expansion of a colony across surfaces driven surfactant production in conjunction with the force of cell division. This form of migration is passive as groups of cells oriented in different directions expand as a single unit. It has been observed in many bacteria, from *Vibrio cholerae* to *Mycobacterium smegmatis*, and is a common mechanism for bacterial translocation across surfaces (103, 104).

B. Flagella-Dependent Motility

One of the most widespread structures used by bacteria for motility is the flagellum, a membrane-bound propeller that is complex in its structure, assembly, and regulation. The flagellum is the best-studied structure used for motility, and flagellar motility is used by members of the Archaea and both Gram-positive and Gram-negative bacteria (95). Flagella drive translocation of individual cells through aqueous environments, called swimming (105). Whereas swimming is an individual endeavor, swarming is undertaken by a group of cells which collectively traverse solid surfaces using their rotating flagella (106). Flagellar motility requires the assembly of an intact flagellum which is produced in response to elegant gene regulation (107-109). Following assembly, flagellar rotation is influenced by chemotaxis (110). A few models for flagellar assembly, regulation, and chemotaxis exist for different classes of bacteria. *P. mirabilis* is a member of the Gram-negative enteric bacteria along with *E. coli* and *S. enterica*. As such, the models for the (i) structure and (ii) regulation of flagellar assembly and (iii) chemotaxis described for this class of bacteria will be discussed.

i. The Flagellum

The flagellum is commonly divided into three substructures: the basal body, the hook, and the filament. The structures of the basal body anchor the flagellum to the

membrane and comprise the motor that generates flagellar rotation (111). The hook acts as the joint to connect the basal body to the filament (112). Thousands of flagellin protein subunits polymerize to form the filament which extends from the cell body to propel the bacterium forward (105, 113).

Flagella are self-assembled in a multi-stage process that begins with the coordinated assembly of the flagellar type III secretion system (T3SS) and some of the basal body structures. The structures of the basal body important for anchoring the flagellum to the cell are a series of rings and a rod. The MS-ring (located on both sides of the cytoplasmic membrane) and the C-ring (located at the cytoplasmic face) form a scaffold for the assembly of the flagellar T3SS cytoplasmic components. The P-ring and the L-ring (present only in Gram-negative bacteria) are incorporated, respectively, into the planes of the peptidoglycan and lipopolysaccharide as the flagellar T3SS assembles (114). The assembled T3SS is now provided with a channel for the export of the basal body rod, followed by the hook proteins, and finally the flagellar filament (115). Late proteins that move through the T3SS to comprise the hook or filament can be contained within secretion chaperones (116-118). Export is driven by an ATPase complex that associates with the cytoplasmic C-ring (119), and is controlled by capping proteins of the hook, rod, and filament. The capping protein of the filament is released by a late secretion chaperone to signal the end of complex assembly (120-122).

The motor behind flagellar rotation is driven by proton motive force. The two parts of the motor are the rotor (rotating basal structure) and the stator (stationary ion-conducting complexes). The rotor is made of the C-ring, located at the base of the newly assembled flagellum, the MS-ring, and the rod (123). The C-ring is composed of three

proteins known as the "switch complex" (124). The stator is made up of two proteins: MotA, which interacts with the switch complex, and MotB, a membrane-embedded protein that holds the complex in place and shuffles proteins through the motor (125, 126). Protonation of MotB induces a conformational change in MotA resulting in a charge-charge interaction between MotA and the switch complex (127, 128). This induces movement of the switch complex, generating torque, which is transmitted by the MS-ring to the rod, hook, and lastly, the filament (127, 129).

ii. Regulation of Flagellar Assembly

Much like its assembly, regulation of flagellar genes is hierarchal and based on three promoter classes in Gram-negative enteric bacteria. At the top of the flagellar gene hierarchy is the flagellar master operon *flhDC* expressed from a class I promoter. The decision to assemble flagella is dependent on *flhDC* expression which is highly regulated in response to changes in the environment, including nutrient availability, pH, osmolarity, and temperature (130-134). The regulation of *flhDC* will be discussed in detail later in this chapter. The FlhD and FlhC proteins encoded by the *flhDC* operon comprise the hetero-hexameric $FlhD_4C_2$ transcriptional regulator. $FlhD_4C_2$ binds large asymmetric repeats present in class II promoters to support σ^{70}-dependent transcription of these genes. Genes transcribed from class II promoters (9 operons, 38 genes) encode proteins of the hook and basal body substructures (HBB) and regulators which drive the expression of class III promoters. These regulators include *fliA* (σ^{28}), *flgM* (anti-σ^{28}), *flgN*, and *fliT*. The regulator σ^{28} drives the expression of class III promoters (16 operons, 29 genes) encoding flagellar filament structural proteins, hook associated proteins, the flagellar motor, and chemotactic proteins (135).

The class II regulators can have dual roles as secretion chaperones and transcriptional regulators. Chaperones were once thought to prevent proteolysis of a substrate before secretion or direct localization of a substrate to the secretion machinery. Alas, a mechanism has emerged in which secretion chaperones function as transcriptional regulators allowing for strict calibration in the assembly of complex structures such as a flagellum. Secretion chaperones that are dual regulators in the flagellar transcriptional cycle are FliA (σ^{28}), FlgN, and FliT (116, 118). Each affects transcription of flagellar genes in a different manner following secretion of their substrates at the HBB. The secretion chaperone FliA drives transcription of class III promoters, and the secreted substrate of FliA is FlgM (anti-σ^{28}). Both are expressed from class II and class III promoters (118, 136). Class II-expressed FlgM serves as an internal checkpoint in flagellar assembly by binding to FliA in the cytoplasm and preventing interaction of σ^{28} with RNA polymerase (137, 138). Once the HBB is completed, the flagellar T3SS changes its affinity for HBB structural proteins to late secreted substrates. Following secretion of FlgM by FliA the ratio of bound σ^{28} in the cytoplasm decreases, and class III promoter transcription can occur (137, 139). The FliA/FlgM regulatory system is further complicated by the fact that both are transcribed from class II and class III promoters. As a result, excess FlgM prevents class III expression of both genes whereas excess σ^{28} increases class III expression of both genes. Additionally, the secretion chaperone FlgN increases translation of FlgM (140).

Another secretion chaperone that functions as a transcriptional regulator is FliT (116). FliT inhibits *flhDC* activation of class II promoters encoding the structural HBB proteins. Before HBB completion, FliT is bound by its late secreted substrate FliD, the

filament capping protein (116). Following HBB completion, FliT and σ^{28} are freed from the interaction with their substrates. FliT promotes ClpXP-mediated proteolysis of FlhC to inhibit $FlhD_4C_2$ formation (141), and it binds to intact $FlhD_4C_2$ to prevent its interaction with class II promoters (142, 143). Concurrently, σ^{28} initiates the expression of class III promoters (136). Overall, the expression of late flagellar genes (class III) coincides with the inhibition of early flagellar genes (class II).

Additional regulators with varying roles in the flagellar transcriptional cycle are also encoded within the class II and class III genes. FliZ, encoded in the same operon with FliA, promotes $FlhD_4C_2$ activation of class II operons by inhibiting expression of *ydiV*, encoding a gene that subjects $FlhD_4C_2$ to proteolytic degradation in *S. enterica* (133, 144). In *Xenorhabdus nematophilus*, FliZ directly activates *flhDC* expression, while the *E. coli* FliZ acts as a direct *flhDC* repressor (145, 146). In *E. coli*, FliA (σ^{28}) also activates its own transcription leading to increased class III expression in the absence of *flhDC.*

Flagellar structural proteins can also play a role in transcriptional feedback which may play a role in hyperflagellion of certain bacteria. FlhA is a membrane bound HBB protein involved in the secretion of late export proteins. In *P. mirabilis,* a mutant of *flhA* does not swarm and produces less *flhDC* transcript. The expression of *flhA* coincides with cycles of swarmer cell formation in *P. mirabilis*, indicating it may form a positive feedback loop with *flhDC* (147, 148). In *B. subtilis*, it has been shown that following secretion of the filament capping protein FliD, FliT stays associated with FlhA at the membrane (117). Thus, FlhA may control the amount of free FliT it the cytoplasm to prevent modulation of $FlhD_4C_2$ activity. In *S. enterica* the secretion chaperone FlgN

negatively affects flagellation; in *P. mirabilis*, it is important for swarming motility. Mutants of *flgN* have decreased *flhDC* expression resulting in flagellation sufficient for swimming but not swarming motility (149). Due to the importance of FlhA and FlgN to *flhDC* expression suggests positive feedback from flagellum completion to new filament production. This feedback could be utilized for the hyperflagellation required by *P. mirabilis* for swarming on surfaces.

iii. Chemotaxis

Bacteria can have bi-directional flagellar motors which permit changes in the direction of flagellar rotation. Tumbling results from clockwise (CW) flagellar rotation, and running is caused by counter-clockwise (CCW) rotation (124). Bacteria will alter the direction of locomotion in response to the presence or absence of attractants and repellents in the environment, called chemotaxis. Examples of attractants are primarily nutrients, including amino acids, sugars, and dipeptides, though the interspecies quorum sensing signal AI-2 and pyrimidines also serve as attractants for *E. coli* (150, 151). Some examples of repellents include fatty acids, aliphatic alcohols, aromatic compounds, inorganic ions, and mercaptans (152). Chemotaxis affects the migration of swimming cells which move forward (run) and change direction (tumble) in response to gradients of attractants or repellents. Chemotactic behavior causes seemingly chaotic swimming patterns that result from rapid succession between running and tumbling. However, motility is rarely random. Bacteria have evolved intricate and incredibly sensitive chemosensory systems which promote their survival in various environments (110, 153, 154).

The chemotactic system that affects swimming motility in Gram-negative enteric bacteria is an atypical two component system that affects the phosphorylation state of the response regulator (RR) CheY. This system has been best-studied in *E. coli* and *S. enterica* (154). The chemosensory proteins that are activated by attractant or repellent molecules are stable, dimeric, transmembrane proteins called methyl-accepting chemotaxis proteins (MCPs). The periplasmic domains of different MCPs have little homology as they "sense" or bind different molecules. Within the cytoplasmic domain of MCPs is a highly conserved signaling domain where the adaptor protein CheW interacts with the cytoplasmic histidine kinase (HK) CheA (155). When the MCP binds a ligand, the signal is transmitted to CheA which, upon activation, phosphorylates the RR CheY (156). Phosphorylated CheY (CheY~P) binds to the switch complex within the flagellar motor to promote CW rotation of the flagellum and tumbling occurs. CheY~P can be dephosphorylated by CheZ to terminate the signal (155, 157). The CW and CCW rotations of flagella exist in equilibrium with CCW rotation being favored unless CheY~P formation is initiated (154).

Another method to reset signal transduction is through altering the methylation state of the MCP so it can sense future environmental signals and react accordingly. Methylation of the signaling domain is mediated by the RR and methyl esterase CheB, which requires phosphorylation to be active, and the constitutive methyl transferase CheR. The HK CheA can bind CheB in addition to CheY (155). If CheB becomes phosphorylated, it competes with CheR to demethylate the signaling domain of the MCP. Demethylation alters the topology of the signaling domain resulting in decreased signal transduction and activity of the HK CheA (155, 158).

As expected, there are differences from this mechanism of chemotaxis in other bacteria. Attractants inhibit the HK CheA in *E. coli* but stimulate the CheA of *Bacillus subtilis* (159). *B. subtilis* can deamidate the signaling domain of some of its MCPs, catalyzed by CheD and not CheB, indicating *B. subtilis* has MCPs similar to those in Archaea which this mechanism of adaption is specific to (42, 160). Additionally, CheZ is exclusive to the β- and γ-proteobacteria so other bacteria employ different mechanisms to terminate the CheY-induced signal. To modulate CheY~P levels in *B. subtilis*, one of the proteins in the motor switch complex hydrolyzes CheY~P; a separate protein, CheC, hydrolyzes CheY~P in conjunction with CheD (160-162). A mechanism dubbed the "phosphate sink" is used by the α-proteobacteria *Sinorhizobium meliloti* and *Rhodobacter sphaeroides*. They encode multiple CheY homologs which are phosphorylated by CheA; however, only one interacts with the motor switch to influence the flagellar rotation (163, 164). *P. aeruginosa* encodes multiple clusters of chemotaxis genes: two for swimming motility (165) and one for twitching motility (166).

While important for the behavior of swimming and twitching cells, the role of chemotaxis in swarming is poorly understood. Chemotaxis appears to be suppressed in swarming cells (167, 168) and is only mechanically required for swarming in *E. coli*, *S. enterica*, *Serratia marcescens*, and *B. subtilis* (169-171). Null mutants in the chemotaxis pathway (Che) locked in flagellar rotation (either CW or CCW) do not swarm unless surface hydration is provided exogenously. Thus, the role chemotaxis plays in swarming in these bacteria appears to be limited to providing surface hydration. In *P. mirabilis*, *che* or MCP mutants are impaired in their ability to swarm. However, it is currently unknown if chemotaxis affects swarming motility by providing surface hydration or mediating

cell-to-cell signaling in this bacterium (17, 59). Overall, the chemotaxis systems employed by these organisms are important for individual and group survival in the diverse niches they inhabit.

C. Swimming as Individuals

Flagella drive translocation of individual cells through aqueous environments or within semi-liquid substrates, called swimming (105). Swimmer cells can be likened to pioneers in search of a more favorable environment mediated by chemotaxis. There are different patterns of flagellation in prokaryotes: including a single, polar flagellum (monotrichous), several flagella at one pole (lophotrichous), flagella at both poles (amphitrichous), or flagella distributed along the cell surface (peritrichous). Different patterns of flagellation, cell shape, swimming velocity, and mechanisms of running/tumbling affect the three-dimensional manner bacteria swim and tolerate viscous environments.

Gram-negative enteric bacteria (*E. coli*, *S. enterica*, and *P. mirabilis*) are peritrichously flagellated when swimming. *E. coli* and *S. enterica* typically have 6-8 flagellar filaments while *P. mirabilis* has 4-10. The hook of each flagellar filament is flexible and permits rotation up to angles of 90°. Flexibility of the hook is essential for normal swimming, as artificially stiffening it impedes swimming motility (172). Each flagellar filament spends the majority of the time (95%) rotating CCW, forcing them to form a bundle which propels these bacteria through the environment. The switch of individual filaments to CW rotation in response to environmental changes forces the bundle apart and results in tumbling. Each flagellum has its own switching frequency and the rate of tumbling is dependent on the number of flagella that change rotation at any

time (173, 174). *E. coli* and *S. enterica* swim at speeds between 15 μm/s and 30 μm/s (175, 176). *P. mirabilis* swims at a rate of 25 μm/s but low pH and high salinity reduce swimming speeds (92). *E. coli* and *S. enterica* are model organisms for the study of flagellar assembly and chemotaxis. However, the mechanisms employed by these bacteria to exploit their respective niches are not shared by other bacteria. Examples of swimming behavior in non-enteric bacteria are discussed below.

The photosynthetic bacterium *Rhodobacter sphaeroides* has a single, polar flagellum that only rotates CW. This bacterium does not exhibit the "run and tumble" behavior seen in enteric bacteria. Rather, *R. sphaeroides* changes direction by stopping and starting flagellar rotation. Starvation for a specific metabolite causes *R. sphaeroides* to increase its speed from 5 μm/s to 50 μm/s, and when chemotactically stimulated, only a subset of cells respond to the gradient (177).

Amphitrichously flagellated bacteria with a single flagellum at each cell pole are often helical shaped such as the gastrointestinal human pathogen *Campylobacter jejuni*. In liquid, the swimming pattern of *C. jejuni* is similar to enteric bacteria with rapid oscillations between runs and tumbles promoting speeds up to 40 μm/s. In viscous environments, *C. jejuni* uses its helical shape in coordination with flagellar rotation to run for longer periods with increased speed, called darting, followed by pauses rather than tumbles. Curiously, *C. jejuni* has increased motility in viscous medium with velocities reaching 75 μm/s (178).

Another human pathogen that is helical in shape but lophotrichously flagellated is gastric pathogen *Helicobacter pylori*. To maintain high velocities in viscous environments, such as the gastric mucosa, *H. pylori* changes its shape and number of

flagella (179). Lophotrichously flagellated bacteria are propelled forward by the CW rotation of flagellar filaments, and tumbling results from asynchronous slowing of the filaments which causes chaotic flagellar movement (180). The swimming pattern of *H. pylori* consists of random darting movements with frequent tumbles and short runs with speeds reaching 20 μm/s. In response to acid, the bacteria increase swimming velocity, swim in arcs, and do not tumble in order to translocate from acid (181). This behavior could be utilized to colonize its niche, as *H. pylori* must quickly traverse the low pH of the stomach to penetrate the gastric mucosa.

Aquatic bacteria *Vibrio parahaemolyticus* and *Aeromonas hydrophila* are unique in their possession of two distinct flagellar systems that are differentially expressed in response to the environment. In liquid culture, swimming is propelled by a single polar flagellum (Fla) permitting speeds up to 60 μm/s. On solid media, mixed flagellation occurs as Fla is accompanied by the expression of numerous lateral flagella (Laf) to promote swarming motility.

Many of the genes encoding the *V. parahaemolyticus* polar flagellum are homologous to flagellar genes in *E. coli*. However, the flagellum is comprised of six different flagellins, it is sheathed, and the motor is powered by sodium motive force rather than proton motive force (PMF). An entirely different set of genes encode the Laf flagella which are composed of one flagellin, are unsheathed, and utilize PMF, much like Gram-negative enteric flagella (182). Regulation of Fla is governed by a 4-tiered flagellar gene hierarchy similar to *P. aeruginosa* (135). Surface-induced inhibition of Fla results in the expression of Laf, triggering the formation of numerous peritrichous flagella on the cell surface. This is an example of mechanosensing: the process by which cells undergo

physiological changes in response to mechanical cues in the environment. The class I flagellar regulator for Fla becomes dispensable, as the class I Laf regulator can activate the expression of both the Laf and Fla structural genes, ensuring constitutive formation of both (107, 183).

The evolution of inducible flagellar systems in these bacteria ensures survival in their aquatic niche. Swimming enables them to migrate toward favorable environments, and the polar flagellum promotes surface attachment. These bacteria can now form biofilms or colonize surfaces via swarming motility (183, 184). Mechanosensing is not limited to *V. parahaemolyticus*. The viscosity of the environment and the presence of attachment substrates can induce physiological changes in other swimming bacteria allowing them to adopt surface-assoicated lifestyles (185, 186).

III. Swarming in a Group

Swarming is the flagella-dependent translocation of a bacterial population across a solid surface. Swarming migration necessitates the cohesion of cells sharing the same shape, density, and flagellar mechanics, called rafting. Cells recruited to a raft participate in swarming migration while cells lost from the raft are immobile. Additionally, a reduction of surface tension mediated by damp substrates or surfactant synthesis is required for swarming. A final feature of swarming bacteria is the “swarming lag” where swimming cells are immobile for a period of time following surface contact likely to undergo physiological rearrangements required for swarming.

Moving as a collective group provides swarming bacteria with benefits not shared by their swimming counterparts. Swarming bacteria exhibit increased resistance to antibiotics which is attributed to altered metabolic activity and outer membrane

composition which leads to an increased oxidative response and reduced membrane permeability, respectively (187-192). As well, the multicellular nature of swarming promotes altruism, as only a subset of the population dies upon antibiotic exposure which provides a protective barrier for survivors. This phenomenon is dependent on cell density as individual surviving swarmer cells undergo cell death when exposed to antibiotics. Movement at higher velocities also promotes increased resistance. This raises the question as to whether swarming is altruistic or selfish behavior – as cell death would be inevitable for slower cells. Overall, the behavior promotes survival of the group at the cost of some individuals (188). Some bacteria couple the expression of virulence factors with swarming motility. Increased expression of hemolysin, IgA protease, and urease are coupled to swarming motility in *P. mirabilis* (64, 75, 78). The operon encoding phospholipase in *S. marcescens* is a part of the flagellar regulon (193). Additionally, the flagellar T3SS has been shown to act as a secretion apparatus for virulence proteins (194). Overall, swarming would provide a bacterial pathogen with the machinery to migrate to, exploit, and disperse from a site of infection.

Swarming motility has been identified under laboratory conditions in the (i) firmicutes, (ii) α-proteobacteria, and (iii) γ-proteobacteria. These bacteria swarm under different conditions to form distinct patterns on agar plates as a result of unique regulatory mechanisms. Swarming in each of these groups is briefly discussed below.

i. Firmicutes: Swarming and Bistability in *B. subtilis*

Many laboratory strains of *B. subtilis* do not exhibit swarming motility, but the discovery of robust swarming in an undomesticated strain permitted characterization of swarming behavior in this bacterium (195). *B. subtilis* swarms on Luria-Burtani plates

with agar concentrations between 0.5 and 0.7%. In any bacterium, motility on agar concentrations greater than 0.5% is indicative of swarming as the agar is no longer porous enough to promote swimming. The pattern formed on agar plates by swarming *B. subtilis* is a sheer, unadorned monolayer known as a "featureless mat". The swarming population is heterogeneous with swarmer cells forming the highly mobile, advancing colony edge and a population of small, non-motile chaining cells comprising the interior. Individual swarmer cells exhibit hyperflagellation, a 3-fold increase in volume, and a modest increase in length compared to swimming cells (171). In the firmicutes *Bacillus thuringiensis* and *Clostridium septicum*, swarmer cells are elongated and multinucleated (196, 197). The morphological change *B. subtilis* undergoes to swarm is less dramatic: they are not filamentous and possess two curiously compact nucleoids formed by cell division inhibition (171). Lastly, swarming is dependent on synthesis of the lipopolypeptide surfactant, surfactin (198, 199).

The reason for the lack of swarming motility in domesticated *B. subtilis* strains is due to a frameshift mutation in *sfp* which is required for surfactin production (200). Domesticated strains with this mutation can form a "whirl and jet" swarm pattern on wet agar only if accompanied by an epigenetic switch in another gene (201). The identification of *swrA* gene explained the non-swarming behavior of certain domesticated strains in the presence of purified surfactin (171). The *swrA* mutation inadvertently selected for in laboratory strains results from a single A/T base pair insertion in a poly-(A/T) nucleotide tract within the *swrA* opening reading frame. In combination with the *sfp* mutation, domesticated strains were further blocked for surface motility.

One mechanism for the regulation of swarming motility in *B. subtilis* may be phase variation mediated by SwrA (202). Insertions and deletions in the *swrA* poly-(A/T) nucleotide tract occur at a high frequency on par with a molecular mechanism of phase variation known as slipped-strand mispairing (203). SwrA is essential for swarming, and it regulates peritrichous flagellation in *B. subtilis*. However, SwrA is not considered a master regulator of motility because *swrA* mutants still swim (199, 204, 205). Additionally, SwrA plays a role in *B. subtilis* population heterogeneity through the transcription factor for motility, σ^D (202, 206, 207).

Growing *B. subtilis* cells exist as a mixed population where σ^D is active (ON) or σ^D is inactive (OFF). σ^D-ON cells express flagella and lytic enzymes to separate individual cells from chains. σ^D-OFF cells exist in long, sessile chains. This heterogeneity results from bistable expression of σ^D and the activator of σ^D-directed gene expression, SwrB. Genes encoding these proteins are located in the same operon (*fla*/*che*) with other flagellar genes (202). SwrA biases the population to σ^D-ON by activating the *fla*/*che* operon subsequently increasing the amounts of σ^D and SwrB. In turn, σ^D and SwrB activate the expression of other flagellar genes, and σ^D activates *swrA* expression (208). Overexpression of *swrA* results in a homogenous populations of motile cells (202). How SwrA biases in the population to σ^D-ON has not been completely elucidated. It could result from the positive feedback interaction between σ^D and SwrA (208). However, the role of SwrA in motility is further complicated by its interaction with the two-component regulatory system DegS/DegU which is also required for swarming in *B. subtilis* (208, 209).

A model exists in *B. subtilis* where the cell envelope acts as a sensor to initiate swarming. Upon surface contact, the sensor kinase DegS phosphorylates the response regulator DegU (DegU~P) which forms a complex with SwrA. Formation of the DegU~P/SwrA complex protects SwrA from Lon protease degradation (210). Additionally, binding of SwrA to *fla*/*che* is dependent upon phosphorylated DegU~P. DegU~P represses the *fla*/*che* operon in the absence of SwrA while DegU activates it (211). The repression of *fla*/*che* by DegU~P is counteracted when SwrA is present; together, the two proteins form a complex to bind and activate *fla*/*che* (209). The regulation of both swimming and swarming motility in *B. subtilis* is complex. Other regulators of swarming likely exist but remain to be identified (108).

ii. α-proteobacteria: Mechano- and Quorum-Sensing Required

Lateral flagellar systems are not limited to *Vibrio* and *Aeromonas spp*. In fact, lateral flagellar systems are used for the initiation of swarming motility in the α-proteobacteria.

Rhodospirillum centenum is a purple photosynthetic bacterium that undergoes differentiation from vibrioid swimming cells with a single sheathed, polar flagellum into rod-shaped swarming cells that have a polar flagellum plus numerous, unsheathed lateral flagella (212). Whereas *V. parahaemolyticus* does not require its polar flagellum for swarming motility, *R. centenum* does. Additionally, the polar flagellum of *R. centenum* is not required for surface-sensing and the subsequent expression of lateral flagella (213). *R. centenum* swarms when swimming cells are grown on agar at concentrations up to 1.5%. Hyperflagellation and surfactant synthesis accompany *R. centenum* swarming on solid surfaces, but swarmer cell elongation only occurs at 42°C (213). Interestingly, swarm

colonies of this bacterium can migrate on 0.8% agar towards or away from light, depending on the wavelength of excitation, a phenomenon known as phototaxis (212).

Azospirillum spp. are nitrogen-fixing rhizobacteria which promote the growth of plants. Motility and chemotaxis are thought to be important factors for efficient plant colonization by these bacteria (214). The polar flagellum of *A. brasilense* is highly glycosylated to promote adhesion to plant roots (215). Disrupting the rotation of the polar flagellum is the signal for lateral flagella (Laf) induction which allows swarming on agar concentrations up to 1.0% at 30°C. The transcription of *laf* rises concurrently with increasing agar concentrations (216). This bacterium, like undomesticated *B. subtilis*, forms a featureless mat when swarming (217). A phase variant of *A. lipoferum* lacking a polar flagellum constitutively expresses high levels Laf in liquid and on solid agar. Formation of lateral flagella increases upon surface contact in this strain suggesting lateral flagella can be involved in mechanosensing in this species (218, 219).

Members of *Rhizobium spp*. are nitrogen fixing bacteria that co-exist with legumes. Motility provides a fitness advantage in this bacteria (220). *Rhizobium spp.* swarms on soft agar (0.5 – 0.8%) in nutrient-rich media at lower temperatures (22°C - 30°C). Swarming is accompanied by hyperflagellation in these species but not by a change in cell length. The swarm pattern formed by *Rhizobium* differs between species: *R. leguminosarum* forms a dendritic pattern while swarm colonies of *R. etli* contain extrusions at the interior, due to changes in viscosity, and scalloping at the swarm edge (221, 222). A glistening film follows the swarm front of *R. etli* suggesting surfactant production. It was later shown that surfactant in this species is unique; it is composed of *N*-(3-hydroxy-7-*cis*-tetradecenoyl) homoserine lactone produced by the CinIR quorum

sensing system. For these bacteria, quorum sensing signals have a dual role in swarming: as signals and biosurfactants (223).

iii. γ-proteobacteria: Diverse Mechanisms of Swarming

E. coli and *S. enterica* are temperate swarmers lacking a transcriptional program to activate swarming motility or the upregulation of flagella. Both swarm optimally on 0.5-0.7% agar, and *E. coli* requires the presence of Eiken agar to supply a hydrated surface. *S. enterica* can swarm on standard agar if glucose is provided in the media. Minimal media does not support swarming of either bacterium. Temperature affects the ability of these organisms to swarm. *E. coli* swarms optimally at 30°C while its ability to swarm is reduced at 37°C. In contrast, 37°C is the optimal temperature for *S. enterica* swarming (224). These bacteria do not undergo dramatic changes in cell morphology in the transition from swimming to swarming; rather, they suppress cell division, double in size, and the resulting cells have twice the number of flagella (225). This uneventful change in morphology corresponds with the fact neither organism undergoes transcriptional changes that would lead to hyperflagellation or cell elongation during swarming (226, 227).

Neither *E. coli* nor *S. enterica* secretes surfactant (228, 229), therefore exogenous hydration must be provided in order for these bacteria to swarm (230, 225). This is thought to occur through flagellar rotation which promotes an insurgence of water from the agar to hydrate the colony. Supporting this, hyperflagellation or increased flagellar motor activity promotes swarming under non-permissive conditions (225, 227). The interchange between CW and CCW flagellar rotation mediated by chemotaxis is mechanically required for this phenomenon (169-171), and chemotaxis is activated upon

surface contact when the flagellum becomes stuck to the agar surface (230). Lipopolysaccharide (LPS) also plays a role in hydration. Stripped LPS penetrates the agar and attracts water to the surface, acting as an osmolyte. LPS mutants are incapable of swarming, and genes encoding the LPS structure are upregulated on surfaces (226, 231). Additionally, a high osmolytic agent at the front of *E. coli* swarms is thought to be LPS (232).

Swimming *P. aeruginosa* uses a single polar flagellum; to swarm, an additional polar flagellum is expressed, and cells slightly elongate to migrate on 0.5 – 0.7% agar supplemented with peptone or casamino acids. Cells with two flagella are found at the interior of the swarm colony, and elongated swarmer cells (~2-fold increase in size), propelled by an alternative stator, comprise the edge of the colony (233, 234). *P. aeruginosa* swarms in defined groups referred to as tendrils which respond to other groups of cells and migrate accordingly to form a dendrite pattern. This pattern is mediated by the LasIR and RhlIR quorum sensing systems and which produce a secondary metabolite: rhamnolipid, the *P. aeruginosa* surfactant (235, 236).

Mechanosensing for swarming initiation in *P. aeruginosa* is complex. The flagellum, the type-IV pili (T4P), and the cell envelope all play separate roles in sensing surfaces and ultimately influencing the surface-associated lifestyle undertaken by the bacterium. Viscous environments promote swarming behavior through flagellar reversals (189, 237), while mechanosensing mediated by the envelope and T4P leads to increases in cyclic-di-GMP which induces biofilm formation (238, 239). Swarmer cells have increased expression of certain virulence factors, while biofilms allows *P. aeruginosa* to

persist in its niche. Overall, both behaviors contribute to *P. aeruginosa* survival in the environment and during human infections.

Another temperate swarmer belonging to the Gram-negative enteric bacteria is the pigmented, opportunistic pathogen *Serratia marcescens*. This bacterium mimics swarming behavior in *P. mirabilis* more closely than any other organism. *S. marcescens* is a peritrichously flagellated (up to 5 flagella) rod (1 - 2 µm) that undergoes a dramatic transformation into highly flagellated (up to 100 flagella), polyploid, elongated swarmer cells (30 - 50 µm) on 0.75 – 1.0 % agar at 30°C (240). At agar concentrations higher than 1.0 %, cells remain rod-shaped thus viscosity is an important factor for differentiation. Swarming *S. marcescens* forms a terraced pattern on minimal media driven by the migration of swarming cells followed by consolidation into rod-shaped cells, similar to *P. mirabilis* (240-242), but *S. marcescens* does not form terraces on rich media. Swarming is coupled to the production to the lipopeptide surfactant, serrawettin, which is dependent on a Swr, a LuxIR-family quorum sensing system. *S. marcescens* can swarm in the absence of serrawettin if a hydrated agar surface is provided (243).

Swarming in *S. marcescens* is dependent on Swr and the *flhDC* master operon which have different regulons (244, 245). While quorum sensing is not required for swarming in *P. mirabilis*, *flhDC* is essential and *P. mirabilis* experiences a 30-fold increase in *flhDC* expression following surface contact (78, 246). In contrast, *flhDC* expression is similar for *S. marcescens* grown in liquid and swarming cells, and *swr* mutants cannot swarm (245). If *flhDC* is overexpressed in liquid, *S. marcescens* forms swarmer cells whereas *P. mirabilis* does not (247, 248). The Rcs phosphorelay signal transduction system also plays a role in modulating *flhDC* in both bacteria, though its

activity is inhibited by two different surface signals. In *S. marcescens*, enterobacterial common antigen (ECA) modulates Rcs activity (249). In *P. mirabilis*, the signal is transduced by membrane perturbations mediated by O-antigen. ECA has no effect on swarming in *P. mirabilis* (250). Overall, the signals triggering swarmer cell differentiation upon surface contact in these bacteria are a combination of different cues which affect different regulatory networks. With the exception of *V. parahaemolyticus*, none of the aforementioned species are robust swarmers. As such, much remains to be discovered concerning mechanisms driving the robust swarming motility of *P. mirabilis*.

IV. Swarming in *Proteus mirabilis*

Compared to other members of the Gram-negative enteric bacteria, *P. mirabilis* is a robust swarmer. This bacterium can swarm on agar at concentrations up to 3.0 % without hydration being provided exogenously, on different kinds of media, at a variety of temperatures (22°C to 42°C), and under aerobic and anaerobic conditions (18, 251). Follow the transfer of liquid cultures of vegetative cells to agar plates, *P. mirabilis* experiences a non-motile swarming lag phase of ~4 h as the population undergoes the necessary physiological rearrangements required for differentiation. The lag phase is affected by the age of the starting culture and its cell density. Additionally, it can be overcome by transferring swarming cells to a new plate; existing swarmer cells do not experience swarming lag (18).

Following lag phase, a subset of the starting vegetative population undergoes differentiation into swarmer cells. Differentiation transforms vegetative cells (~2 μm in length; 4 - 10 flagella) into highly flagellated (500 - 5000 flagella), elongated (20 - 80 μm), multinucleate but aseptate swarmer cells (16, 17, 252). Following differentiation,

swarmer cells move outward in compact groups, called rafts, in which they are aligned and propelled forward by entwined, rotating flagella (17). The duration of migration is affected by the concentration of agar, temperature, and media composition (16, 18). Active migration is followed by a phenomenon known as consolidation where swarmer cells revert back to the vegetative morphotype. The four stages: (i) lag phase prefacing swarming (ii) differentiation of swarmer cells (iii) active swarming migration, and (iv) consolidation are cyclical and yield terraces or the bull's eye pattern formed by *P. mirabilis* on an agar plate. Each stage is governed by a myriad of intrinsic and external elements which give rise to a bifurcated population of cells transcriptionally and physiologically distinct from one another. Phenomena specific to *P. mirabilis* swarming are discussed below.

i. Swarming Lag

Following inoculation of vegetative cells onto an agar plate, a period of non-motile behavior is observed prior to swarmer cell differentiation. During lag phase, the initial population of cells divides and presumably undergoes physiological events necessary for swarming motility such as the inhibition of cell division, the continued extension of the cell body, and the expression of numerous flagella. Moreover, drastic biochemical rearrangements must occur within the colony to prevent dehydration and allow the colony to overcome surface tension so cells can migrate. The lag phase can be reduced by increasing the density of the starting culture, but a threshold is reached where the phenomenon no longer occurs, indicating nutrient depletion in the lag phase colony may contribute to the initiation of swarming (18, 107, 171). The time spent in lag phase can also be overcome by certain mutants (171, 202, 248, 253), reduced by exogenous

addition of certain molecules (22, 23, 25, 254), and abolished if existing swarmer cells are transferred to a new agar plate (171, 255). Following swarmer cell differentiation at the colony periphery the overall population of cells becomes heterogeneous. Interestingly, the remaining immobile cells that do not differentiate are maintained throughout swarm colony development which has yet to be explained (18, 256).

ii. Differentiation

A. Surface Sensing

P. mirabilis in liquid exists in its vegetative form: short, peritrichously flagellated rod-shaped cells. Mechanosensing following surface contact triggers swarmer cell differentiation. The flagella and LPS are two structures used by *P. mirabilis* to sense surfaces.

Much like *V. parahaemolyticus* and other members of the γ-proteobacteria, the flagella of *P. mirabilis* act as mechanosensors. Flagella freely rotate in liquid. However, by increasing the viscosity of the environment, adding anti-flagellin antibodies, or adding cells to a solid surface, the inhibition of flagellar rotation creates torque on the motor, triggering differentiation (25, 257). Correct flagellar assembly is required, as mutants of the major flagellin subunit *flaA* and the secretion chaperone *flgN* do not differentiate (149, 258). Additionally, mutants of flagellar basal body proteins responsible for torque generation have been shown to constitutively elongate under non-permissive conditions. These include mutants in FliG, a switch complex protein of the rotor; FliM, which forms the MS-ring within the rotor; and FliL, a protein that stabilizes the MotAB stator. All of these proteins are essential for powering the flagellar filament (257, 259). The behavior of these mutants results from a defect in mechanosensing, the consequences of which are

cells that behave as though they are perpetually in contact with surfaces. Overall, the *P. mirabilis* flagellum acts as mechanosensor by sensing and responding to external forces on the flagellar motor.

The O-antigen subunit within the LPS is also important for surface sensing. Mutants in genes involved in LPS and O-antigen biosynthesis can swim but do not swarm due to inefficient cell elongation (258). Mutants in *waaL* encoding O-antigen ligase and *wzz*, which determines O-antigen chain length, do not activate the flagellar gene cascade (250). Overall, cell membrane perturbations mediated by LPS and O-antigen following surface contact are sensed by regulatory networks which affect swarmer cell differentiation. These regulatory networks include the Umo proteins and the Rcs phosphorelay which are discussed below.

Surface contact is sensed by the membrane proteins UmoA-D (upregulator of master operon) which activate expression of the flagellar master operon *flhDC*. UmoA is outer membrane associated, UmoC and UmoD are periplasmic, and UmoB is associated with the inner membrane. Mutants in *umoA-D* have reduced *flhDC* transcript levels, with no *flhDC* transcript being detected in *umoB* mutants. Swarming migration is decreased in *umoA-D* mutants, with *umoB* and *umoD* mutants unable to differentiate. It is thought that UmoD acts upstream of UmoB to control its activity and subsequently *flhDC* expression. Expression of *umoA* and *umoD* are expressed coordinately with *flhDC* on solid surfaces, suggesting positive feedback, and these genes are subject to negative regulation when flagellar assembly is blocked (260). It is currently unknown if expression of *umoA-D* is directly activated by $FlhD_4C_2$. Overall, the Umo proteins independently and differentially activate *flhDC*, with UmoB and UmoD being critical for *flhDC* expression and

differentiation of swarming cells (260). A mechanism for *flhDC* activation by the Umo proteins has been described. It involves the interaction of these proteins with the Rcs phosphorelay, a complex signal transduction system (261).

Bacteria constantly monitor the growth, assembly, and status of their envelopes as they are structural barriers essential for cell viability. Envelope defects are sensed by systems such as the Rcs phosphorelay which, upon activation, alter gene expression accordingly. In addition to inducing the expression of genes essentially for maintaining membrane integrity, the Rcs phosphorelay affects genes involved in biofilm formation, virulence, and motility. Rcs activation ultimately results in the phosphorylated response regulator RcsB which binds to DNA. One target is the *flhDC* operon which is repressed by RcsB (261, 262). RcsB phosphorylation results from phosphotransfer via the relay protein RcsD which was previously phosphorylated by activated RcsC, the histidine kinase located at the inner membrane (263). An additional protein, RcsF, transmits stress signals to RcsC, activating it and subsequently the phosphorelay (264). The inability of LPS or O-antigen mutants to swarm can be explained by increased Rcs activity. In order for swarmer cell differentiation to occur in wild-type cells, the activity of the Rcs phosphorelay must be dampened following surface contact.

Rcs activation correlates with the repression of swarming motility. In order for differentiation to occur, its activity must decrease. Following contact with a solid surface, forces acting on O-antigen create membrane perturbations with dual effects. Surface contact may create a transient increase in the distance between the inner and outer membranes, preventing repression of UmoB by RcsF. Alternatively, it may increase the activity of UmoD which interacts with and increases the activity of UmoB. Activated

UmoB attenuates the activity of the Rcs phosphorelay, possibly by inhibiting RcsC activation or interfering with phosphotransfer, which reduces the amount of phosphorylated RcsB. As a result, de-repression of *flhDC* occurs and cells can differentiate. Supporting this model, the swarming defect of *umoB* and *umoD* mutants can be eliminated by mutating *rcsB.* Additionally, *umoB rcsB* and *umoD rcsB* double mutants swarm at the same rate at the *rscB* single mutant. Lastly, artificial overexpression of *umoB* in an isogenic *rscB* mutant did not affect the hyperswarming phenotype exhibited by *rcsB* mutants (261). Overall, these data suggests UmoD, UmoB, and RcsB act in same pathway.

Perturbations mediated by flagella are thought to act through outer membrane protein UmoA, as *umoA* expression is increased in the constitutive elongated *fliL* mutant (265). Whether UmoA modulates Rcs activity is unknown. There are no homologs of UmoA, and *umoA* mutants can still swarm albeit less efficiently (260). UmoA may interact with RcsF to modulate its activity, as both are located on the cell surface, or UmoA may dampen RcsC activity directly albeit to a lesser extent than UmoB. Overall, mechanosensing by cell surface structures dampens the activity of the Rcs phosphorelay to promote differentiation.

B. Changes in Cell Morphology

In order for vegetative cells to form highly elongated and flagellated swarmer cells, drastic morphological changes involving the inhibition of cell division, the continuous extension of the cell via peptidoglycan remodeling, and the expression and integration of numerous flagella into the cell body must occur. Certain extracellular triggers have also been shown to promote differentiation.

To prevent septation, cell division inhibition must occur, and the Min cell division inhibition system has been shown to be involved in this process (266). The three MinC-E proteins comprise the system, and their pole-to-pole oscillation during cell division promotes cell elongation and prevents septum formation at the cell poles (267, 268). Expression of *minCDE* peaks 2 - 3 h following surface contact, preventing septation and promoting elongation of swarmer cells. Its expression decreases following differentiation, the result being an end to cell division inhibition during consolidation (266). During consolidation, it is upregulated once more in order to promote a second period of swarming (65). Supporting this, a *minC* mutant produces insufficiently elongated swarmer cells, less detectable flagella, and exhibits a defect in swarming migration (266). FtsA and FtsZ, responsible for septum formation, are implicated in this process, but creating mutations in the corresponding genes is lethal (269).

Extensive peptidoglycan and cell surface remodeling occurs during differentiation. *P. mirabilis* peptidoglycan (PG) is a combination of unmodified and *O*-acetylated peptidoglycan. *O*-acetylation has clinical and biological significance as it promotes bacterial resistance to lysozyme, intracellular PG autolysins, and prevents insertion of structures such as type III secretion systems or flagella into the cell body (270). Reports of *O*-acetylation in *P. mirabilis* range from 20 to 53 % depending on the strain (271). *O*-acetylation would not be ideal for swarming as it would inhibit consolidation and hyperflagellation. As such, extensive PG remodeling occurs during differentiation. The PG of vegetative cells and cells in lag phase has similar levels of *O*-acetylation from 50 to 55%. In contrast, the PG of consolidated cells is approximately 30% *O*-acetylated (272). Thus, the level of *O*-acetylation of *P. mirabilis* PG decreases by

approximately half upon differentiation. Moreover, the activity of the AmiC autolysin specific for *O*-acetylated PG exhibits higher activity in lag phase colonies. Its activity is diminished following differentiation only to increase once more in consolidation phase. MltF, an enzyme involved in the crosslinking of unmodified PG is highly expressed by differentiating cells (272). Overall, AmiC removes *O*-acetylated PG from *P. mirabilis* while MltF incorporates unmodified PG, permitting the incorporation of numerous flagella through the cell wall as it elongates during differentiation.

Other notable morphological changes during differentiation include a change in membrane fluidity, polyploidy, and the appearance of flagellar filaments. Differentiated swarmer cells have approximately 20 nucleoids, and as cells elongate the number of nucleoids increase (273). This coincides with the upregulation *minCDE* and genes involved in chromosomal partitioning during consolidation, where elongation would occur once more (65). Differentiated swarmer cells have altered membrane fluidity compared to lag phase cells, with longer fatty acid chains comprising the membrane lipids of swarmer cells (274). This could increase the velocity of cells in slime, aid cell-to-cell contact within rafts, or have a regulatory function by changing the activity of membrane proteins. Lastly, an increase in flagellar filament detection occurs 2 h following surface contact. The number of flagellar filaments peaks after 4 h, coinciding with the end of differentiation and the first round of swarming motility (273).

C. Influence by Molecules

A cell density threshold is required for the differentiation of swarmer cells to occur. However, quorum sensing has not been shown to be involved (246) so cell-to-cell communication may occur through alternative pathways.

Putrescine triggers differentiation once an appropriate cell density is reached. This molecule is continuously produced and accumulates during growth of *P. mirabilis* via a biosynthetic pathway comprised of SpeA and SpeB. SpeA converts L-arginine to agmatine; in turn SpeB converts agmatine to putrescine. Putrescine is a component of the LPS core subunit in some strains of *P. mirabilis* (275). Mutants in *speA* or *speB* experience a severe delay in the onset of differentiation. This defect can be restored by the addition of exogenous putrescine (22) or ornithine (23), which is converted to putrescine via an alternative SpeF-mediated pathway. Uptake of putrescine by the PlaP putrescine importer is also necessary for normal swarming, and *plaP speA* double mutants cannot swarm in the presence of extracellular putrescine (254). Moreover, *speB* is upregulated in consolidation compared to swarming cells (65). Perhaps once cell density reaches a threshold during consolidation phase and enough putrescine has accumulated, it acts as a signal for cells to begin another period of migration. Overall, these studies suggest putrescine acts as an important cell-to-cell signaling molecule essential for differentiation.

Exogenous histidine promotes swarming under non-permissive conditions which is dependent on intact putrescine and glutamine biosynthetic pathways. A mutant in the histidine biosynthetic pathway *hisG* experienced a delay in the onset of differentiation and subsequently swarming. The swarming defect of this mutant could be rescued by the addition of extracellular histidine (23). The role of histidine in swarming motility may be connected to the Leucine-responsive regulatory protein (Lrp), a bacterial nucleoid associated protein (NAP) and global transcriptional regulator. Lrp responds to the abundance of amino acids in the environment (27), including histidine, and Lrp is

required for swarmer cell differentiation (24). Thus, histidine trigger differentiation through its interaction with Lrp.

iii. Migration

Following differentiation, the highly flagellated and elongated swarmer cells that emerge from the colony periphery must align to form multicellular bodies known as rafts. *P. mirabilis* swarm rafts are characterized by elongated cells similar in length arranged in parallel. The flagellar filaments are localized between neighboring cells and interwoven to form organized helical connections (17). Once rafts form, migration across surfaces occurs, with adjacent rafts migrating independently and outward from the initial population of cells. Swarming migration is successive; as more swarm cells emerge from the lag phase colony, migration occurs on top of the previous congregation of swarming cells. Overall, each terrace is created by the initial migration of multiple rafts, is multi-layered, and rough at the edge due to the sequential migration of swarmer cells. A myriad of factors contribute to efficient migration, discussed below.

A. Rafting

In order to form a raft, cells must be of similar size and their flagella must interweave so the population can move forward. Mutants devoid of flagella, insufficiently flagellated, or possess flagella that do not form helical connections swarm less efficiently. If cells are not of similar length, insufficiently elongated, or disorganized, migration will be insufficient (17). One well studied mutant, *ccmA* (curved cell morphology), was found to differentiate and efficiently elongate but was unable to swarm (276). The inability of this mutant to swarm is due to its curved shape which prevents proper alignment of swarmer cells and subsequent rafting. Expression of *ccmA* is high during differentiation

and migration (65, 276). Its function is currently unknown, but CcmA is hypothesized to aid in the linearity of elongated swarming cells perhaps by mediating peptidoglycan assembly (276).

Another mutant which is capable of differentiation and hyperflagellation but has reduced swarming velocity is in *cmfA* (colony migration factor) encoding a capsular polysaccharide (CPS) (277). The structure of the CPS in one strain of *P. mirabilis* was determined to be an acidic tetrasaccharide repeat (278). CPS may play an important role in cellular interactions within a raft or aid in population migration through the slime *P. mirabilis* secretes for surface migration.

B. Overcoming Surfaces Conditions

In order to swarm, bacteria must be able to overcome surface tension and dehydration on the agar surface. *P. mirabilis* produces an acidic extracellular polysaccharide matrix (ECM), or slime, prior to differentiation (279). The ECM constitutes 20% of the mass in a lag phase colony. The composition of the ECM has partially been characterized. Exopolysaccharides (EPS) comprise 30% of the ECM and are predominated by two types of sugars: one of low molecular weight (~1 kDa) which contains rhamnose and glucose, and one of high molecular weight (~300 kDa) which consists of rhamnose, galactosamine, glucose, and mannose. Lipids comprise 15% of the ECM with a novel phenoglycolipid (PGL) being present. Additionally, an osmoprotectant, glycinebetaine, was found a constituent of the ECM (280). The presence of PGL may aid in the vasoelasticity of swarm colonies while the presence of small sugars and glycinebetaine in the ECM suggests *P. mirabilis* faces drastic osmotic conditions and prepare accordingly to support swarming (273). Moreover, the ratio of the

two EPS sugars changes drastically following differentiation. Slime is not only used for colony expansion, but its constituents may be acting as signals for differentiation (273, 280, 281). Overall, the *P. mirabilis* ECM is a mixture of complex molecules, the proportions of which are altered at each phase of swarming to promote migration and hydration of the population.

C. Amino Acids

The amino acid arginine promotes swarming under non-permissive conditions, particularly those of low pH, but arginine biosynthesis mutants swarm normally indicating the intracellular production of this amino acid does not contribute to swarming under normal laboratory conditions (23). However, the mechanism by which extracellular arginine and SpeA (arginine decarboxylase) contribute to swarming was later elucidated. The SpeA-mediated conversion of arginine to agmatine consumes intracellular protons, conserving the proton gradient and proton motive force during swarming in low pH environments (282).

Glutamine is required for swarming, and *P. mirabilis* encodes genes specific for glutamine synthesis and transport (23, 25). On media non-permissive for swarming motility, only glutamine was able to initiate differentiation (25). Mutants in *glnA* encoding glutamine synthetase are completely unable to swarm on rich media, and only L-glutamine restored swarming in this mutant. However, no data exists suggesting exogenous glutamine triggers differentiation, though cells migrate for slightly longer distances prior to consolidation (23). Glutamine may promote migration but it does not seem to trigger differentiation.

Overall, amino acids have been shown to trigger differentiation and promote migration. They may be sensed by *P. mirabilis* to determine if surroundings are ideal for the initiation of swarming or if entry into consolidation phase is warranted.

D. Dienes Lines

P. mirabilis has been observed to form boundaries called "Dienes lines" resulting from intersecting swarm fronts of different strains (283). Dienes lines do not form between swarm fronts of the same strain which suggests *P. mirabilis* possesses a mechanism to distinguish self from non-self. This mechanism was recently found to be mediated by the *ids* (identification of self) and *idr* loci (284, 285). Ids and Idr function independently of each other but share the same type-VI secretion system (*tss*) (285). Type-VI secretion systems in Gram-negative bacteria can deliver toxins into neighboring bacteria causing cell death (286). Conflicting results exist as to whether the boundaries formed by different *P. mirabilis* strains result from killing (287) or strain-to-strain avoidance mediated by a diffusible signal (284, 288). The *ids* and *idr* discrimination loci are only expressed in swarming bacteria as if they anticipate combat with other bacteria as they move through their environment. The study of these systems will shed light on multicellular interactions and niche dominance.

iv. Consolidation

Little is known concerning consolidation phase. No conclusive signals have been identified that trigger the end of consolidation. Swarming migration is intensive, and consolidation was once thought to be a resting phase. However, it was shown that during consolidation, cells are metabolically active and a marked increase in the expression of

genes involved in nutrient uptake, peptidoglycan remodeling, metabolism, and respiration occurs (65, 192).

Recently, it was proposed that the interplay between water and the *P. mirabilis* ECM plays a role in the initiation of consolidation (280, 281). The ECM is subject to reorganization, which *P. mirabilis* readily does, to increase the influx of water into the swarming population to prevent osmotic shock. However, as successive cycles of swarming cells form a multi-layered swarm terrace, water incorporation and ECM elasticity eventually becomes increasingly impossible. Thus, the inability of the cells to swarm triggers consolidation (280, 281). This theory may have merit but it does not explain the transcriptional distinction between swarming cells and cells in consolidation phase. Thus, some genetic element must contribute to the initiation of consolidation, and mutants have been identified which could explicate the phenomenon of consolidation and the maintenance of vegetative cells at the swarm colony interior.

V. Regulation of *flhDC* in *P. mirabilis*

An essential factor for swarmer cell differentiation in *P. mirabilis* is the flagellar master operon, *flhDC*. Expression of *flhDC* is activated following surface contact, peaks prior to differentiation, and sharply decreases following the initiation of swarming (147, 248). Slight changes in *flhDC* expression affect the manner in which *P. mirabilis* swarms. Overexpression of *flhDC* results in hyperswarming, an increase in flagellar number, and enables cells to overcome swarming lag phase (289), while *flhDC* mutants do not swarm (257, 289). As swarming is an intensive process, *flhDC* is tightly regulated. Direct transcriptional repressors identified in *P. mirabilis* include the Rcs phosphorelay (248, 253), the MR/P fimbrial operon regulator MrpJ (88, 290), and the Uca fimbrial operon

regulator UcaJ (87). Transcriptional activators include the leucine-responsive regulatory protein Lrp (24). Class II flagellar assembly protein FlhA (148) and the Umo proteins activate *flhDC* expression (260), and their expression coincides with *flhDC* expression on solid surfaces. The Umo proteins mediate their effect on *flhDC* expression by modulation of the Rcs phosphorelay (261), while it is currently unknown how FlhA mediates its positive effect on *flhDC*. Additionally, the Lon protease is the primary mediator of $FlhD_4C_2$ cleavage thus contributing to its short half-life, and it also reduces *flhDC* expression (291, 292).

To understand the mechanism regulating the spatial control of differentiation and consolidation, the characterization of mutants that dampen these stages during swarming is required. A mutant of *rcsB* encoding the response regulator of the Rcs phosphorelay, and mutants with transposon-mediated cassette insertions upstream of *flhDC* have unique swarming phenotypes. These mutants spend less time in both swarming lag and consolidation phase to different degrees.

Consistent with previous studies of mutants in histidine kinase *rcsC* and relay protein *rcsD*, the *rcsB* mutant also hyperswarms. It initiates swarming approximately 1 h prior to wild-type, spends one half of the amount of time in consolidation phase, and migrates 2.5-fold the distance of wild-type (248, 266). This is likely due to increased *flhDC* expression, which is especially apparent between 3 and 5 h following surface contact in this mutant. Curiously, the *rcsB* mutant also differentiates to form swarmer cells in liquid culture, a non-permissive condition, and even strains overexpressing *flhDC* do not exhibit this behavior (248). Due to this phenotype, the Rcs phosphorelay is likely regulating other genes important for swarmer cell differentiation.

The intergenic region upstream of *flhDC* is curiously large (3.3 kb) and AT-rich (75% A/T). Expression of the upstream region in *trans* in wild-type cells enhances swarming, likely due to the titration of *flhDC* repressors. Additionally, two mutants previously characterized by our laboratory exhibit a dramatic phenotype when placed on agar surfaces. These mutant phenotypes are conferred by mini-Tn*5lacZ* insertions either 325 bp (Mutant SS-P) or 740 bp (mutant SS-N) upstream of the *flhDC* transcriptional start site in a region with no obvious open reading frames. Both mutants migrate 5-fold farther than wild-type after 12 h of incubation on LB agar, they do not undergo consolidation, and both express constitutively high levels of *flhDC*. While the *rcsB* mutant elongates in liquid culture, these mutants remain in their short-rod shaped form, indicating these sites are essential for modulating *flhDC* activity following surface contact (248).

The following chapters will describe the newly discovered contributions of the Rcs phosphorelay and $FlhD_4C_2$ to the multifaceted lifestyles of *P. mirabilis* with a focus on swarming motility. The contribution of an Rcs-activated locus, *minCDE,* to swarmer cell elongation is covered at length in Chapter 2. Additionally, the RcsB regulon identified using RNA-Sequencing is discussed in Chapter 3 along with experimental confirmation that RcsB is important for other behaviors in *P. mirabilis*. Lastly, Chapter 4 covers a novel mechanism of *flhDC* regulation and the contribution of the *flhDC* intergenic region to modulation of *flhDC* expression following surface contact. Lastly, what remains to be understood concerning these regulators and how this work has contributed to our knowledge of swarming behavior in *P. mirabilis* is discussed.

References.

1. **O'Hara CM, Brenner FW, Miller JM.** 2000. Classification, identification, and clinical significance of Proteus, Providencia, and Morganella. Clin Microbiol Rev **13:**534-546.
2. **Peerbooms PG, Verweij AM, Oe PL, MacLaren DM.** 1986. Urinary pathogenicity of Proteus mirabilis strains isolated from faeces or urine. Antonie Van Leeuwenhoek **52:**53-62.
3. **Hauser G.** 1885. Über Fäulnisbakterien und deren Beziehungen zur Septicämie. Ein Beitrag zur Morphologie der Spaltpilze. Vogel, Leipzig**:**34.
4. **Jacobsen SM, Stickler DJ, Mobley HL, Shirtliff ME.** 2008. Complicated catheter-associated urinary tract infections due to Escherichia coli and Proteus mirabilis. Clin Microbiol Rev **21:**26-59.
5. **Matthews SJ, Lancaster JW.** 2011. Urinary tract infections in the elderly population. Am J Geriatr Pharmacother **9:**286-309.
6. **Papazafiropoulou A, Daniil I, Sotiropoulos A, Balampani E, Kokolaki A, Bousboulas S, Konstantopoulou S, Skliros E, Petropoulou D, Pappas S.** 2010. Prevalence of asymptomatic bacteriuria in type 2 diabetic subjects with and without microalbuminuria. BMC Res Notes **3:**169.
7. **Mathur S, Sabbuba NA, Suller MT, Stickler DJ, Feneley RC.** 2005. Genotyping of urinary and fecal Proteus mirabilis isolates from individuals with long-term urinary catheters. Eur J Clin Microbiol Infect Dis **24:**643-644.
8. **Lubart E, Segal R, Haimov E, Dan M, Baumoehl Y, Leibovitz A.** 2011. Bacteremia in a multilevel geriatric hospital. J Am Med Dir Assoc **12:**204-207.

9. **Adams-Sapper S, Sergeevna-Selezneva J, Tartof S, Raphael E, Diep BA, Perdreau-Remington F, Riley LW.** 2012. Globally dispersed mobile drug-resistance genes in gram-negative bacterial isolates from patients with bloodstream infections in a US urban general hospital. J Med Microbiol **61:**968-974.

10. **Sader HS, Flamm RK, Jones RN.** 2014. Frequency of occurrence and antimicrobial susceptibility of Gram-negative bacteremia isolates in patients with urinary tract infection: results from United States and European hospitals (2009-2011). J Chemother **26:**133-138.

11. **Nicolle LE.** 2005. Catheter-related urinary tract infection. Drugs Aging **22:**627-639.

12. **Morris NS, Stickler DJ, McLean RJ.** 1999. The development of bacterial biofilms on indwelling urethral catheters. World J Urol **17:**345-350.

13. **Dedeic-Ljubovic A, Hukic M.** 2009. Catheter-related urinary tract infection in patients suffering from spinal cord injuries. Bosn J Basic Med Sci **9:**2-9.

14. **Kunin CM.** 1989. Blockage of urinary catheters: role of microorganisms and constituents of the urine on formation of encrustations. J Clin Epidemiol **42:**835-842.

15. **Ronald A.** 2003. The etiology of urinary tract infection: traditional and emerging pathogens. Dis Mon **49:**71-82.

16. **Williams FD, Schwarzhoff RH.** 1978. Nature of the swarming phenomenon in Proteus. Annu Rev Microbiol **32:**101-122.

17. **Jones BV, Young R, Mahenthiralingam E, Stickler DJ.** 2004. Ultrastructure of Proteus mirabilis swarmer cell rafts and role of swarming in catheter-associated urinary tract infection. Infect Immun **72:**3941-3950.

18. **Rauprich O, Matsushita M, Weijer CJ, Siegert F, Esipov SE, Shapiro JA.** 1996. Periodic phenomena in Proteus mirabilis swarm colony development. Journal of Bacteriology **178:**6525-6538.

19. **Sabbuba N, Hughes G, Stickler DJ.** 2002. The migration of Proteus mirabilis and other urinary tract pathogens over Foley catheters. BJU Int **89:**55-60.

20. **Stickler D, Hughes G.** 1999. Ability of Proteus mirabilis to swarm over urethral catheters. Eur J Clin Microbiol Infect Dis **18:**206-208.

21. **Williams GJ, Stickler DJ.** 2008. Some observations on the migration of Proteus mirabilis and other urinary tract pathogens over foley catheters. Infect Control Hosp Epidemiol **29:**443-445.

22. **Sturgill G, Rather PN.** 2004. Evidence that putrescine acts as an extracellular signal required for swarming in Proteus mirabilis. Mol Microbiol **51:**437-446.

23. **Armbruster CE, Hodges SA, Mobley HL.** 2013. Initiation of swarming motility by Proteus mirabilis occurs in response to specific cues present in urine and requires excess L-glutamine. J Bacteriol **195:**1305-1319.

24. **Hay NA, Tipper DJ, Gygi D, Hughes C.** 1997. A nonswarming mutant of Proteus mirabilis lacks the Lrp global transcriptional regulator. J Bacteriol **179:**4741-4746.

25. **Allison C, Lai HC, Gygi D, Hughes C.** 1993. Cell differentiation of Proteus mirabilis is initiated by glutamine, a specific chemoattractant for swarming cells. Mol Microbiol **8:**53-60.

26. **Tan IK, Gajra B.** 2006. Plasma and urine amino acid profiles in a healthy adult population of Singapore. Ann Acad Med Singapore **35:**468-475.

27. **Hart BR, Blumenthal RM.** 2011. Unexpected coregulator range for the global regulator Lrp of Escherichia coli and Proteus mirabilis. J Bacteriol **193:**1054-1064.

28. **Griffith DP, Musher DM, Itin C.** 1976. Urease. The primary cause of infection-induced urinary stones. Invest Urol **13:**346-350.

29. **Stickler DJ, Lear JC, Morris NS, Macleod SM, Downer A, Cadd DH, Feast WJ.** 2006. Observations on the adherence of Proteus mirabilis onto polymer surfaces. J Appl Microbiol **100:**1028-1033.

30. **Jones BV, Mahenthiralingam E, Sabbuba NA, Stickler DJ.** 2005. Role of swarming in the formation of crystalline Proteus mirabilis biofilms on urinary catheters. J Med Microbiol **54:**807-813.

31. **Stickler DJ.** 2008. Bacterial biofilms in patients with indwelling urinary catheters. Nat Clin Pract Urol **5:**598-608.

32. **Sabbuba NA, Mahenthiralingam E, Stickler DJ.** 2003. Molecular epidemiology of Proteus mirabilis infections of the catheterized urinary tract. J Clin Microbiol **41:**4961-4965.

33. **Morris NS, Stickler DJ.** 1998. Encrustation of indwelling urethral catheters by Proteus mirabilis biofilms growing in human urine. J Hosp Infect **39:**227-234.

34. **Pearson MM, Sebaihia M, Churcher C, Quail MA, Seshasayee AS, Luscombe NM, Abdellah Z, Arrosmith C, Atkin B, Chillingworth T, Hauser H, Jagels K, Moule S, Mungall K, Norbertczak H, Rabbinowitsch E, Walker D, Whithead S, Thomson NR, Rather PN, Parkhill J, Mobley HL.** 2008. Complete genome sequence of uropathogenic Proteus mirabilis, a master of both adherence and motility. J Bacteriol **190:**4027-4037.

35. **Mobley HL, Chippendale GR, Tenney JH, Mayrer AR, Crisp LJ, Penner JL, Warren JW.** 1988. MR/K hemagglutination of Providencia stuartii correlates with adherence to catheters and with persistence in catheter-associated bacteriuria. J Infect Dis **157:**264-271.

36. **Yakubu DE, Old DC, Senior BW.** 1989. The haemagglutinins and fimbriae of Proteus penneri. J Med Microbiol **30:**279-284.

37. **Zunino P, Geymonat L, Allen AG, Legnani-Fajardo C, Maskell DJ.** 2000. Virulence of a Proteus mirabilis ATF isogenic mutant is not impaired in a mouse model of ascending urinary tract infection. FEMS Immunol Med Microbiol **29:**137-143.

38. **Scavone P, Iribarnegaray V, Caetano AL, Schlapp G, Härtel S, Zunino P.** 2016. Fimbriae have distinguishable roles in Proteus mirabilis biofilm formation. Pathogens and Disease doi:10.1093/femspd/ftw033.

39. **Wray SK, Hull SI, Cook RG, Barrish J, Hull RA.** 1986. Identification and characterization of a uroepithelial cell adhesin from a uropathogenic isolate of Proteus mirabilis. Infect Immun **54:**43-49.

40. **Pellegrino R, Scavone P, Umpierrez A, Maskell DJ, Zunino P.** 2013. Proteus mirabilis uroepithelial cell adhesin (UCA) fimbria plays a role in the colonization of the urinary tract. Pathog Dis **67:**104-107.

41. **Lee KK, Harrison BA, Latta R, Altman E.** 2000. The binding of Proteus mirabilis nonagglutinating fimbriae to ganglio-series asialoglycolipids and lactosyl ceramide. Can J Microbiol **46:**961-966.

42. **Ortaldo JR, Sharrow SO, Timonen T, Herberman RB.** 1981. Determination of surface antigens on highly purified human NK cells by flow cytometry with monoclonal antibodies. J Immunol **127:**2401-2409.

43. **Bahrani FK, Cook S, Hull RA, Massad G, Mobley HL.** 1993. Proteus mirabilis fimbriae: N-terminal amino acid sequence of a major fimbrial subunit and nucleotide sequences of the genes from two strains. Infect Immun **61:**884-891.

44. **Johnson DE, Bahrani FK, Lockatell CV, Drachenberg CB, Hebel JR, Belas R, Warren JW, Mobley HL.** 1999. Serum immunoglobulin response and protection from homologous challenge by Proteus mirabilis in a mouse model of ascending urinary tract infection. Infect Immun **67:**6683-6687.

45. **Massad G, Lockatell CV, Johnson DE, Mobley HL.** 1994. Proteus mirabilis fimbriae: construction of an isogenic pmfA mutant and analysis of virulence in a CBA mouse model of ascending urinary tract infection. Infect Immun **62:**536-542.

46. **Zunino P, Sosa V, Allen AG, Preston A, Schlapp G, Maskell DJ.** 2003. Proteus mirabilis fimbriae (PMF) are important for both bladder and kidney colonization in mice. Microbiology **149:**3231-3237.

47. **Zunino P, Geymonat L, Allen AG, Preston A, Sosa V, Maskell DJ.** 2001. New aspects of the role of MR/P fimbriae in Proteus mirabilis urinary tract infection. FEMS Immunol Med Microbiol **31:**113-120.

48. **Bahrani FK, Massad G, Lockatell CV, Johnson DE, Russell RG, Warren JW, Mobley HL.** 1994. Construction of an MR/P fimbrial mutant of Proteus mirabilis: role in virulence in a mouse model of ascending urinary tract infection. Infect Immun **62:**3363-3371.

49. **Li X, Lockatell CV, Johnson DE, Mobley HL.** 2002. Identification of MrpI as the sole recombinase that regulates the phase variation of MR/P fimbria, a bladder colonization factor of uropathogenic Proteus mirabilis. Mol Microbiol **45:**865-874.

50. **Jansen AM, Lockatell V, Johnson DE, Mobley HL.** 2004. Mannose-resistant Proteus-like fimbriae are produced by most Proteus mirabilis strains infecting the urinary tract, dictate the in vivo localization of bacteria, and contribute to biofilm formation. Infect Immun **72:**7294-7305.

51. **Zhao H, Li X, Johnson DE, Blomfield I, Mobley HL.** 1997. In vivo phase variation of MR/P fimbrial gene expression in Proteus mirabilis infecting the urinary tract. Mol Microbiol **23:**1009-1019.

52. **Pearson MM, Yep A, Smith SN, Mobley HL.** 2011. Transcriptome of Proteus mirabilis in the murine urinary tract: virulence and nitrogen assimilation gene expression. Infect Immun **79:**2619-2631.

53. **Andrews SC, Robinson AK, Rodriguez-Quinones F.** 2003. Bacterial iron homeostasis. FEMS Microbiol Rev **27:**215-237.

54. **Hood MI, Skaar EP.** 2012. Nutritional immunity: transition metals at the pathogen-host interface. Nat Rev Microbiol **10:**525-537.

55. **Massad G, Zhao H, Mobley HL.** 1995. Proteus mirabilis amino acid deaminase: cloning, nucleotide sequence, and characterization of aad. J Bacteriol **177:**5878-5883.

56. **Himpsl SD, Pearson MM, Arewang CJ, Nusca TD, Sherman DH, Mobley HL.** 2010. Proteobactin and a yersiniabactin-related siderophore mediate iron acquisition in Proteus mirabilis. Mol Microbiol **78:**138-157.

57. **Gaisser S, Hughes C.** 1997. A locus coding for putative non-ribosomal peptide/polyketide synthase functions is mutated in a swarming-defective Proteus mirabilis strain. Mol Gen Genet **253:**415-427.

58. **Flannery EL, Mody L, Mobley HL.** 2009. Identification of a modular pathogenicity island that is widespread among urease-producing uropathogens and shares features with a diverse group of mobile elements. Infect Immun **77:**4887-4894.

59. **Burall LS, Harro JM, Li X, Lockatell CV, Himpsl SD, Hebel JR, Johnson DE, Mobley HLT.** 2004. Proteus mirabilis Genes That Contribute to Pathogenesis of Urinary Tract Infection: Identification of 25 Signature-Tagged Mutants Attenuated at Least 100-Fold. Infection and Immunity **72:**2922-2938.

60. **Piccini CD, Barbe FM, Legnani-Fajardo CL.** 1998. Identification of iron-regulated outer membrane proteins in uropathogenic Proteus mirabilis and its relationship with heme uptake. FEMS Microbiol Lett **166:**243-248.

61. **Nielubowicz GR, Smith SN, Mobley HL.** 2008. Outer membrane antigens of the uropathogen Proteus mirabilis recognized by the humoral response during experimental murine urinary tract infection. Infect Immun **76:**4222-4231.

62. **Wang S, Fleming RT, Westbrook EM, Matsumura P, McKay DB.** 2006. Structure of the Escherichia coli FlhDC Complex, a Prokaryotic Heteromeric Regulator of Transcription. Journal of Molecular Biology **355:**798-808.

63. **Nielubowicz GR, Smith SN, Mobley HL.** 2010. Zinc uptake contributes to motility and provides a competitive advantage to Proteus mirabilis during experimental urinary tract infection. Infect Immun **78:**2823-2833.

64. **Fraser GM, Claret L, Furness R, Gupta S, Hughes C.** 2002. Swarming-coupled expression of the Proteus mirabilis hpmBA haemolysin operon. Microbiology **148:**2191-2201.

65. **Pearson MM, Rasko DA, Smith SN, Mobley HL.** 2010. Transcriptome of swarming Proteus mirabilis. Infect Immun **78:**2834-2845.

66. **Mobley HL, Chippendale GR, Swihart KG, Welch RA.** 1991. Cytotoxicity of the HpmA hemolysin and urease of Proteus mirabilis and Proteus vulgaris against cultured human renal proximal tubular epithelial cells. Infect Immun **59:**2036-2042.

67. **Chippendale GR, Warren JW, Trifillis AL, Mobley HL.** 1994. Internalization of Proteus mirabilis by human renal epithelial cells. Infect Immun **62:**3115-3121.

68. **Coker C, Poore CA, Li X, Mobley HL.** 2000. Pathogenesis of Proteus mirabilis urinary tract infection. Microbes Infect **2:**1497-1505.

69. **Swihart KG, Welch RA.** 1990. Cytotoxic activity of the Proteus hemolysin HpmA. Infect Immun **58:**1861-1869.

70. **Alamuri P, Eaton KA, Himpsl SD, Smith SN, Mobley HL.** 2009. Vaccination with proteus toxic agglutinin, a hemolysin-independent cytotoxin in vivo, protects against Proteus mirabilis urinary tract infection. Infect Immun **77:**632-641.

71. **Mobley HL, Belas R, Lockatell V, Chippendale G, Trifillis AL, Johnson DE, Warren JW.** 1996. Construction of a flagellum-negative mutant of Proteus mirabilis: effect on internalization by human renal epithelial cells and virulence in a mouse model of ascending urinary tract infection. Infect Immun **64:**5332-5340.

72. **Alamuri P, Mobley HL.** 2008. A novel autotransporter of uropathogenic Proteus mirabilis is both a cytotoxin and an agglutinin. Mol Microbiol **68:**997-1017.

73. **Wassif C, Cheek D, Belas R.** 1995. Molecular analysis of a metalloprotease from Proteus mirabilis. J Bacteriol **177:**5790-5798.

74. **Senior BW, Loomes LM, Kerr MA.** 1991. The production and activity in vivo of Proteus mirabilis IgA protease in infections of the urinary tract. J Med Microbiol **35:**203-207.

75. **Belas R, Manos J, Suvanasuthi R.** 2004. Proteus mirabilis ZapA metalloprotease degrades a broad spectrum of substrates, including antimicrobial peptides. Infect Immun **72:**5159-5167.

76. **Walker KE, Moghaddame-Jafari S, Lockatell CV, Johnson D, Belas R.** 1999. ZapA, the IgA-degrading metalloprotease of Proteus mirabilis, is a virulence factor expressed specifically in swarmer cells. Mol Microbiol **32:**825-836.

77. **Phan V, Belas R, Gilmore BF, Ceri H.** 2008. ZapA, a virulence factor in a rat model of Proteus mirabilis-induced acute and chronic prostatitis. Infect Immun **76:**4859-4864.

78. **Allison C, Coleman N, Jones PL, Hughes C.** 1992. Ability of Proteus mirabilis to invade human urothelial cells is coupled to motility and swarming differentiation. Infect Immun **60:**4740-4746.

79. **Allison C, Lai HC, Hughes C.** 1992. Co-ordinate expression of virulence genes during swarm-cell differentiation and population migration of Proteus mirabilis. Mol Microbiol **6:**1583-1591.

80. **Liaw SJ, Lai HC, Ho SW, Luh KT, Wang WB.** 2001. Characterisation of p-nitrophenylglycerol-resistant Proteus mirabilis super-swarming mutants. J Med Microbiol **50:**1039-1048.

81. **Mathoera RB, Kok DJ, Verduin CM, Nijman RJ.** 2002. Pathological and therapeutic significance of cellular invasion by Proteus mirabilis in an enterocystoplasty infection stone model. Infect Immun **70:**7022-7032.

82. **Li X, Zhao H, Lockatell CV, Drachenberg CB, Johnson DE, Mobley HL.** 2002. Visualization of Proteus mirabilis within the matrix of urease-induced bladder stones during experimental urinary tract infection. Infect Immun **70:**389-394.

83. **Yu Y, Sikorski P, Bowman-Gholston C, Cacciabeve N, Nelson KE, Pieper R.** 2015. Diagnosing inflammation and infection in the urinary system via proteomics. J Transl Med **13**.

84. **Schaffer JN, Norsworthy AN, Sun TT, Pearson MM.** 2016. Proteus mirabilis fimbriae-and urease-dependent clusters assemble in an extracellular niche to initiate bladder stone formation. Proc Natl Acad Sci U S A **113:**4494-4499.

85. **Johnson DE, Bahrani FK, Lockatell CV, Drachenberg CB, Hebel JR, Belas R, Warren JW, Mobley HLT.** 1999. Serum Immunoglobulin Response and Protection from Homologous Challenge by Proteus mirabilis in a Mouse Model of Ascending Urinary Tract Infection. Infection and Immunity **67:**6683-6687.

86. **Bahrani FK, Mobley HL.** 1994. Proteus mirabilis MR/P fimbrial operon: genetic organization, nucleotide sequence, and conditions for expression. J Bacteriol **176:**3412-3419.

87. **Lane MC, Li X, Pearson MM, Simms AN, Mobley HL.** 2009. Oxygen-limiting conditions enrich for fimbriate cells of uropathogenic Proteus mirabilis and Escherichia coli. J Bacteriol **191:**1382-1392.

88. **Pearson MM, Mobley HL.** 2008. Repression of motility during fimbrial expression: identification of 14 mrpJ gene paralogues in Proteus mirabilis. Mol Microbiol **69:**548-558.

89. **Bode NJ, Debnath I, Kuan L, Schulfer A, Ty M, Pearson MM.** 2015. Transcriptional analysis of the MrpJ network: modulation of diverse virulence-associated genes and direct regulation of mrp fimbrial and flhDC flagellar operons in Proteus mirabilis. Infect Immun **83:**2542-2556.

90. **Belas R.** 1994. Expression of multiple flagellin-encoding genes of Proteus mirabilis. J Bacteriol **176:**7169-7181.

91. **Murphy CA, Belas R.** 1999. Genomic rearrangements in the flagellin genes of Proteus mirabilis. Mol Microbiol **31:**679-690.

92. **Manos J, Belas R.** 2004. Transcription of Proteus mirabilis flaAB. Microbiology **150:**2857-2863.

93. **Manos J, Artimovich E, Belas R.** 2004. Enhanced motility of a Proteus mirabilis strain expressing hybrid FlaAB flagella. Microbiology **150:**1291-1299.

94. **O'Toole G, Kaplan HB, Kolter R.** 2000. Biofilm Formation as Microbial Development. Annual Review of Microbiology **54:**49-79.

95. **P. Stoodley, K. Sauer, D. G. Davies, Costerton JW.** 2002. Biofilms as Complex Differentiated Communities. Annual Review of Microbiology **56:**187-209.

96. **Henrichsen J.** 1972. Bacterial surface translocation: a survey and a classification. Bacteriol Rev **36:**478-503.

97. **Mattick JS.** 2002. Type IV Pili and Twitching Motility. Annual Review of Microbiology **56:**289-314.

98. **Merz AJ, So M, Sheetz MP.** 2000. Pilus retraction powers bacterial twitching motility. Nature **407:**98-102.

99. **Skerker JM, Berg HC.** 2001. Direct observation of extension and retraction of type IV pili. Proceedings of the National Academy of Sciences **98:**6901-6904.

100. **McBride MJ.** 2001. Bacterial Gliding Motility: Multiple Mechanisms for Cell Movement over Surfaces. Annual Review of Microbiology **55:**49-75.

101. **Wolgemuth C, Hoiczyk E, Kaiser D, Oster G.** 2002. How myxobacteria glide. Curr Biol **12:**369-377.

102. **Mignot T, Shaevitz JW, Hartzell PL, Zusman DR.** 2007. Evidence that focal adhesion complexes power bacterial gliding motility. Science **315:**853-856.

103. **Halfen LN, Castenholz RW.** 1970. Gliding in a blue-green alga: a possible mechanism. Nature **225:**1163-1165.

104. **Recht J, Kolter R.** 2001. Glycopeptidolipid Acetylation Affects Sliding Motility and Biofilm Formation in Mycobacterium smegmatis. Journal of Bacteriology **183:**5718-5724.

105. **Brown II, Häse CC.** 2001. Flagellum-Independent Surface Migration ofVibrio cholerae and Escherichia coli. Journal of Bacteriology **183:**3784-3790.

106. **Berg HC, Anderson RA.** 1973. Bacteria swim by rotating their flagellar filaments. Nature **245:**380-382.

107. **Kearns DB.** 2010. A field guide to bacterial swarming motility. Nat Rev Micro **8:**634-644.

108. **Belas R, Simon M, Silverman M.** 1986. Regulation of lateral flagella gene transcription in Vibrio parahaemolyticus. Journal of Bacteriology **167:**210-218.

109. **Patrick JE, Kearns DB.** 2012. Swarming motility and the control of master regulators of flagellar biosynthesis. Molecular Microbiology **83:**14-23.

110. **Aldridge P, Hughes KT.** 2002. Regulation of flagellar assembly. Curr Opin Microbiol **5:**160-165.

111. **Szurmant H, Ordal GW.** 2004. Diversity in chemotaxis mechanisms among the bacteria and archaea. Microbiol Mol Biol Rev **68:**301-319.

112. **Kubori T, Matsushima Y, Nakamura D, Uralil J, Lara-Tejero M, Sukhan A, Galan JE, Aizawa SI.** 1998. Supramolecular structure of the Salmonella typhimurium type III protein secretion system. Science **280:**602-605.

113. **Samatey FA, Matsunami H, Imada K, Nagashima S, Shaikh TR, Thomas DR, Chen JZ, Derosier DJ, Kitao A, Namba K.** 2004. Structure of the bacterial flagellar hook and implication for the molecular universal joint mechanism. Nature **431:**1062-1068.

114. **Yonekura K, Maki-Yonekura S, Namba K.** 2003. Complete atomic model of the bacterial flagellar filament by electron cryomicroscopy. Nature **424:**643-650.

115. **Abrusci P, Vergara-Irigaray M, Johnson S, Beeby MD, Hendrixson DR, Roversi P, Friede ME, Deane JE, Jensen GJ, Tang CM, Lea SM.** 2013. Architecture of the major component of the type III secretion system export apparatus. Nat Struct Mol Biol **20:**99-104.

116. **Minamino T.** 2014. Protein export through the bacterial flagellar type III export pathway. Biochimica et Biophysica Acta (BBA) - Molecular Cell Research **1843:**1642-1648.

117. **Fraser GM, Bennett JCQ, Hughes C.** 1999. Substrate-specific binding of hook-associated proteins by FlgN and FliT, putative chaperones for flagellum assembly. Molecular Microbiology **32:**569-580.

118. **Bange G, Kummerer N, Engel C, Bozkurt G, Wild K, Sinning I.** 2010. FlhA provides the adaptor for coordinated delivery of late flagella building blocks to the type III secretion system. Proc Natl Acad Sci U S A **107:**11295-11300.

119. **Aldridge PD, Karlinsey JE, Aldridge C, Birchall C, Thompson D, Yagasaki J, Hughes KT.** 2006. The flagellar-specific transcription factor, sigma28, is the Type III secretion chaperone for the flagellar-specific anti-sigma28 factor FlgM. Genes Dev **20:**2315-2326.

120. **Minamino T, Namba K.** 2008. Distinct roles of the FliI ATPase and proton motive force in bacterial flagellar protein export. Nature **451:**485-488.

121. **Shibata S, Takahashi N, Chevance FF, Karlinsey JE, Hughes KT, Aizawa S.** 2007. FliK regulates flagellar hook length as an internal ruler. Mol Microbiol **64:**1404-1415.

122. **Kutsukake K.** 1997. Hook-length control of the export-switching machinery involves a double-locked gate in Salmonella typhimurium flagellar morphogenesis. J Bacteriol **179:**1268-1273.

123. **Auvray F, Thomas J, Fraser GM, Hughes C.** 2001. Flagellin polymerisation control by a cytosolic export chaperone. J Mol Biol **308:**221-229.

124. **Kubori T, Yamaguchi S, Aizawa S.** 1997. Assembly of the switch complex onto the MS ring complex of Salmonella typhimurium does not require any other flagellar proteins. J Bacteriol **179:**813-817.

125. **Park SY, Lowder B, Bilwes AM, Blair DF, Crane BR.** 2006. Structure of FliM provides insight into assembly of the switch complex in the bacterial flagella motor. Proc Natl Acad Sci U S A **103:**11886-11891.

126. **Blair DF, Berg HC.** 1990. The MotA protein of E. coli is a proton-conducting component of the flagellar motor. Cell **60:**439-449.

127. **Kojima S, Blair DF.** 2004. The bacterial flagellar motor: structure and function of a complex molecular machine. Int Rev Cytol **233:**93-134.

128. **Zhou J, Lloyd SA, Blair DF.** 1998. Electrostatic interactions between rotor and stator in the bacterial flagellar motor. Proc Natl Acad Sci U S A **95:**6436-6441.

129. **Kojima S, Blair DF.** 2001. Conformational change in the stator of the bacterial flagellar motor. Biochemistry **40:**13041-13050.

130. **Minamino T, Imada K, Kinoshita M, Nakamura S, Morimoto YV, Namba K.** 2011. Structural insight into the rotational switching mechanism of the bacterial flagellar motor. PLoS Biol **9:**e1000616.

131. **Adler J, Templeton B.** 1967. The effect of environmental conditions on the motility of Escherichia coli. J Gen Microbiol **46:**175-184.

132. **Walker SL, Sojka M, Dibb-Fuller M, Woodward MJ.** 1999. Effect of pH, temperature and surface contact on the elaboration of fimbriae and flagella by Salmonella serotype Enteritidis. J Med Microbiol **48:**253-261.

133. **Soutourina OA, Krin E, Laurent-Winter C, Hommais F, Danchin A, Bertin PN.** 2002. Regulation of bacterial motility in response to low pH in Escherichia coli: the role of H-NS protein. Microbiology **148:**1543-1551.

134. **Koirala S, Mears P, Sim M, Golding I, Chemla YR, Aldridge PD, Rao CV.** 2014. A Nutrient-Tunable Bistable Switch Controls Motility in Salmonella enterica Serovar Typhimurium. mBio **5**.

135. **Soutourina O, Kolb A, Krin E, Laurent-Winter C, Rimsky S, Danchin A, Bertin P.** 1999. Multiple control of flagellum biosynthesis in Escherichia coli: role of H-NS protein and the cyclic AMP-catabolite activator protein complex in transcription of the flhDC master operon. J Bacteriol **181:**7500-7508.

136. **Chevance FFV, Hughes KT.** 2008. Coordinating assembly of a bacterial macromolecular machine. Nat Rev Micro **6:**455-465.

137. **Ohnishi K, Kutsukake K, Suzuki H, Iino T.** 1990. Gene fliA encodes an alternative sigma factor specific for flagellar operons in Salmonella typhimurium. Mol Gen Genet **221:**139-147.

138. **Karlinsey JE, Tanaka S, Bettenworth V, Yamaguchi S, Boos W, Aizawa SI, Hughes KT.** 2000. Completion of the hook-basal body complex of the Salmonella typhimurium flagellum is coupled to FlgM secretion and fliC transcription. Mol Microbiol **37:**1220-1231.

139. **Hughes KT, Gillen KL, Semon MJ, Karlinsey JE.** 1993. Sensing structural intermediates in bacterial flagellar assembly by export of a negative regulator. Science **262:**1277-1280.

140. **Barembruch C, Hengge R.** 2007. Cellular levels and activity of the flagellar sigma factor FliA of Escherichia coli are controlled by FlgM-modulated proteolysis. Mol Microbiol **65:**76-89.

141. **Aldridge P, Karlinsey J, Hughes KT.** 2003. The type III secretion chaperone FlgN regulates flagellar assembly via a negative feedback loop containing its chaperone substrates FlgK and FlgL. Mol Microbiol **49:**1333-1345.

142. **Sato Y, Takaya A, Mouslim C, Hughes KT, Yamamoto T.** 2014. FliT selectively enhances proteolysis of FlhC subunit in FlhD4C2 complex by an ATP-dependent protease, ClpXP. J Biol Chem **289:**33001-33011.

143. **Yamamoto S, Kutsukake K.** 2006. FliT acts as an anti-FlhD2C2 factor in the transcriptional control of the flagellar regulon in Salmonella enterica serovar typhimurium. J Bacteriol **188:**6703-6708.

144. **Imada K, Minamino T, Kinoshita M, Furukawa Y, Namba K.** 2010. Structural insight into the regulatory mechanisms of interactions of the flagellar type III chaperone FliT with its binding partners. Proc Natl Acad Sci U S A **107:**8812-8817.

145. **Wada T, Tanabe Y, Kutsukake K.** 2011. FliZ Acts as a Repressor of the ydiV Gene, Which Encodes an Anti-FlhD(4)C(2) Factor of the Flagellar Regulon in Salmonella enterica Serovar Typhimurium. J Bacteriol **193:**5191-5198.

146. **Lanois A, Jubelin G, Givaudan A.** 2008. FliZ, a flagellar regulator, is at the crossroads between motility, haemolysin expression and virulence in the insect pathogenic bacterium Xenorhabdus. Molecular Microbiology **68:**516-533.

147. **Pesavento C, Hengge R.** 2012. The global repressor FliZ antagonizes gene expression by σ(S)-containing RNA polymerase due to overlapping DNA binding specificity. Nucleic Acids Res **40:**4783-4793.

148. **Gygi D, Bailey MJ, Allison C, Hughes C.** 1995. Requirement for FlhA in flagella assembly and swarm-cell differentiation by Proteus mirabilis. Mol Microbiol **15:**761-769.

149. **Furness RB, Fraser GM, Hay NA, Hughes C.** 1997. Negative feedback from a Proteus class II flagellum export defect to the flhDC master operon controlling cell division and flagellum assembly. Journal of Bacteriology **179:**5585-5588.

150. **Gygi D, Fraser G, Dufour A, Hughes C.** 1997. A motile but non-swarming mutant of Proteus mirabilis lacks FlgN, a facilitator of flagella filament assembly. Molecular Microbiology **25:**597-604.

151. **Hegde M, Englert DL, Schrock S, Cohn WB, Vogt C, Wood TK, Manson MD, Jayaraman A.** 2011. Chemotaxis to the quorum-sensing signal AI-2 requires the Tsr chemoreceptor and the periplasmic LsrB AI-2-binding protein. J Bacteriol **193:**768-773.

152. **Neumann S, Hansen CH, Wingreen NS, Sourjik V.** 2010. Differences in signalling by directly and indirectly binding ligands in bacterial chemotaxis. Embo j **29:**3484-3495.

153. **Tso WW, Adler J.** 1974. Negative chemotaxis in Escherichia coli. J Bacteriol **118:**560-576.

154. **Zhao K, Liu M, Burgess RR.** 2007. Adaptation in bacterial flagellar and motility systems: from regulon members to 'foraging'-like behavior in E. coli. Nucleic Acids Research **35:**4441-4452.

155. **Armitage JP.** 1999. Bacterial Tactic Responses, p 229-289. *In* Poole RK (ed), Advances in Microbial Physiology, vol Volume 41. Academic Press.

156. **Hess JF, Oosawa K, Kaplan N, Simon MI.** 1988. Phosphorylation of three proteins in the signaling pathway of bacterial chemotaxis. Cell **53:**79-87.

157. **Hess JF, Bourret RB, Simon MI.** 1988. Histidine phosphorylation and phosphoryl group transfer in bacterial chemotaxis. Nature **336:**139-143.

158. **McEvoy MM, Bren A, Eisenbach M, Dahlquist FW.** 1999. Identification of the binding interfaces on CheY for two of its targets, the phosphatase CheZ and the flagellar switch protein fliM. J Mol Biol **289:**1423-1433.

159. **Anand GS, Goudreau PN, Stock AM.** 1998. Activation of methylesterase CheB: evidence of a dual role for the regulatory domain. Biochemistry **37:**14038-14047.

160. **Garrity LF, Ordal GW.** 1997. Activation of the CheA kinase by asparagine in Bacillus subtilis chemotaxis. Microbiology **143:**2945-2951.

161. **Kristich CJ, Ordal GW.** 2002. Bacillus subtilis CheD Is a Chemoreceptor Modification Enzyme Required for Chemotaxis. Journal of Biological Chemistry **277:**25356-25362.

162. **Szurmant H, Bunn MW, Cannistraro VJ, Ordal GW.** 2003. Bacillus subtilis Hydrolyzes CheY-P at the Location of Its Action, the Flagellar Switch. Journal of Biological Chemistry **278:**48611-48616.

163. **Szurmant H, Muff TJ, Ordal GW.** 2004. Bacillus subtilis CheC and FliY are members of a novel class of CheY-P-hydrolyzing proteins in the chemotactic signal transduction cascade. J Biol Chem **279:**21787-21792.

164. **Porter SL, Armitage JP.** 2002. Phosphotransfer in Rhodobacter sphaeroides Chemotaxis. Journal of Molecular Biology **324:**35-45.

165. **Sourjik V, Schmitt R.** 1998. Phosphotransfer between CheA, CheY1, and CheY2 in the Chemotaxis Signal Transduction Chain of Rhizobium meliloti. Biochemistry **37:**2327-2335.

166. **Masduki A, Nakamura J, Ohga T, Umezaki R, Kato J, Ohtake H.** 1995. Isolation and characterization of chemotaxis mutants and genes of Pseudomonas aeruginosa. Journal of Bacteriology **177:**948-952.

167. **Kearns DB, Robinson J, Shimkets LJ.** 2001. Pseudomonas aeruginosa Exhibits Directed Twitching Motility Up Phosphatidylethanolamine Gradients. Journal of Bacteriology **183:**763-767.

168. **Harshey RM.** 2003. Bacterial Motility on a Surface: Many Ways to a Common Goal. Annual Review of Microbiology **57:**249-273.

169. **Darnton NC, Turner L, Rojevsky S, Berg HC.** 2010. Dynamics of bacterial swarming. Biophys J **98:**2082-2090.

170. **Mariconda S, Wang Q, Harshey RM.** 2006. A mechanical role for the chemotaxis system in swarming motility. Mol Microbiol **60:**1590-1602.

171. **Burkart M, Toguchi A, Harshey RM.** 1998. The chemotaxis system, but not chemotaxis, is essential for swarming motility in Escherichia coli. Proc Natl Acad Sci U S A **95:**2568-2573.

172. **Kearns DB, Losick R.** 2003. Swarming motility in undomesticated Bacillus subtilis. Mol Microbiol **49:**581-590.

173. **Darzins A.** 1994. Characterization of a Pseudomonas aeruginosa gene cluster involved in pilus biosynthesis and twitching motility: sequence similarity to the chemotaxis proteins of enterics and the gliding bacterium Myxococcus xanthus. Mol Microbiol **11:**137-153.

174. **Brown MT, Steel BC, Silvestrin C, Wilkinson DA, Delalez NJ, Lumb CN, Obara B, Armitage JP, Berry RM.** 2012. Flagellar hook flexibility is essential for bundle formation in swimming Escherichia coli cells. J Bacteriol **194:**3495-3501.

175. **Macnab RM, Ornston MK.** 1977. Normal-to-curly flagellar transitions and their role in bacterial tumbling. Stabilization of an alternative quaternary structure by mechanical force. J Mol Biol **112:**1-30.

176. **Macnab RM, Han DP.** 1983. Asynchronous switching of flagellar motors on a single bacterial cell. Cell **32:**109-117.

177. **Magariyama Y, Sugiyama S, Kudo S.** 2001. Bacterial swimming speed and rotation rate of bundled flagella. FEMS Microbiology Letters **199:**125-129.

178. **Berg HC, Purcell EM.** 1977. Physics of chemoreception. Biophysical Journal **20:**193-219.

179. **Porter SL, Wadhams GH, Armitage JP.** 2008. Rhodobacter sphaeroides: complexity in chemotactic signalling. Trends Microbiol **16:**251-260.

180. **Szymanski CM, King M, Haardt M, Armstrong GD.** 1995. Campylobacter jejuni motility and invasion of Caco-2 cells. Infection and Immunity **63:**4295-4300.

181. **Martinez LE, Hardcastle JM, Wang J, Pincus Z, Tsang J, Hoover TR, Bansil R, Salama NR.** 2016. Helicobacter pylori strains vary cell shape and flagellum number to maintain robust motility in viscous environments. Mol Microbiol **99:**88-110.

182. **Merritt PM, Danhorn T, Fuqua C.** 2007. Motility and Chemotaxis in Agrobacterium tumefaciens Surface Attachment and Biofilm Formation. Journal of Bacteriology **189:**8005-8014.

183. **Croxen MA, Sisson G, Melano R, Hoffman PS.** 2006. The Helicobacter pylori Chemotaxis Receptor TlpB (HP0103) Is Required for pH Taxis and for Colonization of the Gastric Mucosa. Journal of Bacteriology **188:**2656-2665.

184. **McCarter LL.** 2001. Polar flagellar motility of the Vibrionaceae. Microbiol Mol Biol Rev **65:**445-462, table of contents.

185. **Merino S, Shaw JG, Tomás JM.** 2006. Bacterial lateral flagella: an inducible flagella system. FEMS Microbiology Letters **263:**127-135.

186. **Kirov SM.** 2003. Bacteria that express lateral flagella enable dissection of the multifunctional roles of flagella in pathogenesis. FEMS Microbiology Letters **224:**151-159.

187. **Persat A, Nadell Carey D, Kim Minyoung K, Ingremeau F, Siryaporn A, Drescher K, Wingreen Ned S, Bassler Bonnie L, Gitai Z, Stone Howard A.** 2015. The Mechanical World of Bacteria. Cell **161:**988-997.

188. **Chaban B, Hughes HV, Beeby M.** 2015. The flagellum in bacterial pathogens: For motility and a whole lot more. Seminars in Cell & Developmental Biology **46:**91-103.

189. **Kim W, Killam T, Sood V, Surette MG.** 2003. Swarm-Cell Differentiation in Salmonella enterica Serovar Typhimurium Results in Elevated Resistance to Multiple Antibiotics. Journal of Bacteriology **185:**3111-3117.

190. **Butler MT, Wang Q, Harshey RM.** 2010. Cell density and mobility protect swarming bacteria against antibiotics. Proceedings of the National Academy of Sciences **107:**3776-3781.

191. **Overhage J, Bains M, Brazas MD, Hancock REW.** 2008. Swarming of Pseudomonas aeruginosa Is a Complex Adaptation Leading to Increased Production of Virulence Factors and Antibiotic Resistance. Journal of Bacteriology **190:**2671-2679.

192. **Kim W, Surette MG.** 2004. Metabolic differentiation in actively swarming Salmonella. Molecular Microbiology **54:**702-714.

193. **Turnbull AL, Surette MG.** 2010. Cysteine biosynthesis, oxidative stress and antibiotic resistance in Salmonella typhimurium. Research in Microbiology **161:**643-650.

194. **Armitage JP.** 1981. Changes in metabolic activity of Proteus mirabilis during swarming. J Gen Microbiol **125:**445-450.

195. **Givskov M, Eberl L, Christiansen G, Benedik MJ, Molin S.** 1995. Induction of phospholipase- and flagellar synthesis in Serratia liquefaciens is controlled by expression of the flagellar master operon flhD. Mol Microbiol **15:**445-454.

196. **Young GM, Schmiel DH, Miller VL.** 1999. A new pathway for the secretion of virulence factors by bacteria: the flagellar export apparatus functions as a protein-secretion system. Proc Natl Acad Sci U S A **96:**6456-6461.

197. **Kearns DB, Losick R.** 2003. Swarming motility in undomesticated Bacillus subtilis. Molecular Microbiology **49:**581-590.

198. **Macfarlane S, Hopkins MJ, Macfarlane GT.** 2001. Toxin Synthesis and Mucin Breakdown Are Related to Swarming Phenomenon in Clostridium septicum. Infection and Immunity **69:**1120-1126.

199. **Ghelardi E, Celandroni F, Salvetti S, Beecher DJ, Gominet M, Lereclus D, Wong ACL, Senesi S.** 2002. Requirement of flhA for Swarming Differentiation, Flagellin Export, and Secretion of Virulence-Associated Proteins in Bacillus thuringiensis. Journal of Bacteriology **184:**6424-6433.

200. **Arima K, Kakinuma A, Tamura G.** 1968. Surfactin, a crystalline peptidelipid surfactant produced by Bacillus subtilis: isolation, characterization and its inhibition of fibrin clot formation. Biochem Biophys Res Commun **31:**488-494.

201. **Kearns DB, Chu F, Rudner R, Losick R.** 2004. Genes governing swarming in Bacillus subtilis and evidence for a phase variation mechanism controlling surface motility. Molecular Microbiology **52:**357-369.

202. **Nakano MM, Corbell N, Besson J, Zuber P.** 1992. Isolation and characterization of sfp: a gene that functions in the production of the lipopeptide biosurfactant, surfactin, in Bacillus subtilis. Mol Gen Genet **232:**313-321.

203. **Mendelson NH, Bourque A, Wilkening K, Anderson KR, Watkins JC.** 1999. Organized cell swimming motions in Bacillus subtilis colonies: patterns of short-lived whirls and jets. J Bacteriol **181:**600-609.

204. **Kearns DB, Losick R.** 2005. Cell population heterogeneity during growth of Bacillus subtilis. Genes & Development **19:**3083-3094.

205. **Henderson IR, Owen P, Nataro JP.** 1999. Molecular switches — the ON and OFF of bacterial phase variation. Molecular Microbiology **33:**919-932.

206. **Guttenplan SB, Shaw S, Kearns DB.** 2013. The cell biology of peritrichous flagella in Bacillus subtilis. Mol Microbiol **87:**211-229.

207. **Calvio C, Celandroni F, Ghelardi E, Amati G, Salvetti S, Ceciliani F, Galizzi A, Senesi S.** 2005. Swarming Differentiation and Swimming Motility in Bacillus subtilis Are Controlled by swrA, a Newly Identified Dicistronic Operon. Journal of Bacteriology **187:**5356-5366.

208. **Verhamme DT, Kiley TB, Stanley-Wall NR.** 2007. DegU co-ordinates multicellular behavior exhibited by Bacillus subtilis. Mol Microbiol **65**.

209. **Tokunaga T, Rashid MH, Kuroda A, Sekiguchi J.** 1994. Effect of degS-degU mutations on the expression of sigD, encoding an alternative sigma factor, and autolysin operon of Bacillus subtilis. J Bacteriol **176**.

210. **Calvio C, Osera C, Amati G, Galizzi A.** 2008. Autoregulation of swrAA and Motility in Bacillus subtilis. Journal of Bacteriology **190:**5720-5728.

211. **Mordini S, Osera C, Marini S, Scavone F, Bellazzi R, Galizzi A, Calvio C.** 2013. The Role of SwrA, DegU and P_{D3} in <italic>fla/che</italic> Expression in <italic>B. subtilis</italic>. PLoS ONE **8:**e85065.

212. **Mukherjee S, Bree AC, Liu J, Patrick JE, Chien P, Kearns DB.** 2015. Adaptor-mediated Lon proteolysis restricts Bacillus subtilis hyperflagellation. Proceedings of the National Academy of Sciences **112:**250-255.

213. **Kobayashi K.** 2007. Gradual activation of the response regulator DegU controls serial expression of genes for flagellum formation and biofilm formation in Bacillus subtilis. Mol Microbiol **66**.

214. **Ragatz L, Jiang ZY, Bauer CE, Gest H.** 1995. Macroscopic phototactic behavior of the purple photosynthetic bacterium Rhodospirillum centenum. Arch Microbiol **163:**1-6.

215. **Jiang ZY, Rushing BG, Bai Y, Gest H, Bauer CE.** 1998. Isolation of Rhodospirillum centenum Mutants Defective in Phototactic Colony Motility by Transposon Mutagenesis. J Bacteriol **180:**1248-1255.

216. **Zhulin IB, Armitage JP.** 1993. Motility, chemokinesis, and methylation-independent chemotaxis in Azospirillum brasilense. J Bacteriol **175:**952-958.

217. **Moens S, Michiels K, Vanderleyden J.** 1995. Glycosylation of the flagellin of the polar flagellum of Azospirillum brasilense, a Gram-negative nitrogen-fixing bacterium. Microbiology **141:**2651-2657.

218. **Moens S, Schloter M, Vanderleyden J.** 1996. Expression of the structural gene, laf1, encoding the flagellin of the lateral flagella in Azospirillum brasilense Sp7. Journal of Bacteriology **178:**5017-5019.

219. **Hall PG, Krieg NR.** 1983. Swarming of Azospirillum brasilense on solid media. Canadian Journal of Microbiology **29:**1592-1594.

220. **Vial L, Lavire C, Mavingui P, Blaha D, Haurat J, Moënne-Loccoz Y, Bally R, Wisniewski-Dyé F.** 2006. Phase Variation and Genomic Architecture Changes in Azospirillum. J Bacteriol **188:**5364-5373.

221. **Alexandre G, Rohr R, Bally R.** 1999. A Phase Variant of Azospirillum lipoferum Lacks a Polar Flagellum and Constitutively Expresses Mechanosensing Lateral Flagella. Appl Environ Microbiol **65:**4701-4704.

222. **Ames P, Bergman K.** 1981. Competitive Advantage Provided by Bacterial Motility in the Formation of Nodules by Rhizobium meliloti. Journal of Bacteriology **148:**728-729.

223. **Braeken K, Daniels R, Vos K, Fauvart M, Bachaspatimayum D, Vanderleyden J, Michiels J.** 2008. Genetic determinants of swarming in Rhizobium etli. Microb Ecol **55:**54-64.

224. **Tambalo DD, Yost CK, Hynes MF.** 2010. Characterization of swarming motility in Rhizobium leguminosarum bv. viciae. FEMS Microbiology Letters **307:**165-174.

225. **Daniels R, Reynaert S, Hoekstra H, Verreth C, Janssens J, Braeken K, Fauvart M, Beullens S, Heusdens C, Lambrichts I, De Vos DE, Vanderleyden J, Vermant J, Michiels J.** 2006. Quorum signal molecules as biosurfactants affecting swarming in Rhizobium etli. Proceedings of the National Academy of Sciences **103:**14965-14970.

226. **Harshey RM, Matsuyama T.** 1994. Dimorphic transition in Escherichia coli and Salmonella typhimurium: surface-induced differentiation into hyperflagellate swarmer cells. Proceedings of the National Academy of Sciences **91:**8631-8635.

227. **Partridge JD, Harshey RM.** 2013. More than motility: Salmonella flagella contribute to overriding friction and facilitating colony hydration during swarming. J Bacteriol **195:**919-929.

228. **Wang Q, Frye JG, McClelland M, Harshey RM.** 2004. Gene expression patterns during swarming in Salmonella typhimurium: genes specific to surface growth and putative new motility and pathogenicity genes. Molecular Microbiology **52:**169-187.

229. **Girgis HS, Liu Y, Ryu WS, Tavazoie S.** 2007. A comprehensive genetic characterization of bacterial motility. PLoS Genet **3:**1644-1660.

230. **Chen BG, Turner L, Berg HC.** 2007. The Wetting Agent Required for Swarming in Salmonella enterica Serovar Typhimurium Is Not a Surfactant. Journal of Bacteriology **189:**8750-8753.

231. **Be'er A, Harshey Rasika M.** 2011. Collective Motion of Surfactant-Producing Bacteria Imparts Superdiffusivity to Their Upper Surface. Biophysical Journal **101:**1017-1024.

232. **Wang Q, Suzuki A, Mariconda S, Porwollik S, Harshey RM.** 2005. Sensing wetness: a new role for the bacterial flagellum. The EMBO Journal **24:**2034-2042.

233. **Toguchi A, Siano M, Burkart M, Harshey RM.** 2000. Genetics of Swarming Motility in Salmonella enterica Serovar Typhimurium: Critical Role for Lipopolysaccharide. Journal of Bacteriology **182:**6308-6321.

234. **Ping L, Wu Y, Hosu BG, Tang JX, Berg HC.** 2014. Osmotic pressure in a bacterial swarm. Biophys J **107:**871-878.

235. **Toutain CM, Zegans ME, O'Toole GA.** 2005. Evidence for two flagellar stators and their role in the motility of Pseudomonas aeruginosa. J Bacteriol **187:**771-777.

236. **Kohler T, Curty LK, Barja F, van Delden C, Pechere JC.** 2000. Swarming of Pseudomonas aeruginosa is dependent on cell-to-cell signaling and requires flagella and pili. J Bacteriol **182:**5990-5996.

237. **Deziel E, Lepine F, Milot S, Villemur R.** 2003. rhlA is required for the production of a novel biosurfactant promoting swarming motility in Pseudomonas aeruginosa: 3-(3-hydroxyalkanoyloxy)alkanoic acids (HAAs), the precursors of rhamnolipids. Microbiology **149:**2005-2013.

238. **Latifi A, Foglino M, Tanaka K, Williams P, Lazdunski A.** 1996. A hierarchical quorum-sensing cascade in Pseudomonas aeruginosa links the transcriptional activators LasR and RhIR (VsmR) to expression of the stationary-phase sigma factor RpoS. Molecular Microbiology **21:**1137-1146.

239. **Caiazza NC, Merritt JH, Brothers KM, O'Toole GA.** 2007. Inverse Regulation of Biofilm Formation and Swarming Motility by Pseudomonas aeruginosa PA14. Journal of Bacteriology **189:**3603-3612.

240. **Luo Y, Zhao K, Baker AE, Kuchma SL, Coggan KA, Wolfgang MC, Wong GC, O'Toole GA.** 2015. A hierarchical cascade of second messengers regulates Pseudomonas aeruginosa surface behaviors. MBio **6**.

241. **Persat A, Inclan YF, Engel JN, Stone HA, Gitai Z.** 2015. Type IV pili mechanochemically regulate virulence factors in Pseudomonas aeruginosa. Proc Natl Acad Sci U S A **112:**7563-7568.

242. **Alberti L, Harshey RM.** 1990. Differentiation of Serratia marcescens 274 into swimmer and swarmer cells. J Bacteriol **172:**4322-4328.

243. **O'Rear J, Alberti L, Harshey RM.** 1992. Mutations that impair swarming motility in Serratia marcescens 274 include but are not limited to those affecting chemotaxis or flagellar function. Journal of Bacteriology **174:**6125-6137.

244. **Eberl L, Molin S, Givskov M.** 1999. Surface motility of serratia liquefaciens MG1. J Bacteriol **181:**1703-1712.

245. **Lindum PW, Anthoni U, Christophersen C, Eberl L, Molin S, Givskov M.** 1998. N - Acyl-l-Homoserine Lactone Autoinducers Control Production of an Extracellular Lipopeptide Biosurfactant Required for Swarming Motility of Serratia liquefaciens MG1. Journal of Bacteriology **180:**6384-6388.

246. **Eberl L, Christiansen G, Molin S, Givskov M.** 1996. Differentiation of Serratia liquefaciens into swarm cells is controlled by the expression of the flhD master operon. Journal of Bacteriology **178:**554-559.

247. **Givskov M, Östling J, Eberl L, Lindum PW, Christensen AB, Christiansen G, Molin S, Kjelleberg S.** 1998. Two Separate Regulatory Systems Participate in Control of Swarming Motility of Serratia liquefaciensMG1. Journal of Bacteriology **180:**742-745.

248. **Schneider R, Lockatell CV, Johnson D, Belas R.** 2002. Detection and mutation of a luxS-encoded autoinducer in Proteus mirabilis. Microbiology **148:**773-782.

249. **Tolker-Nielsen T, Christensen AB, Holmstrøm K, Eberl L, Rasmussen TB, Sternberg C, Heydorn A, Molin S, Givskov M.** 2000. Assessment of flhDC mRNA Levels inSerratia liquefaciens Swarm Cells. Journal of Bacteriology **182:**2680-2686.

250. **Clemmer KM, Rather PN.** 2007. Regulation of flhDC expression in Proteus mirabilis. Research in Microbiology **158:**295-302.

251. **Castelli ME, Véscovi EG.** 2011. The Rcs Signal Transduction Pathway Is Triggered by Enterobacterial Common Antigen Structure Alterations in Serratia marcescens. Journal of Bacteriology **193:**63-74.

252. **Morgenstein RM, Clemmer KM, Rather PN.** 2010. Loss of the waaL O-antigen ligase prevents surface activation of the flagellar gene cascade in Proteus mirabilis. J Bacteriol **192:**3213-3221.

253. **Jin T, Murray RG.** 1988. Further studies of swarmer cell differentiation of Proteus mirabilis PM23: a requirement for iron and zinc. Can J Microbiol **34:**588-593.

254. **HOENIGER JFM.** 1965. Development of Flagella by Proteus mirabilis. Microbiology **40:**29-42.

255. **Belas R, Schneider R, Melch M.** 1998. Characterization of Proteus mirabilis precocious swarming mutants: identification of rsbA, encoding a regulator of swarming behavior. J Bacteriol **180:**6126-6139.

256. **Kurihara S, Sakai Y, Suzuki H, Muth A, Phanstiel Ot, Rather PN.** 2013. Putrescine importer PlaP contributes to swarming motility and urothelial cell invasion in Proteus mirabilis. J Biol Chem **288:**15668-15676.

257. **Williams FD, Anderson DM, Hoffman PS, Schwarzhoff RH, Leonard S.** 1976. Evidence against the involvement of chemotaxis in swarming of Proteus mirabilis. J Bacteriol **127:**237-248.

258. **Morrison RB, Scott ANN.** 1966. Swarming of Proteus[mdash]A Solution to an Old Problem? Nature **211:**255-257.

259. **Belas R, Suvanasuthi R.** 2005. The ability of Proteus mirabilis to sense surfaces and regulate virulence gene expression involves FliL, a flagellar basal body protein. J Bacteriol **187:**6789-6803.

260. **Belas R, Goldman M, Ashliman K.** 1995. Genetic analysis of Proteus mirabilis mutants defective in swarmer cell elongation. J Bacteriol **177:**823-828.

261. **Partridge JD, Nieto V, Harshey RM.** 2015. A New Player at the Flagellar Motor: FliL Controls both Motor Output and Bias. mBio **6**.

262. **Dufour A, Furness RB, Hughes C.** 1998. Novel genes that upregulate the Proteus mirabilis flhDC master operon controlling flagellar biogenesis and swarming. Molecular Microbiology **29:**741-751.

263. **Morgenstein RM, Rather PN.** 2012. Role of the Umo proteins and the Rcs phosphorelay in the swarming motility of the wild type and an O-antigen (waaL) mutant of Proteus mirabilis. J Bacteriol **194:**669-676.

264. **Tierrez A, García-del Portillo F.** 2004. The Salmonella Membrane Protein IgaA Modulates the Activity of the RcsC-YojN-RcsB and PhoP-PhoQ Regulons. J Bacteriol **186:**7481-7489.

265. **Takeda S, Fujisawa Y, Matsubara M, Aiba H, Mizuno T.** 2001. A novel feature of the multistep phosphorelay in Escherichia coli: a revised model of the RcsC --> YojN --> RcsB signalling pathway implicated in capsular synthesis and swarming behaviour. Mol Microbiol **40:**440-450.

266. **Castanie-Cornet MP, Cam K, Jacq A.** 2006. RcsF is an outer membrane lipoprotein involved in the RcsCDB phosphorelay signaling pathway in Escherichia coli. J Bacteriol **188:**4264-4270.

267. **Cusick K, Lee YY, Youchak B, Belas R.** 2012. Perturbation of FliL interferes with Proteus mirabilis swarmer cell gene expression and differentiation. J Bacteriol **194:**437-447.

268. **Howery KE, Clemmer KM, Simsek E, Kim M, Rather PN.** 2015. Regulation of the Min Cell Division Inhibition Complex by the Rcs Phosphorelay in Proteus mirabilis. Journal of Bacteriology **197:**2499-2507.

269. **de Boer PA, Crossley RE, Rothfield LI.** 1990. Central role for the Escherichia coli minC gene product in two different cell division-inhibition systems. Proc Natl Acad Sci U S A **87:**1129-1133.

270. **Ward JE, Jr., Lutkenhaus J.** 1985. Overproduction of FtsZ induces minicell formation in E. coli. Cell **42:**941-949.

271. **Howery KE, Clemmer KM, Rather PN.** 2016. The Rcs regulon in Proteus mirabilis: implications for motility, biofilm formation, and virulence. Curr Genet doi:10.1007/s00294-016-0579-1.

272. **Moynihan PJ, Clarke AJ.** 2011. O-Acetylated peptidoglycan: controlling the activity of bacterial autolysins and lytic enzymes of innate immune systems. Int J Biochem Cell Biol **43:**1655-1659.

273. **Clarke AJ.** 1993. Extent of peptidoglycan O acetylation in the tribe Proteeae. Journal of Bacteriology **175:**4550-4553.

274. **Strating H, Vandenende C, Clarke AJ.** 2012. Changes in peptidoglycan structure and metabolism during differentiation of Proteus mirabilis into swarmer cells. Can J Microbiol **58:**1183-1194.

275. **Gué M, Dupont V, Dufour A, Sire O.** 2001. Bacterial Swarming: A Biochemical Time-Resolved FTIR−ATR Study of Proteus mirabilis Swarm-Cell Differentiation. Biochemistry **40:**11938-11945.

276. **Gue M, Dupont V, Dufour A, Sire O.** 2001. Bacterial swarming: a biochemical time-resolved FTIR-ATR study of Proteus mirabilis swarm-cell differentiation. Biochemistry **40:**11938-11945.

277. **Vinogradov E, Perry MB.** 2000. Structural analysis of the core region of lipopolysaccharides from Proteus mirabilis serotypes O6, O48 and O57. Eur J Biochem **267:**2439-2446.

278. **Hay NA, Tipper DJ, Gygi D, Hughes C.** 1999. A novel membrane protein influencing cell shape and multicellular swarming of Proteus mirabilis. J Bacteriol **181:**2008-2016.

279. **Gygi D, Rahman MM, Lai HC, Carlson R, Guard-Petter J, Hughes C.** 1995. A cell-surface polysaccharide that facilitates rapid population migration by differentiated swarm cells of Proteus mirabilis. Mol Microbiol **17:**1167-1175.

280. **Rahman MM, Guard-Petter J, Asokan K, Hughes C, Carlson RW.** 1999. The structure of the colony migration factor from pathogenic Proteus mirabilis. A capsular polysaccharide that facilitates swarming. J Biol Chem **274:**22993-22998.

281. **Stahl SJ, Stewart KR, Williams FD.** 1983. Extracellular slime associated with Proteus mirabilis during swarming. Journal of Bacteriology **154:**930-937.

282. **Lahaye E, Aubry T, Kervarec N, Douzenel P, Sire O.** 2007. Does Water Activity Rule P. mirabilis Periodic Swarming? I. Biochemical and Functional Properties of the Extracellular Matrix. Biomacromolecules **8:**1218-1227.

283. **Lahaye E, Qin Y, Jamme F, Aubry T, Sire O.** 2014. A multi-scale approach of the mechanisms underlying exopolysaccharide auto-organization in the Proteus mirabilis extracellular matrix. Analyst **139:**4879-4886.

284. **Armbruster CE, Hodges SA, Smith SN, Alteri CJ, Mobley HLT.** 2014. Arginine promotes Proteus mirabilis motility and fitness by contributing to conservation of the proton gradient and proton motive force. MicrobiologyOpen **3:**630-641.

285. **Dienes L.** 1946. Reproductive processes in Proteus cultures. J Bacteriol **51:**585.

286. **Gibbs KA, Urbanowski ML, Greenberg EP.** 2008. Genetic determinants of self identity and social recognition in bacteria. Science **321:**256-259.

287. **Wenren LM, Sullivan NL, Cardarelli L, Septer AN, Gibbs KA.** 2013. Two independent pathways for self-recognition in Proteus mirabilis are linked by type VI-dependent export. MBio **4**.

288. **Costa TRD, Felisberto-Rodrigues C, Meir A, Prevost MS, Redzej A, Trokter M, Waksman G.** 2015. Secretion systems in Gram-negative bacteria: structural and mechanistic insights. Nat Rev Micro **13:**343-359.

289. **Alteri CJ, Himpsl SD, Pickens SR, Lindner JR, Zora JS, Miller JE, Arno PD, Straight SW, Mobley HLT.** 2013. Multicellular Bacteria Deploy the Type VI Secretion System to Preemptively Strike Neighboring Cells. PLoS Pathog **9:**e1003608.

290. **Cardarelli L, Saak C, Gibbs KA.** 2015. Two Proteins Form a Heteromeric Bacterial Self-Recognition Complex in Which Variable Subdomains Determine Allele-Restricted Binding. MBio **6:**e00251.

291. **Furness RB, Fraser GM, Hay NA, Hughes C.** 1997. Negative feedback from a Proteus class II flagellum export defect to the flhDC master operon controlling cell division and flagellum assembly. J Bacteriol **179:**5585-5588.

292. **Li X, Rasko DA, Lockatell CV, Johnson DE, Mobley HLT.** 2001. Repression of bacterial motility by a novel fimbrial gene product. The EMBO Journal **20:**4854-4862.

293. **Claret L, Hughes C.** 2000. Rapid Turnover of FlhD and FlhC, the Flagellar Regulon Transcriptional Activator Proteins, duringProteus Swarming. Journal of Bacteriology **182:**833-836.

294. **Clemmer KM, Rather PN.** 2008. The Lon protease regulates swarming motility and virulence gene expression in Proteus mirabilis. Journal of Medical Microbiology **57:**931-937.

Chapter 2: Regulation of the Min Cell Division Inhibition Complex by the Rcs Phosphorelay in *Proteus mirabilis*

Kristen E. Howery[1], Katy M. Clemmer[2], Emrah Şimşek[3], Minsu Kim[3], and Philip N. Rather[1, 2]

[1]Department of Microbiology and Immunology, Emory University, Atlanta, Georgia

[2]Research Service, Atlanta VA Medical Center, Decatur, Georgia

[3]Department of Physics, Emory University, Atlanta, Georgia

Published in:
Journal of Bacteriology, 2015
Vol. 197, No. 5
p. 2499-2507

This manuscript was written by K.E.H and edited by P.N.R.

All experiments were performed by K.E.H. with the exception of Fig. 6C.

Abstract.

A key regulator of swarming in *Proteus mirabilis* is the Rcs phosphorelay, which represses *flhDC* encoding the master flagellar regulator $FlhD_4C_2$. Mutants in *rcsB*, the response regulator in the Rcs phosphorelay, hyperswarm on solid agar and differentiate into swarmer cells in liquid, demonstrating this system also influences the expression of genes central to differentiation. To gain a further understanding of RcsB regulated genes involved in swarmer cell differentiation, RNA-Seq was used to examine the RcsB regulon. Among the 133 genes identified, *minC* and *minD,* encoding cell division inhibitors were identified as RcsB activated genes. A third gene, *minE*, was shown to be part of an operon with *minCD.* To examine *minCDE* regulation, the *min* promoter was identified by 5'-RACE and both transcriptional *lacZ* fusions and qRT-PCR were used to confirm that the *minCDE* operon was RcsB activated. Purified RcsB was capable of directly binding the *minC* promoter region. To determine the role of RcsB mediated activation of *minCDE* in swarmer cell differentiation, a polar *minC* mutation was constructed. This mutant formed minicells during growth in liquid, produced shortened swarmer cells during differentiation and exhibited decreased swarming motility.

Importance.

This work describes the regulation and role of the MinCDE cell division system in *P. mirabilis* swarming and swarmer cell elongation. Previous to this study, the mechanisms that inhibit cell division and allow for swarmer cell elongation were unknown. In addition, this work outlines for the first time the RcsB regulon in *P. mirabilis.* Taken together, the data presented in this study begins to address how *P. mirabilis* elongates upon contact with a solid surface.

Introduction.

Proteus mirabilis, a Gram-negative member of the family *Enterobacteriaceae*, is a bacterium well-known for its ability to swarm. Swarming is a specialized form of motility displayed by multicellular groups of flagellated bacteria across a solid or semi-solid surface. In liquid culture, *P. mirabilis* exists as a peritrichously flagellated, rod-shaped cell. However, after coming into contact with a solid surface, the cells undergo differentiation into elongated, highly flagellated, multinucleate swarmer cells. Swarmer cells are 20 to 50-fold longer than vegetative cells and express thousands of flagella (1). Together, these swarmer cells form multicellular rafts, which they utilize to move across a solid surface (2). After a period of migration, the swarmer cells undergo consolidation (or de-differentiation) and revert back to vegetative rods. The repeated interchange from differentiation to consolidation is responsible for the characteristic bull's eye pattern that *P. mirabilis* forms on an agar plate (3, 4). Reviews on *P. mirabilis* swarming provide additional details on this process (5, 6).

The switch from a rod shaped cell to a swarmer cell is a complex process involving several global regulatory factors. The regulator of colonic acid capsule synthesis (Rcs) phosphorelay is one of these important regulators. The Rcs phosphorelay consists of a sensor kinase (RcsC), a response regulator (RcsB), and a phosphotransferase (RcsD), which mediates the transfer of the phosphate from RcsC to RcsB (7, 8). An additional protein, RcsF, is an outer-membrane lipoprotein that increases the levels of RcsC phosphorylation by some unknown mechanism (9). Once the system is activated, it results in phosphorylated RcsB, which represses *flhDC* (10). *flhDC* encodes the master regulator for flagellar synthesis, $FlhD_4C_2$, which controls genes central to flagellin

production (11). The levels of *flhDC* increase in swarming cells (10, 12), and *flhDC* mutants do not swarm (10, 11). Factors that influence *flhDC* expression, such as activated RcsB, can have dramatic effects on the ability of *P. mirabilis* to swarm. When the Rcs system is active, for example, the cells exist as vegetative rods due to repression of *flhDC*; however, in *rcs* mutants, *P. mirabilis* cells hyperswarm due, in part, to increased *flhDC* expression (10, 13, 14). Another interesting phenotype of *rcs* mutants in *P. mirabilis* is the ability of cells to differentiate into swarmer cells in liquid; this phenomenon does not occur in wild-type cells or in cells overexpressing *flhDC* (10, 13, 14), suggesting that other genes within the Rcs regulon are involved in swarmer cell elongation. External factors that influence the expression of the Rcs phosphorelay and $FlhD_4C_2$ and subsequently the cycles of differentiation and consolidation are unknown. Cell-to-cell contact (4, 15) and extracellular signaling (16) are among hypothesized factors that could play a role in these genetic and morphological cycles.

In *Escherichia coli* and other members of the *Enterobacteriaceae*, RcsB activates genes involved in cell division (17, 18), cell wall synthesis (17, 18), and virulence (19), while repressing genes involved in motility (10, 20). The rationale for investigating genes regulated by the Rcs phosphorelay in *P. mirabilis* lies in the observation that *rcs* mutants hyperswarm on solid agar and differentiate into swarmer cells in liquid culture. Therefore, it is inferred that the Rcs phosphorelay regulates the expression of genes important for swarmer cell formation, including elongation. One subset of genes activated by RcsB in other bacteria are those involved in cell division (17, 18). However, the role of the cell division machinery in *P. mirabilis* swarmer cell formation has not been investigated.

Cell division in many prokaryotes is dictated by the placement of the FtsZ-mediated Z-ring (21), whose positioning is determined by a group of negative regulators known as the Min system. The Min system is comprised of three proteins, MinC, MinD, and MinE, whose oscillation prevents the formation of the Z-ring at the poles of a rod-shaped cell (22, 23). MinC acts as the effector of this system by preventing FtsZ polymerization (23, 24). MinD binds the cell membrane in an ATP-dependent manner (25), where it recruits MinC and activates it 25- to 50-fold (24). The ATPase activity of MinD, which causes it to disassociate with the cell membrane, is induced by MinE (26). This trait of MinE, along with its ability to suppress the activity of MinCD (27), restricts cell division inhibition to one pole at a time and is responsible for the oscillating nature of the complex. When MinE stimulates disassociation of the complex at one pole, MinD-ADP moves to the opposite pole, where it recruits MinC, and the process begins again. A *min* mutant produces anucleate minicells from the pole of a mother cell, which, as a result of minicell production, is slightly enlarged (28). Though cells elongate during cell division inhibition, the potential role these three proteins play in swarmer cell formation and motility has not yet been investigated.

In this study, we elucidate the regulation and role of the Min system in *P. mirabilis* swarming. We found a *minC::kan*^{R} mutation resulted in aberrant cell division in both vegetative and swarmer cells and decreased swarming motility. Additionally, we identified the transcriptional start site of the *minCDE* operon and demonstrated that the region encompassing this start site is bound by RcsB, the response regulator in the Rcs phosphorelay. Overall, our data demonstrates that the cell division inhibition machinery contributes to swarmer cell formation and identifies an important regulator of the Min

system.

Materials and Methods.

Bacterial growth conditions. Except where indicated, *P. mirabilis* and *E. coli* strains were grown in modified Luria-Bertani (LB) broth (10 g tryptone, 5 g yeast extract, 5 g NaCl per liter) at 37°C with shaking at 250 rpm. All strains were incubated at 37°C. *E. coli* strains were grown on 1.5% LB agar and *P. mirabilis* strains were grown on 3.0% LB agar to prevent swarming. Antibiotic selection for *E. coli* contained the following concentrations: 100 μg/ml ampicillin, 20 μg/ml kanamycin, and 25 μg/ml streptomycin. *P. mirabilis* antibiotic selection used 300 μg/ml ampicillin, 20 μg/ml kanamycin, 35 μg/ml streptomycin, and 15 μg/ml tetracycline. When appropriate, a concentration of 12 μg/ml 5-bromo-4-chloro-indolyl-β-d-galactopyranoside (X-Gal) was used for the selection of blue or white colonies for both *E. coli* and *P. mirabilis*. For induction of protein expression, a concentration of 1 mM isopropyl β-D-1-thiogalactopyranoside (IPTG) was used.

DNA manipulations and transformations. All PCR amplifications were done using Phusion Hot Start II high-fidelity DNA polymerase (Thermo Scientific) and verified by DNA sequencing. All ligations were performed using the *Fast-Link*™ DNA Ligation Kit (Epicentre). For electroporation of plasmids into both *E. coli* and *P. mirabilis*, 30 ml of cells were grown to an OD_{600} of 0.3-0.5 in LB broth. Cells were pelleted by centrifugation at 3,000 x g for 5 min at 4°C before being washed twice with 1 ml of ice cold 10% glycerol and resuspended in 60 μl of ice cold 10% glycerol per electroporation. Electroporations were done in Bio-Rad Gene Pulser 0.2-cm diameter cuvettes with a Bio-Rad MicroPulser electroporator. Cells were plated on the appropriate antibiotics after 1.5 h shaking at 250 rpm at 37°C. For *P. mirabilis* transformations, competent cells were

incubated for 30 min with plasmid DNA on ice prior to electroporation. *P. mirabilis* electroporations were allowed to recover for 3 h.

Construction of strains. For bacterial conjugations, overnight cultures were washed 3X in 1 ml of fresh LB broth. 100 µl of each strain was combined in a 1.5 ml microcentrifuge tube before being added to a pre-dried 1.5% LB agar plate. 200 µl of each strain alone was added to separate plates to serve as controls. After 7 h of incubation at 37°C, cells were resuspended in 4 ml LB broth. The mating mixture and the individual control strains were plated on 3% LB agar containing the appropriate antibiotics and incubated overnight at 37°C.

To construct a *minC* mutant, the *minC* gene was amplified using minC-F and minC-R primers (Table 2) and ligated into pBluescript SK (Stratagene) digested with *Xba*I and *Bam*HI (New England Biolabs). The cloned *minC* gene was then mutagenized using EZ-Tn5^{TM} <Kan-2> TNP Transposome Kit (Epicentre). A *minC*::EZ-Tn5 insertion in the center of the *minC* at a position 387 bp into the 702 bp *minC* ORF was identified by restriction enzyme analysis and confirmed by DNA sequencing. This is hereafter described as *minC::kan*^{R}. This was then subcloned into pKNG101, creating pMinC. pKNG101 is a suicide vector harboring streptomycin resistance, used to select for initial pKNG101 integration, and the *sacB* gene which selects for the loss of the pKNG101 in the presence of 10% sucrose. pMinC was maintained in *E. coli* SM10 λ*pir*. This strain was conjugated with wild-type PM7002, and selection for PM7002 harboring the Campbell-type insertion at the *minC* locus was done on LB plates containing tetracycline (15 µg/ml) and streptomycin (35 µg/ml). An exconjugant was grown in LB only for approximately 10 generations and then plated on LSW agar containing 10% sucrose and

kanamycin to select for clones that had lost pMinC, but contained the *minC* locus harboring the EZ-Tn5 Kan^R insertion. Clones that were Str^S, Kan^R and sucrose resistant were subject to Southern blot analysis to confirm they harbored the *minC::kan*^{R} mutation. One of these strains, PMKH1 (PM7002 *minC::kan*^{R}), was used for future experiments.

To construct PMKH4 (PM7002 *minC::kan*^{R}, *rcsB::str*^{R}), SM10 pKNG101::*rcsB* containing an internal fragment of *rcsB* (10) was conjugated to PMKH1. Exconjugants that were resistant to tetracycline, kanamycin, and streptomycin were confirmed using Southern blot analysis as having a disruption in the *rcsB* gene.

To complement the *minC* mutation, the *minCDE* region was amplified from PM7002 genomic DNA using minCDE-F and minCDE-R (Table 2). The *minCDE* containing fragment was cloned into the *Sma*I site of pBC creating pBCMinCDE. *minCDE* was digested out of pBCMinCDE using *Bam*HI and *Xho*I and cloned into the *Bam*HI/*Sal*I sites of pKNG101, creating pMinCDE (pKNG101 + *minCDE*). pMinCDE was maintained in *E. coli* SM10 λ*pir*, and conjugated to PMKH1. Exconjugants that were resistant to tetracycline, kanamycin, and streptomycin were confirmed using Southern blot analysis, and one of the clones, PMKH5, was used for future experiments.

pMinClacZ was created by PCR amplification of the *minC* upstream region using PminC-F and PminC-R, and ligating it into the *Bam*HI and *Sal*I sites of pQF50, a low-copy number vector harboring a promoterless *lacZ* which can be used to quantify promoter activities (29). pMinClacZ was electroporated into *E. coli* DH5α and clones were selected on LB agar plates containing X-gal and ampicillin. One of these confirmed clones was purified using the Qiagen Plasmid Mini-Kit and 5 µl of this DNA was used to

electroporate PM7002 and PM7002 *rcsB::str*^{R}, creating PMKH6 and PMKH7, respectively.

5'-RACE. 5'-RACE was performed on 1.5 µg of RNA isolated from PM7002 using the 5'-RACE System (Invitrogen) according to version 2.0 of the manufacturer's protocol. First strand cDNA synthesis was performed using GSP1 (Table 2). PCR amplification of the dC-tailed cDNA was done using GSP2 (Table 2) and the provided Abridged Anchor Primer. Nested PCR amplification of the diluted PCR product was done with Phusion Hot Start II high-fidelity DNA polymerase (Thermo Scientific) using the provided AUAP and GSP2. The resulting product was ligated into the *Sma*I site of pBC.SK and transformed into *E. coli* DH5α. The transformation was plated on ampicillin and X-gal, and white colonies that were confirmed to have the 5'-RACE generated product were sequenced to identify the 5'end of the *minC* gene.

Phase contrast microscopy. All images were captured with an Infinity 2-1 CCD Camera (Lumenera) using an Olympus BX51 Microscope. For imaging liquid cultures, cells were grown to mid-log and 1.5 µl was pipetted onto a glass slide (VWR International). A coverslip (VWR International) was placed on top of the culture, and images were taken at 1,000 X magnification using oil-immersion. Swarm fronts were imaged by adding 650 µl of LB agar to CoverWell^{TM} Imaging Chambers (1 X 20mm dia X 2.3mm depth) then adding 4 µl of an overnight culture to the solidified agar. The cells were grown in a humidified environment at 37°C until they began to swarm. A coverslip was placed on top of the imaging chamber containing the swarming cells, and images were taken at 1,000 X magnification using oil-immersion. When applicable, antibiotics and IPTG were added to the media.

β-galactosidase assays. Overnight cultures were standardized to the same optical density before 300 µl of each culture was spread plated onto 1.5% LB agar containing ampicillin and incubated at 37°C for 2 or 4 h. After the appropriate incubation period, cells were harvested from agar plates using 2 ml of ice-cold LB broth and 0.9 ml of the harvested culture was pelleted by centrifugation at 13,000 rpm for 4 min. Pelleted cells were placed on ice for 20 min before lysis using chloroform and 0.1% SDS. β-galactosidase activity was quantified as described by Miller (30).

Electrophoretic mobility shift assays (EMSA). EMSAs were performed on digoxigenin-ddUTP labeled probes created by PCR amplification using Phusion Hot Start II high-fidelity DNA polymerase (Thermo Scientific) and primers containing *Eco*RI recognition sites at the end (Table 2). Amplified DNA was digested with *Eco*RI for 3 h at 37°C, cleaned up using a PCR purification kit (Qiagen) and boiled for 10 min. After boiling, the digested DNA was placed immediately on ice, and 250 ng was incubated with 1µl Dig-11-dUTP (Roche), 1 mM dATP (Roche), 4 µl Buffer B (6 mM Tris-HCl, 6 mM $MgCl_2$, 50mM NaCl, pH 7.5) and 1 µl Klenow enzyme (Roche). The labeling reaction incubated at 37°C for 1 h followed by 10 min incubation at 65°C to heat-inactivate the Klenow enzyme. After labeling, the probe was cleaned up using the PCR purification kit.

Binding reactions were done by incubating 0.5 µl of labeled probe with 10 X binding buffer (500 mM Tris-HCl, 1 M NaCl, 1 mM EDTA, 0.5 µg/µl BSA, 100 mM DTT), 1µg/µl poly(dIdC), 0 to 320 pmol of purified RcsB-His_6 and brought to a final volume of 20 µl with molecular biology grade water (Fisher). The reactions incubated for 30 min at room temperature before being loaded with 5X DNA loading dye on a pre-run Mini-

PROTEAN® 5% TBE Precast Gel (BioRad). The gel was run at 100 V for approximately 3-4 h at 4°C, until the loading dye was no longer visible on the gel. DNA was transferred onto a 0.22 micron nylon membrane (MagnaGraph) at 15 V with a 0.4 mA limit for 45 min using a Bio-Rad Transblot SD Semi-Dry Transfer Cell. DNA was crosslinked to the membrane using a Stratagene Crosslinker. 10X blocking reagent (Roche) was prepared in maleate buffer (100 mM maleic acid [pH 7.5], 150 mM NaCl), and the membrane was blocked for 30 min at room temperature using 1X of the blocking solution diluted in maleic acid wash buffer (maleate buffer with 0.3% Tween 20). The membrane was then incubated for 30 min with a 1:1,000 dilution of anti-digoxigenin coupled to alkaline phosphatase (Roche) in maleic acid wash buffer. The membrane was washed 2 X 15 min with maleic acid wash buffer. The membrane was equilibrated in detection Buffer (100 mM Tris-HCl [pH 9.5], 100 mM NaCl) for 2 min then incubated with a 1 mL 1:10 dilution of CDP-Star (Roche), for 5 min. After briefly blotting the membrane with Whatman paper, it was placed in a sealable plastic bag and exposed to film.

Swarm assays. Overnight cultures were standardized to the same optical density, and 4 µl of each culture was pipetted onto the same pre-dried 1.5% LB agar plate. The culture was allowed to dry into the LB plate before being incubated at 37°C. Measurements of the swarm diameter in centimeters were taken every 30 min until the cells reached consolidation. Antibiotics were included in the agar plate when appropriate. The values represent the average diameter of duplicate sets (4 total) with standard deviations.

RNA-Seq. HI4320 and *rcsB::str*^{R} (PMKM2) cells were harvested at an OD_{600}= 1.1 in triplicate. RNAprotect Bacteria Reagent was used at a 1:1 ratio (Qiagen). Total RNA was isolated using MasterPure RNA Purification Kit (Epicentre) and contaminating DNA

was removed using Turbo DNA-Free Kit (Ambion). RNA purity was confirmed on the Agilent 2100 Bioanalyzer (Agilent Technologies). DNA-free samples were then enriched for mRNA using MICROB*Express*™ Bacterial mRNA Enrichment Kit (Ambion). Two rounds of rRNA depletion were performed and RNA purity was confirmed on an Agilent 2100 Bioanalyzer (Agilent Technologies). cDNA libraries were constructed from HI4320 and *rcsB::str*^{R} mRNA using the SuperScript Double-Stranded cDNA Synthesis Kit (Invitrogen). The cDNA libraries were purified by phenol extraction and ethanol precipitation. Sequences were analyzed on an Illumina HiSeq2000 instrument with 50 bp paired end reads and matched to the HI4320 genome using CLC Genomics Workbench (CLC Bio-Qiagen, Aarhus Denmark). The total number of reads mapped per transcript was determined and used to determine the reads per kilobase per million reads (RPKM). Three separate sets of RNA samples were analyzed and the average of samples from two sets was reported in Supplemental Table 1.

Quantitative RT-PCR (qRT-PCR) The same RNA used for RNA-Seq was used for qRT-PCR. Briefly, the RNA was transcribed into cDNA using iScript^{TM} Selected cDNA Synthesis Kit (Bio-Rad) per the manufacturer's instructions. qRT-PCR was performed using a 1:10 dilution of the generated cDNA in iQ^{TM} SYBR® Green Supermix (Bio-Rad). The reaction was completed in an iCycler iQ^{TM} Real-Time PCR Detection System (Bio-Rad) and values were normalized to 16S rRNA expression for each sample. The expression of *minC*, *minD*, and *minE* in HI4320 was calculated relative to PMKM2 (HI4320 *rcsB::str*^{R}) using the $\Delta\Delta C_T$ method (31). The primers used to quantify the expression of each gene can be found in Table 2.

Semi-quantitative RT-PCR. Total RNA was harvested at hourly intervals (T_1, T_2, T_4,

T_6) after placing cells on 1.5% LB agar plates using MasterPure RNA Purification Kit (Epicentre). The T_0 sample represents cells immediately before being placed on agar surfaces. Contaminating DNA was removed using Turbo DNA-Free Kit (Ambion). Purified RNA was transcribed into cDNA using iScript™ Selected cDNA Synthesis Kit (Bio-Rad). PCR amplification was performed using 16S-F and 16S-R (Table 2) and aliquots from the PCR reaction were taken after 5, 10, and 15 cycles in order to equilibrate cDNA samples relative to 16S rRNA expression. Once equilibrated, *minC* expression was examined using minC-F and minC-R (Table 2) and *flhD* expression was examined using flhD-F and flhD-R (Table 2) at cycles 20, 25, 30, and 35.

Western blot analysis. Overnight cultures grown to stationary phase in LB were equilibrated to the same optical density then 300 µl was spread onto a 1.5% LB agar before incubation at 37°C for 5 h. Cells were gently resuspended in cold LB broth to the same optical density and 1.5 ml was pelleted and stored at -80°C. Cell pellets were lysed using 400 µl CellLytic™ B Cell Lysis Reagent (Sigma). Equivalent protein levels for each sample were confirmed using a Bradford assay. Cell lysates were resuspended at a 1:1 ratio in Laemmli sample buffer. Samples were run on a 12% Mini-PROTEAN™ TGX (Bio-RAD) gel and transferred to a nitrocellulose membrane. The primary antibody used was rabbit anti-FlaA obtained from Robert Belas at the University of Maryland. The secondary antibody was ECL™ peroxidase labelled anti-rabbit antibody (Life Sciences).

DAPI (*4',6* - Diamidino - 2 - phenylindole, dihydrochloride*)* staining and microscopy. Swarmer cells were harvested after 5 h of incubation on 1.5% LB agar and resuspended in 1X phosphate buffered saline (PBS). Cell suspensions were chemically fixed by the addition of formaldehyde (Sigma) to a 3% (v/v) final concentration and

incubated for 10 min by gentle rocking. Fixed bacteria were attached to a poly-L-lysine (Sigma-Aldrich) coated coverglass and incubated with DAPI (AnaSpec, Inc) (at 2 μg/mL of final concentration in 1X PBS) for 5 minutes in the dark. The excessive DAPI solution was removed by washing with 1X PBS. The entire staining procedure was performed at room temperature. DAPI-stained cells were imaged at room temperature using phase contrast light- and wide field fluorescence microscopy with an Olympus IX83 microscope. An oil immersion 100x objective and a standard DAPI filter were employed for microscopy. Images were acquired using a Neo 5.5 sCMOS camera (Andor) and the MetaMorph software (Molecular Devices). The image was prepared for publication using ImageJ software (NIH).

Results.

The *minCDE* operon is positively regulated by RcsB. Mutations in *rcsB* result in a hyperswarming phenotype and differentiation into swarmer cells in liquid, indicating that RcsB regulates genes important for swarmer cell differentiation (10). To identify these genes, RNA-Seq was performed on RNA isolated from liquid cultures of *P. mirabilis* HI3420 and an isogenic *rcsB::str*^{R} mutant derivative at an optical density A_{600} of 1.1. At this optical density, cells of the *rcsB* mutant were highly elongated, in contrast to the short rods of wild-type cells. When a cutoff of 2-fold or greater was applied, 87 genes were found to be RcsB repressed and 46 were RcsB activated (Supplemental Table 1). Among the RcsB regulated genes, we were interested in those that might contribute to cell elongation, and initially focused on cell division genes. Expression of the *ftsA* and *ftsZ* genes was reduced 2.4 and 3.3-fold, respectively, in the *rcsB* mutant. However, the essential nature of these genes precluded a direct analysis of their role in cell elongation during swarming. Therefore, we focused on the *minC* and *minD* genes encoding components of a cell division inhibition complex, where expression decreased 3.4 and 6.7-fold, respectively, in the *rcsB* mutant relative to wild-type cells. The *minE* gene, located immediately downstream of *minD* was not identified in the RNA-Seq as RcsB regulated, which was surprising as *minE* is part of an operon with *minCD* in other bacteria (32, 33). To determine if the *minCDE* genes formed an operon in *P. mirabilis,* a primer specific to *minE* was used to prime cDNA synthesis and this was used in a PCR to amplify the *minC-E* region. The *minC-E* region was amplified using this cDNA, but no product was observed with the RNA only, indicating that the *minCDE* genes form an operon (data not shown).

To confirm the RNA-Seq data, the expression of *minC* and *minD* was examined using quantitative real-time reverse transcriptase PCR (qRT-PCR) using the same RNA used for RNA-Seq. A 7.4-fold decrease in *minC* expression was observed in the *rcsB* mutant relative to wild-type and a 6.3-fold decrease in *minD* was observed (Fig. 1C). In addition, qRT-PCR analysis indicated that the expression of *minE* was reduced 2.4-fold in the *rcsB* mutant. (Fig. 1C) These results indicate that RcsB positively regulates the *minCDE* operon.

Identification of the *minC* transcriptional start site and analysis of a *minC-lacZ* transcriptional fusion. The *minC* promoter region was identified by first determining the 5'-end of the *minC* mRNA using 5'-RACE with RNA harvested from wild-type PM7002. Two alternative transcriptional start sites were identified 65 and 66 bp upstream of the *minC* start codon. Upstream of the identified start sites were putative -10 and -35 regions and a possible RcsB binding site based on the *E. coli* consensus TAAGAATAATCCTA (Fig.1B). To confirm that this region represented the *min* promoter, a DNA fragment encompassing from -169 to +371 relative to the transcriptional start site and containing the putative –10 and –35 regions was amplified using PCR. This fragment was ligated into pQF50, a low-copy number vector harboring a promoterless *lacZ* gene (29) in order to quantify the *minC* promoter activity. This construct, pMinClacZ, was transformed into PM7002 and PM7002 *rcsB*::*str*^{R} and cells were collected after 2 (T_2) and 4 h (T_4) of incubation on agar plates at 37°C. The expression of β-galactosidase from pMinClacZ was 2-fold lower in the *rcsB* mutant at T_2 relative to wild-type, and was approximately 4-fold lower at T_4 (Fig. 1D).

RcsB directly regulates *minCDE* expression. The above data indicated that RcsB

positively regulated *minCDE* expression. Next, to determine whether RcsB exerted its effect on *minCDE* expression directly, electrophoretic mobility shift assays (EMSA) were performed using purified His-tagged RcsB and a 292 bp region upstream of *minCDE*. This 292 bp region included the transcriptional start site identified using 5'-RACE, and extended from -208 to + 82 relative to the transcriptional start site. A partial shift was observed when 75 pmol of RcsB was added to the reaction and this shift further increased at RcsB concentrations of 170 pmol and above (Fig. 2A). To confirm that the binding of RcsB was specific to the region upstream of *minC*, a competitive EMSA was performed using the unlabeled 292 bp *minC* promoter fragment and a 249 bp fragment containing the *abaI* gene from *Acinetobacter nosocomialis* strain M2 using the abaI-F and abaI-R primers (Table 2). At a concentration 50 times that of the labeled *minC* fragment, the unlabeled *minC* DNA prevented a shift. However, the unlabeled 249 bp *abaI* fragment did not affect the shift of the labeled *minC* fragment (Fig. 2B). Together, these data indicate that RcsB binds the region containing the *minC* promoter and this binding is specific.

Expression of the *minCDE* operon during swarmer cell differentiation. To determine if *minCDE* expression varied during swarmer cell differentiation, expression was examined by semi-quantitative RT-PCR from cells collected at hourly intervals after differentiation was initiated by placing cells on agar plates. The expression of *minC* increased sharply by T_2 and then decreased to undetectable levels by T_4 (Fig. 3). As a marker for swarmer cell differentiation, *flhD* was also examined, where expression began to increase at T_1, peaked at T_2- T_4 and then decreased by T_6 (Fig. 3).

A *minC* mutation results in aberrant cell division and minicell production. Since

RcsB regulates genes important for swarmer cell differentiation, it seemed likely that the identification of the MinCDE cell division inhibitors as RcsB regulated indicated they had a likely role in swarmer cell elongation. To address the effect of the *min* system on *P. mirabilis* cell division and swarmer cell formation, a *minC::kan*^{R} mutant was constructed. Cell morphologies were first examined in liquid media and imaged by phase contrast microscopy. PM7002 produced short rod-shaped cells in liquid with an average length of 2.3 μ ± 0.6 (n=147), while the *minC::kan*^{R} mutant produced a typical *min* mutant phenotype with both enlarged cells and minicells, resulting in an average length of 3.72 μ ± 1.8 (n = 102) (Fig. 4). In contrast, there were no minicells observed in wild-type cells. The *minC::kan*^{R} mutation was complemented using the *minCDE* operon in single copy as PMKH5 (PM7002 *minC::kan*^{R} + pMinCDE) shared the division phenotype of PM7002, with an average cell length of 2.37 μ ± 0.6 (n= 82) (Fig. 4).

The *minC::kan*^{R} mutation reduces swarming motility. To investigate whether the *min* system was important for swarming in both wild-type and *rcsB::str*^{R} mutant backgrounds, wild-type PM7002, a *minC::kan*^{R} mutant, a *rcsB::str*^{R} mutant, and the *minC::kan*^{R}**,** *rcsB::str*^{R} double mutant were subject to swarm assays. Measurements of the swarm diameter were taken every 30 minutes until the strains reached the first consolidation phase. PM7002 initiated swarming at approximately 4 h (T_4) after being spotted onto an agar plate (Fig. 5A). In contrast, the *minC::kan*^{R} mutant experienced a half-hour delay in the onset of swarming, and did not reach wild-type levels of swarming until the consolidation phase at T_6. The swarming phenotype of the *minC::Kan*^{R} mutant complemented with pMinCDE was not significantly different than the *minC::Kan*^{R} alone (Fig. 5A) and the possible basis for this is discussed below. As expected, the *rcsB* mutant

hyperswarmed and initiated swarming an hour before wild-type (Fig. 5B). The *minC::kan*^{R}*, rcsB::str*^{R} double mutant initiated swarming at the same time as *rcsB::str*^{R} mutant, but migration was 50% lower (Fig. 5B).

Since the *minC::kan*^{R} mutation in both wild-type and *rcsB::str*^{R} mutant backgrounds resulted in deficient swarming, the basis for this defect was examined by: (i) analyzing cell morphology at the swarm fronts, (ii) determining the levels of flagellin expressed in wild-type and *minC::kan*^{R} mutant strains, and (iii) examining the nucleoid distribution in wild-type and *minC::kan*^{R} mutant cells using DAPI staining. The PM7002 swarm front consisted of highly elongated, multinucleate swarm cells on the exterior and rod-shaped cells on the interior (Fig. 6A). In contrast, the *minC::kan*^{R} mutant swarm front was a heterologous population of swollen and slightly elongated rod-shaped cells and minicells (Fig. 6A). The altered swarmer cell morphology at the swarm fronts of the *minC::kan*^{R} mutant could be complemented by reintroducing the *minCDE* operon in single copy (Fig. 6A). The levels of flagellin (FlaA) detected by Western blot were approximately 2-fold lower in the *minC::kan*^{R} mutant at T_5 (Fig. 6B). However, complementation with pMinCDE did not restore flagellin expression in the *minC::kan*^{R} mutant. In both the *minC::kan*^{R} mutant and the *minC::kan*^{R} mutant, the reduced flagellin likely contributes to the reduction in swarming. The basis for the ability of pMinCDE to complement the defect in cell morphology, but not the reduced flagellin expression is unknown. There are no genes immediately downstream of *minCDE* in *P. mirabilis* which might have decreased expression due to a polar effect of the *minC::kan*^{R} mutation, or could have been affected by introducing pMinCDE into the chromosome at the *min* locus. The lack of complementation with respect to swarming may have resulted from

expression differences that failed to mimic the physiological level of MinCDE required for normal swarming, but were able to rescue the morphological defect. For example, in *E. coli*, the *min* operon must be present 1-10 times the physiological level in order to complement a *min* deletion mutant (32). Lastly, in both wild-type and *minC::kan*^{R} mutant cells, multiple chromosomes typical of swarmer cells were present and similar in appearance in each strain (Fig. 6C).

Discussion.

Previous studies have demonstrated that mutations which inactivate the Rcs phosphorelay in *P. mirabilis* result in hyperswarming on agar surfaces and constitutive swarmer cell formation in liquid media, a normally non-permissive condition (10, 13, 14). The basis for the hyperswarming phenotype is due, in part, to the overexpression of the *flhDC* operon, which then activates genes involved in the production of flagella. However, overexpression of *flhDC* alone does not result in cell elongation, therefore, the Rcs phosphorelay must also regulate genes involved in swarmer cell elongation (10). Since *rcs* mutants constitutively elongate to swarmer cells in liquid media, this condition was chosen to identify RcsB regulated genes that contributed to cell elongation by using RNA-Seq analysis. Based on this analysis, we chose to focus on two genes, *minC* and *minD* that were activated by the Rcs phosphorelay and encoded components of the MinCDE cell division inhibition complex. Interestingly, a third gene, *minE*, which is typically co-transcribed with *minC* and *minD* did not show up in the RNA-Seq analysis as RcsB regulated. However, our work demonstrated that *minE* was co-transcribed with *minCD* and thus the three genes formed an operon. The inability to identify *minE* in the RNA-Seq analysis may have been due to a reduced sensitivity of this technique when compared to the qRT-PCR, which showed a 2.4-fold reduction in the *rcsB* mutant (Fig. 1C). To confirm the activation of the *minCDE* operon by RcsB, a combination of transcriptional *lacZ* fusions and real-time PCR was used. In addition, purified RcsB was capable of binding the *minCDE* promoter region indicating the regulation was direct. A possible RcsB binding site (TAAGAATAATCCTA) was present immediately upstream of the -35 region of the promoter (Fig. 1B). Additional studies including mutagenesis of

this putative RcsB binding site or demonstrating its ability to confer RcsB-dependent regulation on a heterologous promoter will be needed to confirm the role of this sequence in RcsB binding.

Identification of the MinCDE cell division inhibition complex as regulated by the Rcs phosphorelay prompted our investigation of its function in swarmer cell elongation and swarming motility. We hypothesized that the expression of *minCDE* had to be tightly regulated during swarmer cell differentiation. During swarmer cell differentiation, there is a sharp increase in *minCDE* expression approximately 2 hours after contact with an agar surface (T_2) and the increased levels of MinCDE likely contributed to the inhibition of cell division (Fig. 3). Consistent with this, we have observed that even slight increases in *minCDE* expression from an IPTG inducible promoter resulted in a block in cell division and the formation of highly elongated cells (data not shown). Then, as the activity of the Rcs phosphorelay begins to decrease at T_3, the resulting decrease in levels of MinCDE would partially alleviate the block in cell division and allow cells to prepare for the consolidation phase where they divide again. Consistent with this, a *minC* mutant was unable to elongate normally during swarmer cell differentiation and formed shorter cells than wild-type (Fig. 6). In addition, the *minC* mutant did not swarm as efficiently as wild-type (Fig. 5). This decrease in swarming was likely due to the decreased flagellin expression and the abnormal morphology in the *minC* mutant, which may affect the ability of the cells to form multicellular rafts. For example, it has been shown that a *ccmA* mutant in *P. mirabilis* produces curved cells that cannot align properly to form rafts during swarming. This mutant is able to differentiate into elongated, C-shaped swarmer cells, but is unable to swarm (34).

To our knowledge, this is the first study to investigate the contribution of a cell division system to swarmer cell differentiation in *P. mirabilis*. In other bacteria, a *minC* mutation was found to reduce motility in *Helicobacter pylori*, but this mutant was highly elongated in liquid culture, which the authors hypothesized was the cause of reduced motility (35). In contrast, a mutation in a *minE* homolog in the Gram-positive bacterium *Clostridium perferingens* resulted in hypermotility and hyper-elongation (36). In *P. mirabilis*, a null allele in *minC*, the proprietor of cell division inhibition in the Min system, did not induce hyper-elongation in liquid culture or on solid surfaces in our study. The difference seen between these studies and ours highlights the underlying complexities and varying roles of the Min system in different organisms.

Acknowledgements.

We are grateful to Robert Belas for providing the FlaA antibody. This work was supported by a Merit Review award from the Department of Veterans Affairs and by a Research Career Scientist award (P.N.R). K.H. is supported by the Burroughs Wellcome Fund's Molecules to Mankind program.

References.

1. **Hoeniger, JFM.** 1965. Development of flagella by *Proteus mirabilis*. J Gen Microbiol **40:**29-42.
2. **Jones BV, Young R, Mahenthiralingam E, Stickler DJ.** 2004. Ultrastructure of *Proteus mirabilis* swarmer cell rafts and role of swarming in catheter associated urinary tract infection. Infect Immun **72:**3941-3950.
3. **Rauprich O, Matsushita M, Weijer CJ, Siegert F, Esipov SE, Shapiro JA.** 1996. Periodic phenomena in *Proteus mirabilis* swarm colony development. J Bacteriol **178:**6525-6538.
4. **Williams FD, Schwarzhoff RH.** 1978. Nature of the swarming phenomenon in *Proteus.* Annu Rev Microbiol **32**:101–122.
5. **Armbruster CE, Mobley HLT.** 2012. Merging mythology and morphology: the multifaceted lifestyle of *Proteus mirabilis*. Nat Rev Microbiol **10**:743-754.
6. **Rather PN.** 2005. Swarmer cell differentiation in *Proteus mirabilis.* Environmen Microbiol **7**:1065-1073.
7. **Stout V, Gottesman S.** 1990. RcsB and RcsC: A two-component regulator of capsule synthesis in *Escherichia coli*. J Bacteriol **172:**659-669.
8. **Takeda S, Fujisawa Y, Matsubara M, Aiba H, Mizuno T.** 2001. A novel feature of the multistep phosphorelay in *Escherichia coli*: A revised model of the RcsC –> YojN –> RcsB signalling pathway implicated in capsular synthesis and swarming behavior. Mol Microbiol **40:**440–450.
9. **Gervais FG, Drapeau GR.** 1992. Identification, cloning, and characterization of *rcsF*, a new regulator gene for exopolysaccharide synthesis that suppresses the division mutation *ftsZ84* in *Escherichia coli* K-12. J Bacteriol **174:**8016–8022.

10. **Clemmer KM, Rather PN.** 2008. Regulation of *flhDC* expression in *Proteus mirabilis*. Res Microbiol **158:**295-302.

11. **Claret L, Hughes C.** 2000. Functions of the subunits of the $FlhD_2C_2$ transcriptional master regulator of bacterial flagellum biosynthesis and swarming. J Mol Biol **303:**467-478.

12. **Pearson MM, Rasko DA, Smith SN, Mobley HLT.** 2010. Transcriptome of swarming *Proteus mirabilis*. Infect Immun **78**(6)**:**2834-2845.

13. **Belas R, Schneider R, Melch M.** 1998. Characterization of *Proteus mirabilis* precocious swarming mutants: identification of *rsbA*, encoding a regulator of swarming behavior. J Bacteriol **180**(23):6126-39.

14. **Liaw SJ, Lia HC, Ho SW, Luh KT, Wang WB.** 2001. Characterisation of p-nitrophenylglycerol-resistant *Proteus mirabilis* super-swarming mutants. J Med Microbiol **50**(12):1039-1048.

15. **Belas R.** *Proteus mirabilis* and other swarming bacteria. In: Shapiro J, Dworkin M, editors. Bacteria as multicellular organisms. New York, N.Y: Oxford University Press; 1997. pp. 183–219.

16. **Sturgill G, Rather PN.** 2004. Evidence that putrescine acts as an extracellular signal required for swarming in *Proteus mirabilis.* Mol Microbiol **51**:437-446.

17. **Carballès F, Bertrand C, Bouche JP, Cam K.** 1999. Regulation of *Escherichia coli* cell division genes *ftsA* and *ftsZ* by the two-component system *rcsC–rcsB.* Mol Microbiol **34**(3)**:**442–450.

18. **Gervais FG, Phoenix P, Drapeau GR.** 1992. The *rcsB* gene, a positive regulator of colonic acid biosynthesis in *Escherichia coli*, is also an activator of *ftsZ* expression. J

Bacteriol **174:**3964–3971.

19. **Detweiler CS, Monack DM, Brodsky IE, Mathew H, Falkow S.** 2003. *virK, somA* and *rcsC* are important for systemic *Salmonella enterica* serovar Typhimurium infection and cationic peptide resistance. Mol Microbiol **48:**385–400.

20. **Francez-Charlot A, Laugel B, Van Gemert A, Dubarry N, Wiorowski F, Castanié-Cornet MP, Gutierrez C, Cam K.** 2003. RcsCDB His-Asp phosphorelay system negatively regulates the *flhDC* operon in *Escherichia coli*. Mol Microbiol **49**:823–832.

21. **Bi EF, Lutkenhaus J.** 1991. FtsZ ring structure associated with cell division in *Escherichia coli*. Nature **354**:161-164.

22. **Ward JE, Lutkenhaus J.** 1985. Overproduction of FtsZ induces minicell formation in *E. coli*. Cell **42**:941-949.

23. **de Boer PA, Crossley RE, Rothfield LI.** 1990. Central role for the *Escherichia coli minC* gene product in two different cell division-inhibition systems. Proc Natl Acad Sci USA **87**:1129-1133.

24. **de Boer PA, Crossley RE, Rothfield LI.** 1992. Roles of the MinC and MinD in the site-specific septation block mediated by the MinCDE system of *Escherichia coli*. J Bacteriol **174**(1):63-70.

25. **Hu Z, Gogol EP, Lutkenhaus J.** 2003. Dynamic assembly of MinD on phospholipid vesicles regulated by ATP and MinE. Proc Natl Acad Sci USA **99**:671-676.

26. **Hu Z, Lutkenhaus J.** 2001. Topological regulation of cell division in *E.coli* spatiotemporal oscillation of MinD requires stimulation of its ATPase by MinE and phospholipid. Mol Cell **7**(6):1337-1343.

27. **Zhao CR, de Boer PA, Rothfield LI.** 1995. Proper placement of the *Escherichia coli*

division site requires two functions that are associated with different domains of the MinE protein. Proc Natl Acad Sci USA. **92**(10):4313-7.

28. **Adler HI, Fisher WD, Cohen A, Hardigree AA.** 1967. Miniature *Escherichia coli* cells deficient in DNA. Proc Natl Acad Sci USA **57**(2):321-326.

29. **Farinha MA, Kropinski AM.** 1990. Construction of broad-host-range plasmid vectors for easy visible selection and analysis of promoters. J Bacteriol **172**:3496–3499.

30. **Miller JH.** 1972. Experiments in molecular genetics. Cold Springs Harbor Laboratory, Cold Spring Harbor, NY.

31. **Livak KJ, Schmittgen TD.** 2001. Analysis of relative gene expression data using real-time quantitative PCR and the 2(-Delta Delta C(T)) Method. Methods **25**:402-408.

32. **de Boer PA, Crossley RE, Rothfield LI.** 1988. Isolation and properties of *minB*, a complex genetic locus involved in correct placement of the division site in *Escherichia coli.* J Bacteriol **170**(5):2106-2112.

33. **de Boer PA, Crossley RE, Rothfield LI.** (1989) A division inhibitor and a topological specificity factor coded for by the minicell locus determine proper placement of the division septum in *E. coli*. Cell **56**:641-649.

34. **Hay NA, Tipper D J, Gygi D, Hughes C.** 1999. A novel membrane protein influencing cell shape and multicellular swarming of *Proteus mirabilis*. J Bacteriol **181**:2008–2016.

35. **Chiou P, Luo C, Chang K, Lin N.** 2013. Maintenance of the cell morphology by MinC in *Helicobacter pylori*. PLoS ONE **8**(8):e71208.

36. **Liu H, McCord KD, Howarth J, Popham DL, Jensen RV, Melville SB.** 2014. Hypermotility in *Clostridium perfringens* strain SM101 is due to spontaneous mutations in genes linked to cell division. J Bacteriol **196**(13):2405-2412.

37. **Manoil C, Beckwith J.** 1985. TnphoA: a transposon probe for protein export signals. Proc Natl Acad Sci USA **82**:8129-8133.

38. **Miller V L, Mekalanos JJ.** 1988. A novel suicide vector and its use in construction of insertion mutations: osmoregulation of outer membrane proteins and virulence determinants in *Vibrio cholerae* requires *toxR*. J Bacteriol **170**:2575-2583.

39. **Mobley HLT, Warren JW.** 1987. Urease-positive bacteriuria and obstruction of long-term urinary catheters. J Clin Microbiol **25**:2216–2217.

40. **Kaniga K, Delor I, Cornelis GR.** 1991. A wide-host-range suicide vector for improving reverse genetics in gram-negative bacteria: inactivation of the *blaA* gene in *Yersinia enterocolitica*. Gene **109**:137-141.

41. **Amann E, Ochs B, Abel KJ.** 1988. Tightly regulated tac promoter vectors useful for the expression of unfused and fused proteins in *Escherichia coli*. Gene **69**(2):301-315.

Table 1. Stains and plasmids used in this study

Strain or plasmid	Description/genotype	Source
***E. coli* strains**		
DH5α	F- Φ80d*lacZ*ΔM15 Δ(*lacZYA-argF'*)U169 *endA1 recA1 hsdR17(*r_k- m_k-)*deoR thi-1 supE44* λ- *gyrA96 relA1*	Laboratory stock
CC118 λ*pir*	*araD139 Δ(ara leu)7697 ΔlacZ74 phoAΔ20 galE galK thi rpsE rpoB argE(Am) recA1*	(37)
SM10 λ*pir*	*thi thr leu tonA supE recA* RP4-2Tc::Mu Kan^R λ*pir*	(38)
BL21 (DE3)	F^- *dcm ompT hsdS* (r^-_B m^-_B) g*al* λ(DE3)	Stratagene
***P. mirabilis* strains**		
PM7002	Wild type; Tc^R	ATCC
HI4320	Wild type; Tc^R	(39)
PMKH1	PM7002 *minC::kan*^{R}	This study
PMKM1	PM7002 *rcsB::str*^{R}	(10)
PMKH4	PM7002 *minC::kan*^{R}, *rcsB::str*^{R}	This study
PMKH5	PM7002 *minC::kan*^{R} + pMinCDE	This study
PMKH6	PM7002 + pMinClacZ	This study
PMKH7	PM7002 *rcsB::str*^{R} + pMinClacZ	This study
PMKM2	HI4320 *rcsB::str*^{R}	This study
Plasmids		
pBluescriptII SK(−)	ColE1 replicon *lacZ*α; Amp^R	Stratagene
pBC	High copy; Cm^R	Stratagene
pKNG101	R6K replicon *mob*$^+$ *sacB*$^+$*R*$^+$; Str^R	(40)
pTrc99a	ColE1replicon trcPO $lacI^Q$; Amp^R	(41)
pQF50	pRO1600 replicon *lacZ*α (promoterless); Amp^R	(29)
pET21a	T7 expression vector; Amp^R	Novagen
pRcsB	pKNG101::*rcsB* (internal fragment); Str^R	(10)
pMinC	pKNG101 + *minC*::Kan^R ; Str^R	This study
pBCMinCDE	pBC + *minCDE*; Cm^R	This study
pMinCDE	pKNG101 + *minCDE*; Str^R	This study
pMinClacZ	pQF50 + $minC_P$; Amp^R	This study
pETRcsB	pET21a + *rcsB*; Amp^R	This study

Kan^R, kanamycin resistant; Tc^R, tetracycline; Str^R, streptomycin; Amp^R, ampicillin
Cm^R, chloramphenicol

Table 2. Primer sequences used in this study

Primer	Sequence (5' →3')	Purpose
minC-F	TTTTTCTAGATTTTTGAGCGAGGCCGGTAG	*minC* mutation
minC-R	TTTTGGATCCAGCGACTTGCCTGAATATTTTAGT	*minC* mutation
PminC-F	TTTTGTCGACGCGCGAGATCTAGCAACATT	*minC* promoter activity
PminC-R	TTTTGGATCCCCTGAGCTGCTGGCTTAGTT	*minC* promoter activity
GSP1	CCAATATTGACCAGCAATGGAAACT	5'-RACE
GSP2	ACACCATAAATATGTACATTACCGTCT	5'-RACE
minCSS-F	TTAAGAATTCCGCGAGATCTAGCAACATTGCA	DNA binding studies
minCSS2-F	TTAAGAATTCAGCGACTTGCCTGAATATTTTAGT	DNA binding studies
minCSS2-R	TTAAGAATTCAATGGGCGTGTTTGACATCT	DNA binding studies
abaI-F	AAGTTAATCGCTTCTTGCAG	DNA binding studies
abaI-R	AGCTTATGTGGTCGCTCAAG	DNA binding studies
minCDE-F	ATAATTAAAACACAGAGCC	complementing strain
minCDE-R	CCAGATTATAGAAAATTTAC	complementing strain
minCqRT-F	CCCAAGCGCCTCAATTTCTG	qRT-PCR studies
minCqRT-R	TTCCCACAACACGTAAGCCA	qRT-PCR studies
minDqRT-F	CCACCAACCCAGAAGTCTCC	qRT-PCR studies
minDqRT-R	CGGCCTGGATTATAGCGTGT	qRT-PCR studies
minEqRT-F	CGCGTAAAAAGTCGACAGCA	qRT-PCR studies
minEqRT-R	TAAGCTGGCTCAGTATCGCC	qRT-PCR studies
16S-F	GGCTCAGATTGAACGCTGGC	qRT-PCR studies
16S-R	CGAAGAGCCCCTGGTTTGG	qRT-PCR studies
flhD-F	TTGGTTAAGTTGGCTGAAAC	semi-quantitative RT-PCR
flhD-R	TTTGTAGCAGAGGTATCATG	semi-quantitative RT-PCR
minE-R	CTTAGGTGATTCTTCATTTTCAGG	operon study
rcsB-F	ACAGTCTAGAGATCCGACAGTTGCTGTAGC	RcsB protein purification
rcsB-R	AGACGTCGACCGGGTTAATGATGATGATGATGATGG CTTTCTCCGTTAATTTCCTTATC	RcsB protein purification

Figure legends.

Figure 1. *minC* is positively regulated by RcsB. (A) The organization of the *minCDE* open reading frame. *minC* (702 bp), *minD* (813 bp) and *minE* (207 bp) are located in the same operon. The non-coding region upstream of *minC* is 127 bp long. Two transcriptional start sites for *minCDE* are located at positions -65 (the white arrow) and -66 (the grey arrow) upstream of the *minC* start codon. (B) The sequence upstream of *minCDE*. The start codon of *minC* is found in bold. The two transcriptional start sites identified using 5'-RACE are underlined and in bold. They are 65 and 66 bp upstream of the start codon. Upstream of the two identified start sites are putative -10 (highlighted in grey) and -35 (grey) regions. A potential RcsB binding site is underlined based on the *E. coli* consensus sequence (TAAGAATAATCCTA). (C) qRT-PCR analysis of *minC, minD, and minE* expression levels in *P. mirabilis* HI4320 and *P. mirabilis* HI4320 *rcsB::str*^{R} (PMKM2). *minC* expression is 7.5 times lower in PMKM2 relative to wild-type; *minD* expression is 6.3 times lower in PMKM2 relative to wild-type, and *minE* expression is 2.4 times lower in PMKM2 relative to wild-type. (D) β-galactosidase activity of pMinCLacZ in PM7002 wild-type (PMKH6, dark grey bars) and PM7002 *rcsB::str*^{R} (PMKH7, light grey bars). The activity of the *minC* promoter is decreased 2-fold in PMKH7 compared to PMKH6 after 2 h on solid agar, and is decreased 4-fold in PMKH7 after 4 h on solid agar. An asterisk indicates a *P* value <0.05.

Figure 2. **RcsB binds to the *minC* promoter region.** Binding of purified His-tagged RcsB to the *minC* promoter region. (A) Binding of the *minC* upstream region (290 bp) with increasing concentrations of RcsB. Lane 1, free labelled *minC* probe; lane 2, *minC* probe with 40 pmol RcsB; lane 3, *minC* probe with 75 pmol RcsB; lane 4, *minC* probe

with 170 pmol RcsB; lane 5, *minC* probe with 340 pmol RcsB. (B) The digoxigenin labelled 290-bp fragment was incubated with 340 pmol His-tagged RcsB. This binding was competed with unlabeled *minC* DNA (290 bp) and unlabeled *abaI* DNA (249 bp). Lane 1, free *minC* probe without RcsB or competitor; lane 2, *minC* probe with 340 pmol RcsB; lane 3, *minC* probe with 340 pmol RcsB and unlabeled *minC* DNA; lane 4, *minC* probe with 340 pmol RcsB and unlabeled *abaI* DNA.

Figure 3. Semi-quantitative RT-PCR of *minC, flhD,* and 16S RNA expression during swarmer cell differentiation. Total RNA was harvested at hourly intervals (T_1, T_2, T_4, T_6) after placing cells on agar plates. The T_0 sample represents cells immediately before being placed on agar surfaces. PCR on cDNA samples prepared from RNA at each time point were amplified for 10 cycles (16S rRNA), 30 cycles (*minC*) or 25 cycles (*flhD*).

Figure 4. A *minC::kan*^{R} mutation results in aberrant cell division in liquid culture. The cell division phenotypes for wild-type strain PM7002 (top panel), PMKH1 (PM7002 *minC::kan*^{R}, middle panel), and PMKH5 (PM7002 *minC::kan*^{R} + pMinCDE, bottom panel) are shown. Cells were grown to mid-log and 1.5 µl was imaged using phase contrast microscopy. Liquid cultures of PM7002 exist as rod shaped cells, often as doublets, with septa positioned at the center of cells. The *minC::kan*^{R} mutation causes a large percentage of cells to divide at the poles (see inlets in middle panel). Minicells are often present. The division phenotype can be complemented by the addition of *minCDE* in single copy (bottom panel). Images were taken at 1,000 X magnification. All cell sizes in the inlets have been increased equally.

Figure 5. A *minC* mutation reduces *P. mirabilis* swarming in wild-type and *rcsB::str*^{R} backgrounds. (A) The *minC::kan*^{R} mutation was introduced into PM7002 (wild-type) in order to create PMKH1 (PM7002 *minC::kan*^{R}). The complementing strain was created by introducing pMinCDE (pKNG101 + *minCDE*) into PMKH1. (B) The *minC::kan*^{R} mutation was also introduced into PMKM1 (PM7002 *rcsB::str*^{R}) in order to create PMKH4 (PM7002 *minC::kan*^{R}, *rcsB::str*^{R}). All 5 strains were grown overnight in LB containing the appropriate antibiotics, then equilibrated to the same optical density. To investigate their ability to swarm, 4 µl droplets of the equilibrated inocula were spotted onto the same plate, and the migration distance was measured every 30 min. The average of four measurements is shown for PM7002, PMKH1, PMKM1, PMKH4, and PMKH5.

Figure 6. The *minC::kan*^{R} mutation causes an atypical swarm front. (A) Stationary phase cultures of PM7002 (wild-type), PMKH1 (PM7002 *minC::kan*^{R}), and PMKH5 (PM7002 *minC::kan*^{R} + pMinCDE) were grown overnight in LB broth were equilibrated to the same optical density then spotted onto 1.5% LB agar contained in a Coverwell™ Imaging Chamber. Once the cells began to swarm, phase contrast images at 1,000X magnification of PM7002 (left), PMKH1 (center), and PMKH5 (right) were taken of the swarm front. (B) Western blot analysis of flagellin (FlaA) expression in PM7002 wild-type (lane 1), PM7002 *minC::kan*^{R} (lane 2), and PM7002 *minC::kan*^{R} and PM7002 *minC::kan*^{R} + pMinCDE (lane 3) cells harvested after 5 h of growth on LB agar plates. (C) DAPI staining of chromosomes in PM7002 (wild-type) and PMKH1 (PM7002 *minC::kan*^{R}) swarmer cells.

Figure 1

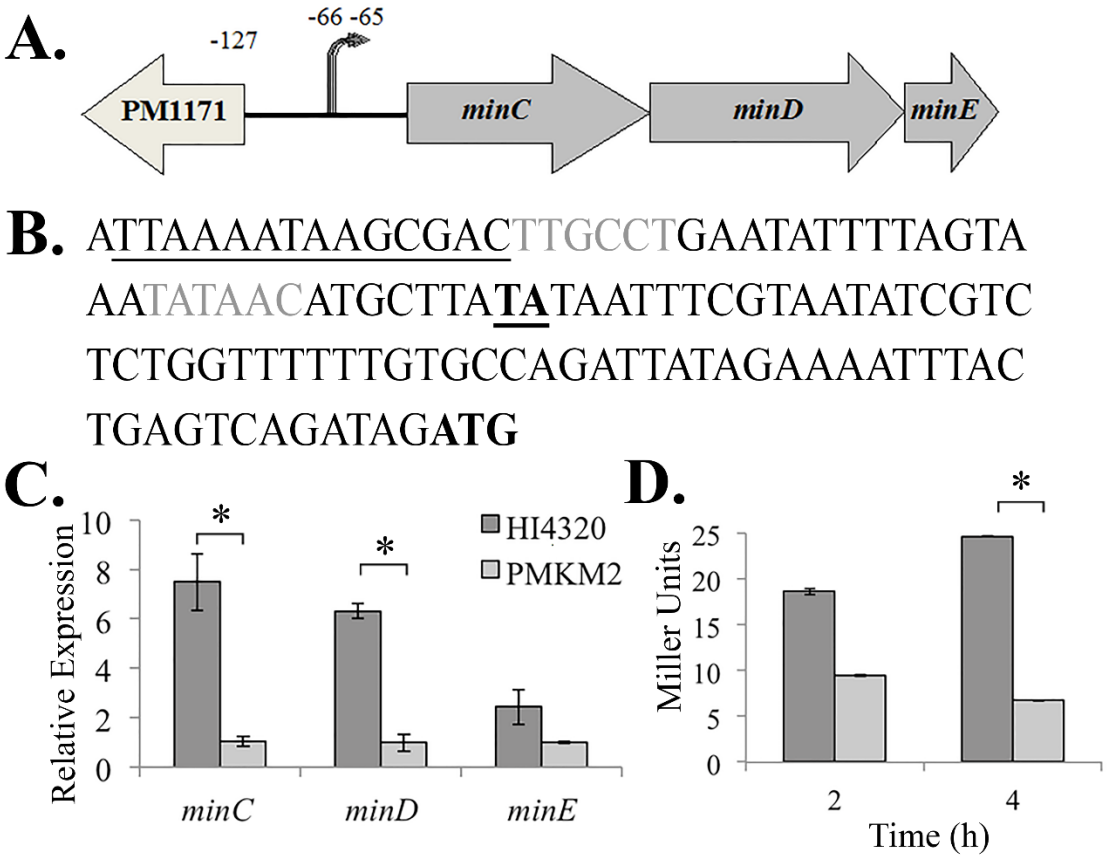
A.
-127
-66 -65
PM1171
minC
minD
minE
B.
ATTAAAATAAGCGACTTGCCTGAATATTTTAGTA
AATATAACATGCTTATATAATTTCGTAATATCGTC
TCTGGTTTTTTGTGCCAGATTATAGAAAATTTAC
TGAGTCAGATAGATG
C.
Relative Expression
10
8
6
4
2
0
*
*
HI4320
PMKM2
minC
minD
minE
D.
Miller Units
25
20
15
10
5
0
*
2
4
Time (h)

Figure 2

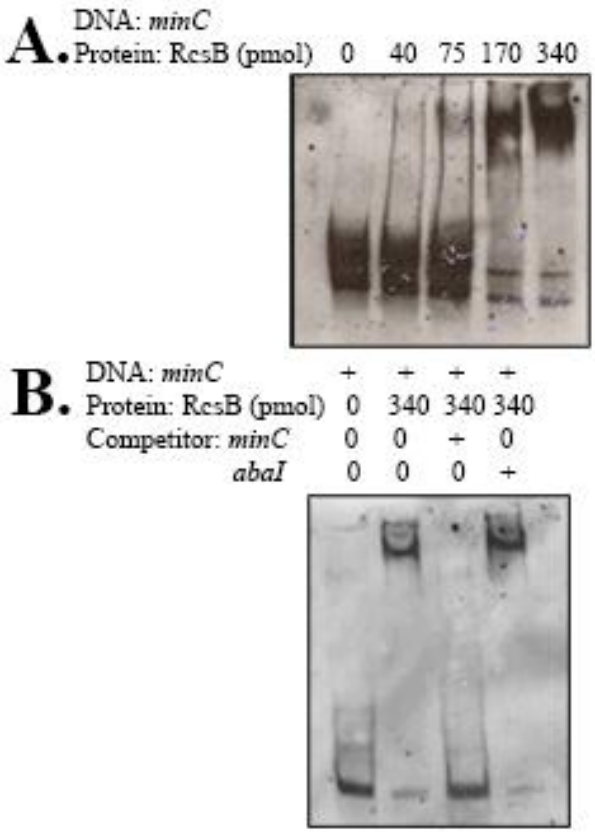
A.
DNA: minC
Protein: RcsB (pmol) 0 40 75 170 340
B.
DNA: minC + + + +
Protein: RcsB (pmol) 0 340 340 340
Competitor: minC 0 0 + 0
abaI 0 0 0 +

Figure 3

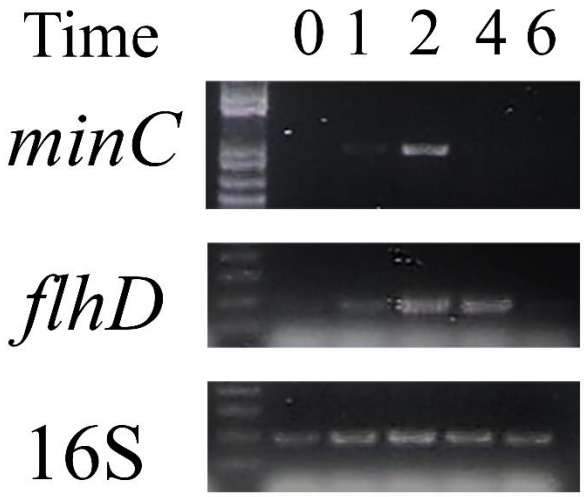

Figure 4

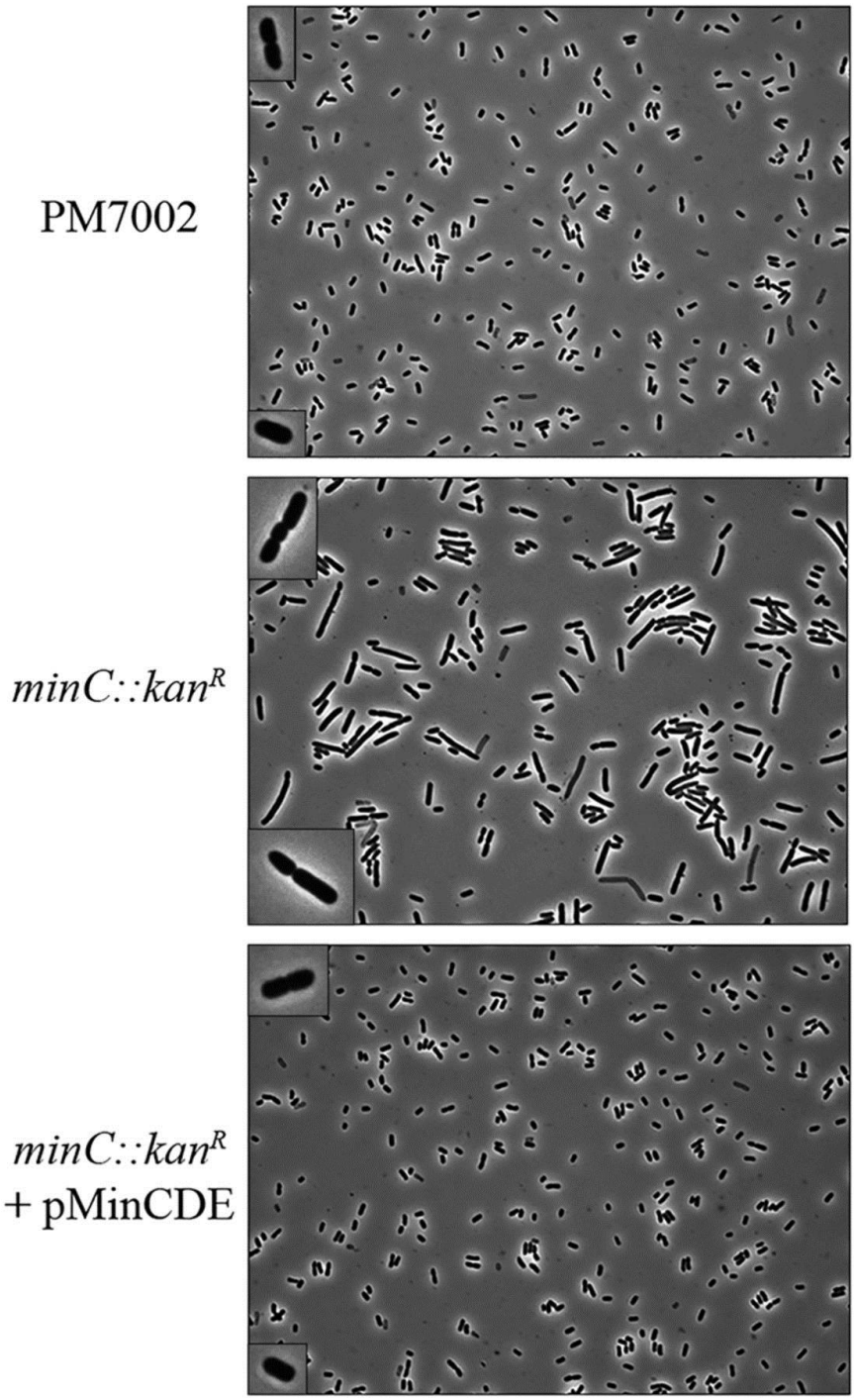

Figure 5

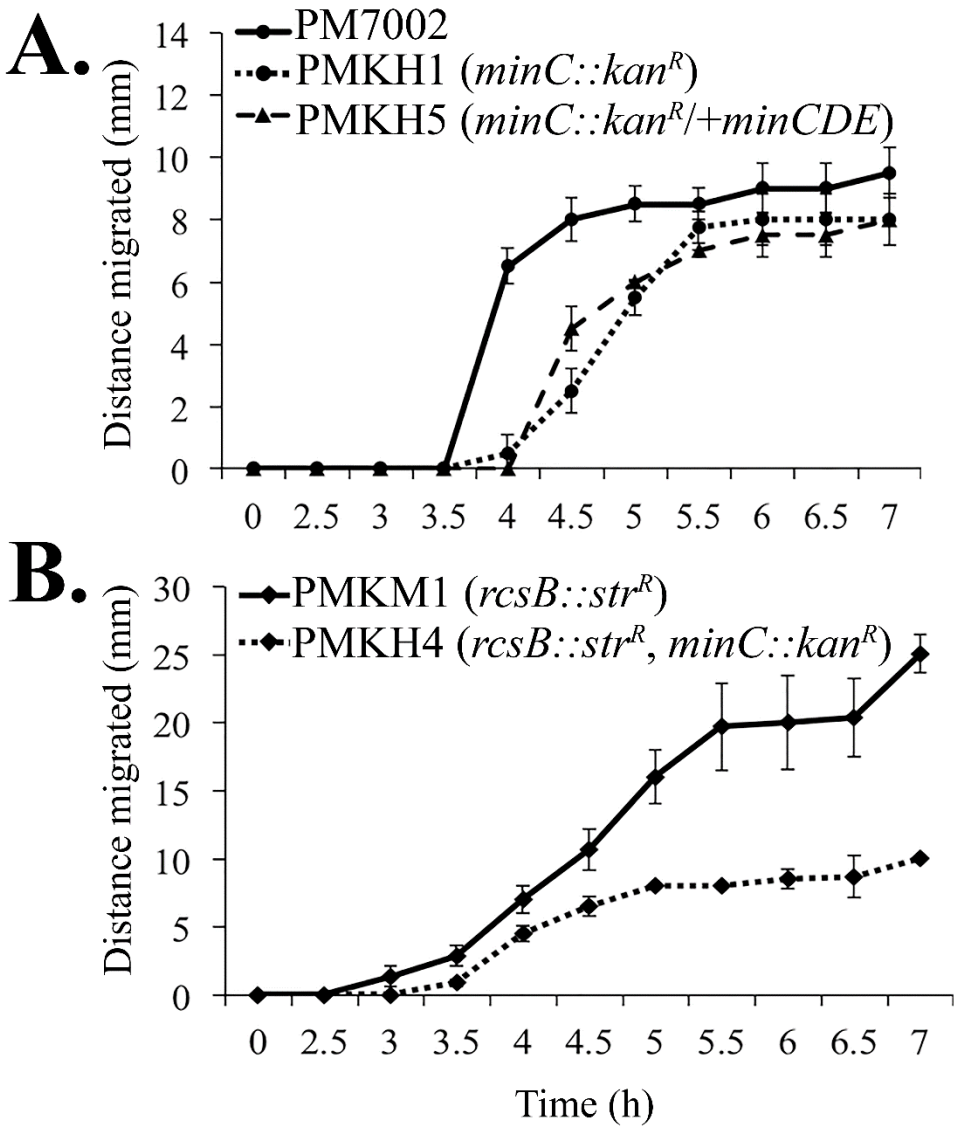
A.
PM7002
PMKH1 (minC::kan^R)
PMKH5 (minC::kan^R/+minCDE)
Distance migrated (mm)
0
2
4
6
8
10
12
14
0 2.5 3 3.5 4 4.5 5 5.5 6 6.5 7
B.
PMKM1 (rcsB::str^R)
PMKH4 (rcsB::str^R, minC::kan^R)
Distance migrated (mm)
0
5
10
15
20
25
30
0 2.5 3 3.5 4 4.5 5 5.5 6 6.5 7
Time (h)

Figure 6

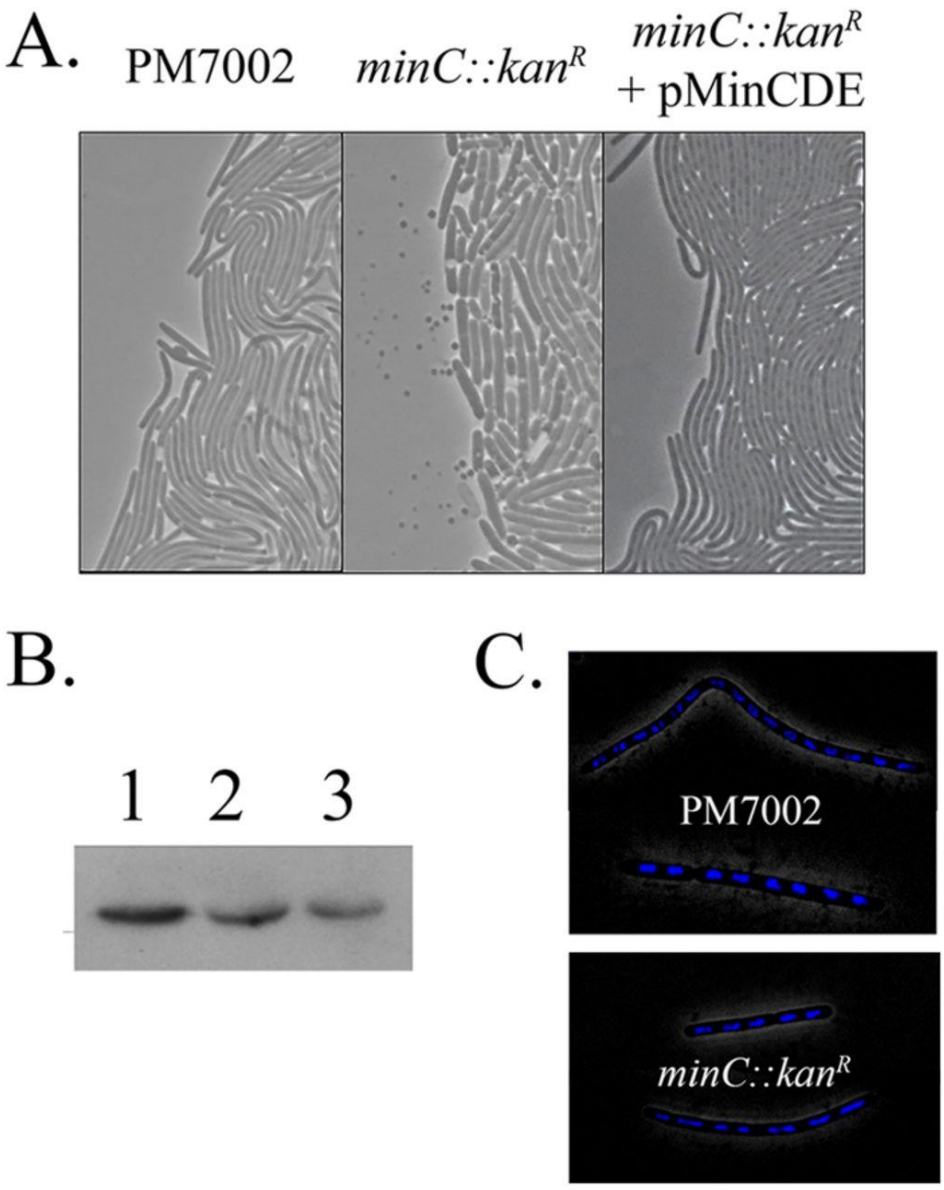

Chapter 3: The Rcs Regulon in *Proteus mirabilis*: Implications for Motility, Biofilm Formation, and Virulence

Kristen E. Howery[1], Katy M. Clemmer[2], and Philip N. Rather[1,2]

[1] Department of Microbiology and Immunology, Emory University, Atlanta, Georgia,
[2] Research Service, Atlanta VA Medical Center, Decatur, Georgia, USA

Published in:
Current Genetics, 2016
DOI: 10.1007/s00294-016-0579-1
p. 1-15

The manuscript was written by K.E.H. The manuscript was edited by K.M.C and P.N.R. K.M.C did RNA-sequencing and the data was analyzed by K.E.H. K.E.H performed the experiment for Fig. 1. P.N.R performed the experiment for Fig. 2.

Abstract.

The overall role of the Rcs phosphorelay in *Proteus mirabilis* is largely unknown. Previous work had demonstrated that the Rcs phosphorelay represses the *flhDC* operon and activates the *minCDE* cell division inhibition system. To identify additional cellular functions regulated by the Rcs phosphorelay, an analysis of RNA-Seq data was undertaken. In this report, the results of the RNA-sequencing are discussed with an emphasis on the predicted roles of the Rcs phosphorelay in swarmer cell differentiation, motility, biofilm formation, and virulence. RcsB is shown to activate genes important for differentiation and fimbriae formation, while repressing the expression of genes important for motility and virulence. Additionally, to follow up on the RNA-Seq data, we demonstrate that an *rcsB* mutant is deficient in its ability to form biofilm and exhibits enhanced virulence in a *Galleria mellonella* waxworm model. Overall, these results indicate the Rcs regulon in *P. mirabilis* extends beyond flagellar genes to include those involved in biofilm formation and virulence**.** Furthermore, the information presented in this study may provide clues to additional roles of the Rcs phosphorelay in other members of the *Enterobacteriaceae*.

Introduction.

The regulator of colonic acid capsule synthesis (Rcs) phosphorelay is a complex signal transduction system present in many members of the *Enterobacteriaceae*. In the swarming bacterium *P. mirabilis*, the Rcs phosphorelay controls swarmer cell differentiation, represses the *flhDC* operon and activates the *minCDE* cell division system (79, 253, 266) However, our knowledge of the role for the Rcs phosphorelay in other cellular functions in *P. mirabilis* is limited. Because of the importance of *P. mirabilis* as a human pathogen, we sought to identify additional functions for the Rcs phosphorelay in the physiology of this bacterium.

The Rcs phosphorelay was first identified during a screen to find genes necessary for capsular polysaccharide synthesis in *Escherichia coli* (293). Further studies revealed that it was not just a simple two-component system but a multifaceted variation known as a phosphorelay. The Rcs phosphorelay is comprised of a sensor kinase (RcsC) located at the inner membrane, a response regulator (RcsB) (293-295) and a phosphotransfer protein (RcsD). RcsD, previously known as YojN, mediates the transfer of the phosphate group from RcsC to RcsB (263). An additional protein, RcsA, is an auxiliary protein that assists RcsB binding at sites denoted as RcsAB boxes (296). Finally, the outer membrane lipoprotein RcsF transmits signals induced by membrane stress or other elements to RcsC thereby activating the phosphorelay (264, 297).

In addition to *cps*, other targets for Rcs regulation have been identified in *E. coli.* The cell division septum protein, FtsZ, responsible for Z-ring formation at the future site of cytokinesis is activated by RcsB (298). A related cell division protein, FtsA, which tethers FtsZ to the cell membrane, was also shown to be Rcs regulated (299). OsmC, a

reducer of organic hydroperoxides, and two other osmotically induced proteins, encoded by *osmB* and *osmY*, are all Rcs-activated genes (300, 301). RprA, a regulatory RNA also activated by RcsB, affects translation of RpoS, which connects the Rcs phosphorelay to the RpoS regulon (302). One target in particular, *flhDC*, encoding the regulator for flagellar synthesis, $FlhD_4C_2$, is repressed by the Rcs phosphorelay in *E. coli* (303) and *Salmonella enterica* (304). The relationship between the Rcs phosphorelay and *flhDC* regulation is one that has strong implications for motility and virulence, particularly for organisms that use motility as a means to establish infection.

P. mirabilis is a highly motile bacterium noted for its ability to change shape from short vegetative rod cells into elongated swarmer cells during a process known as differentiation. Differentiated swarmer cells are 20 to 50-fold longer than their vegetative counterparts and express thousands of flagella (252). Swarmer cells utilize a flagellum-dependent, multicellular form of motility known as swarming which is different from swimming motility. Swimming occurs when a single cell propels itself through liquid or soft agar. Swarming is a multicellular process where a group of cells producing massive amounts of interweaving flagella collectively align and form rafts which facilitate movement across a solid surface (17). Differentiation of rod-shaped cells into swarmer cells occurs upon contact with a solid surface. Elements that contribute to this process include O-antigen mediated cell surface perturbation (250), inhibition of flagellar rotation (18), and cell-to-cell signaling (22, 116, 257). After a period of migration, swarmer cells undergo consolidation or de-differentiation, which was once thought to be a resting period. However, during consolidation, cells are more metabolically active than swarming cells (192) and a prominent upregulation of genes involved in cell wall

synthesis, nutrient uptake, metabolism, and respiration occurs relative to swarming cells (65), indicating the cells are preparing for another period of energy-expensive swarming. The bulls-eye pattern *P. mirabilis* forms on agar plates is due to the oscillation between swarming and consolidation.

At the center of swarmer cell differentiation is the *flhDC* master operon, whose expression is dictated by a myriad of factors (22, 79, 250, 253, 260, 292, 305). The product of *flhDC*, $FlhD_4C_2$, is central to the activation of class II flagellar genes (148, 306), and hyper-flagellation is essential for the formation of swarmer cells (147). Expression of *flhDC* is high during initiation of swarming, but sharp decreases in *flhDC* expression can be observed shortly after differentiation occurs (148, 248) In addition to strict transcriptional control, the FlhD and FlhC proteins are tightly regulated post-translationally via proteolytic degradation (291). Modest changes in *flhDC* expression can have dramatic effects on the swarm phenotype. Overexpression of *flhDC* results in a hyperswarming phenotype (148), also known as precocious swarming, and *flhDC* mutants do not swarm.

Other mutations that result in hyperswarming include those in the RppAB two-component system (307) and the Rcs phosphorelay. It is common in bacteria to employ more than one two-component system to control differentiation (308). The first *rcs* mutations resulting in hyperswarming were in *rcsC* and *rcsD* (previously *rsbA*) (309). An *rcsB* mutant was later constructed, and it shared the hyperswarming phenotype with other mutants of the Rcs phosphorelay. The hyperswarming phenotype of the *rcsB* mutant is likely related to increased levels of *flhDC* observed in this strain (33), and RcsB has been shown to bind to the upstream region of *flhDC* in *E. coli* (16). In addition to

hyperswarming, *rcs* mutants elongate in liquid media, a non-permissive condition for differentiation, suggesting the Rcs phosphorelay influences the expression of genes important for differentiation. Interestingly, *flhDC* overexpression alone does not induce an elongated phenotype in liquid indicating additional *rcs* regulated genes control elongation (33).

Recently, RNA sequencing was performed on an *rcsB* mutant in *P. mirabilis* to identify Rcs regulated genes important for differentiation (3). This data set was compiled from three independent RNA-Seq analyses between wild-type and an RcsB mutant. However, when re-evaluating these data sets, additional RcsB regulated genes were identified resulting in 221 genes that were differentially regulated in an *rcsB* mutant when a 2-fold or greater cutoff is employed (Supplemental Table 1). To aid in determining whether RcsB is acting directly or indirectly on genes within its regulon, a bioinformatic approach was used to identify putative RcsB binding sites. The results of the RNA-Seq have predicted additional functions that may be controlled by the Rcs regulon in *P. mirabilis.* Specifically, the role of the Rcs regulon in differentiation, motility, self-recognition, adherence, biofilm formation and virulence are discussed. Lastly, to confirm these predictions, we experimentally verify that the Rcs phosphorelay is important for biofilm formation and influences virulence in *P. mirabilis*.

Materials and Methods.

Bacterial growth conditions. Except where indicated, *P. mirabilis* strains were grown in modified Luria-Bertani (LB) broth (10 g tryptone, 5 g yeast extract, 5 g NaCl per liter) at 37°C with shaking at 250 rpm. Agar was used at 30 g/L in plates to prevent swarming. Antibiotic selections included 35 µg/ml streptomycin.

Biofilm assays. *P. mirabilis* strain HI4320 or the isogenic *rcsB::Str*^{R} were grown overnight in LB with appropriate antibiotics at 37°C without shaking. Cells were equilibrated to the same optical density (A_{600}) and a 1:100 dilution of each strain was made in LB only. For the biofilm assays in 96-well polystyrene microtiter plates (Costar®), 150 µl of the diluted cultures were added to 8 wells of the microtiter plate and incubated in a humidified environment at 37°C for 8 or 24 h. The A_{600} was determined for each well to measure growth. Biofilms were stained with by adding 15 µl 0.4% crystal violet to the well and incubating for 15 min. Afterward, stained biofilms were rinsed with deionized water three times, and biofilms were resuspended in 200 µl 33% acetic acid. Biofilm was quantified by reading each sample at 580 nm and dividing that value by the A_{600} value for the same sample well. For biofilm assays on catheter, tweezers and scissors were pre-sterilized in 100% ethanol for 20 min. Siliconized latex catheters (Mentor) were cut into 0.25 inch pieces, flamed briefly, and 5 pieces of catheter were fused per well to the bottom of a 6-well plate (Costar®). 9.5 ml of a 1:100 diluted culture was added in duplicate to the plate containing catheter pieces to submerge them. An LB only control was used in duplicate. After 8 or 24 h of incubation in a humidified environment, 1 ml of the culture was removed to determine the A_{600}. If any piece of catheter detached from the bottom of the plate, it was discarded prior to staining.

Biofilms were stained by added 0.85 ml of 0.4% crystal violet to each well and incubated for 15 min. Liquid was removed from the wells, and catheters were rinsed three times by adding 10 ml deionized water to each well to remove planktonic cells. After rinsing, catheter pieces were removed and added to individual 1.5 ml microcentrifuge tubes where they were resuspended in 0.9 ml 33% acetic acid and vortexed for 2 min. Catheter pieces were removed from tubes and each sample tube was read at 580 nm. A_{580} values were adjusted for each strain by subtracting the average A_{580} value for catheter incubated in LB only. Biofilm was quantified by dividing the A_{580} value by the A_{600} value of the well where catheters were incubated.

Identification of potential RcsB binding sites of RcsB regulated genes. Based on known RcsB binding sites in *E. coli*, the pattern NNNGANNNNCNNN was used as the input for Computational Microbiology Laboratory (CMBL) Pattern Locator (PATLOC) program (63). The search was restricted to intergenic regions within the *P. mirabilis* HI4320 chromosome (NCBI RefSeq NC_010554.1). Genomic hits returned by PATLOC were compiled using a SAS program to restrict binding sites to RcsB-regulated genes identified using the RNA sequencing data. To confirm location and presence on the direct DNA strand, potential RcsB binding patterns were input into Nucleotide Basic Local Alignment Search Tool (BLAST) (38) version 2.2.32 adjusted for highly similar (megablast) and short input nucleotide sequences. Potential RcsB binding sequences located near defined or putative transcriptional regulatory regions were aligned to the consensus *E. coli* RcsAB box, TAAGAATATTCCTA, using a SAS program. Previously identified RcsB binding sequences in *E. coli* were also aligned. The SAS programs

written to compile genomic hits and align binding sequences are available from the authors upon request.

***Galleria mellonella* killing assays.** Cells of wild-type PM7002 or the isogenic *rcsB::Sm* mutant (33) were grown by shaking at 250 rpm in 2.5 ml of LB broth at 37^{o}C to an optical density (A_{600}) of 0.45. A 10^{-6} dilution was prepared in sterile LB and 5 µl representing 10 CFU for each strain was used to inject *G. mellonella* waxworms (200-250 mg each) in the second proleg. The *G. mellonella* worms were incubated at 37^{o}C in a humidified incubator and were checked at 24 hour intervals for killing. Worms were considered dead if they did not move when prodded with a pipette tip and were dark brown or black in color. A total of three independent experiments were conducted representing 28 worms for wild-type and 29 worms for the *rcsB* mutant.

Results.

RcsB activated genes identified by RNA-Seq

(i) Cell division and differentiation. Genes involved in cell division and thus septation have long been hypothesized to play a role in swarmer cell elongation, since the prevention of septation in *E. coli* results in filamentation (39). However, during a previous study to identify genes important for elongation in *P. mirabilis,* only *gidA,* involved in glucose-inhibited cell division, was isolated (40). Rcs activated genes involved in cell division include the Min cell division inhibition system, *ftsZ,* and *ftsA* (Table 1). The Min system is composed of three proteins, MinC, MinD, and MinE, which oscillate from pole to pole during cell division in order to keep FtsZ-mediated Z ring formation at the cell center (39,41). As previously noted, expression of *minC* and *minD* were reduced 3.4- and 6.74-fold respectively, in the *rcsB* mutant relative to wild-type (Table 1)(3). FtsZ is the bacterial homolog of tubulin and mediator of the Z ring (42). FtsA, which is structurally related to actin, is the protein that anchors the Z ring to the site of septation (43). *ftsZ* expression was reduced 3.33 fold- and *ftsA* expression was reduced 2.38-fold in *rcsB* mutant relative to wild-type (Table 1). This is consistent with previous studies demonstrating that *ftsZ* and *ftsA* were RcsB activated in *E. coli* (11, 12).

An additional Rcs-activated gene important for differentiation was *speB,* where expression was reduced 2.69-fold in the *rcsB* mutant relative to wild-type. SpeB functions as an agmatinase required for the conversion of agmatine to putrescine. Mutations in *speB* result in a delay in the onset of differentiation and shorter migration periods. This swarming defect could be rescued by the addition of extracellular putrescine (23).

(ii) Fimbriae production. *P. mirabilis* is known in a clinical setting for its ability to cause catheter-associated urinary tract infections (CAUTIs) which can lead to pyelonephritis, urolithiasis, and cystitis. It is not often found in patients undergoing short-term catheterization (44), but can be isolated from the urine of approximately 40% of patients undergoing long-term catheterization (45, 46). The first step in establishing a CAUTI is adherence to a catheter, which *P. mirabilis* readily does (47, 48). Fimbriae from other urinary tract pathogens have been implicated in the adherence to catheter material (49, 50). There are 17 putative fimbrial operons in the *P. mirabilis* HI4320 genome (51). The major fimbrial subunits of the mannose-resistant *Proteus*-like (MRP) fimbriae, the *P. mirabilis* fimbriae (PMF), and the Uroepithelial cell adhesin fimbriae (UCA) were all identified as Rcs-activated genes. Expression of *mrpA*, *pmfA* and *ucaA* was reduced 68.69-, 63.93-, and 6.96-fold, respectively, in the *rcsB* mutant relative to wild-type (Table 1). Additionally, the expression of an *mrpJ* paralog (PMI0261) and a fimbrial adhesin, *mrpH*, paralog (PMI0260) were reduced 28.86- and 12.15-fold (Table 1).

Given the importance of fimbriae to biofilm formation (52) (53) the Rcs-mediated activation of certain fimbrial genes in *P. mirabilis*, and the contribution of Rcs to biofilm formation in other bacteria (54, 55) biofilm assays were performed using *P. mirabilis* strain HI4320 and an isogenic *rcsB* mutant. After 8 h of incubation in 96-well polystyrene microtiter plates, the *rcsB* mutant was unable to form biofilm (Fig. 1A). After 24 h of incubation, the *rcsB* mutant formed 2.9-fold less biofilm than wild-type cells. The reduction in biofilm formation seen in the *rcsB* mutant at 24 h is unlikely to be the result of increased *flhDC* expression as a wild-type strain that overexpresses *flhDC* on a

plasmid (pACYC-*flhDC*) forms the same level of biofilm as cells containing the vector alone (Fig. S1). At 48 h the difference in biofilm formation was not statistically significant, although at this time point the wild-type biofilm had decreased 6.8-fold compared to 24 h. Biofilm reduction after longer periods of incubation is not an uncommon phenomenon and can be seen in other organisms (56, 57). The reduction over time in wild-type is not seen in the *rcsB* mutant, where only a 0.6-fold reduction in biofilm occurred between 24 and 48 h (Fig. 1A).

To examine the importance of *rcsB* to establishing CAUTIs, additional biofilm assays were performed using siliconized latex catheters. Recapitulating the results of the previous biofilm assays, the *rcsB* mutant did not form detectable biofilm on catheter after 8 h of incubation. After 24 h of incubation, the *rcsB* mutant did form biofilm, but 2.7-fold less than wild-type (Fig. 1B). Overall biofilm formation for both strains was higher on catheter material, with the exception of the *rcsB* mutant after 8 h of incubation. In fact, the wild-type strain formed 6.3-fold more biofilm on catheter (Fig. 1B) compared to polystyrene (Fig. 1A) after 8 h of incubation.

RcsB repressed genes

(i) Motility. As the Rcs phosphorelay is a well-characterized repressor of swarming, it was not surprising that a large number of flagellar genes were identified as Rcs-repressed (Table 2). There are 15 proteins that comprise the external structural proteins of the flagellum, and 13 of those were recognized as Rcs-repressed. They include the proximal rod (FlgB, FlgC, FlgF), the distal rod (FlgG) and rod cap (FlgJ), the hook (FlgE), the hook cap (FlgD), hook-length control protein (FliK), the hook-flagellar junction proteins (FlgK, FlgL), the major flagellar subunit (FlaA) and flagellar cap (FliD), and the anti-σ^{28}

regulatory protein (FlgM) (Table 2). Secretion of the structural proteins involves 7 proteins located within the flagellar basal body, 4 of which have been identified as Rcs-repressed (FlhB, FliF, FliO, and FliP). All 3 proteins which comprise the ATPase that drives export of flagellar components (FliI, FliH, and FliJ), the secretion chaperones (FlgN, FliS and FliT), and the alternative sigma factor FliA (σ^{28}) were all negatively regulated by RcsB (Table 2).

Additional flagellar proteins that were identified as Rcs-repressed are within the basal body and the flagellar motor. They include the flagellar basal body protein FliL, the L-ring protein FlgH, the P-ring proteins FlgA and FlgI, the MS-ring protein FliF, and the C ring proteins (FliG, FliM, and FliN). *motA*, *motB*, and all genes encoding members of the chemosensory (Che) complex with the exception of *cheW*, and two putative methyl-accepting chemotaxis proteins, PMI2808 and PMI2809, were also identified as negatively regulated by RcsB (Table 2).

Important regulators of flagellar synthesis, in addition to *fliA* (σ^{28}) and *flgM* (anti-σ^{28}), were repressed by RcsB. They include the class I operon for flagellar synthesis, *flhDC*; *umoA* and *umoD* (which were named for the upregulated expression of *flhDC*), and *fliZ*. Finally, *ccmA*, a gene important for cell shape and motility but unrelated to flagella production (58) was identified as Rcs-repressed (Table 2).

(ii) Virulence genes. RcsB influences the expression of two well-studied virulence genes, the IgA-degrading protease *zapA* and hemolysin (*hpmBA*). Both *zapA* and *zapB*, encoding a type-1 secretion ATP-binding protein, and *zapD*, encoding a Type I secretion outer membrane protein, were found to be Rcs-repressed. The expression of *zapA*, *zapB*, and *zapD* were upregulated 43.44-, 39.44-, and 13.87-fold, respectively, in the *rcsB*

mutant relative to wild-type (Table 2). Expression of the hemolysin encoding genes, *hpmA* and *hpmB,* was also up-regulated 12.51 and 10.41-fold, respectively, in the *rcsB* mutant relative to wild-type (Table 2).

The RNA-Seq data suggested that the virulence of an *rcsB* mutant might be enhanced as the *hpmBA* hemolysin and *zapAB* protease genes were overexpressed. To examine this, we used an invertebrate *G. mellonella* waxworm model. In three independent experiments, the average killing at day 1 after infection was 92% for the *rcsB* mutant versus 34% for wild-type cells (Fig. 2). At day 2, the percent killing was 96% for the *rcsB* mutant and 53% for wild-type and at day 3, the *rcsB* mutant killed 96% of the worms versus 60% for wild-type cells.

(iii) Self-recognition. *P. mirabilis* undergoes an interesting phenomenon during swarming where different strains will form boundaries (Dienes lines) between swarming colonies, but swarming colonies of the same strain will merge (59). The ability to distinguish between self and non-self has been well studied in *P. mirabilis* strain BB2000. Two systems, *ids* and *idr*, are important for self-recognition, and their products are exported by a type VI secretion system encoded by *tss* (60-62). The BB2000 homologs of *idsA* (PMI2990), *idrA* (PMI0750), and *idrB* (PMI0751) were all negatively regulated by RcsB (Table 2). PMI1117 (*hcp*) is a paralog of PMI0750, and PMI1118 is a paralog of PMI0751; both were identified as Rcs-repressed. Several homologs of the *tss* system were identified as Rcs-repressed. They include *tssA* (PMI0749), *tssB* (PMI0748), *tssC* (PMI0747), *tssE* (PMI0745), *tssF* (PMI0744), *tssH* (PMI0742), *tssI* (PMI0741), *tssJ* (PMI0740), and *tssL* (PMI0738) (Table 2). The *idr* and *tss* operons neighbor one another, are positioned divergently, and are separated by a large intergenic region (1,899 bp) on

the BB2000 chromosome. This organization is mimicked in HI4320 with PMI0250 being separated by an intergenic region of 2,396 bp from the BB2000 homolog of *tss*. However, none of the genes downstream of PMI0251 had significant sequence similarity to *idrC*, *idrD*, or *idrE*. Other Rcs-repressed genes, which could be involved in self-recognition include PMI1331, which shares 56 percent identity with IdsB, and PMI1332, which shares 44 percent identity with IdsF.

Identification of putative RcsB binding sites upstream of RcsB-regulated genes. As RcsB modulates the expression of known transcriptional regulators such as *flhDC*, *crp*, *rpoN*, and *rpoE*, a bioinformatic approach was used to identify potential RcsB binding sites upstream of genes identified by the RNA sequencing data. After aligning previously identified RcsB binding sites (12, 13, 16), it is clear that the guanine at position 4, the adenine at position 5, and the cytosine at position 10 are the most conserved residues within RcsB binding sites.

In addition, if point mutations are introduced into the adenine at position 5 or the cytosine at position 10, repression of *flhDC* expression is reduced in *E. coli* (16). In an *S. enterica* mutant where the Rcs system is constitutively active, a point mutation of the adenine, cytosine, or guanine at position 4 was able to restore swimming motility in the previously non-motile strain (17). These three sites within the RcsAB box are the only residues conserved across strains and multiple genes, both activated and repressed. Therefore, NNNGANNNNNCNNN was used as the input sequence for the Pattern Locator (PATLOC) program (63) against the *P. mirabilis* strain HI4320 genome. When used as the input for PATLOC, 4,605 genomic hits were returned. 21.47 % were within pseudogenes, 73.05% were intergenic, and 5.48% were partial overlaps. These hits were

compiled to be specific for genes identified using the RNA sequencing data. After compilation, the number of hits was reduced to intergenic or partially overlapping regions of 126 genes identified using RNA sequencing. Since PATLOC did not take into account whether the putative site was on the top or bottom strand, each potential sequence was input into BLAST to confirm its location and position. Previously proposed or experimentally identified transcriptional start sites and promoter regions were considered when determining a potential binding site. Thirty-four putative RcsB-binding sites were identified for RcsB-activated genes (Table 3), and thirty-one putative RcsB-binding sites were identified for RcsB-repressed genes (Table 4). These binding sites were aligned to the original consensus RcsAB box TAAGAATATTCCTA (64) based on the number of shared residues. The consensus RcsAB box was chosen for alignment as it is the originally defined binding sequence for RcsB, though there is divergence amongst identified RcsB binding sequences, and the RcsB binding site in *P. mirabilis* is unknown. Shared residues in aligned sequences are shown in red. In addition to putative binding sites, the known RcsA-independent RcsB binding sites for the promoters of *flhD, ftsA,* and *osmC* in *E. coli* are also aligned (12, 13, 16). The sequence for the RcsA-dependent RcsB binding site for the *flhD* promoter is also included (16). Their inclusion in the tables illustrates the divergence of identified RcsB binding sites from the consensus sequence. The fold-change in gene expression based on the RNA sequencing data and the location of binding site relative to important residues are also included in the table. Unfortunately, for many of the identified genes, no transcriptional start sites or promoters have been mapped and the relevance of the putative binding sites is unclear.

Of the Rcs-activated genes, *cfa* (encoding a cyclopropane fatty acyl phospholipid synthase), *eco* (encoding the protease inhibitor ecotin), and *mrpA* shared the most residues with the RcsB consensus sequence, with 11 out of 14 base pairs aligning with the sequence (Table 3). The location of the RcsB binding site of *mrpA* is next to the -35 region of a putative σ^{70} promoter, which was identified when the *mrp* operon was first sequenced (65). The *mrp* transcriptional start site and another σ^{70} promoter were recently identified within the invertible repeat region when the phase variable *mrp* operon is in ON phase (66). This places the putative binding site 100 base pairs downstream of the transcriptional start site. Regulatory elements of *cfa* or *eco* have not been identified.

Genes directly regulated by RcsB in other organisms, which were identified in *P. mirabilis* using RNA sequencing include *osmB* and *ftsA.* Their putative binding sites are located 60 and 396 base pairs, respectively, upstream of their start codons. The *osmB* sequences shares 9 out of 14 identities with the consensus RcsAB box and shares 10 out of 14 residues with the *osmCp1* RcsB binding sequence (13). The *ftsA* binding sequence shares 7 residues with the consensus sequence, but 9 with the *ftsA1p* binding site of *E. coli*. The putative RcsB binding site and the *ftsA1p* binding site are found in similar locations: at the center of *ftsQ* (12).

Of the Rcs-repressed genes, the identified RcsB binding site of *flhD* shared 11 out of 14 residues with the RcsAB consensus sequence and the RcsAB binding site of *flhD* in *E. coli* (16). It shared 9 residues with the RcsA-independent binding site *flhD3p* described in the same manuscript (Table 4). The putative *flhD* binding site is located two base pairs upstream of the mapped transcriptional start site (30, 33, 66). The putative RcsB binding sites of PMI1359, which encodes a putative attachment invasion outer

membrane protein, and PMI1075, a hypothetical protein with a domain of unknown function (DUF1795) aligned 10 of 14 residues with the RcsAB box. Many of the motility-associated genes have putative RcsB-binding sites overlapping their promoters (*hpmB*, *flaD*, *fliF*), start codons (*flgB*, *flgM*, *motA*) or transcriptional start sites (*flhB*). Additionally, the genes encoding self-recognition proteins PMI1117 (*hcp*/*idrA* homolog), PMI0750 (*idrA* paralog), and PMI2990 (*idsA* homolog) all share the same putative RcsB binding sequence in the same location (Table 4).

Discussion.

The importance of the Rcs phosphorelay in *P. mirabilis* has long been associated with the control of swarming via the negative regulation of *flhDC*. Through RNA sequencing, we have shown that the impact of Rcs on gene expression extends far beyond the inhibition of swarming-related genes. RcsB is not just a repressor of *flhDC*, but a repressor of many genes essential for motility, including flagella, chemotactic proteins, and positive regulators of motility. In addition, it represses the expression of virulence factors associated with swarmer cells, including *zapA* and hemolysin, and genes important for self-recognition. In contrast, RcsB is an activator of genes important for swarmer cell differentiation, including *minCDE* and *speB*, and also fimbrial genes, which are important for adherence and biofilm formation. This work will pave the way for future studies to identify the specific RcsB-regulated genes that carry out the above functions. In addition, the role of downstream transcriptional regulators in the overall RcsB regulon can be assessed.

As expected, RcsB was shown to negatively regulate the expression of flagellar structural genes and known activators of flagellar synthesis. The negative effect of RcsB on motility is seen in a myriad of bacterial species (8, 17, 55). A putative RcsB binding site was identified for the master operon for flagellar synthesis, *flhDC* (Table 4); this site shares high sequence homology to the RcsAB consensus binding site and is located in a similar region as the RcsB binding site of *flhD* in *E. coli*. RcsB-mediated regulation of *flg*, *fli*, or *flhBA* operons could be indirect, as $FlhD_4C_2$ has been shown to bind directly to these operons in *E. coli* (67). FliA, which also has a predicted RcsB binding motif (Table

4) has also been shown to bind directly upstream of *motAB-cheAW*, predicted methyl-accepting chemotaxis proteins, and the *E. coli* homolog of *flaA* (68).

The RNA sequencing data has revealed new processes controlled by RcsB. First, the expression of self-recognition systems involved in the territoriality of swarmer cells (*ids*, *idr*, *tss*) were repressed by RcsB. Since self-recognition systems are primarily observed under swarming permissive conditions, the increased expression of these genes when swarming has initiated would make biological sense. Second, expression of the *speB* gene, encoding agmatinase, was reduced 2.69-fold in the RcsB mutant (Table 1). SpeB is required for the production of putrescine and *speB* mutants exhibit a both delay in the onset of differentiation and a crippled swarming phenotype.

RcsB also regulated expression of the major fimbrial subunits of the uroepithelial cell adhesion (UCA), the *P. mirabilis* fimbriae (PMF), and the mannose-resistant *Proteus*-like (MR/P) fimbriae, which were highly down-regulated in the *rcsB* mutant relative to wild-type. Additional genes within each of these fimbrial operons were identified as Rcs-regulated. However, due to low levels of transcript reads, the *p*-values for each gene were too high to be deemed significant, and they were not included. RcsB has been shown to directly bind to the promoter region of the *mat* fimbriae and activate its expression in the *E. coli* (69). It also activates the transcription of the *fim* operon in *E. coli* by influencing the orientation of the *fimAp* invertible repeat (70). In addition, *fim* genes are positively regulated by RcsB in *S. enterica* serovar typhimurium (17). Identification of major fimbrial subunits in *P. mirabilis* as RcsB regulated is important, as all three systems have been implicated in virulence. Though the contribution of *P. mirabilis* fimbriae to catheter adherence has not been well-characterized, their importance

to the establishment of urinary tract infections has been recognized. Mutations in *ucaA* lead to impaired adhesion to uroepithelial cells and in the ability to colonize the kidneys of mice (71). Mutants of *pmfA* have been shown to be deficient in bladder colonization in a mouse model of ascending urinary tract infection, but able to colonize the kidneys (72). Another study showed that *pmfA* mutants were unable to colonize the bladder and the kidneys (73). The ability of a *pmfA* mutant to adhere to uroepithelial cells also differed between these two reports. The differences seen between these two studies could be due to the route of infection, different strains of mice, uroepithelial cells, and *P. mirabilis*. Mutants of *mrpA* reduce *P. mirabilis* colonization of the bladder, kidneys, and urine of mice (74, 75). M/RP fimbriae are also important for adherence to uroepithelial cells (75) and biofilm formation in *P. mirabilis* (52).

mrpJ has 14 paralogues in *P. mirabilis* strain HI4320, and many of them repress motility (76). MrpJ itself has been shown to directly repress *flhDC* expression (66, 77). One *mrpJ* paralog, PMI0261, was highly repressed in the *rcsB* mutant based on our RNA sequencing data. The neighboring *mrpH* paralog, PMI0260, was also significantly down-regulated in the *rcsB* relative to wild-type. Expression of the *mrpA* paralog of this operon (PMI0254) was also reduced in the *rcsB* mutant relative to wild-type as well as other members of the paralog operon. Their exclusion is due to a high *p*-value which resulted from low transcript levels. Why the two terminal genes of this operon produced more read transcript relative to the rest of operon members is unknown. An internal promoter could exist or perhaps more levels of *mrpH* and *mrpJ* are required to initiate transcription of the operon, as *mrpJ* binds and activates expression of *mrpA* (66), and assembly of the fimbriae, which *mrpH* is essential for (78). However, PMI0256, encoding a fimbrial

chaperone *mrpD* paralog, is a pseudogene due to the presence of a stop codon. This likely renders this *mrp* paralog non-functional. Overexpression of PMI0261 has been shown to reduce motility in *P. mirabilis* (76) in the same manner as *mrpJ*, illustrating its function in counteracting motility is intact. The negative impact fimbrial activators have on motility makes biological sense as motile bacteria would not want to express adherence factors and vice versa.

The formation of biofilms was strongly impacted by the *rcsB* mutation. Two different biofilm assays were performed, one using polystyrene (Fig.1A) and the other using catheter sections as biofilm substrates (Fig. 1B). With polystyrene as the substrate, the *rcsB* mutant formed no detectable biofilm after 8 h of incubation, formed 2.9-fold less biofilm than wild-type after 24 h, and formed similar amounts of biofilm as wild-type after 48 h of incubation. The wild-type strain exhibited a large reduction in biofilm formation between 24 and 48 h of incubation which was not as exaggerated in the *rcsB* mutant (Fig. 1A). The inability of the *rcsB* mutant to form biofilm was recapitulated when assays were performed on catheters. Again, it did not form detectable biofilm after 8 h of incubation, and formed 2.7-fold less biofilm than wild-type after 24 h of incubation (Fig. 1B). The inability of the *rcsB* mutant to form biofilm initially may be due to the down-regulation of adherence factors, such as the major fimbrial subunits (*ucaA*, *pmfA*, and *mrpA*). Rcs mutants of *Yersinia pseudotuberculosis* are deficient in their ability to adhere to HEp-2 cells and form biofilm on abiotic surfaces; fimbrial proteins are a part of its RcsB regulon (55). Our RNA-Seq data also showed that outer membrane protein A (*ompA*) is highly repressed in the *rcsB* mutant; it has been shown to bind abiotic surfaces, which could contribute to initial adherence (79). However, other factors are likely

mediating adherence as the *rcsB* mutant does form biofilm after 24 h of incubation. Like wild-type cells, biofilm production of the *rcsB* mutant decreases after 48 h. Overall these data, combined with a previous report that a *P. mirabilis rcsD* mutant is deficient in biofilm production (37), reiterate the contribution of the Rcs phosphorelay to biofilm formation in *P. mirabilis*. These results also suggest a preference for *P. mirabilis* to form biofilm on catheter versus polystyrene, a medically relevant finding, as the wild-type strain formed 6.8-fold more biofilm on catheter versus polystyrene after 8 h of incubation.

The virulence genes *zapAB* and *hpmBA* were strongly upregulated in the *rcsB* mutant; both have increased expression in swarming bacteria (80, 81). ZapA is a metalloprotease, which cleaves immunoglobulins (82), host cytoskeletal and matrix proteins, complement (C1q and C3), and antimicrobial peptides (human beta-defensin 1 and LL-37) (83). It is important for the colonization and subsequent infection of the urinary tract (84). HpmA functions as a hemolysin (85, 86) and induces cytotoxicity (87). Virulence proteins are RcsB regulated in *Y. psuedotuberculosis*, and genes within the *Salmonella enterica* serovar typhimurium SP-2 pathogenicity island are highly repressed by RcsB (17, 55). Additionally, a mutant of *S. enterica* with a constitutively activated Rcs system is attenuated in virulence within a mouse (88). Based on these studies and our RNA-Seq data, it was hypothesized that RcsB would regulate virulence in *P. mirabilis.* This was tested using a *Galleria mellonella* waxworm model. It should be noted that this model has not been previously used in *P. mirabilis,* although it has been used in other bacteria, where a good correlation has been observed with mammalian virulence (89-93). Moreover, the relevance of this model to a mouse model of urinary tract infection is

unknown, but this model was only intended to measure general differences in virulence. One day after inoculation, the *rcsB* mutant had killed 94 percent of worms versus 37 percent for wild-type HI4320. By day three, the *rcsB* mutant had killed 96 percent of worms versus 60 percent of wild-type.

A putative RcsB binding sequence lies upstream of the *hpmBA* operon, but not upstream of the *zap* operon. RcsB has been shown to directly bind to the promoter region of the hemolysin homolog (*shlBA*) in *Serratia marcescens* (94), and our putative RcsB binding site does overlap the σ^{28} promoter identified by Fraser et al. However, a limitation exists in our identification of putative RcsB binding sites. By using NNNGANNNNCNNN as the input, many genomic hits were returned to due the sequence being nonspecific. The input sequence retaining only 3 of 14 base pairs is due to the variability in known RcsB binding sites. The original RcsAB Box was defined as TaAGaataTCctA, with capital letters being the most conserved residues (64). This binding site was defined based on the RcsA-dependent RcsB binding site of 12 promoters that were RcsAB regulated. It does not take into account sequence of RcsA-independent RcsB binding sites of multiple genes. Presently, the RcsB binding site in *P. mirabilis* is unknown.

The role of the Rcs phosphorelay in establishing CAUTIs has not been determined, but likely depends on whether the swarmer cell or swimmer cell is more important for colonization of the urinary tract. Conflicting data exist concerning this topic. Studies have shown that differentiated swarmer cells invade uroepithelial cells more efficiently than vegetative cells (95), and non-swarming mutants are unable to establish ascending urinary tract infections or kill mice (96, 97). Other studies have

shown swimmer cells, not swarmer cells, are the dominant cell morphology in a mouse model of ascending urinary tract infection (98) and non-flagellated *P. mirabilis* were isolated from a human infection (99). Corroborating these studies is one that showed flagellar genes were down-regulated during the early stages of ascending urinary tract infection. Fimbrial genes, associated with swimmer cells, were upregulated during early infection (100). Perhaps swarmer cells are needed to establish infection, as *P. mirabilis* readily moves across catheters (101), but the antigenic potential due to flagellar components and cell length leads to immune recognition. This leads to the selection of swimmer cells in the urinary tract. The upregulation of fimbriae during colonization offers another set of antigens subject to immune recognition. To counteract this, *P. mirabilis* may differentiate into swarmer cells during later stages of infection, consistent with a previous study where fimbrial gene expression decreased while the expression of some flagellar genes increased during the later stages of a mouse ascending urinary tract infection (100). The possibility of cycling differentiation and consolidation during infection reiterates the origin of the name *Proteus*, named for a god who changed shape to avoid capture and questioning. The interplay of the Rcs phosphorelay, together with additional important genetic factors contributes to this elusive change in cell morphology and affects motility, biofilm formation, and virulence in *P. mirabilis*.

Acknowledgements. This work was supported by a Merit Review award 1IOIBX001725 and by a Research Career Scientist award to P.N.R., both from the Department of Veterans Affairs. K.H. was supported by the Burroughs Wellcome Fund's Molecules to Mankind program. The authors thank Lewis Jordan, PhD for aid in the bioinformatic identification of RcsB binding sites.

References.

1. **Belas R, Schneider R, Melch M.** 1998. Characterization of Proteus mirabilis precocious swarming mutants: identification of rsbA, encoding a regulator of swarming behavior. J Bacteriol **180:**6126-6139.
2. **Liaw SJ, Lai HC, Ho SW, Luh KT, Wang WB.** 2001. Characterisation of p-nitrophenylglycerol-resistant Proteus mirabilis super-swarming mutants. J Med Microbiol **50:**1039-1048.
3. **Howery KE, Clemmer KM, Simsek E, Kim M, Rather PN.** 2015. Regulation of the Min Cell Division Inhibition Complex by the Rcs Phosphorelay in Proteus mirabilis. Journal of Bacteriology **197:**2499-2507.
4. **Gottesman S, Trisler P, Torres-Cabassa A.** 1985. Regulation of capsular polysaccharide synthesis in Escherichia coli K-12: characterization of three regulatory genes. J Bacteriol **162:**1111-1119.
5. **Brill JA, Quinlan-Walshe C, Gottesman S.** 1988. Fine-structure mapping and identification of two regulators of capsule synthesis in Escherichia coli K-12. J Bacteriol **170:**2599-2611.
6. **Stout V, Gottesman S.** 1990. RcsB and RcsC: a two-component regulator of capsule synthesis in Escherichia coli. J Bacteriol **172:**659-669.
7. **Majdalani N, Heck M, Stout V, Gottesman S.** 2005. Role of RcsF in signaling to the Rcs phosphorelay pathway in Escherichia coli. J Bacteriol **187:**6770-6778.
8. **Takeda S, Fujisawa Y, Matsubara M, Aiba H, Mizuno T.** 2001. A novel feature of the multistep phosphorelay in Escherichia coli: a revised model of the RcsC --> YojN -->

RcsB signalling pathway implicated in capsular synthesis and swarming behaviour. Mol Microbiol **40:**440-450.

9. **Pristovsek P, Sengupta K, Lohr F, Schafer B, von Trebra MW, Ruterjans H, Bernhard F.** 2003. Structural analysis of the DNA-binding domain of the Erwinia amylovora RcsB protein and its interaction with the RcsAB box. J Biol Chem **278:**17752-17759.

10. **Castanie-Cornet MP, Cam K, Jacq A.** 2006. RcsF is an outer membrane lipoprotein involved in the RcsCDB phosphorelay signaling pathway in Escherichia coli. J Bacteriol **188:**4264-4270.

11. **Gervais FG, Phoenix P, Drapeau GR.** 1992. The rcsB gene, a positive regulator of colanic acid biosynthesis in Escherichia coli, is also an activator of ftsZ expression. J Bacteriol **174:**3964-3971.

12. **Carballes F, Bertrand C, Bouche JP, Cam K.** 1999. Regulation of Escherichia coli cell division genes ftsA and ftsZ by the two-component system rcsC-rcsB. Mol Microbiol **34:**442-450.

13. **Davalos-Garcia M, Conter A, Toesca I, Gutierrez C, Cam K.** 2001. Regulation of osmC gene expression by the two-component system rcsB-rcsC in Escherichia coli. J Bacteriol **183:**5870-5876.

14. **Hagiwara D, Sugiura M, Oshima T, Mori H, Aiba H, Yamashino T, Mizuno T.** 2003. Genome-wide analyses revealing a signaling network of the RcsC-YojN-RcsB phosphorelay system in Escherichia coli. J Bacteriol **185:**5735-5746.

15. **Majdalani N, Hernandez D, Gottesman S.** 2002. Regulation and mode of action of the second small RNA activator of RpoS translation, RprA. Mol Microbiol **46:**813-826.

16. **Francez-Charlot A, Laugel B, Van Gemert A, Dubarry N, Wiorowski F, Castanie-Cornet MP, Gutierrez C, Cam K.** 2003. RcsCDB His-Asp phosphorelay system negatively regulates the flhDC operon in Escherichia coli. Mol Microbiol **49:**823-832.

17. **Wang Q, Zhao Y, McClelland M, Harshey RM.** 2007. The RcsCDB signaling system and swarming motility in Salmonella enterica serovar typhimurium: dual regulation of flagellar and SPI-2 virulence genes. J Bacteriol **189:**8447-8457.

18. **HOENIGER JFM.** 1965. Development of Flagella by Proteus mirabilis. Microbiology **40:**29-42.

19. **Jones BV, Young R, Mahenthiralingam E, Stickler DJ.** 2004. Ultrastructure of Proteus mirabilis swarmer cell rafts and role of swarming in catheter-associated urinary tract infection. Infect Immun **72:**3941-3950.

20. **Morgenstein RM, Clemmer KM, Rather PN.** 2010. Loss of the waaL O-antigen ligase prevents surface activation of the flagellar gene cascade in Proteus mirabilis. J Bacteriol **192:**3213-3221.

21. **Rauprich O, Matsushita M, Weijer CJ, Siegert F, Esipov SE, Shapiro JA.** 1996. Periodic phenomena in Proteus mirabilis swarm colony development. Journal of Bacteriology **178:**6525-6538.

22. **Fraser GM, Bennett JCQ, Hughes C.** 1999. Substrate-specific binding of hook-associated proteins by FlgN and FliT, putative chaperones for flagellum assembly. Molecular Microbiology **32:**569-580.

23. **Sturgill G, Rather PN.** 2004. Evidence that putrescine acts as an extracellular signal required for swarming in Proteus mirabilis. Mol Microbiol **51:**437-446.

24. **Belas R, Suvanasuthi R.** 2005. The ability of Proteus mirabilis to sense surfaces and regulate virulence gene expression involves FliL, a flagellar basal body protein. J Bacteriol **187:**6789-6803.

25. **Armitage JP.** 1981. Changes in metabolic activity of Proteus mirabilis during swarming. J Gen Microbiol **125:**445-450.

26. **Pearson MM, Rasko DA, Smith SN, Mobley HL.** 2010. Transcriptome of swarming Proteus mirabilis. Infect Immun **78:**2834-2845.

27. **Dufour A, Furness RB, Hughes C.** 1998. Novel genes that upregulate the Proteus mirabilis flhDC master operon controlling flagellar biogenesis and swarming. Molecular Microbiology **29:**741-751.

28. **Stevenson LG, Rather PN.** 2006. A novel gene involved in regulating the flagellar gene cascade in Proteus mirabilis. J Bacteriol **188:**7830-7839.

29. **Clemmer KM, Rather PN.** 2008. The Lon protease regulates swarming motility and virulence gene expression in Proteus mirabilis. Journal of Medical Microbiology **57:**931-937.

30. **Furness RB, Fraser GM, Hay NA, Hughes C.** 1997. Negative feedback from a Proteus class II flagellum export defect to the flhDC master operon controlling cell division and flagellum assembly. Journal of Bacteriology **179:**5585-5588.

31. **Claret L, Hughes C.** 2000. Functions of the subunits in the FlhD(2)C(2) transcriptional master regulator of bacterial flagellum biogenesis and swarming. J Mol Biol **303:**467-478.

32. **Gygi D, Bailey MJ, Allison C, Hughes C.** 1995. Requirement for FlhA in flagella assembly and swarm-cell differentiation by Proteus mirabilis. Mol Microbiol **15:**761-769.

33. **Clemmer KM, Rather PN.** 2007. Regulation of flhDC expression in Proteus mirabilis. Research in Microbiology **158:**295-302.

34. **Claret L, Hughes C.** 2000. Rapid Turnover of FlhD and FlhC, the Flagellar Regulon Transcriptional Activator Proteins, duringProteus Swarming. Journal of Bacteriology **182:**833-836.

35. **Wang WB, Chen IC, Jiang SS, Chen HR, Hsu CY, Hsueh PR, Hsu WB, Liaw SJ.** 2008. Role of RppA in the regulation of polymyxin b susceptibility, swarming, and virulence factor expression in Proteus mirabilis. Infect Immun **76:**2051-2062.

36. **Kovacs AT.** 2016. Bacterial differentiation via gradual activation of global regulators. Curr Genet **62:**125-128.

37. **Liaw SJ, Lai HC, Wang WB.** 2004. Modulation of swarming and virulence by fatty acids through the RsbA protein in Proteus mirabilis. Infect Immun **72:**6836-6845.

38. **Altschul SF, Madden TL, Schaffer AA, Zhang J, Zhang Z, Miller W, Lipman DJ.** 1997. Gapped BLAST and PSI-BLAST: a new generation of protein database search programs. Nucleic Acids Res **25:**3389-3402.

39. **de Boer PA, Crossley RE, Rothfield LI.** 1990. Central role for the Escherichia coli minC gene product in two different cell division-inhibition systems. Proc Natl Acad Sci U S A **87:**1129-1133.

40. **Belas R, Goldman M, Ashliman K.** 1995. Genetic analysis of Proteus mirabilis mutants defective in swarmer cell elongation. J Bacteriol **177:**823-828.

41. **Ward JE, Jr., Lutkenhaus J.** 1985. Overproduction of FtsZ induces minicell formation in E. coli. Cell **42:**941-949.

42. **Bi EF, Lutkenhaus J.** 1991. FtsZ ring structure associated with division in Escherichia coli. Nature **354:**161-164.

43. **Pichoff S, Lutkenhaus J.** 2005. Tethering the Z ring to the membrane through a conserved membrane targeting sequence in FtsA. Mol Microbiol **55:**1722-1734.

44. **Matsukawa M, Kunishima Y, Takahashi S, Takeyama K, Tsukamoto T.** 2005. Bacterial colonization on intraluminal surface of urethral catheter. Urology **65:**440-444.

45. **O'Hara CM, Brenner FW, Miller JM.** 2000. Classification, identification, and clinical significance of Proteus, Providencia, and Morganella. Clin Microbiol Rev **13:**534-546.

46. **Jacobsen SM, Stickler DJ, Mobley HL, Shirtliff ME.** 2008. Complicated catheter-associated urinary tract infections due to Escherichia coli and Proteus mirabilis. Clin Microbiol Rev **21:**26-59.

47. **Roberts JA, Fussell EN, Kaack MB.** 1990. Bacterial adherence to urethral catheters. J Urol **144:**264-269.

48. **Stickler DJ, Lear JC, Morris NS, Macleod SM, Downer A, Cadd DH, Feast WJ.** 2006. Observations on the adherence of Proteus mirabilis onto polymer surfaces. J Appl Microbiol **100:**1028-1033.

49. **Mobley HL, Chippendale GR, Tenney JH, Mayrer AR, Crisp LJ, Penner JL, Warren JW.** 1988. MR/K hemagglutination of Providencia stuartii correlates with adherence to catheters and with persistence in catheter-associated bacteriuria. J Infect Dis **157:**264-271.

50. **Yakubu DE, Old DC, Senior BW.** 1989. The haemagglutinins and fimbriae of Proteus penneri. J Med Microbiol **30:**279-284.

51. **Pearson MM, Sebaihia M, Churcher C, Quail MA, Seshasayee AS, Luscombe NM, Abdellah Z, Arrosmith C, Atkin B, Chillingworth T, Hauser H, Jagels K, Moule S, Mungall K, Norbertczak H, Rabbinowitsch E, Walker D, Whithead S, Thomson NR, Rather PN, Parkhill J, Mobley HL.** 2008. Complete genome sequence of uropathogenic Proteus mirabilis, a master of both adherence and motility. J Bacteriol **190:**4027-4037.

52. **Jansen AM, Lockatell V, Johnson DE, Mobley HL.** 2004. Mannose-resistant Proteus-like fimbriae are produced by most Proteus mirabilis strains infecting the urinary tract, dictate the in vivo localization of bacteria, and contribute to biofilm formation. Infect Immun **72:**7294-7305.

53. **Rocha SP, Pelayo JS, Elias WP.** 2007. Fimbriae of uropathogenic Proteus mirabilis. FEMS Immunol Med Microbiol **51:**1-7.

54. **Ferrieres L, Clarke DJ.** 2003. The RcsC sensor kinase is required for normal biofilm formation in Escherichia coli K-12 and controls the expression of a regulon in response to growth on a solid surface. Mol Microbiol **50:**1665-1682.

55. **Hinchliffe SJ, Howard SL, Huang YH, Clarke DJ, Wren BW.** 2008. The importance of the Rcs phosphorelay in the survival and pathogenesis of the enteropathogenic yersiniae. Microbiology **154:**1117-1131.

56. **Jackson DW, Suzuki K, Oakford L, Simecka JW, Hart ME, Romeo T.** 2002. Biofilm formation and dispersal under the influence of the global regulator CsrA of Escherichia coli. J Bacteriol **184:**290-301.

57. **Berne C, Kysela DT, Brun YV.** 2010. A bacterial extracellular DNA inhibits settling of motile progeny cells within a biofilm. Mol Microbiol **77:**815-829.

58. **Hay NA, Tipper DJ, Gygi D, Hughes C.** 1999. A novel membrane protein influencing cell shape and multicellular swarming of Proteus mirabilis. J Bacteriol **181:**2008-2016.

59. **Dienes L.** 1946. Reproductive processes in Proteus cultures. J Bacteriol **51:**585.

60. **Gibbs KA, Urbanowski ML, Greenberg EP.** 2008. Genetic determinants of self identity and social recognition in bacteria. Science **321:**256-259.

61. **Wenren LM, Sullivan NL, Cardarelli L, Septer AN, Gibbs KA.** 2013. Two independent pathways for self-recognition in Proteus mirabilis are linked by type VI-dependent export. MBio **4**.

62. **Alteri CJ, Himpsl SD, Pickens SR, Lindner JR, Zora JS, Miller JE, Arno PD, Straight SW, Mobley HLT.** 2013. Multicellular Bacteria Deploy the Type VI Secretion System to Preemptively Strike Neighboring Cells. PLoS Pathog **9:**e1003608.

63. **Mrazek J, Xie S.** 2006. Pattern locator: a new tool for finding local sequence patterns in genomic DNA sequences. Bioinformatics **22:**3099-3100.

64. **Wehland M, Bernhard F.** 2000. The RcsAB box. Characterization of a new operator essential for the regulation of exopolysaccharide biosynthesis in enteric bacteria. J Biol Chem **275:**7013-7020.

65. **Bahrani FK, Mobley HL.** 1994. Proteus mirabilis MR/P fimbrial operon: genetic organization, nucleotide sequence, and conditions for expression. J Bacteriol **176:**3412-3419.

66. **Bode NJ, Debnath I, Kuan L, Schulfer A, Ty M, Pearson MM.** 2015. Transcriptional analysis of the MrpJ network: modulation of diverse virulence-associated genes and direct regulation of mrp fimbrial and flhDC flagellar operons in Proteus mirabilis. Infect Immun **83:**2542-2556.

67. **Claret L, Hughes C.** 2002. Interaction of the atypical prokaryotic transcription activator FlhD2C2 with early promoters of the flagellar gene hierarchy. J Mol Biol **321:**185-199.

68. **Fitzgerald DM, Bonocora RP, Wade JT.** 2014. Comprehensive mapping of the Escherichia coli flagellar regulatory network. PLoS Genet **10:**e1004649.

69. **Lehti TA, Bauchart P, Dobrindt U, Korhonen TK, Westerlund-Wikstrom B.** 2012. The fimbriae activator MatA switches off motility in Escherichia coli by repression of the flagellar master operon flhDC. Microbiology **158:**1444-1455.

70. **Schwan WR, Shibata S, Aizawa S, Wolfe AJ.** 2007. The two-component response regulator RcsB regulates type 1 piliation in Escherichia coli. J Bacteriol **189:**7159-7163.

71. **Pellegrino R, Scavone P, Umpierrez A, Maskell DJ, Zunino P.** 2013. Proteus mirabilis uroepithelial cell adhesin (UCA) fimbria plays a role in the colonization of the urinary tract. Pathog Dis **67:**104-107.

72. **Massad G, Lockatell CV, Johnson DE, Mobley HL.** 1994. Proteus mirabilis fimbriae: construction of an isogenic pmfA mutant and analysis of virulence in a CBA mouse model of ascending urinary tract infection. Infect Immun **62:**536-542.

73. **Zunino P, Sosa V, Allen AG, Preston A, Schlapp G, Maskell DJ.** 2003. Proteus mirabilis fimbriae (PMF) are important for both bladder and kidney colonization in mice. Microbiology **149:**3231-3237.

74. **Bahrani FK, Massad G, Lockatell CV, Johnson DE, Russell RG, Warren JW, Mobley HL.** 1994. Construction of an MR/P fimbrial mutant of Proteus mirabilis: role in virulence in a mouse model of ascending urinary tract infection. Infect Immun **62:**3363-3371.

75. **Zunino P, Geymonat L, Allen AG, Preston A, Sosa V, Maskell DJ.** 2001. New aspects of the role of MR/P fimbriae in Proteus mirabilis urinary tract infection. FEMS Immunol Med Microbiol **31:**113-120.

76. **Pearson MM, Mobley HL.** 2008. Repression of motility during fimbrial expression: identification of 14 mrpJ gene paralogues in Proteus mirabilis. Mol Microbiol **69:**548-558.

77. **Li X, Rasko DA, Lockatell CV, Johnson DE, Mobley HLT.** 2001. Repression of bacterial motility by a novel fimbrial gene product. The EMBO Journal **20:**4854-4862.

78. **Li X, Johnson DE, Mobley HL.** 1999. Requirement of MrpH for mannose-resistant Proteus-like fimbria-mediated hemagglutination by Proteus mirabilis. Infect Immun **67:**2822-2833.

79. **Lower BH, Yongsunthon R, Vellano FP, 3rd, Lower SK.** 2005. Simultaneous force and fluorescence measurements of a protein that forms a bond between a living bacterium and a solid surface. J Bacteriol **187:**2127-2137.

80. **Walker KE, Moghaddame-Jafari S, Lockatell CV, Johnson D, Belas R.** 1999. ZapA, the IgA-degrading metalloprotease of Proteus mirabilis, is a virulence factor expressed specifically in swarmer cells. Mol Microbiol **32:**825-836.

81. **Fraser GM, Claret L, Furness R, Gupta S, Hughes C.** 2002. Swarming-coupled expression of the Proteus mirabilis hpmBA haemolysin operon. Microbiology **148:**2191-2201.

82. **Senior BW, Loomes LM, Kerr MA.** 1991. The production and activity in vivo of Proteus mirabilis IgA protease in infections of the urinary tract. J Med Microbiol **35:**203-207.

83. **Belas R, Manos J, Suvanasuthi R.** 2004. Proteus mirabilis ZapA metalloprotease degrades a broad spectrum of substrates, including antimicrobial peptides. Infect Immun **72:**5159-5167.

84. **Phan V, Belas R, Gilmore BF, Ceri H.** 2008. ZapA, a virulence factor in a rat model of Proteus mirabilis-induced acute and chronic prostatitis. Infect Immun **76:**4859-4864.

85. **Mobley HL, Chippendale GR, Swihart KG, Welch RA.** 1991. Cytotoxicity of the HpmA hemolysin and urease of Proteus mirabilis and Proteus vulgaris against cultured human renal proximal tubular epithelial cells. Infect Immun **59:**2036-2042.

86. **Chippendale GR, Warren JW, Trifillis AL, Mobley HL.** 1994. Internalization of Proteus mirabilis by human renal epithelial cells. Infect Immun **62:**3115-3121.

87. **Swihart KG, Welch RA.** 1990. Cytotoxic activity of the Proteus hemolysin HpmA. Infect Immun **58:**1861-1869.

88. **Garcia-Calderon CB, Garcia-Quintanilla M, Casadesus J, Ramos-Morales F.** 2005. Virulence attenuation in Salmonella enterica rcsC mutants with constitutive activation of the Rcs system. Microbiology **151:**579-588.

89. **Jander G, Rahme LG, Ausubel FM.** 2000. Positive correlation between virulence of Pseudomonas aeruginosa mutants in mice and insects. J Bacteriol **182:**3843-3845.

90. **Seed KD, Dennis JJ.** 2008. Development of Galleria mellonella as an alternative infection model for the Burkholderia cepacia complex. Infect Immun **76:**1267-1275.

91. **Mukherjee K, Altincicek B, Hain T, Domann E, Vilcinskas A, Chakraborty T.** 2010. Galleria mellonella as a model system for studying Listeria pathogenesis. Appl Environ Microbiol **76:**310-317.

92. **Fedhila S, Buisson C, Dussurget O, Serror P, Glomski IJ, Liehl P, Lereclus D, Nielsen-LeRoux C.** 2010. Comparative analysis of the virulence of invertebrate and mammalian pathogenic bacteria in the oral insect infection model Galleria mellonella. J Invertebr Pathol **103:**24-29.

93. **Ramarao N, Nielsen-Leroux C, Lereclus D.** 2012. The insect Galleria mellonella as a powerful infection model to investigate bacterial pathogenesis. J Vis Exp doi:10.3791/4392**:**e4392.

94. **Di Venanzio G, Stepanenko TM, Garcia Vescovi E.** 2014. Serratia marcescens ShlA pore-forming toxin is responsible for early induction of autophagy in host cells and is transcriptionally regulated by RcsB. Infect Immun **82:**3542-3554.

95. **Allison C, Coleman N, Jones PL, Hughes C.** 1992. Ability of Proteus mirabilis to invade human urothelial cells is coupled to motility and swarming differentiation. Infect Immun **60:**4740-4746.

96. **Allison C, Emody L, Coleman N, Hughes C.** 1994. The role of swarm cell differentiation and multicellular migration in the uropathogenicity of Proteus mirabilis. J Infect Dis **169:**1155-1158.

97. **Mobley HL, Belas R, Lockatell V, Chippendale G, Trifillis AL, Johnson DE, Warren JW.** 1996. Construction of a flagellum-negative mutant of Proteus mirabilis: effect on internalization by human renal epithelial cells and virulence in a mouse model of ascending urinary tract infection. Infect Immun **64:**5332-5340.

98. **Jansen AM, Lockatell CV, Johnson DE, Mobley HL.** 2003. Visualization of Proteus mirabilis morphotypes in the urinary tract: the elongated swarmer cell is rarely observed in ascending urinary tract infection. Infect Immun **71:**3607-3613.

99. **Zunino P, Piccini C, Legnani-Fajardo C.** 1994. Flagellate and non-flagellate Proteus mirabilis in the development of experimental urinary tract infection. Microb Pathog **16:**379-385.

100. **Pearson MM, Yep A, Smith SN, Mobley HL.** 2011. Transcriptome of Proteus mirabilis in the murine urinary tract: virulence and nitrogen assimilation gene expression. Infect Immun **79:**2619-2631.

101. **Sabbuba N, Hughes G, Stickler DJ.** 2002. The migration of Proteus mirabilis and other urinary tract pathogens over Foley catheters. BJU Int **89:**55-60.

102. **Belas R.** 1994. Expression of multiple flagellin-encoding genes of Proteus mirabilis. J Bacteriol **176:**7169-7181.

Table 1: Rcs-activated genes discussed in this article

	Gene	Fold change (*rcsB*::*Str*^{R} relative to wild-type)
Differentiation	*minD*	-6.74
	minC	-3.40
	ftsZ	-3.33
	ftsA	-2.38
	speB	-2.69
Fimbriae	*mrpA*	-68.69
	pmfA	-63.93
	PMI0261 (*mrpJ* paralog)	-28.86
	PMI0260 (*mrpH* paralog)	-12.15
	ucaA	-6.97

Table 2: Rcs-repressed genes discussed in this article

	Gene	Fold change (*rcsB::Str*^{R} relative to wild-type)
Virulence factors	*zapA*	43.44
	zapB	39.44
	zapD	13.87
	hpmA	12.51
	hpmB	10.41
Motility	*fliO*	26.61
	fliJ	25.48
	umoD	21.51
	flhB	21.16
	ccm	15.90
	flhC	15.71
	fliP	15.02
	fliK	13.28
	flgC	13.26
	fliZ	13.13
	flgF	12.76
	fliA	11.51
	flgD	11.34
	flgK	10.31
	flgE	9.47
	fliI	9.29
	flgJ	9.03
	fliH	8.71
	fliF	7.99
	flgG	7.97
	flhD	7.89
	fliG	7.33
	flgA	7.07
	flaD	6.99
	fliL	6.52
	umoA	5.86
	flaA, flgB	5.67
	PMI2809	4.93
	fliT	4.87
	fliM	4.50
	fgL	4.15
	cheA	4.06
	flgN	3.98
	motA	3.87
	fliN	3.85
	fliS	3.84

Motility	*flgH*	3.63
	motB	3.59
	flgI	3.43
	cheZ	2.91
	PMI2808	2.63
	cheB	2.52
	flgM	2.45
	cheR	2.26
	cheY	2.20
Self-recognition	PMI1332 (*idsF* paralog)	35.45
	PMI0749 (*tssA*)	10.29
	PMI0748 (*tssB*)	9.01
	PMI0747 (*tssC*)	7.85
	PMI1331 (*idsB* paralog)	6.89
	PMI0741 (*tssI*)	5.90
	PMI1118 (*idrB* paralog)	5.38
	PMI0740(*tssJ*)	4.49
	PMI0738 (*tssL*)	4.10
	PMI0745 (*tssE*)	3.90
	PMI1117 (*hcp*/*idrA*	3.89
	PMI0742 (*tssH*)	3.66
	PMI0744 (*tssF*)	3.39
	PMI0751 (*idrB*)	3.21
	PMI0750 (*idrA*)	3.11
	PMI2990 (*idsA*)	2.39

Table 3: Location and putative binding sites of Rcs-activated genes

Gene name	Binding Sequence	Location	Count
RcsAB box [64]	TAA**GA**ATATT**C**CTA		14
cfa	TAGGAAAATTCTTA	272 bp upstream of start codon	11
eco	TCAGAATAATCCTC	124 bp upstream of start codon	11
mrpA	TAGGAATAATCCAA	-40 [66]; +100 [65]	11
ompA	TAAGATAAGTCATA	289 bp upstream of start codon	10
aspA	TAAGAAGGTTCTCA	Overlapping start codon	10
PMI3699	TAAGACTTTTCTCA	98 bp upstream of ATG	10
dnaK	AATGAATATTCATC	54 bp upstream of ATG	10
osmB	CCCGAATATTCTGA	60 bp upstream of start ATG	9
osmCp1 RcsB box*	TCGGAATATCCTGC	-48 [13]	8
PMI0805	TTGGACTAACCATA	29 bp upstream of ATG	8
PMI0250	TGAGAGAAATCTGA	177 bp upstream of ATG	8
katA	TTAGATTTTTCAAT	182 bp upstream of ATG	8
crp	TCCGAATTCTCAGG	95 bp upstream of ATG	7
PMI3443	TATGAACAACCGAT	83 bp upstream GTG	7
pepD	TTTGAGCGTTCAAA	264 bp upstream of GTG	7
PMI2837	TATGATAAATCAAT	30 bp upstream of ATG	7
frdA	ACCGAGAATTCTTG	247 bp upstream of ATG	7
rpoB	ATGGAAAATTCTAT	100 bp upstream of ATG	7
ftsAp1 RcsB box*	GAAGATTCATCTGG	-50 [12]	7
ftsA	GCCGAATTTTCAGT	396 bp upstream of ATG	7
PMI0044	AGCGAAAATTCAAT	287 bp upstream of ATG	7
PMI2772	AATGAGTAATCACT	2 bp upstream of ATG	7
ribF	AGTGAGTAATCGTT	151 bp upstream of ATG	7
udp	ATTGAGGAGTCCGA	2 bp upstream of ATG	7
nrdD	AATGAGCAATCATT	257 bp upstream of GTG	7
rraA	CTGGACTTTCCTGA	20 bp upstream of ATG	6
uspA	ACCGATTAATCAGC	19 bp upstream of ATG	6
pgk	TGTGATAATGCGCG	52 bp upstream of ATG	6
poxB	AGAGATTACCCACT	24 bp upstream ATG	6
PMI1017	AGCGATTTGGCTTA	113 bp upstream of ATG	6
tpx	AGCGAGTTAACTTA	188 bp upstream of ATG	6
rpoN	GAGGATCCATCGCA	6 bp upstream of ATG	6
PMI0657	TTTGATAAGCCTAT	204 bp upstream of start codon	5
rpoE	CGGGAGAGTCCATC	2 bp upstream of ATG	5
PMI1454	TCTGATTTAACGCT	49 bp upstream of ATG	5
PMI1199	TGTGATAGATCACT	50 bp upstream of ATG	5
speB	GTTGATACATCACT	60 bp upstream of ATG	4

*denotes previously reported RcsB binding sequence

Superscript numbers represent the number of the citation where relevant sites were previously defined.

Table 4: Location and putative binding sites of Rcs-repressed genes

Gene name	Binding Sequence	Location	Count
RcsAB box* [64]	TAA**GA**ATATT**C**CTA		14
flhD	TAGGATTATTCTTA	+3 [30, 33, 65]	11
*flhD*3 RcsB box*	TAGGAATTCTCCGA	+5 [16]	10
flhD RcsAB box*	TAGGAAAAATCTTA	+5 [16]	10
PMI1359	TTAGAATAATCAAA	213 bp upstream of ATG	10
PMI1075	AATGAATTTTCCTT	116 bp upstream of ATG	10
PMI1540	TAAGATTTCTCTTT	250 bp upstream of GTG	9
fliA	TATGACCCATCTTA	178 bp upstream of ATG	8
ddg	TAGGAAAAAGCCGT	135 bp upstream of GTG	8
flaA	AATGAATAGGCAAA	26 bp downstream of σ-28 promoter [102]	8
PMI3378	AGAGATAATTCTGA	28 bp upstream of ATG	8
hcp	AGTGACTTATCCTA	167 bp upstream of ATG	8
PMI0750	AGTGACTTATCCTA	167 bp upstream of ATG	8
PMI2990	AGTGACTTATCCTA	167 bp upstream of ATG	8
hpmB	GTAGATAACGCTTA	Overlapping σ-28 promoter [81]	7
PMI1438	AGAGATTAACCTAA	37 bp upstream of ATG	7
PMI0720	ATAGAAATTACTTT	280 bp upstream of ATG	7
coaE	GAAGATTTAGCCAC	160 bp upstream of ATG	7
flgA	ACAGAATAAACGCT	86 bp upstream of +1 [67]	7
flgB	ATAGAAGATGCTCG	Overlaps ATG; 42 bp downstream of +1 [67]	7
flhB	AGAGACATTTCATT	Overlaps +1 [67]	7
rpmE	TATGATCCGCCCCC	98 bp upstream of ATG	6
flgM	AAGGATTTTCCTAT	Overlapping start codon	6
PMI2809	TCAGACAGCACTTT	283 bp upstream of ATG	6
PMI1245	AATGATATAGCCTT	47 bp upstream of ATG	6
flaD	TCCGATAACGCTGT	Overlapping σ-28 promoter [102]	5
fliF	AATGAGACACCTGA	Overlaps putative σ-28 promoter	5
fliL	ACAGAAATAGCGGG	81 bp upstream of ATG	5
PMI2121	CTTGAAAAAACACT	33 bp upstream of ATG	5
PMI2810	TGTGATTTAGCGAT	122 bp upstream of ATG	5
PMI3393	AAAGATATAACGAC	31 bp upstream of ATG	5
PMI1628	GGGGACCCATCAGC	31 bp upstream of ATG	4
motA	AGGGATATCGCGTG	Overlapping start codon	4
PMI2808	GTGGAGCTCCCACT	34 bp upstream of ATG	3

*denotes previously reported RcsB binding sequence

Superscript numbers represent the number of the citation where relevant sites were previously defined

Figure legends.

Figure 1. An *rcsB* mutant is deficient in biofilm formation. In Panel A, *P. mirabilis* strain HI4320 (dark grey bars) or the isogenic *rcsB::Str*^{R} (light grey bars) were grown overnight at 37°C without shaking. Cells were equilibrated to the same optical density (A_{600}), diluted, incubated in polystyrene microtiter plates for 8, 24, and 48 h. Biofilm formation was assessed as described in the Materials and Methods. In Panel B, biofilms were formed on 0.25 in latex catheter pieces for 8 and 24 h. For all experiments, the average of 3 independent experiments is shown. Error bars represent standard deviations. An asterisk indicates a *p*-value < 0.05.

Figure 2. An *rcsB* mutant exhibits enhanced virulence in a *Galleria mellonella* waxworm model. Cells of wild-type PM7002 (light grey bars) or the isogenic *rcsB::Str*^{R} mutant (dark grey bars) were grown to the same optical density. A 10^{-6} dilution was prepared in sterile LB and was used to inject *G. mellonella* in the second proleg. The *G. mellonella* worms were incubated at 37^{o}C in a humidified incubator and were checked at 24 hour intervals for killing. Worms were considered dead if they did not move when prodded with a pipette tip and were dark brown or black in color. A total of three independent experiments were conducted representing 28 worms for wild-type and 29 worms for the *rcsB* mutant. Error bars represent standard deviations.

Supplementary Figure 1. Overexpression of flagellar genes is not responsible for biofilm defect in *rcsB* mutant. Plasmid pACY184 or pACY184-*flhDC* was isolated from *E. coli* strain BL21 and electroporated into *P. mirabilis* strain HI4320 as follows: 30 ml of cells were grown to an OD_{600} of 0.3-0.5 in LB broth. Cells were pelleted by centrifugation at 3,000 x g for 5 min at 4°C before being washed twice with 1 ml of ice

cold 10% glycerol and resuspended in 60 µl of ice cold 10% glycerol per electroporation. Electroporations were done in Bio-Rad Gene Pulser 0.2-cm diameter cuvettes with a Bio-Rad MicroPulser electroporator. Cells were selected on 3% LB agar containing 200 ug/ml chloramphenicol after recovering for 1.5 h shaking at 250 rpm at 37°C. To compare biofilm formation of HI4320 pACY184, HI4320 *rcsB*::*str*^{R}, and HI4320 pACY184-*flhDC, strains were* grown overnight at 37°C without shaking. Cells were equilibrated to the same optical density (A_{600}), diluted, incubated in polystyrene microtiter plates for 24 h. Biofilm formation was assessed as described in the Materials and Methods. The *rcsB* mutant formed 2.5-fold less biofilm than HI4320 pACY184 and HI4320 pACY184-*flhDC* after 24 h of incubation. There was no significant difference in biofilm formation between HI4320 pACY184 and HI4320 pACY184-*flhDC* after 24 h.

Figure 1

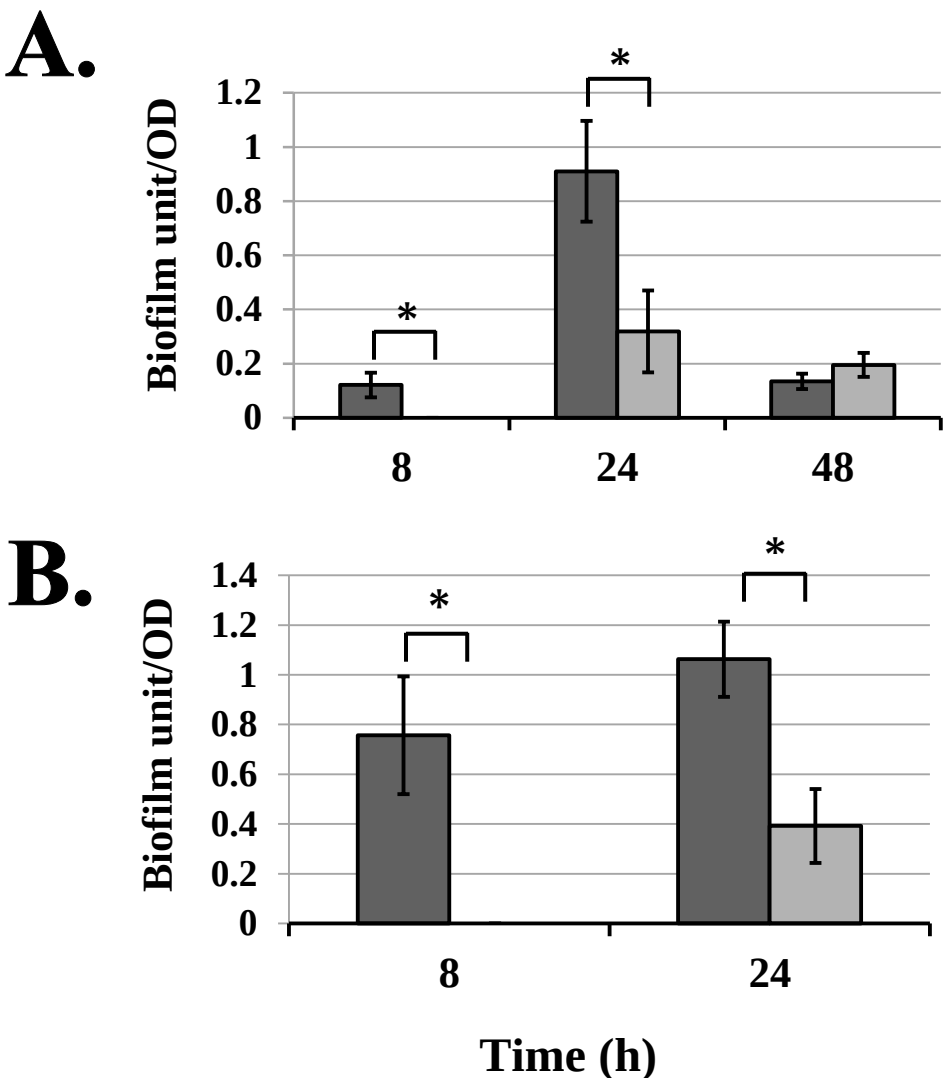
A.
Biofilm unit/OD
1.2
1
0.8
0.6
0.4
0.2
0
*
*
8
24
48
B.
Biofilm unit/OD
1.4
1.2
1
0.8
0.6
0.4
0.2
0
*
*
8
24
Time (h)

Figure 2

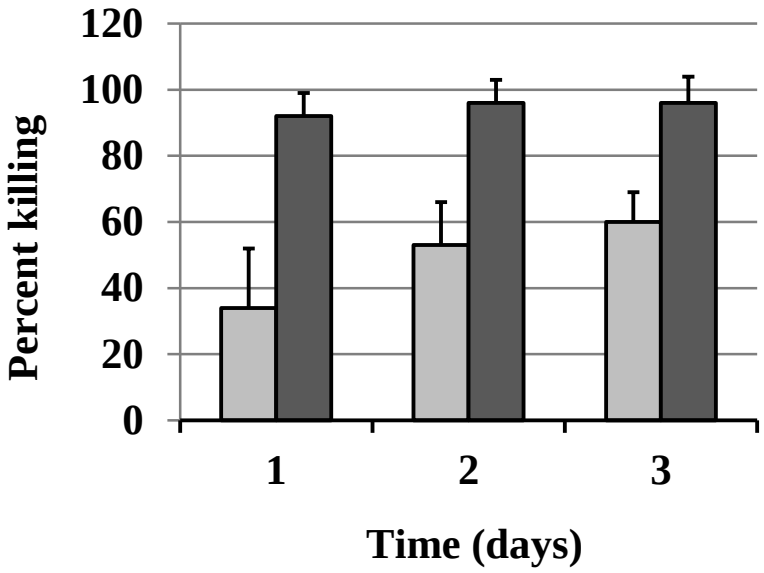

Supplementary Figure 1

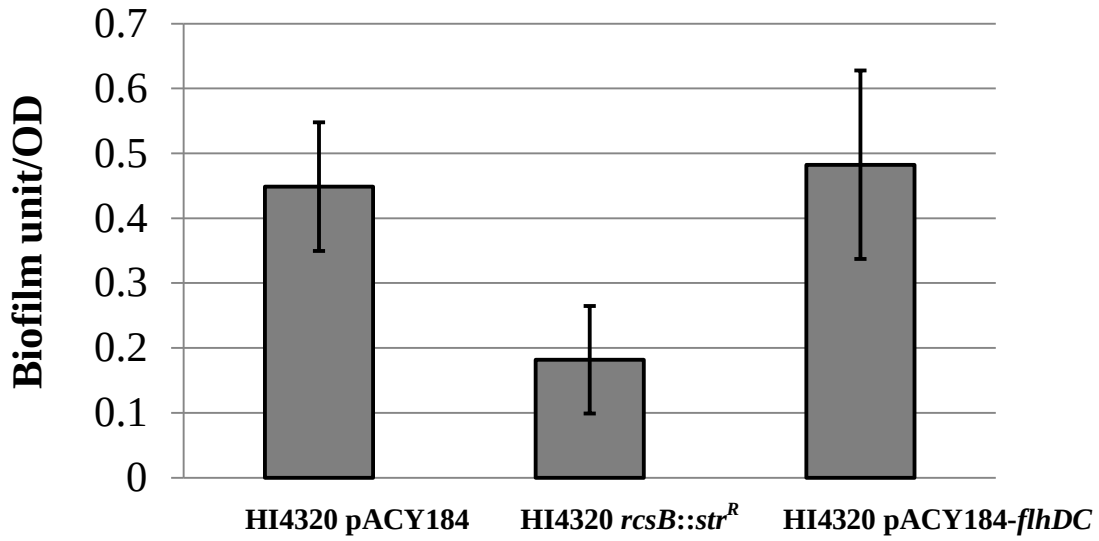

Chapter 4: Expression of the Master Operon for Flagellar Synthesis *flhDC* in a Population of Swarming *Proteus mirabilis* Involves a Bistable Switch

Kristen E. Howery[1], Emrah Şimşek[2], Janet K. Hatt[3], Katy M. Clemmer[3], Daniel Knight[3], Minsu Kim[2], and Philip N. Rather[1, 3]

[1]Department of Microbiology and Immunology, Emory University, Atlanta, Georgia
[2]Department of Physics, Emory University, Atlanta, Georgia
[3]Research Service, Atlanta VA Medical Center, Decatur, Georgia

Manuscript in Preparation

K.E.H wrote the manuscript with the exception of "Time Lapsed Microscopy" under the Materials and Methods which was written by E.S. E.S performed all time lapse microscopy experiments. Images were compiled by K.E.H. K.M.C performed the experiments for Fig. 6. Manuscript was edited by E.S. and P.N.R.

Abstract.

The flagellar master regulator $FlhD_4C_2$ is essential for swarming motility in the bacterium *Proteus mirabilis*. When examining *P. mirabilis* swarm fronts on agar plates, it was noted that cells within the interior of the swarm front remained as short undifferentiated vegetative cells, while differentiated swarmer cells were limited to the exterior portion. To determine if this spatial separation of differentiated swarmer cells resulted from the selective expression of *flhDC*, a strain with a transcriptional *flhDC-gfp* fusion was examined using time-lapse fluorescence microscopy which revealed a potential mechanism of bistable expression. We confirmed $FlhD_4C_2$ activates its own operon via a positive feedback loop and purified FlhC could bind to its own promoter region. To investigate the mechanism responsible for the spatial control of swarmer cell differentiation, a collection of mutants was examined for those that allowed for swarmer cell differentiation to occur in the interior. One previously characterized mutant, SS-P, containing a transposon insertion in the non-coding region 325 upstream of the *flhDC* transcriptional start site, was capable of differentiating within the interior. Time-lapse phase contrast microscopy revealed the SS-P mutant differentiated shortly after surface contact, whereas wild-type *P. mirabilis* only exhibited swarmer cell differentiation after 5 hours of growth and swarmer cells were only visible in the exterior of the developing colony. Deletion analysis of the region upstream of *flhDC* demonstrated that sequences from -322 to -1000 were required to mediate the spatial control of *flhDC* expression within the interior. Lastly, we demonstrate for the first time that the histone-like DNA binding proteins Fis, IHF, HU and the FliZ transcription factor are required for swarmer cell differentiation in *P. mirabilis.*

Introduction.

The Gram-negative bacterium *P. mirabilis* is capable of undergoing a metamorphosis from a short, rod-shaped, vegetative cell into an elongated swarmer cell; a process known as differentiation. Vegetative cells are approximately 2 μm in length and are sparsely but peritrichously flagellated. Differentiated swarmer cells are 20 to 40-fold longer than their vegetative counterparts and express thousands of flagella (1). Swarmer cells utilize a flagellum-dependent, multicellular form of motility known as swarming. Swarming in *P. mirabilis* occurs when a population of swarmer cells cooperatively aligns as their flagella interweave to form rafts which propel group movement across a solid surface (2, 3). Swarming is initiated once vegetative cells come into contact with a solid surface. Following surface contact and a period of cell division, a subset of the population undergoes differentiation into elongated swarming cells which migrate from the initial point of contact. Factors associated with surface contact that facilitate differentiation include O-antigen mediated cell surface perturbation (4), inhibition of flagellar rotation (5-7), and cell-to-cell signaling (6, 8). After an interim period of migration, swarmer cells consolidate (or de-differentiate), once thought to be a resting period following the energetically demanding swarming phase. However, consolidated cells are metabolically active (9) and a marked increase in the expression of genes involved in flagellar synthesis, nutrient uptake, metabolism, cell division, and respiration occurs in consolidation phase cells (10). Following a period in consolidation phase, differentiation occurs once more; the cycling between differentiation and consolidation results in the unique bulls-eye pattern *Proteus* forms on an agar plate (3, 11).

Many bacteria have the ability to utilize swarming motility, and the behavior has been well-characterized in several species. *P. mirabilis* is a vigorous swarmer compared to many other species of bacteria. While *E. coli* can swarm on 0.45% Eiken agar in nutrient rich media (12), *P. mirabilis* can swarm on a variety of media, on 1.0 - 3.0% agar, and at a range of temperatures (25 to 37°C) (3, 11). Like *Bacillus subtilis*, *P. mirabilis* exhibits a "swarming lag" or "lag phase" where, following inoculation of vegetative cells onto an agar plate, the cells actively divide but remain non-motile for a period of time presumably to undergo the necessary transcriptional and physiological rearrangements for swarming initiation (1, 13, 14). The time spent in lag phase can be reduced by increasing the cell density of the inoculum (11, 13, 15), overcome by certain mutants (13, 16-18), and abolished if existing swarmer cells are transferred to a new agar plate (13, 19). Upon the initiation of swarming, the population of *P. mirabilis* cells formerly in lag phase becomes heterogeneous, as swarmer cells form at the edge of the colony periphery. The population of cells that do not differentiate remain as non-motile, vegetative cells and are maintained throughout swarm colony development (10, 11, 13, 14).

Clonal populations of bacteria exhibit unimodal variability in the expression of a gene due to stochastic fluctuations in the availability of the gene product, called noise. Noise may be inherent to the biochemical process of gene expression (instrinsic noise) or arise from incongruity in other factors involved in the expression of a gene (extrinsic noise). Fluctuations in noise are generally small and transient and thus not sufficient to alter cell fate. However, if noise in the expression of a given gene can be amplified, a new pattern of gene expression may arise depending on the regulatory network in which the gene product operates. If cells within a population pass a threshold in the expression of a

master regulatory gene, bimodal gene expression and subsequent bifurcation of the population occurs where some cells express high levels (ON state) or low levels (OFF state) of a gene product (20, 21). This phenomenon is referred to as bistability. One example of bistable gene expression is mediated by a positive feedback loop, where a gene product activates its own expression and downstream targets. Another is a pair of mutually repressing repressors, where one repressor is inactivated due to the stochastic addition of inducer to the system. The other repressor can now be produced, further blocking expression of first repressor while activating the expression of downstream targets (22). In *B. subtilis*, a bistable mechanism for the development of motility in a subset of the overall population has been described (16). Bistable gene expression has been shown to influence other bacterial behaviors, including sporulation (23) and competence (24). Reviews describing bistable gene expression in bacteria can be found in references 20 and 21.

An essential factor for swarmer cell differentiation in *P. mirabilis* is the flagellar master operon, *flhDC*. The products of *flhDC*, FlhD and FlhC comprise the heterohexameric transcriptional regulator $FlhD_4C_2$, which binds and activates the expression of class II flagellar genes (25-27). $FlhD_4C_2$ recognizes large asymmetric repeats present in bacterial promoters and upon binding, bends DNA to affect expression of targets (28, 29). Dimerized FlhC is the DNA-binding component of the complex and can bind DNA independently, though FlhD aids in the stability and fidelity of the FlhC-DNA interaction (26). Expression of *flhDC* increases prior to differentiation, as hyperflagellation is essential for swarming, and sharp decreases in *flhDC* expression are observed following the initiation of swarming (18, 30). This is due to tight transcriptional

(17, 18, 30-32) and post-translational regulation (33, 34). Slight changes in *flhDC* expression can affect the manner in which *P. mirabilis* swarms. Overexpression of *flhDC* results in an increase in the number flagella, hypermotility, and enables cells to overcome swarming lag phase (30), while *flhDC* mutants do not swarm (7, 30).

Regulators of *flhDC* expression in *P. mirabilis* include the repressors RcsB, RppA, MrpJ and UcaJ (17, 18, 35-37) and the activators Lrp and WosA (38-40). However, mechanisms of gene expression that drive swarmer cell differentiation within individual cells in a population have not been described to our knowledge. In this study, we show that swarmer cell differentiation is spatially constrained to cells at the periphery of a growing population. Utilizing a *flhDC-gfp* fusion, expression was only observed within a subpopulation of cells, both prior to and after the initiation of swarming. We quantitatively confirm $FlhD_4C_2$ as a bistable regulator via a positive feedback loop and demonstrate binding of FlhC to its upstream region. In addition, characterization of a mutant that allowed cells to differentiate within the interior of a cell population, combined with deletion analysis of the 5'-region of the *flhDC* promoter has revealed that sequences between -322 and -1000 mediate repression within the interior of a population. DNA affinity chromatography was used to identify proteins that bound to this region and could act as putative repressors. Analysis of these proteins in combination with the construction of defined deletions in their respective genes did not identify new repressors, but revealed for the first time that the histone-like DNA binding proteins Fis, IHF, HU and the FliZ transcription factor are required for swarmer cell differentiation.

Materials and Methods.

Bacterial strains, conditions for growth and mutant selection. The strains used in this study are listed in Table 1. Except where indicated, *P. mirabilis* and *E. coli* strains were grown in modified Luria-Bertani (LB) broth (10 g tryptone, 5 g yeast extract, 5 g NaCl per liter) at 37°C with shaking at 250 rpm. Frozen stocks of all strains were maintained at -80°C in LB media containing 10% glycerol. Strains were newly grown from aliquots of frozen stocks to begin each experiment. LB plates contained 1.5% and 3.0% agar for *E. coli* and *P. mirabilis*, respectively, for the isolation of single colonies. The following antibiotic concentrations were used for the selection and maintenance of constructs in *E. coli*: 150 μg/ml ampicillin, 25 μg/ml streptomycin, and 25 μg/ml chloramphenicol. For *P. mirabilis*, antibiotic concentrations were 300 μg/ml ampicillin, 20 μg/ml kanamycin, 35 μg/ml streptomycin, 15 μg/ml tetracycline, and 200 μg/ml chloramphenicol. When appropriate, a concentration of 12 μg/ml 5-bromo-4-chloro-indolyl-β-d-galactopyranoside (X-Gal) was used for the selection of blue or white colonies for both *E. coli* and *P. mirabilis*. For induction of protein expression, a concentration of 1 mM isopropyl β-D-1-thiogalactopyranoside (IPTG) was used.

For electroporation of plasmids into both *E. coli* and *P. mirabilis*, 30 ml of cells were grown to an OD_{600} of 0.3-0.5 in LB broth. Cells were pelleted by centrifugation at 3,000 x g for 5 min at 4°C before being washed twice with 1 ml of ice cold 10% glycerol and resuspended in 60 μl of ice cold 10% glycerol per electroporation. Electroporations were done in Bio-Rad Gene Pulser 0.2-cm diameter cuvettes with a Bio-Rad MicroPulser electroporator. *E. coli* cells were plated on LB agar plates containing the appropriate antibiotic concentrations after 1.5 h shaking at 250 rpm at 37°C. For *P. mirabilis*

transformations, competent cells were incubated for 30 min with plasmid DNA on ice prior to electroporation. *P. mirabilis* electroporations were allowed to recover for 3 h.

For bacterial conjugations, overnight cultures were washed 3X in 1 ml of fresh LB broth. 100 µl of each strain was combined in a 1.5 ml microcentrifuge tube before being added to a pre-dried 1.5% LB agar plate. 100 µl of each strain alone was added to separate plates to serve as controls. After 7 h of incubation at 37°C, cells were resuspended in 4 ml LB broth. Conjugations and control plates were incubated on 3% LB agar containing the appropriate antibiotics and incubated overnight at 37°C.

Mutagenesis. All PCR amplifications were done using Phusion Hot Start II high-fidelity DNA polymerase (Thermo Scientific) and verified by DNA sequencing. All ligations were performed using the *Fast-Link*™ DNA Ligation Kit (Epicentre).

To construct a merodiploid PM7002 *flhDC*Ωgfp transcriptional fusion strain, an incomplete copy of *flhC* (designated '*flhC*) was amplified from genomic PM7002 DNA using FlhCgfp-F and FlhCgfp-R containing *Bam*HI and *Pst*I sites, respectively, within the oligonucleotide sequence. eGFP was amplified from genomic DNA of MGIBKY (Table 1) with GFP-F and GFP-R containing *Pst*I and *Xba*I sites, respectively, within the sequence. GFP-F anneals upstream of the RBS of eGFP but does not include a promoter fragment within the sequence. To create pFlhCGFP, '*flhC* and eGFP were digested with *Bam*HI and *Pst*I or *Pst*I and *Xba*I and ligated into the *Bam*HI/*Xba*I site of pKNG101. pKNG101 is a suicide vector harboring streptomycin resistance to select for single recombinants and *sacB* to confirm both the integration and loss of pKNG101 in the presence of 10% sucrose (41). pFlhCGFP was maintained in *E. coli* SM10 λ*pir* and

conjugated to PM7002. Str^R, sucrose sensitive PM7002 exconjugants were confirmed to express GFP using fluorescence microscopy. One of these strains, PMKH14, was used for future experiments.

To generate markerless, in-frame deletion mutants of *ihfA*, *ihfB*, *hupA*, *hupB*, *fis*, *hns*, and *fliZ*, a fragment of each gene (IFD1; ~1000 bp) containing the first few codons of the gene and upstream flanking DNA was PCR amplified using primers IFD1-F and IFD1-R (Table 3). Another fragment (IFD2; ~1000 bp) containing the last few codons of the gene and downstream DNA were PCR amplified using primers IFD2-F and IFD2-R (Table 3). Primers IFD1-R and IFD2-F were previously 5'phosphorylated using T4 Polynucleotide Kinase (New England Biolabs). IFD1 and IFD2 were ligated, run on a 1.0% TAE agarose gel, and the fragment corresponding to the appropriate ligated product size (~2000 bp) was gel purified (UltraClean® 15 DNA Purification Kit, MO BIO Laboratories) and PCR amplified using IFD1-F and IFD2-R. The amplified fragment was cloned into the *Eco*RV site of pBluescript KS(-) (Stratagene) and later subcloned into pKNG101 using *Xba*I and *Sal*I (New England Biolabs), and electroporated into CC118 λ*pir* (42) and single colonies were screened for the correct construct, referred to hereafter as pIFD. pIFD was electroporated into *E. coli* SM10 λ*pir* (43) for conjugation with PM7002. Selection for PM7002 harboring the Campbell-type insertion at the locus of interest was done on LB plates containing tetracycline (15 µg/ml) and streptomycin (35 µg/ml). A Str^R, sucrose sensitive exconjugant was grown in LB only for approximately 10 generations and plated on LSW agar with 10% sucrose incubated at room temperature to select for double recombinants. To generate mutants of *hns*, *ihfA*, *ihfB*, and the *ihfA*, *ihfB* double mutant, plates were incubated at 37°C as room temperature sucrose selection failed to generate

these mutants. Clones that were Str^S and sucrose resistant were screened via PCR using primers outside of the locus of interest (Table 3) to confirm gene deletions.

The null *flhC* mutation was introduced into SS-P to create PMKH10. To do this, *E. coli* SM10 λ*pir* harboring BB4 (pKNG101 +*flhC*$^-$) (44) was conjugated to SS-P, and selection for single recombinants was done on 3% LB agar containing Kan^{20}, Str^{35}, and Tet^{15}. A sucrose sensitive exconjugant was inoculated from its frozen stock the morning of selection and grown to mid-log in LB only to prevent the development of second site suppressor mutations. Cells were plated on LSW agar with 10% sucrose and incubated at room temperature to select for the loss of BB4. Double recombinants that did not appear to swarm were patched on 1.5% LB agar to confirm loss of swarming, and non-swarmers were restreaked on 1.5% LB and LB/Str^{35} to confirm streptomycin sensitivity. To verify mutated *flhC,* genomic DNA was prepared from non-swarming mutants and the *flhC* gene was amplified using flhC-F and flhC-R (Table 2). The *flhC* fragment was digested confirm the presence of a base pair insertion at the *Eco*NI site, and the SS-P mutant containing mutated *flhC,* PMKH10, was used for future experiments.

To examine the effect of *flhDC* overexpression on *flhDC* transcription, the merodiploid PM7002 *flhDC*ΩlacZ strain constructed using pLX7801 from the Mobley lab (45) was transformed with 3 µl of pACYC184 (46) or pFDCH1 (pACYC184 + *flhDC*) (47) prepared via the QIAPrep® Spin Miniprep Kit from DH5α. Single colonies were grown in LB and chloramphenicol; PMKH8 (PM7002 *flhDCΩlacZ* pACYC184) and PMKH9 (PM7002 *flhDCΩlacZ* pFDCH1) were used for studies. Similarly, to examine the activity of the *flhDC* promoter extending 2100 base pairs upstream from the transcriptional start site in wild-type versus the *flhC* mutant, pFlhDCLacZ (pQF50 (48) + *flhDCp* [-2100])

was prepared using the Qiagen Plasmid Mini-Kit, and 5 µl was transformed into PM7002 and BB7 (PM7002 *flhC*$^-$) (44) to create PMKH11 and PMKH12, respectively.

For expression and purification of FlhC, the coding region with the exception of the stop codon was amplified from PM7002 genomic DNA using primers found in Table 2. The fragments were ligated separately into the *Nde*I/*Xho*I site of pET21a, a bacterial protein expression vector which utilizes an IPTG-inducible T7 promoter. Ligation into the *Nde*I/*Xho*I site eliminates the N-terminal T7 tag present on the vector but enables C-terminal His_6 tagging of protein. This construct was electroporated into BL21, creating pFlhC, and induction was confirmed via Coomassie staining and α-His_6 Western blot.

Time lapsed microscopy. For imaging of the cells, frozen stocks of all used strains were maintained at -80°C in LB broth media containing 25% glycerol. Strains were inoculated directly from aliquots of frozen stocks to begin each experiment. To begin an experiment, the cells were first inoculated into 2 ml of LB broth liquid culture and incubated overnight at 37°C without shaking. The following morning, 1 µl from the overnight culture was re-inoculated into 2 ml of fresh LB broth at an initial cell density such that the culture would reach an OD_{600}=0.005-0.02, as measured using a Genesys20 spectrophotometer (Thermo-Fisher) with a standard cuvette (16.100-Q-10/Z8.5, Starna Cells Inc.), after completing at least two doublings of cell growth at 37°C with shaking at 250 rpm. Once the culture reached to an OD_{600}=0.005-0.02, a 2 µl aliquot was loaded onto one chamber of a sterile 35 mm four chamber glass bottom Petri dish (InVitro Scientific) and confined with an LB agar/agarose pad. For preparation of the pad, 3 ml of LB broth medium was supplemented with agar (1.5% w/v) or agarose (1% w/v; Invitrogen), and microwaved to obtain a sterile gel. Then, 0.6 ml of the resultant gel was

poured into each one of the chambers of the sterile 35 mm four chamber glass bottom Petri dish and allowed to solidify for 30 min at room temperature before storage at 4°C. Prior to incubation with cells, the pad was pre-warmed to 37°C. Then, for each of the chambers used for inoculation, the LB agar/agarose pad was gently removed with the help of a sterile spatula, and the glass bottom of the dish was quickly dried by aspiration. Promptly, 2 µl from an exponential phase culture of a OD_{600}= 0.005-0.02 was pipetted onto the glass bottom of the dish, and the LB agar/agarose pad was replaced back on top of the cells by gently pressing it down using a flat ended sterile spatula. Unused chambers, if any, were filled by 0.6 ml sterile nanopure water to maintain humidity, and the dish was sealed using parafilm to limit water evaporation while rendering oxygenation of the interior of the dish possible. Streptomycin was added into LB broth or the LB agar/agarose pad at a final concentration of 35 µg/ml for selection, when applicable.

The cells in the dish were imaged using an automated microscope (Olympus IX83), which includes an automated mechanical stage and focus system. A microscope incubator (InVivo Scientific) was used to keep the dish at 37°C. An oil immersion 60x objective was used. Images were acquired using a Neo 5.5 sCMOS camera (Andor) and the MetaMorph software (Molecular Devices). The image analyses were manually performed using ImageJ software (49).

Phase contrast imaging of swarm colonies grown on agar plates. All images were captured with an Infinity 2-1 CCD Camera (Lumenera) using an Olympus BX51 Microscope. For imaging cells from agar plates, cells were removed from the agar plate, resuspended in cold LB broth, and 1.5 µl of the resuspension was immediately pipetted

onto a glass slide (VWR International). A coverslip (VWR International) was placed on top of the culture, and images were taken at 100 X magnification using oil-immersion. Swarm fronts were imaged by adding 650 µl of LB agar to CoverWell™ Imaging Chambers (1 X 20mm dia X 2.3mm depth) then adding 4 µl of a stationary overnight culture to the solidified agar. The cells were grown in a humidified environment at 37°C until they began to swarm. A coverslip was placed on top of the imaging chamber containing the swarming cells, and images were taken at 1,000 X magnification using oil-immersion.

β-galactosidase assays. Cultures grown at 37°C without shaking were equilibrated to the same OD_{600} with LB plus antibiotics and 300 µl of each culture was plated onto 1.5% LB agar containing the appropriate antibiotics and incubated at 37°C for 2 or 4 h. Cells were harvested from agar plates using ice-cold LB broth, and 0.9 ml of the harvested culture was pelleted by centrifugation at 13,000 rpm for 4 min. Pelleted cells were placed on ice for 20 min before lysis using chloroform and 0.1% SDS. β-Galactosidase activity was quantified as described by Miller (50).

Quantitative RT-PCR (qRT-PCR). Cultures of PM7002, PM7002 *flhC*$^-$, SS-P, and SS-P *flhC*$^-$ were incubated overnight at 37°C without shaking. Cultures were equilibrated to the same OD_{600} and 300 µl of each strain were spread plated on individual 1.5% LB agar plates. After 2 and 4 h of incubation at 37°C, cells were harvested from plates in ice cold LB to an OD_{600} ~ 0.4. Cells were spun down at 12,000 rpm for 4 min at 4°C, and RNA was extracted from pellets using MasterPure™ RNA Purification Kit (Epicentre). Nucleic acid extracts were DNase treated using TURBO™ DNase (Ambion™), and RNA was precipitated overnight at -80°C. PCR was used to confirm DNA-free RNA extracts.

RNA was quantified using the NanoDrop® ND-1000 Spectrophotometer, and reverse transcribed using iScript™ Selected cDNA Synthesis Kit (Bio-Rad) per the manufacturer's instructions. qRT-PCR was performed using a 1:10 dilution of the generated cDNA in iQ™ SYBR® Green Supermix (Bio-Rad). The reaction was completed in an iCycler iQ™ Real-Time PCR Detection System (Bio-Rad) and values were normalized to expression of *clpX*. Expression of *flhD* was quantified using the $\Delta\Delta C_T$ method (51). Primers used to quantify gene expression are found in Table 2.

Protein Purification. To purify FlhC from BL21, an overnight culture of BL21 pFlhC was inoculated in 500 ml of LB with ampicillin and grown to OD600 ~ 0.5 at 37°C with shaking. Cells were induced for 2 h before centrifugation at 12,000 rpm for 20 min at 4°C. Supernatant was removed, and pellets were stored at -80°C until further use. To purify protein, pellets were resuspended in 20 ml xTractor™ Buffer (Clontech) with 200 µl protease inhibitor cocktail for histidine tagged proteins (Sigma) and 10 µl DNase (Invitrogen). Cells were French pressed 3 x 600 psi in a cooled large cell. Pressed lysate was spun at 7,000 rpm for 15 min at 4°C and the resulting supernatant underwent another centrifugation for 30 min at 4°C and 13,000 rpm. The HisTALON™ Gravity Column Purification Kit (Clontech) was used to purify protein from cleared lysate per the manufacturer's instructions. Elution fractions were monitored for protein by quantifying the A_{280} of each fraction using a NanoDrop® ND-1000 Spectrophotometer. Fractions containing protein were aliquoted into Spectra/Por® 2 Dialysis Membrane (Spectrum Labs), dialyzed overnight at 4°C in Buffer 1 (20 mM HEPES [pH 7.5], 5 mM $MgCl_2$, 100 mM KCl, 10% glycerol) with gentle stirring. Dialyzed fractions were aliquoted into 1.5

ml microcentrifuge tubes and stored at -20°C. Coomassie staining and α-His_6 Western blot were used to confirm the purity and presence of purified FlhC.

Electrophoretic mobility shift assays (EMSA). This technique for EMSA was previously utilized by our lab (52) with a few modifications: digoxigenin-ddUTP labeled probes were created via PCR amplification with a high-fidelity DNA polymerase for no more than 30 cycles to ensure the integrity of the native sequence and primers containing *Eco*RI recognition sites (Table 2). Amplified DNA was digested with *Eco*RI-HF (New England Biolabs) for 1 h at 37°C and cleaned up using a PCR purification kit (Qiagen). Digested DNA was incubated with Dig-11-dUTP, dATP (Roche), Buffer B (6 mM Tris-HCl [pH 7.5], 6 mM $MgCl_2$, 50mM NaCl) and Klenow enzyme (Roche) for 1 h at 37°C followed by 10 min at 65°C to heat-inactivate Klenow. After labelling, the probe was cleaned up using the same PCR purification kit.

Binding reactions were incubated at room temperature for 30 min with 10 X binding buffer (500 mM Tris-HCl [pH 7.5], 1 M NaCl, 1 mM EDTA, 0.5 µg/µl BSA, 100 mM DTT), 1µg/µl poly(dIdC), labeled probe, and 0 to 160 pmol of purified FlhC-His_6 to a volume of 20 µl with molecular biology grade water (Fisher). Reactions were loaded with 5X DNA loading dye on a pre-run Mini-PROTEAN® 5% TBE Precast Gel (BioRad) in 0.5X TBE and run at 100 V at 4°C for approximately 4 h (2 h after loading dye was no longer visible on the gel). Gel and a 0.22 micron nylon membrane (MagnaGraph) were incubated for 10 min in 0.5X TBE and DNA was transferred to the membrane using a Bio-Rad Transblot SD Semi-Dry Transfer Cell. Crosslinking was done using a Stratagene Crosslinker. 10X blocking reagent (Roche) was previously prepared via boiling in maleate buffer (100 mM maleic acid [pH 7.5], 150 mM NaCl) until in solution and

autoclaved. Membrane was blocked for 45 min at room temperature in blocking solution (1X blocking reagent in maleic acid wash buffer [maleate buffer plus 0.3% Tween 20]) followed by a 45 min incubation with anti-digoxigenin coupled to alkaline phosphatase (Roche) in the same blocking solution. Membranes were washed 2 X 15 min with maleic acid wash buffer, equilibrated in detection Buffer (100 mM Tris-HCl [pH 9.5], 100 mM NaCl) for 2 min, and treated with a 1:1 dilution of CDP-Star (Roche) for 5 min. Membranes were blotted briefly with Whatman paper to remove excess substrate, placed in a sealable plastic bag , and exposed to film.

DNA Affinity Chromatography Pulldown assay. Method is based on published techniques (53, 54) with a few modifications. Probes were PCR amplified from genomic PM7002 using a high fidelity DNA polymerase and a primer set where one primer contained a 5' biotin moiety. To ensure the native DNA sequence was conserved, PCR cycles did not exceed 30. Biotinylated DNA probes were purified via Qiagen PCR Purification Kit, ethanol precipitated to concentrate samples, and stored at -20°C until use. Buffers for assay are as follows: THES Buffer (50 mM Tris-HCl [pH 7.5], 10 mM EDTA, 20% sucrose (m/v), 140 mM NaCl, and 0.7% Protease Inhibitor Cocktail (Sigma) and 0.1% Phosphatase Inhibitor Cocktail (Sigma) which were added the day of the experiment), 5X BS Buffer (50 mM HEPES, 25 mM CaCl2, 250 mM KCl, 60% glycerol), 2X B/W Buffer (10 mM Tris-HCl [pH 7.5], 1 mM EDTA, 2 M NaCl), and Elution buffer (25 mM Tris-HCl (pH 7.5) M NaCl). Buffers were filter sterilized and stored at 4°C. To prepare cell lysate for incubation with DNA probes, PM7002 was inoculated in 250 mL LB broth and grown to an OD_{600} ~ 0.6 the day prior to assay execution. Cells were spun down at 12,000 rpm for 20 min at 4°C and pellets were stored

at -80°C. The day of the experiment, pellets were resuspended in 15 ml BS/THES Buffer with protease and phosphatase inhibitors [For 50 mL, 22.15 ml THES Buffer, 10 ml 5X BS Buffer, 150 µl protease inhibitor cocktail, 20 µl phosphatase inhibitor cocktail brought to volume with molecular biology grade water (Fisher Scientific)]. Cells were French pressed 3 x 600 psi in a cooled large cell, pressed lysate was spun at 13,000 rpm for 30 min at 4°C. Supernatants were kept on ice while DNA probes were coupled to streptavidin beads. To couple DNA to streptavidin beads, 100 µl of Dynabeads M280 Streptavidin (Invitrogen) were mixed well and transferred to a sterile 1.5 microcentrifuge tube. Beads were pulled down by securing the tube to a PolyATtract System 1000 (Promega) magnetic column for 2 min. Supernatant was removed carefully and discarded, and beads were washed 3 X with 200 µl 2X B/W buffer (2X beads volume). For all washes unless otherwise specified, tubes were removed from the magnetic stand, beads were resuspended in buffer, tubes were replaced on stand, and buffer was removed 2 min after beads had re-aggregated toward stand. Following the initial wash, beads were incubated in the DNA suspension which contained 1 µg of DNA per 10 µl of beads (10 µg of DNA probe, 400 µl 2X B/W Buffer, and molecular grade water to a volume of 800 µl [4X bead volume]) by rolling at room temperature for 30 min. Beads were separated from suspension by placement on the magnetic stand, and DNA was quantified from the supernatant using the NanoDrop® ND-1000 Spectrophotometer to confirm successful coupling of DNA to beads. The beads were washed 3X 200 µl TE. Prior to incubation with cell lysate, beads were washed 2X with 200 µl BS/THES Buffer and once with 200 µl BS/THES buffer supplemented with 1 mg/mL poly(dI-dC). The lysate suspension (320 µl BS/THES buffer, 10 µg/ml poly(dI-dC), 1240 µl cell lysate) was incubated with the

probe-bead complex for 1 h at room temperature. Due to the large volume, the lysate and bead suspension were split into two 1.5 ml microcentrifuge tubes to allow for efficient interaction between protein and DNA. Beads were recombined after incubation well cell lysate, washed 5 X 200 µl BS/THES buffer with 10 µg/ml poly(dI-dC), and twice with 300 µl BS/THES buffer. Proteins were eluted in 200 µl Elution buffer X 3. Elution fractions were combined and TCA/Acetone precipitated. If submitting entire eluate, precipitated protein pellets were resuspended in 20 µl of Elution Buffer, and an aliquot of the eluate was stored until submission for mass spectrometry analysis. The rest of the protein precipitate was recombined in 2X Laemmli buffer with 5% β-mercaptoethanol, boiled for 10 min, and run on a 12% Mini-PROTEAN® TGX™ Precast Gel (BioRad) in Tris/Glycine/SDS buffer. Cell lysate was run as a positive control for staining. Gels were stained using SYPRO©Ruby (Invitrogen) per the manufacturer's instructions and proteins were visualized on a UV Illuminator (Fisher Scientific). Individual protein bands or eluates were submitted to the Emory University Integrated Proteomics Core for LC-LC/MS analysis using the LTQ Orbitrap XL™ Hybrid Ion Trap-Orbitrap Mass Spectrometer (Thermo Scientific) for protein identification.

Swarm assays. Overnight cultures were standardized to the same optical density, and 4 µl of each culture were pipetted onto a 1.5% LB agar and incubated at 37°C. Measurements of the swarm diameter were taken every 30 min. Antibiotics were included in the agar plate when appropriate. The values represent the average diameter of duplicate with standard deviations. Each experiment was repeated in triplicate.

Results.

***P. mirabilis* preferentially differentiates into swarmer cells at the periphery of a cell population.** Swarming colonies of *P. mirabilis* have been well studied (1, 3, 11). However, little is known concerning factors that influence the initiation of swarming in a developing colony and the spatial distribution of swarmer cells within this population. Ultimately, the subpopulation of cells that undergo differentiation are responsible for the swarm front and subsequent colonization of the agar plate. In contrast, the cells that do not differentiate remain as vegetative, short-rod shaped cells that do not migrate and are maintained throughout colony development.

To determine if there is a spatial distribution of swarmer cell differentiation when *P. mirabilis* cells are placed as a small lawn on an agar surface, multiple methods of microscopy were utilized. First, phase contrast images were taken of a *P. mirabilis* ATCC 7002 (PM7002) swarm front on an agar plate immediately upon the initiation of swarming. We observed elongated, highly flagellated swarmer cells only at the edge of the inoculum, while the population at the interior remained short, rod-shaped vegetative cells (Fig. 1A). This morphology was confirmed by taking cells from both the exterior and interior of the growing population and analyzing their morphology by phase contrast microscopy. Within the interior, swarmer cells were not represented within the population (Fig. 1C), but they comprised the exterior of the swarm colony (Fig. 1D).

As this technique did not permit long-term monitoring of swarm colony development and only allowed visualization of the swarm colony at one time-point, time-lapse phase contrast microscopy was used to examine single-cells of PM7002 as they formed swarming microcolonies over time. In this method of analysis, single cells divide

as short, rod shaped cells until 5.5 h after surface contact after which differentiation of swarmer cells occurs only at the colony periphery (Fig. 1B; Supplemental Movie 1).

***flhDC* exhibits bistable gene expression in a population of swarming *P. mirabilis*.** Upon surface contact, *flhDC* expression immediately increases, and continues to do so until approximately 4 hours after surface contact, prior to the initiation of swarming. Its expression goes down once swarming has initiated, only to increase again during consolidation (18, 30). Since *flhDC* is essential for swarmer cell formation and its expression coincides with the initiation of differentiation, we hypothesized a subset of the initial population of vegetative cells would express high levels of *flhDC* prior to the initiation of swarming and that these cells would be limited to the exterior of the cell population, thus forming the swarmer cell population at the colony periphery.

To address this hypothesis, a transcriptional GFP fusion was used to monitor *flhDC* expression in swarming *P. mirabilis*. This construct was created by ligating an incomplete copy of *flhC* and a promoterless GFP into pKNG101 (41) then introducing it into the PM7002 chromosome. The resulting merodiploid strain, PM7002 *flhDCΩgfp*, harbors the *flhDC* operon fused to GFP with pKNG101 and the non-functional copy of *flhC* integrated in the chromosome (Fig. S1). To examine the spatial distribution of *flhDC-gfp* expression, time-lapse fluorescence microscopy was performed on single cells as they divided, formed microcolonies, and began to swarm. Surprisingly, high levels of GFP expression in rod-shaped cells were present early in microcolonies – hours prior to the initiation of swarming (Supplemental Movie 2). High levels of GFP expression were present within subpopulations throughout the microcolony, indicating that this is a stochastic event (Fig. 2A) Once swarming had initiated, all swarmer cells expressed high

levels of GFP (Fig. 2B). This experiment unveiled a potential mechanism of bistable *flhDC* expression as GFP expression was high in cell subpopulations. Additionally, high *flhDC* expression was necessary but not sufficient for swarmer cell differentiation, as rod-shaped cells were expressing high levels of GFP hours prior to differentiation, and instances of *flhDC* expression being inherited by daughter cells was observed (Fig. 2C).

$FlhD_4C_2$ is a bistable regulator via a direct positive feedback loop. As *flhDC* expression was high in subpopulations of cells, we hypothesized that the product of *flhDC*, $FlhD_4C_2$, was acting as a bistable regulator via a positive feedback loop. To quantitatively address this hypothesis, multiple experiments were performed. First, the expression of chromosomal *flhDC-lacZ* fusion was examined in both liquid cultures and on solid agar in cells that artificially overexpressed *flhDC* in *trans* by the *lacI* promoter on a medium copy plasmid. PM7002 *flhDC-lacZ* with pACYC184 (46) or pACYC184 + *flhDC* was grown to mid- and late- logarithmic growth phase in LB broth, cells were harvested, and β-galactosidase activity was quantified as described by Miller (50). Transcriptional activity of *flhDC* was 5.1-and 8-fold higher when *flhDC* is artificially overexpressed at mid- and late-log, respectively (Fig. 3A). In the same strains grown on LB agar after 2 (T_2) and 4 (T_4) h, the activity of the *flhDC-lacZ* increased 3- and 5-fold, respectively, at T_2 and T_4 in when *flhDC* was overexpressed relative to empty vector (Fig. 3B).

To quantify the activity of the *flhDC* promoter in wild-type PM7002 versus a *flhC* null mutant, a DNA-fragment extending from intragenic *flhD* to from -2100 relative to the transcriptional start site was ligated into pQF50, a low-copy number vector harboring a promoterless *lacZ* gene (48), creating pFlhDCLacZ (-2100). The reasoning behind

examining transcriptional activity of such a large region is due to the very large 3,321 bp *flhDC* upstream region in PM7002 and regulatory elements up to -2100 affect *flhDC* expression (Fig. 6) (18). pFlhDCLacZ (-2100) was electroporated into PM7002 and an isogenic *flhC* null mutant (44), and promoter activity was quantified in cells after 2 and 4 h of incubation on LB agar containing ampicillin. A significant 2.4-fold decrease in pFlhDCLacZ activity is observed in the *flhC* mutant at T_4 relative to wild-type; no significant difference in expression was observed at T_2 (Fig. 3C).

To independently confirm the data generated by the β-galactosidase assays, quantitative reverse transcriptase PCR (qRT-PCR) analysis was utilized to examine *flhD* expression in PM7002 and the isogenic *flhC* mutant. Cells of PM7002 and the isogenic *flhC* mutant were harvested after 2 and 4 h of incubation on LB, and qRT-PCR analysis was performed with primers specific to *flhD*. In the null *flhC* mutant, the expression of *flhD* was 1.9-fold lower at T_2 of incubation and 5-fold lower at T_4 relative to PM7002 at T_2. Additionally, while there was a 3.6-fold increase in *flhD* expression between T_2 and T_4 in wild-type, expression of *flhD* in the *flhC* mutant only increased 1.4-fold (Fig. 3D). Overall, these data indicate $FlhD_4C_2$ is subject to autoregulation.

Electrophoretic mobility shift assays (EMSA) were then performed to confirm that this autoregulation was direct. FlhC is the DNA-binding subunit within the $FlhD_4C_2$ complex (26) so purified FlhC-His_6 was used for binding to a 124-bp fragment containing the *flhDC* promoter and transcriptional start site (Fig. 4). To confirm specific FlhC binding to its promoter fragment, a competitive EMSA was performed using 60 pmol of His_6-tagged FlhC with unlabeled 124-bp *flhDC* promoter fragment as specific competitor and an *abaI* PCR fragment amplified from *Acinetobacter nosocomialis* as nonspecific

competitor. At a concentration 50 times that of the labeled *flhDC* promoter, the unlabeled *flhDC* DNA reduced the shift of the labelled probe. However, the unlabeled *abaI* fragment did not affect binding of FlhC-His_6 to the labeled *flhDC* fragment (Fig. 4). Overall, these data indicate that $FlhD_4C_2$ is a bistable, direct positive regulator of its own expression.

Characterization of a mutant that permits swarmer cell differentiation within the population interior. To begin addressing the mechanism that prevented cells in the interior of a population from differentiating to swarmer cells, we reasoned that mutants allowing this to occur would have a hyperswarming phenotype and possibly initiate swarming earlier than wild-type. Based on this assumption, we screened a collection of hyperswarming mutants previously isolated in our laboratory and identified two mutants that allowed for swarmer cell differentiation within the interior of a cell population. These mutants contain mini-Tn*5lacZ* insertions either 325 bp (Mutant SS-P) or 740 bp (mutant SS-N) upstream of the *flhDC* transcriptional start site in a region with no obvious open reading frames. Both mutants migrate ~5 times further than PM7002 after 12 h of swarming on standard LB agar, do not undergo consolidation, and express constitutively high levels of *flhDC* (18).

Time-lapse phase contrast microscopy of SS-P microcolonies revealed that elongation occurred almost immediately following surface contact (Fig. 5A; Supplemental Movie 3). Increased elongation of single cells appeared to coincide with each cell division. As a result, highly elongated swarmer cells were present in the population after 2 h of incubation (Fig. 5A). In contrast, differentiation within PM7002 microcolonies did not occur until 5 to 5.5 h of incubation under the same conditions

(Supplemental Movie 1). Moreover, after 6 h of incubation on solid agar, the starting point of microcolony formation consists entirely of swarmer cells; no rod-shaped cells were maintained in the population (Fig. 5B). While microcolonies of PM7002 can be followed over time, SS-P cells almost immediately become motile after surface contact, which prevented the tracking the swarmer cells over a long period of time.

Due to prior examination of SS-P (18) and the aforementioned experiments, we hypothesize the mutation conferring the phenotype of SS-P biases the entire population to exist in the *flhDC* ON state. To further characterize SS-P as a mutant locked in *flhDC* ON state, qRT-PCR analysis of *flhD* expression was performed to (i) compare expression of *flhD* in PM7002 versus SS-P and (ii) address whether $FlhD_4C_2$ is responsible for propagating the ON state bias in SS-P by introducing a null *flhC* mutation into the SS-P background. When *flhC* is mutated in the SS-P background, the expression of *flhD* was 1.9-fold lower at T_2 and 5.2-fold lower at T_4. Expression of *flhD* increased 3.9-fold between T_2 and T_4 in SS-P while there is only a 1.5-fold increase of *flhD* in SS-P *flhC*- under the same conditions (Fig. 5D). These data indicate $FlhD_4C_2$ largely contributes to maintaining the ON state bias within the SS-P population.

Differential effects of *flhDC* expression mediated by its upstream region. The *flhDC* upstream region is curiously large (3,321 bp) and AT rich (74.7% AT). As mutations conferring precocious swarming are the result of cassette insertions at -325 (for SS-P) or -740 (for SS-N) relative to *flhDC*, the *flhDC* regulatory region was investigated using reporter fusions. The transcriptional activity of four upstream fragments was examined in *trans* by ligating the fragments into a medium-copy plasmid with a promoterless *lacZ* gene and quantifying β-galactosidase activity. These fragments began within the *flhD*

open reading frame and extended to -322, -1000, -1600, or -2100 relative to the transcriptional start site. The fragment that extended to -322 had the highest transcriptional activity; 4-fold higher than the -1000 and -2100 fragments. The -1000 and -2100 fragments had equivalent activity. The fragment that extended to -1600 had the least activity; 14-fold lower than the -322 fragment and 3.5-fold lower than the -1000 and -2100 fragments (Fig. 6A). These results indicate that the region beyond -322 mediates repression of *flhDC* transcription. Maximum attenuation of *flhDC* transcription is conferred by the 600 base pair fragment between -1000 and -1600.

In order to uncover important segments upstream of *flhDC* that affect swarming motility, plasmid DNA was used to interrupt the sequence upstream of different DNA fragments in the *flhDC* regulatory region. These fragments extended to -322, -1000, -1600, -2100, or -2500 and were ligated into the suicide vector pKNG101. Swarm assays were conducted on PM7002 exconjugants containing single crossovers. Interruption of the region beyond the -322 fragment resulted in hyperswarming swarming, like SS-P. When DNA upstream from the -1000 and -2100 fragments was interrupted by pKNG101, crippled swarming occurs, and the strain harboring a disruption upstream of -1600 did not swarm. However, inactivation of the region upstream of -2500 had no effect on swarming (Fig. 6B). These results provide additional insight into potential regulatory mechanisms hidden upstream of *flhDC*. There was minimal effect on swarming motility when the region upstream of -2500 was disrupted indicating elements beyond -2500 do not affect transcriptional activity of *flhDC* enough to induce a phenotype. Meanwhile, removal of the *flhDC* upstream region beyond -322 confers precocious swarming likely by eliminating highly repressive elements between -322 and -2500. The crippled swarming

that resulted by interrupting the regions upstream of -1000 and -2100 indicates deletion of activating elements while retaining repressive components. Finally, the non-swarming phenotypes conferred by deleting the regions upstream of -1600 designate removal of a crucial *flhDC*-activating element. In combination with the pFlhDCLacZ β-galactosidase assays, these results indicate the presence of both activating and repressive elements within the *flhDC* upstream region.

Identification of putative direct regulators of *flhDC* using DNA affinity chromatography assay. In SS-N and SS-P, the transposon insertions do not interrupt any open reading frames, they do not create a new promoter, and the wild-type swarming phenotype cannot be restored by complementation of the *flhDC* regulatory region in *trans* (18). Therefore, we hypothesized the insertions conferring the swarming phenotypes of SS-O and SS-P were interrupting the binding sites of a *trans*-acting repressor. To identify putative repressors, DNA affinity chromatography assay was utilized. This technique utilizes a biotinylated DNA probe, which interacts with streptavidin beads to pull down DNA-binding proteins. Two probes were used for this analysis: probe 1 was amplified from -122 to -585 (443 bp) and included the insertion site conferring the SS-P phenotype, and probe 2 spanned from -558 to -1535 (977 bp) and included the insertion site conferring the SS-N phenotype. Since both SS-P and SS-N mutants also mediates a hyperswimming phenotype, we reasoned that the putative repressors that bound upstream of *flhDC* would not be specific to swarmer cells. Both probes were incubated with cell lysates from PM7002 grown to mid-logarithmic growth phase in LB broth, and proteins eluted from the probes were submitted for identification using LC-LC/MS. A list of proteins that bound the probes can be found in Table 4 with the proteins at the top of the

table having to most peptide spectrum matches identified by LC-LC/MS. Many of the identified proteins were bacterial nucleoid associated proteins (NAPs) including the Histone-Like Nucleoid Structuring protein, H-NS; the Factor for Inversion Stimulation, Fis; the Heat Unstable proteins, HU-α and HU-β; and the Integration Host Factor proteins, IHF-α and IHF-β. The genes encoding these NAPS were deleted from the chromosome (Table 4, bold font). For HU and IHF, double mutants were constructed to eliminate intact complex formation. In addition to the NAPs, two transcriptional regulators were deleted: the global regulatory protein, FliZ, and the *N*-acetyl-D-glucosamine repressor, NagC. The swarming behavior of all these mutants was then assessed (Fig. 7).

Of the deleted genes, no putative repressors were identified. In contrast, most of the deletions greatly decreased swarming. The deletion mutants of PM7002 Δ*fis* (Fig. 7A), Δ*ihfA*, and Δ*ihfA* Δ*ihfB* (Fig. 7C) do not swarm. Δ*hns* was slightly crippled after the second interval of swarming commenced (Fig. 7A). Δ*hupA* and Δ*hupB* were slightly crippled throughout swarming; the Δ*hupA* Δ*hupB* double mutant was severely crippled (Fig. 7B). Unlike Δ*ihfA*, which does not swarm, Δ*ihfB* swarms similarly to the PM7002 parent strain. For the transcriptional regulators deleted, Δ*nagC* experienced a half hour delay in the onset of swarming and a defect in overall migration. The *fliZ* mutant did not swarm (Fig. 7D). None of the single or double deletions shown in Fig. 7 resulted in a growth defect with the exception of Δ*ihfA* (data not shown).

Discussion.

In this study, we sought to understand two features upon the initiation of swarming behavior in *P. mirabilis* (i) why cells only differentiate at the swarm colony periphery and (ii) why vegetative rods are maintained following the initiation of swarming. Despite originating from a clonal population of vegetative cells in liquid, *P. mirabilis* exhibits heterogeneity following surface contact. In LB media, nutrient conditions are rich, but following contact with a solid surface, the fate of the initial population of vegetative cells becomes uncertain. A subset of the population undergoes differentiation while the remainder of the population remains at the swarm colony interior, morphologically indistinguishable yet transcriptomically distinct from the original population of vegetative cells (10). The heterogeneity on solid surfaces enables *P. mirabilis* to "hedge its bets" so that the subpopulation that swarms is able to discover new and perhaps more favorable environments, and the short, rod-shaped cells maintained at the point of surface contact can exploit a niche that has proven suitable. Phenotypic variation manifests to propagate the success of the entire population, as heterogeneous populations are more fit than homogenous ones (55).

Bistability, a phenomenon where a clonal population of cells exhibits heterogeneity due to non-uniform gene expression (21), is a mechanism that promotes population survival in dynamic environments. Phenotypic variation arises from unimodal noise affecting a master regulatory gene, such as $FlhD_4C_2$. Cell-to-cell fluctuations in $FlhD_4C_2$ abundance result from changes in intrinsic or extrinsic noise (55-57). Examples of potential intrinsic noise affecting $FlhD_4C_2$ in *P. mirabilis* include transient *flhDC* expression, the time required for FlhD and FlhC to assemble into the complex, and

protein stability, as both proteins have longer half-lives when assembled as $FlhD_4C_2$ (33). Possible sources of extrinsic noise include transcriptional regulation by the Rcs phosphorelay (17, 18), the MR/P fimbrial operon regulator MrpJ (45, 58), and the leucine responsive regulatory protein Lrp (38). Class II flagellar assembly protein FlhA (59) and the Umo membrane proteins affect *flhDC* expression (60). The Umo proteins mediate their effect on *flhDC* expression by modulation of the Rcs phosphorelay (61). The Lon protease is the primary mediator of $FlhD_4C_2$ cleavage thus contributing to its short half-life, and it also reduces *flhDC* expression (33, 47).

In this study, we uncovered bistable *flhDC* autoregulation in a developing swarm colony of *P. mirabilis* using time-lapse fluorescent microscopy and a strain harboring a transcriptional GFP reporter. We hypothesized *flhDC* expression would increase prior to the onset of swarming, and rod-shaped cells destined to swarm would express high levels of *flhDC* preceding differentiation. However, we observed high levels of *flhDC* expression in single cells hours before the onset of swarming. High levels of expression were present in subpopulations of the dividing microcolony; cells expressing high levels of *flhDC* originated at different locations within the microcolony, and high *flhDC* expression was inherited by daughter cells (Fig. 2C). A form of epigenetic inheritance is one where daughter cells inherit active transcriptional regulators following division. In a positive feedback loop, a positive regulator activates its own promoter to ensure high intracellular levels of the regulator, resulting in ON state, which can continue to be propagated by offspring for generations depending on growth, regulator stability, and other sources of noise (62, 63). Due to the inheritance of high *flhDC* expression, we sought to characterize $FlhD_4C_2$ as a regulator within a positive feedback loop.

Different bistable regulatory mechanisms of *flhDC* expression have been characterized in other organisms. In *Salmonella enterica,* a bistable switch affecting motility involves mutually repressing repressors and occurs in response to nutrient availability (64). Under nutrient limiting conditions, an EAL domain protein homolog, YdiV, is expressed and subsequently destabilizes or prevents the interaction of $FlhD_4C_2$ with its DNA target (65). A regulatory protein FliZ represses *ydiV* expression to abolish the negative effect of YdiV on the $FlhD_4C_2$ regulon (66); both gene products are required for heterogeneity of *S. enterica* motility (67). *S. enterica* represses motility when nutrients are limited while *E. coli* exhibits foraging behavior and becomes motile (65, 68). YdiV acts on $FlhD_4C_2$ similarly in *E. coli* (69), but its expression is not negated by FliZ which acts as direct repressor of *flhDC* (70). There is no homolog of YdiV in *P. mirabilis*.

$FlhD_4C_2$ can also interact with other gene products in autoregulatory feedback loops. Autoregulation of *flhDC* has also been observed in *Serratia marcescens* though the precise mechanism is currently unknown (71), and *flhDC* is a part of its own regulon in *E. coli* (68, 72). In *S. enterica*, $FlhD_4C_2$ can fine tune its own expression by directly activating *rflM* encoding a LuxR homolog that represses *flhDC* transcription (73). In contrast, FliZ and $FlhD_4C_2$ are direct transcriptional activators of one another's expression in the insect pathogen *Xenorhabdus nematophila* (74), and FliZ mediates the bimodal expression of flagellar genes in this bacterium (75). The FliZ mutant constructed in this study was unable to swarm (Fig. 7), possibly indicating it is a direct *flhDC* regulator and feasibly a bistable one, due to the aforementioned examples of interplay between the two regulators. Extrinsic factors that affect *flhDC* expression in *P. mirabilis*

have been identified, and due to the diverse mechanisms employed by other bacteria which result in heterogeneous *flhDC* expression, other bistable interactions affecting swarming motility in *P. mirabilis* cannot be ruled out and require further investigation. However, we quantitatively confirmed *flhDC* autoregulation (Fig. 3) and binding of FlhC to its promoter region (Fig. 4) illustrating $FlhD_4C_2$ acts as a bistable regulator in a positive feedback loop in *P. mirabilis*.

To address the maintenance of rod-shaped cells within the heterogeneous population of swarming cells, we utilized a *P. mirabilis* mutant SS-P which does not undergo consolidation (18) and differentiates immediately following surface contact (Fig. 5A). In liquid culture, SS-P exists as vegetative rods, but following surface contact forms a homogeneous population of swarmer cells. The vegetative rods present at the point of inoculation in a wild-type *P. mirabilis* swarm colony are not maintained in this mutant (Fig. 5B). Antibiotic cassette insertions located at -740 and -325 in the *flhDC* upstream region result in this unique form of precocious swarming; interruption of the region upstream of -322 using an integrative plasmid also confers the phenotype (Fig. 6A). While wild-type cells heterogeneously express *flhDC* within the population, SS-P cells solely exist in ON state, expressing constitutively high levels of *flhDC* (Fig. 5C) which is dependent on the presence of intact $FlhD_4C_2$ (Fig. 5D). We hypothesized SS-P perpetually remains in ON state due to the cassette insertion affecting the binding site of a *trans*-acting repressor, and the vegetative cells maintained following surface contact in a wild-type strain do not swarm due in part to repressor binding.

Insertions upstream of *flhDC* that increase motility are not limited to *P. mirabilis*, and the idea that such insertions affect the binding of transcriptional repressors has been

proposed. In *E. coli*, insertion sequence (IS) elements in the regulatory region of *flhDC* give rise to motility in MG1655 by interrupting the binding sites of repressors LhrA and OmpR (76). In *P. mirabilis*, mutants of OmpR (18) and LhrA (10) do not have significantly altered swarming phenotypes. Highly motile *E. coli* mutants have been shown to contain IS element insertions anywhere from the promoter region to ~450 bp upstream of the *flhD* transcriptional start site or single base pair insertions around the *flhDC* promoter. Some of these mutants were motile in the absence of the nucleoid associated protein H-NS which is required for motility in *E. coli* (77, 78). The H-NS mutant constructed in this study had a modest 0.5-fold decrease in migration after 8 h on LB agar, following consolidation phase (Fig 7A).

To identify repressors of the *flhDC* operon that could support the SS-P phenotype and the maintenance of rod-shaped cells in the interior of the swarming population, DNA affinity chromatography was utilized. Proteins bound to the *P. mirabilis flhDC* upstream region included FliZ, the *N*-acetyl-D-glucosamine repressor NagC (79), and bacterial nucleoid associated proteins (NAPs) H-NS, Fis, HU-αβ, and IHF-αβ. None of the proteins that bound the *flhDC* upstream region were identified as *flhDC* repressors. Previous transposon based screens to identify putative *flhDC* repressors have been performed by our laboratory, and despite saturation of the genome, no insertions in genes encoding *trans*-acting factors have been isolated that conferred a phenotype similar that seen in the SS-P mutant. One possibility to explain this is that the repressor may be essential for cell viability. However, deletions in genes encoding the above proteins resulted in significant defects in swarming motility, with the exception of IHF-β, which migrated similarly to wild-type (Fig. 7). The IHF-α mutant exhibited a growth defect that

was recapitulated in the *ihfA ihfB* double mutant. Swarming by Δ*ihfA* could not be restored by artificial overexpression of *flhDC* in *trans*, and the mutant had a cell morphology defect (data not shown) which likely mediates its inability to swarm or grow efficiently in LB broth. The two IHF subunits have their own regulons, and differential effects of *ihfA* and *ihfB* on motility and flagellar gene expression have been observed in other organisms (80), which could explain why Δ*ihfB* did not exhibit a swarming defect while Δ*ihfA* did (Fig. 7C). The single HU subunit deletions were moderately crippled while the *hupA hupB* double mutant was severely crippled. Like IHF, each HU subunit has a unique regulon and subsequent motility phenotypes when deleted (81). Swarming motility in the *hupA hupB* double mutant could be restored by artificial overexpression of *flhDC* in *trans* (data not shown), possibly indicating HU-αβ acts directly on *flhDC*. Of the two transcriptional regulators, the *nagC* mutant was crippled in swarming; it has been shown to be important for swarming motility in *E. coli* (79), and the *fliZ* mutant did not swarm (Fig. 7D). FliZ represses *flhDC* expression in *E. coli*, but is an activator of the operon in *S. enterica* and *X. nematophila.* Since FliZ is a characterized bistable mediator of motility in these organisms, future studies to elucidate a potential bistable interaction with *flhDC* in *P. mirabilis* is warranted (64, 70, 75). Overall, extensive characterization of each of the identified mutants is required to understand the contribution of these genes to swarming motility and *flhDC* regulation in *P. mirabilis*.

In this work, we sought to understand the genetic mechanisms responsible for the ability of cells in the exterior of a population *P. mirabilis* cells to undergo differentiation upon surface contact, while the interior of the population does not. We illustrate differentiation of swarmer cells results from bistable expression of *flhDC,* which is

subject to autoregulation. We further demonstrate the importance of the *flhDC* regulatory region, as different segments upstream from the operon promote or repress its expression. Lastly, we identify putative, novel regulators of *flhDC* expression, and lay the groundwork for future studies to understand the precise contribution of these proteins to *P. mirabilis* physiology. Additionally, to our knowledge, this is the first demonstration of direct $FlhD_4C_2$ autoregulation, a mechanism of gene regulation compatible with the biology of a robustly motile organism.

References.

1. **HOENIGER JFM.** 1965. Development of Flagella by Proteus mirabilis. Microbiology **40:**29-42.
2. **Jones BV, Young R, Mahenthiralingam E, Stickler DJ.** 2004. Ultrastructure of Proteus mirabilis swarmer cell rafts and role of swarming in catheter-associated urinary tract infection. Infect Immun **72:**3941-3950.
3. **Williams FD, Schwarzhoff RH.** 1978. Nature of the swarming phenomenon in Proteus. Annu Rev Microbiol **32:**101-122.
4. **Morgenstein RM, Clemmer KM, Rather PN.** 2010. Loss of the waaL O-antigen ligase prevents surface activation of the flagellar gene cascade in Proteus mirabilis. J Bacteriol **192:**3213-3221.
5. **Gygi D, Bailey MJ, Allison C, Hughes C.** 1995. Requirement for FlhA in flagella assembly and swarm-cell differentiation by Proteus mirabilis. Mol Microbiol **15:**761-769.
6. **Allison C, Lai HC, Gygi D, Hughes C.** 1993. Cell differentiation of Proteus mirabilis is initiated by glutamine, a specific chemoattractant for swarming cells. Mol Microbiol **8:**53-60.
7. **Belas R, Suvanasuthi R.** 2005. The ability of Proteus mirabilis to sense surfaces and regulate virulence gene expression involves FliL, a flagellar basal body protein. J Bacteriol **187:**6789-6803.
8. **Sturgill G, Rather PN.** 2004. Evidence that putrescine acts as an extracellular signal required for swarming in Proteus mirabilis. Mol Microbiol **51:**437-446.
9. **Armitage JP.** 1981. Changes in metabolic activity of Proteus mirabilis during swarming. J Gen Microbiol **125:**445-450.

10. **Pearson MM, Rasko DA, Smith SN, Mobley HL.** 2010. Transcriptome of swarming Proteus mirabilis. Infect Immun **78:**2834-2845.

11. **Rauprich O, Matsushita M, Weijer CJ, Siegert F, Esipov SE, Shapiro JA.** 1996. Periodic phenomena in Proteus mirabilis swarm colony development. Journal of Bacteriology **178:**6525-6538.

12. **Zhang R, Turner L, Berg HC.** 2010. The upper surface of an Escherichia coli swarm is stationary. Proceedings of the National Academy of Sciences **107:**288-290.

13. **Kearns DB, Losick R.** 2003. Swarming motility in undomesticated Bacillus subtilis. Mol Microbiol **49:**581-590.

14. **Morrison RB, Scott ANN.** 1966. Swarming of Proteus[mdash]A Solution to an Old Problem? Nature **211:**255-257.

15. **Belas R, Simon M, Silverman M.** 1986. Regulation of lateral flagella gene transcription in Vibrio parahaemolyticus. Journal of Bacteriology **167:**210-218.

16. **Kearns DB, Losick R.** 2005. Cell population heterogeneity during growth of Bacillus subtilis. Genes & Development **19:**3083-3094.

17. **Belas R, Schneider R, Melch M.** 1998. Characterization of Proteus mirabilis precocious swarming mutants: identification of rsbA, encoding a regulator of swarming behavior. J Bacteriol **180:**6126-6139.

18. **Clemmer KM, Rather PN.** 2007. Regulation of flhDC expression in Proteus mirabilis. Research in Microbiology **158:**295-302.

19. **Williams FD, Anderson DM, Hoffman PS, Schwarzhoff RH, Leonard S.** 1976. Evidence against the involvement of chemotaxis in swarming of Proteus mirabilis. J Bacteriol **127:**237-248.

20. **Dubnau D, Losick R.** 2006. Bistability in bacteria. Mol Microbiol **61:**564-572.

21. **Veening J-W, Smits WK, Kuipers OP.** 2008. Bistability, Epigenetics, and Bet-Hedging in Bacteria. Annual Review of Microbiology **62:**193-210.

22. **Gardner TS, Cantor CR, Collins JJ.** 2000. Construction of a genetic toggle switch in Escherichia coli. Nature **403:**339-342.

23. **Chung JD, Stephanopoulos G, Ireton K, Grossman AD.** 1994. Gene expression in single cells of Bacillus subtilis: evidence that a threshold mechanism controls the initiation of sporulation. Journal of Bacteriology **176:**1977-1984.

24. **Haijema BJ, Hahn J, Haynes J, Dubnau D.** 2001. A ComGA-dependent checkpoint limits growth during the escape from competence. Molecular Microbiology **40:**52-64.

25. **Claret L, Hughes C.** 2002. Interaction of the Atypical Prokaryotic Transcription Activator FlhD2C2 with Early Promoters of the Flagellar Gene Hierarchy. Journal of Molecular Biology **321:**185-199.

26. **Claret L, Hughes C.** 2000. Functions of the subunits in the FlhD2C2 transcriptional master regulator of bacterial flagellum biogenesis and swarming1. Journal of Molecular Biology **303:**467-478.

27. **Liu X, Matsumura P.** 1994. The FlhD/FlhC complex, a transcriptional activator of the Escherichia coli flagellar class II operons. J Bacteriol **176:**7345-7351.

28. **Lee Y-Y, Barker CS, Matsumura P, Belas R.** 2011. Refining the Binding of the Escherichia coli Flagellar Master Regulator, FlhD4C2, on a Base-Specific Level. Journal of Bacteriology **193:**4057-4068.

29. **Wang S, Fleming RT, Westbrook EM, Matsumura P, McKay DB.** 2006. Structure of the Escherichia coli FlhDC Complex, a Prokaryotic Heteromeric Regulator of Transcription. Journal of Molecular Biology **355:**798-808.

30. **Furness RB, Fraser GM, Hay NA, Hughes C.** 1997. Negative feedback from a Proteus class II flagellum export defect to the flhDC master operon controlling cell division and flagellum assembly. J Bacteriol **179:**5585-5588.

31. **Gygi D, Fraser G, Dufour A, Hughes C.** 1997. A motile but non-swarming mutant of Proteus mirabilis lacks FlgN, a facilitator of flagella filament assembly. Molecular Microbiology **25:**597-604.

32. **Fraser GM, Bennett JCQ, Hughes C.** 1999. Substrate-specific binding of hook-associated proteins by FlgN and FliT, putative chaperones for flagellum assembly. Molecular Microbiology **32:**569-580.

33. **Claret L, Hughes C.** 2000. Rapid Turnover of FlhD and FlhC, the Flagellar Regulon Transcriptional Activator Proteins, duringProteus Swarming. Journal of Bacteriology **182:**833-836.

34. **Stevenson LG, Rather PN.** 2006. A Novel Gene Involved in Regulating the Flagellar Gene Cascade in Proteus mirabilis. Journal of Bacteriology **188:**7830-7839.

35. **Liaw SJ, Lai HC, Ho SW, Luh KT, Wang WB.** 2001. Characterisation of p-nitrophenylglycerol-resistant Proteus mirabilis super-swarming mutants. J Med Microbiol **50:**1039-1048.

36. **Pearson MM, Mobley HL.** 2008. Repression of motility during fimbrial expression: identification of 14 mrpJ gene paralogues in Proteus mirabilis. Mol Microbiol **69:**548-558.

37. **Wang WB, Chen IC, Jiang SS, Chen HR, Hsu CY, Hsueh PR, Hsu WB, Liaw SJ.** 2008. Role of RppA in the regulation of polymyxin b susceptibility, swarming, and virulence factor expression in Proteus mirabilis. Infect Immun **76:**2051-2062.

38. **Hay NA, Tipper DJ, Gygi D, Hughes C.** 1997. A nonswarming mutant of Proteus mirabilis lacks the Lrp global transcriptional regulator. J Bacteriol **179:**4741-4746.

39. **Hart BR, Blumenthal RM.** 2011. Unexpected coregulator range for the global regulator Lrp of Escherichia coli and Proteus mirabilis. J Bacteriol **193:**1054-1064.

40. **Hatt JK, Rather PN.** 2008. Characterization of a novel gene, wosA, regulating FlhDC expression in Proteus mirabilis. J Bacteriol **190:**1946-1955.

41. **Kaniga K, Delor I, Cornelis GR.** 1991. A wide-host-range suicide vector for improving reverse genetics in Gram-negative bacteria: inactivation of the blaA gene of Yersinia enterocolitica. Gene **109:**137-141.

42. **Manoil C, Beckwith J.** 1985. TnphoA: a transposon probe for protein export signals. Proc Natl Acad Sci U S A **82:**8129-8133.

43. **de Lorenzo V, Herrero M, Jakubzik U, Timmis KN.** 1990. Mini-Tn5 transposon derivatives for insertion mutagenesis, promoter probing, and chromosomal insertion of cloned DNA in gram-negative eubacteria. Journal of Bacteriology **172:**6568-6572.

44. **Szostek BA, Rather PN.** 2013. Regulation of the Swarming Inhibitor disA in Proteus mirabilis. Journal of Bacteriology **195:**3237-3243.

45. **Li X, Rasko DA, Lockatell CV, Johnson DE, Mobley HLT.** 2001. Repression of bacterial motility by a novel fimbrial gene product. The EMBO Journal **20:**4854-4862.

46. **Chang AC, Cohen SN.** 1978. Construction and characterization of amplifiable multicopy DNA cloning vehicles derived from the P15A cryptic miniplasmid. Journal of Bacteriology **134:**1141-1156.

47. **Clemmer KM, Rather PN.** 2008. The Lon protease regulates swarming motility and virulence gene expression in Proteus mirabilis. Journal of Medical Microbiology **57:**931-937.

48. **Farinha MA, Kropinski AM.** 1990. Construction of broad-host-range plasmid vectors for easy visible selection and analysis of promoters. Journal of Bacteriology **172:**3496-3499.

49. **Moynihan PJ, Clarke AJ.** 2011. O-Acetylated peptidoglycan: controlling the activity of bacterial autolysins and lytic enzymes of innate immune systems. Int J Biochem Cell Biol **43:**1655-1659.

50. **Miller JH.** 1972. Experiments in molecular genetics. Cold Spring Harbor Laboratory.

51. **Livak KJ, Schmittgen TD.** 2001. Analysis of relative gene expression data using real-time quantitative PCR and the 2(-Delta Delta C(T)) Method. Methods **25:**402-408.

52. **Howery KE, Clemmer KM, Simsek E, Kim M, Rather PN.** 2015. Regulation of the Min Cell Division Inhibition Complex by the Rcs Phosphorelay in Proteus mirabilis. Journal of Bacteriology **197:**2499-2507.

53. **Jutras BL, Verma A, Stevenson B.** 2005. Identification of Novel DNA-Binding Proteins Using DNA-Affinity Chromatography/Pull Down, Current Protocols in Microbiology doi:10.1002/9780471729259.mc01f01s24. John Wiley & Sons, Inc.

54. **Farrow JM, Hudson LL, Wells G, Coleman JP, Pesci EC.** 2015. CysB Negatively Affects the Transcription of pqsR and Pseudomonas Quinolone Signal Production in Pseudomonas aeruginosa. Journal of Bacteriology **197:**1988-2002.

55. **Kussell E, Leibler S.** 2005. Phenotypic Diversity, Population Growth, and Information in Fluctuating Environments. Science **309:**2075-2078.

56. **Elowitz MB, Levine AJ, Siggia ED, Swain PS.** 2002. Stochastic Gene Expression in a Single Cell. Science **297:**1183-1186.

57. **Swain PS, Elowitz MB, Siggia ED.** 2002. Intrinsic and extrinsic contributions to stochasticity in gene expression. Proceedings of the National Academy of Sciences **99:**12795-12800.

58. **Bode NJ, Debnath I, Kuan L, Schulfer A, Ty M, Pearson MM.** 2015. Transcriptional analysis of the MrpJ network: modulation of diverse virulence-associated genes and direct regulation of mrp fimbrial and flhDC flagellar operons in Proteus mirabilis. Infect Immun **83:**2542-2556.

59. **Furness RB, Fraser GM, Hay NA, Hughes C.** 1997. Negative feedback from a Proteus class II flagellum export defect to the flhDC master operon controlling cell division and flagellum assembly. Journal of Bacteriology **179:**5585-5588.

60. **Dufour A, Furness RB, Hughes C.** 1998. Novel genes that upregulate the Proteus mirabilis flhDC master operon controlling flagellar biogenesis and swarming. Molecular Microbiology **29:**741-751.

61. **Morgenstein RM, Rather PN.** 2012. Role of the Umo proteins and the Rcs phosphorelay in the swarming motility of the wild type and an O-antigen (waaL) mutant of Proteus mirabilis. J Bacteriol **194:**669-676.

62. **Ajo-Franklin CM, Drubin DA, Eskin JA, Gee EP, Landgraf D, Phillips I, Silver PA.** 2007. Rational design of memory in eukaryotic cells. Genes Dev **21:**2271-2276.

63. **Kaufmann BB, Yang Q, Mettetal JT, van Oudenaarden A.** 2007. Heritable Stochastic Switching Revealed by Single-Cell Genealogy. PLoS Biol **5:**e239.

64. **Koirala S, Mears P, Sim M, Golding I, Chemla YR, Aldridge PD, Rao CV.** 2014. A Nutrient-Tunable Bistable Switch Controls Motility in Salmonella enterica Serovar Typhimurium. mBio **5**.

65. **Wada T, Morizane T, Abo T, Tominaga A, Inoue-Tanaka K, Kutsukake K.** 2011. EAL Domain Protein YdiV Acts as an Anti-FlhD(4)C(2) Factor Responsible for Nutritional Control of the Flagellar Regulon in Salmonella enterica Serovar Typhimurium. J Bacteriol **193:**1600-1611.

66. **Wada T, Tanabe Y, Kutsukake K.** 2011. FliZ Acts as a Repressor of the ydiV Gene, Which Encodes an Anti-FlhD(4)C(2) Factor of the Flagellar Regulon in Salmonella enterica Serovar Typhimurium. J Bacteriol **193:**5191-5198.

67. **Stewart MK, Cookson BT.** 2014. Mutually repressing repressor functions and multi-layered cellular heterogeneity regulate the bistable Salmonella fliC census. Mol Microbiol **94:**1272-1284.

68. **Zhao K, Liu M, Burgess RR.** 2007. Adaptation in bacterial flagellar and motility systems: from regulon members to 'foraging'-like behavior in E. coli. Nucleic Acids Research **35:**4441-4452.

69. **Li B, Li N, Wang F, Guo L, Huang Y, Liu X, Wei T, Zhu D, Liu C, Pan H, Xu S, Wang HW, Gu L.** 2012. Structural insight of a concentration-dependent mechanism by

which YdiV inhibits Escherichia coli flagellum biogenesis and motility. Nucleic Acids Res **40:**11073-11085.

70. **Pesavento C, Hengge R.** 2012. The global repressor FliZ antagonizes gene expression by σ(S)-containing RNA polymerase due to overlapping DNA binding specificity. Nucleic Acids Res **40:**4783-4793.

71. **Jia-Hurng Liu A, Meng-Jiun L, Sunny Ang A, Jwu-Ching S, Po-Chi Soo A, Yu-Tze Horng A, Wen-Ching Yi A, Hsin-Chih Lai A, Kwen-Tay L, Shen-Wu H, Swift S.** 2000. Role of flhDC in the Expression of the Nuclease Gene nucA, Cell Division and Flagellar Synthesis in Serratia marcescens. Journal of Biomedical Science **7:**475-483.

72. **Prüß BM, Liu X, Hendrickson W, Matsumura P.** 2001. FlhD/FlhC-regulated promoters analyzed by gene array and lacZ gene fusions. FEMS Microbiology Letters **197:**91-97.

73. **Singer HM, Erhardt M, Hughes KT.** 2013. RflM Functions as a Transcriptional Repressor in the Autogenous Control of the Salmonella Flagellar Master Operon flhDC. J Bacteriol **195:**4274-4282.

74. **Lanois A, Jubelin G, Givaudan A.** 2008. FliZ, a flagellar regulator, is at the crossroads between motility, haemolysin expression and virulence in the insect pathogenic bacterium Xenorhabdus. Molecular Microbiology **68:**516-533.

75. **Jubelin G, Lanois A, Severac D, Rialle S, Longin C, Gaudriault S, Givaudan A.** 2013. FliZ Is a Global Regulatory Protein Affecting the Expression of Flagellar and Virulence Genes in Individual Xenorhabdus nematophila Bacterial Cells. PLoS Genet **9**.

76. **Barker CS, Prüß BM, Matsumura P.** 2004. Increased Motility of Escherichia coli by Insertion Sequence Element Integration into the Regulatory Region of the flhD Operon. Journal of Bacteriology **186:**7529-7537.

77. **Fahrner KA, Berg HC.** 2015. Mutations That Stimulate flhDC Expression in Escherichia coli K-12. J Bacteriol **197:**3087-3096.

78. **Lee C, Park C.** 2013. Mutations upregulating the flhDC operon of Escherichia coli K-12. J Microbiol **51:**140-144.

79. **Inoue T, Shingaki R, Hirose S, Waki K, Mori H, Fukui K.** 2007. Genome-Wide Screening of Genes Required for Swarming Motility in Escherichia coli K-12. J Bacteriol **189:**950-957.

80. **Mangan MW, Lucchini S, Danino V, Croinin TO, Hinton JC, Dorman CJ.** 2006. The integration host factor (IHF) integrates stationary-phase and virulence gene expression in Salmonella enterica serovar Typhimurium. Mol Microbiol **59:**1831-1847.

81. **Mangan MW, Lucchini S, T OC, Fitzgerald S, Hinton JC, Dorman CJ.** 2011. Nucleoid-associated protein HU controls three regulons that coordinate virulence, response to stress and general physiology in Salmonella enterica serovar Typhimurium. Microbiology **157:**1075-1087.

Table 1. Strains and plasmids used in this study

Strain or plasmid	Description/genotype	Source
***E. coli* strains**		
DH5α	F- Φ80d*lacZ*ΔM15 Δ(*lacZYA-argF'*)U169 *endA1 recA1 hsdR17(*r_k- m_k-)*deoR thi-1 supE44* λ- *gyrA96 relA1*	Laboratory stock
CC118 λ*pir*	*araD139* Δ*(ara leu)7697* Δ*lacZ74 phoA*Δ*20 galE galK thi rpsE rpoB argE(Am) recA1*	(42)
SM10 λ*pir*	*thi thr leu tonA supE recA* RP4-2Tc::Mu Kan^r λ*pir*	(43)
BL21	F^- *ompT hsdS*$_B$(r_B^- m_B^-) *gal dcm* (DE3)	Stratagene
MGIBKY	*km:T:ptet:GFP(intC)*	Kim lab stock
***P. mirabilis* strains**		
PM7002	Wild type; Tc^R	ATCC
SS-P	-325 *flhDC*::Kan^R	(18)
PMKH8	PM7002 *flhDC*Ω*lacZ* pACYC184	This study
PMKH9	PM7002 *flhDC*Ω*lacZ* pFDCH1	This study
BB7	PM7002 *flhC*$^-$	(44)
PMKH10	SS-P *flhC*$^-$	This study
PMKH11	PM7002 + pFlhDCLacZ (-2100)	This study
PMKH12	BB7 + pFlhDCLacZ (-2100)	This study
PMKH14	PM7002 *flhDC*Ω*gfp*	This study
PMJH1-3	PM7002 + pFlhDCLacZ (-322, -1000, or -1600)	This study
PMJH5-9	PM7002 + pFlhDCpINT	This study
Plasmids		
pBluescriptII KS(−)	ColE1 replicon *lacZ*α; Chl^R	Stratagene
pKNG101	R6K replicon *mob*$^+$ *sacB*$^+$*R*$^+$; Sm^R	(41)
pET21a	F1 ori lacI expression vector; Amp^R	Novagen
pQF50	pRO1600 replicon *lacZ*α (promoterless); Amp^R	(48)
pACYC184	p15A ori Tet^R, Cm^R	(46)
pFDCH1	pACYC184 + *flhDC*	(47)
pBB4	pKNG101 +*flhC*$^-$ (frameshift mutation)	(44)
pFlhDCLacZ	pQF50 + *flhDCp* (-322, -1000, -1600, or -2100)	This study
pFlhC	pET21a + *flhC*	This study
pFlhCGFP	pKNG101 + '*flhC*-Egfp	This study
pFlhDCpINT	pKNG101::-322, -1000, -1600, -2100, or -2500 *flhDCp*	This study

Tc, tetracycline; Sm, streptomycin; Amp, ampicillin; Chl, chloramphenicol; Kan, kanamycin

Table 2. Primer sequences used in this study

Primer	Sequence (5' →3')
flhCGFP-F	TTAAGGATCCCGCAATTAAGTCGAGGGCGT
flhCGFP-R	TTAACTGCAGGAATCACATTGCAAACTGTTCAA
GFP-F	TTAACTGCAGGCAGCAGGACGCACTGAC
GFP-R	TTAATCTAGAAAGCTTTTATTTGTATAGTTCATCC
flhC-F	TAACATATGATGAGTGAGAAAAGTATCGTCCGA
flhC-R	TAACTCGAGCATTGCAAACTGTTCAAGACCATC
Probe 1-F	TTATAAGGTAAGATGCATAACTAGGAA
Probe 1-R	CTTGCTGAGAATTAATAAGCGAA
Probe 2-F	GCTAAGGCTACTCTTCTCAAA
Probe 2-R	TTCCTAGTTATGCATCTTACCTTATAA
flhDCp-F	TTTGAATTCGAGGAGCTATGGCAATATATGTTACTG
flhDCp-R	TTTGAATTCTCGCCAATATATCAC
flhDCp2-R	TTTGAATTCGCCCGTTTCTTTGTAGCAGAGG
flhDqRT-F	TTGGTTAAGTTGGCTGAAAC
flhDqRT-R	TTTGTAGCAGAGGTATCATG
clpX-F	CGCATCGGCCATGGTAAAAG
clpX-R	ATATCCTGCTGATTGGCCCG

Table 3. Primers sequences used in this study to make in-frame deletions

hnsIFD1-F	CCAATATTGACCAGCAATGGAAACT
hnsIFD1-R	GCTCATTTTCCTGGTCTCAAA
hnsIFD2-F	GAAGATTTCCTCATCTAATTTAATGCA
hnsIFD2-R	TTGGATCCCAGATTCAGTGAGTATTGCGC
hns-F	CCTTTATTGGCGAAAGATGC
hns-R	AAACGCTCGTTTAATAAAAATGACT
hupAIFD1-F	TTGGATCCTAGAAGAAGCTATTCCTGATGCATCTC
hupAIFD1-R	TTCAGCTTTGTTCATAAA ATAGTCCTT
hupAIFD2-F	GACGCAGTAAAATAATTCCTTTGAACG
hupAIFD2-R	TTGGATCCCAACATAAGCGGGACGAGTTAGAT
hupA-F	CGAAAAGAAGTGGCTCAGGTG
hupA-R	AACAAAAGGGGAGCAACTCCC
hupBIFD1-F	CCACTATCTTGAAGTGGACTACGA
hupBIFD1-R	CATCCCCATAATTTATGCGTTATTTTTTAC
hupBIFD2-F	GACGCAGTAAATCAATAATTGAGTAAATCG
hupBIFD2-R	GGGCTTCTAACTGAATATAGCTCACTT
hupB-F	GGATAAGCAATAAAAGCTTGCCAGTC
hupB-R	GAAAAGCGCATCCTTTAAAGATGCG
ihfAIFD1-F	TTGGATCCTTGATCCGAAGATCCAAAGCTTAC
ihfAIFD1-R	TGTAAGCGCCATAGGTCTAGT
ihfAIFD2-F	GAGTAATACTTAAACACCAAAACGGCT
ihfAIFD2-R	TTGGATCCAATAAGCAGGTGATCCCCAAA
ihfA-F	GGTTATAAGAGCCTCGCTATTAGCT
ihfA-R	GAAGGAGTAAATCGTAGAAGTAAGTCG
ihfBIFD1-F	GAAATTCGACCGTGAGCGTACTCGCGT
ihfBIFD1-F	CTTGGTCATATTACCTCCCTAGACTAC
ihfBIFD1-F	ACGGAATAATAGTTTCCTATCAAATAGGCA
ihfBIFD1-F	CCTGACAATGTTTCTCTTACTGAAACG
ihfB-F	AAACAACGCTATGGCTGAAGCTTT
ihfB-R	GAACGTAACTTAATACCAACCGATAACCC
fisIFD1-F	TTGGATCCGATCCGCTCCGTACAAATTGC
fisIFD1-R	GCGTTGTTCGAACATAGTTCTGTC
fisIFD2-F	GGCATGAATTAATAGAAGTCGTATAATACA
fisIFD2-R	TTGGATCCAAATTGAGAAGTCAATCTTCTGTGGTT
fis-F	TTCAACGCCATAGAGGATGC
fis-R	TTTCGTGGCTATCACCCACTA
fliZIFD1-F	GTAATGCAAGAGAAGTGACACAATCCA
fliZIFD1-R	TGTTGAAACAGACATAAGAGATAAAGCCCT
fliZIFD2-F	AGTGGTCACTAATCGCATTCAAGAGAG
fliZIFD2-R	CAAGGTGCTTTGTCTCTCAGATAATGA
fliZ-F	TTATTTATTAAGACTACAACACAGGGC
fliZ-F	GAGACCACCTTTAACTTACTTATCTATTAA
nagCIFD1-F	TTGGATCCAACGGGTCACGTATTGAGCAG
nagCIFD1-R	GTGACTCATCAGCATTTACATCCA
nagCIFD2-F	GAGTTACTACAATATTTATTCGACAAATAATCTTTT
nagCIFD2-R	TTTCTAGAACTTGAACTCGCACACCTTGC
nagC-F	ATGCGGACGGTACATTAAGTG
nagC-R	CAACGCACAGTTATTTTAGCTGCA

Table 4. Transcriptional regulators bound to *flhDC* upstream region

Probe 1	Probe 2
Lrp	**H-NS**
FliZ	**NagC**
H-NS	PMI1764 (*hexA*)
Fis	Ssb
Ssb	Lrp
IHF-α	**Fis**
IHF-β	PMI1540 (*yjhU* homolog)
ArcA	IclR
HU-α	HdfR
PMI1764 (*hexA*)	PMI0801 (*yafC* homolog)
	ArcA
	HexR
	IHF-α
	IHF-β
	GvaC
	PMI0825 (*ndpA* homolog)
	PMI3003 (*mrpJ* paralog)
	HU-β
	HU-α

*Bold letters indicate proteins where in-frame deletions were constructed in corresponding genes

Figure legends.

Figure 1. Swarming colonies of PM7002 preferentially differentiate at colony periphery. (A) Phase contrast images of PM7002 following the initiation of swarming on 1.5% LB agar. Images were obtained once cells began to swarm using an Olympus BX51 Research System Microscope. Elongated swarmer cells are found at the colony periphery, while the interior consists of non-swarming, short, rod-shaped cells. (B) A microcolony of PM7002 captured using time-lapse phase contrast microscopy. Image was obtained 5.5 h following inoculation of a low-density PM7002 culture onto a petri dish and overlaid with agarose pad. (C) Vegetative rod shaped cells are maintained in the swarming population at the point of inoculation, and (D) swarmer cells are the dominant morphotype during swarm phase. For (C) and (D), cells were removed from the point of inoculation or from cells in swarm phase 8 h following inoculation onto LB agar, resuspended in LB broth, and 1.5 µl was spotted onto a glass side. Images were obtained at 1,000X magnification using oil immersion.

Figure 2. *flhDC* expression is high in subpopulations of non-swarming *P. mirabilis* cells during colony development. GFP expression in PMKH14 (PM7002 *flhDCΩgfp*). PMKH14 was grown overnight in LB + Str^{35} at 37°C without shaking. Cells were subcultured, grown to an OD_{600}~0.01 at 37°C with shaking at 250 rpm then diluted to an OD_{600}~0.0025 in 2 ml of fresh LB + Str^{35}. After 45 min at 37°C with shaking, 2 µl was pipetted onto a glass bottom Petri dish and overlaid with a 1.5% LB agar pad + Str^{35}. Fluorescent images were acquired every 15 min using an Olympus IX83 microscope. (A) A microcolony of PMKH14 after 4.23 h of growth. (B) A microcolony of PMKH14 after 9 h of growth upon initiation of swarming. High GFP expression occurs at microcolony

exterior where swarmer cells form. (C) The image of the microcolony in (A) was cropped to focus on a single cell expressing GFP before (left; t = 4.23 h) and after (right; t = 4.58 h) cell division (indicated by white arrows). GFP expression is inherited and appears to increase in daughter cells. Image adjustments (brightness, contrast, sharpness) were applied equally.

Figure 3. The *flhDC* operon is autoregulated. (A) β-galactosidase activity of PM7002 *flhDC*Ω*lacZ* with or without constitutive *flhDC* expression in liquid. PMKH8 (PM7002 *flhDC*Ω*lacZ* + pACYC184*)* and PMKH9 (PM7002 *flhDC*Ω*lacZ* + pFDCH1) were grown to mid- and late-logarithmic growth phase. Activity of the chromosomal *flhDC*Ω*lacZ* transcriptional fusion increased 5.1-fold at mid-log and 8-fold at late log when harboring pFDCH1 (pACYC184 + *flhDC*) relative to empty pACYC184. (B) β - galactosidase activity of PM7002 *flhDC*Ω*lacZ* with or without constitutive *flhDC* expression on solid agar. Activity of *flhDC*Ω*lacZ* increased 5.2-fold and 3-fold, respectively, after 2 and 4 h of incubation on 1.5% LB agar in PMKH9 relative to PMKH8. (C) β-galactosidase activity of pFlhDCLacZ (pQF50 + *flhDCp* [-2100]) in PMKH11 (PM7002 + pFlhDCLacZ [-2100]) and PMKH12 (PM7002 *flhC*$^{-}$ + pFlhDCLacZ [-2100]). The activity of the *flhDC* promoter is decreased 2.4-fold in a *flhC* mutant background relative to wild-type after 4 h of incubation of solid agar. (D) qRT-PCR analysis of *flhD* expression in PM7002 and BB7 (PM7002 *flhC*$^{-}$). Expression of *flhD* is 1.9-fold lower after 2 h and 5-fold lower after 4 h on solid agar in the *flhC* mutant relative to wild-type. There is a 1.4-fold increase in *flhD* expression in the *flhC* mutant between T_2 and T_4 versus a 3.6-fold increase of *flhD* expression in PM7002. Error bars represent standard deviations. An asterisk indicates a *p*-value <0.05

Figure 4. FlhC binds to the *flhDC* promoter. Shown is the specific binding of purified FlhC-His_6 to the *flhDC* promoter region (*flhDCp*). The 124-bp *flhDCp* probe was incubated with 60 pmol FlhC-$His_{6.}$ This binding was competed with unlabeled *flhDCp* DNA (124 bp) and unlabeled *abaI* DNA (249 bp). Lane 1, free *flhDCp* probe; lane 2, *flhDCp* probe with 60 pmol FlhC; lane 3, *flhDCp* probe with 60 pmol FlhC and unlabeled *flhDCp* DNA; lane 4, *flhDCp* probe with 60 pmol FlhC and unlabeled *abaI* DNA.

Figure 5. Characterization of SS-P, a mutant that differentiates at the swarm colony interior. (A) SS-P differentiates upon contact with a solid surface. (B) Rod shaped cells are not present in the SS-P population following the initiation of swarming. (C) qRT-PCR analysis of *flhD* expression in PM7002 and SS-P on solid agar. Expression of *flhD* increased 9.4-fold after 2 h and 36.7-fold after 4 h of incubation on LB agar in SS-P relative to PM7002 at T_2. (D) qRT-PCR analysis of *flhD* in SS-P and PMKH10 (SS-P *flhC*$^-$). Expression of *flhD* is 1.9-fold lower after 2 h and 5.2-fold lower after 4 h of incubation on solid agar when *flhC* is mutated in the SS-P background. Expression of *flhD* increases 3.9-fold between T_2 and T_4 in SS-P while there is only a 1.5-fold increase of *flhD* in SS-P *flhC*$^-$ under the same conditions. Error bars represent standard deviations. An asterisk indicates a *p*-value <0.05.

Figure 6. Differential effects on *flhDC* transcriptional activity are mediated by its upstream region. (A) β -galactosidase activity of pFlhDCLacZ (pQF50 + *flhDCp*) with different *flhDC* promoter fragments: PMJH1 (PM7002 + pFlhDCLacZ [-322]), PMJH2 (PM7002 + pFlhDCLacZ [-1000]), PMJH3 (PM7002 + pFlhDCLacZ [-1600]) or PMKH11 (PM7002 + pFlhDCLacZ [-2100]).The activity of PM7002 harboring pFlhDCLacZ (-322) is 4-fold higher than pFlhDCLacZ (-1000) and pFlhDCLacZ

(-2100). The -1000 and -2100 fragments have nearly equal activity. pFlhDCLacZ (-322) activity is 14-fold higher than pFlhDCLacZ (-1600). (B) Interrupting different regions of the *flhDC* upstream region affects swarming motility. Overnight cultures of PM7002, JH4 (PM7002 + pKNG101::-322 *flhDCp*), JH5 (PM7002 + pKNG101::-1000 *flhDCp*), JH6 (PM7002 + pKNG101::-1600 *flhDCp*), JH7 (PM7002 + pKNG101::-2100 *flhDCp*), and JH8 (PM7002 + pKNG101::-2500 *flhDCp*) were equilibrated to the same OD600. To measure swarming migration, 1.5 µl droplets of the equilibrated inocula were spotted onto the same plate, and the migration distance was measured every 30 min after $T_{2.5}$. The average of four measurements is shown for PM7002, JH4, JH5, JH6, JH7, and JH8. Error bars represent standard deviations.

Figure 7. Swarming of putative direct *flhDC* regulators identified using DNA affinity chromatography pulldown. Overnight cultures of all strains were grown in LB broth at 37°C without shaking. Strains were equilibrated to the same OD_{600} before inoculation onto a 1.5% LB agar plate. Swarming diameter was measured every 30 min from T_2 to T_8. The average of four measurements is shown for all strains. Error bars represent standard deviations. (A) Swarming of PM7002 and isogenic H-NS and Fis deletion mutants. (B) Swarming of PM7002 and isogenic *hupA*, *hupB*, and a *hupA hupB* double mutant. (C) Swarming of PM7002 and isogenic *ihfA*, *ihfB*, and an *ihfA ihfB* double mutant. (D) Swarming of PM7002 and isogenic *nagC* and *fliZ* mutants.

Supplementary Figure 1. The organization of the transcriptional GFP fusion in the PM7002 chromosome. pFlhCGFP (pKNG101 + '*flhC*-eGFP) integrated at the *flhDC* locus in the PM7002 chromosome. The resulting strain (PMKH14) harbors the *flhDC* operon followed by eGFP with pKNG101 and the non-functional copy of *flhC*.

Figure 1

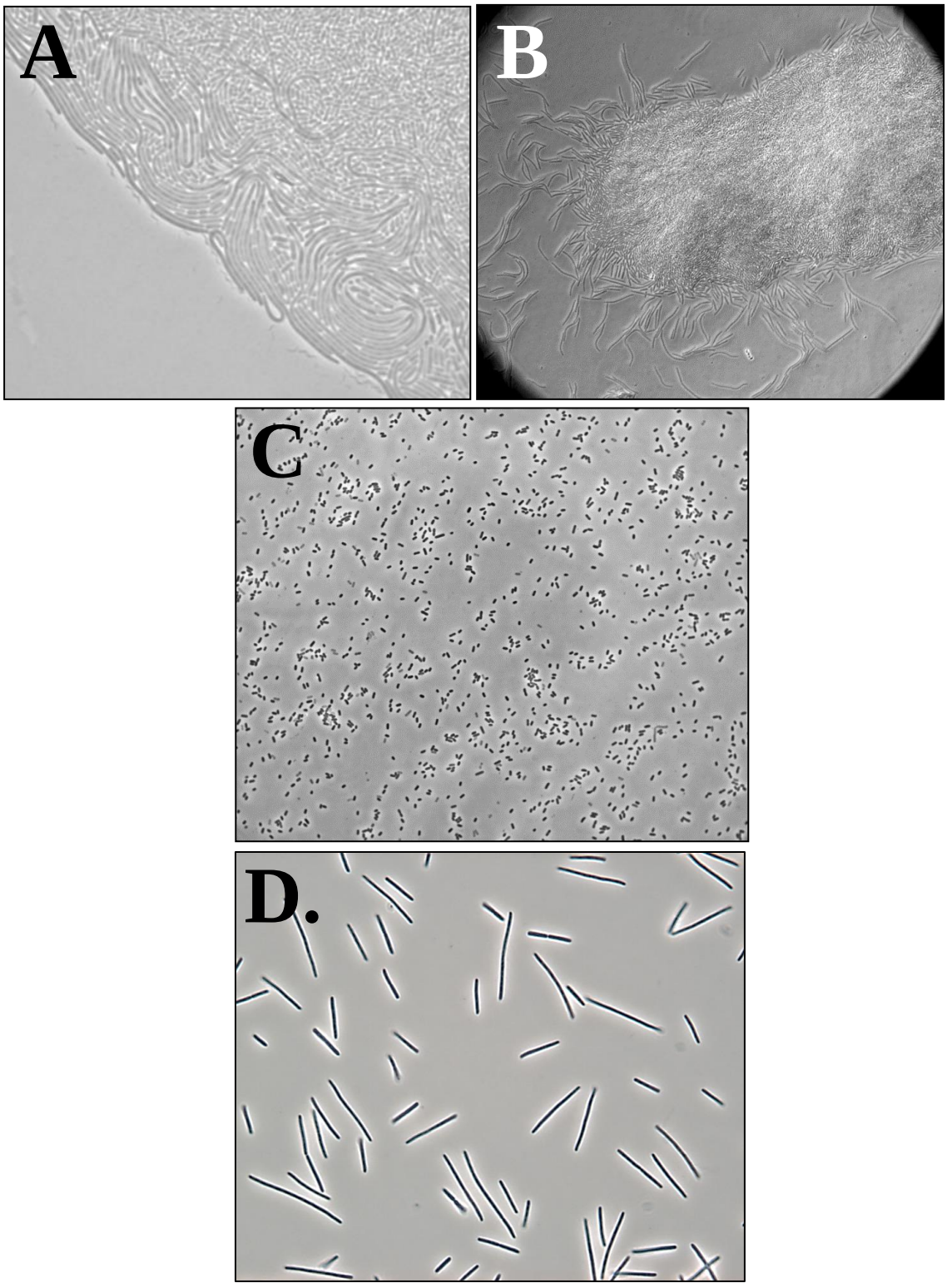

Figure 2

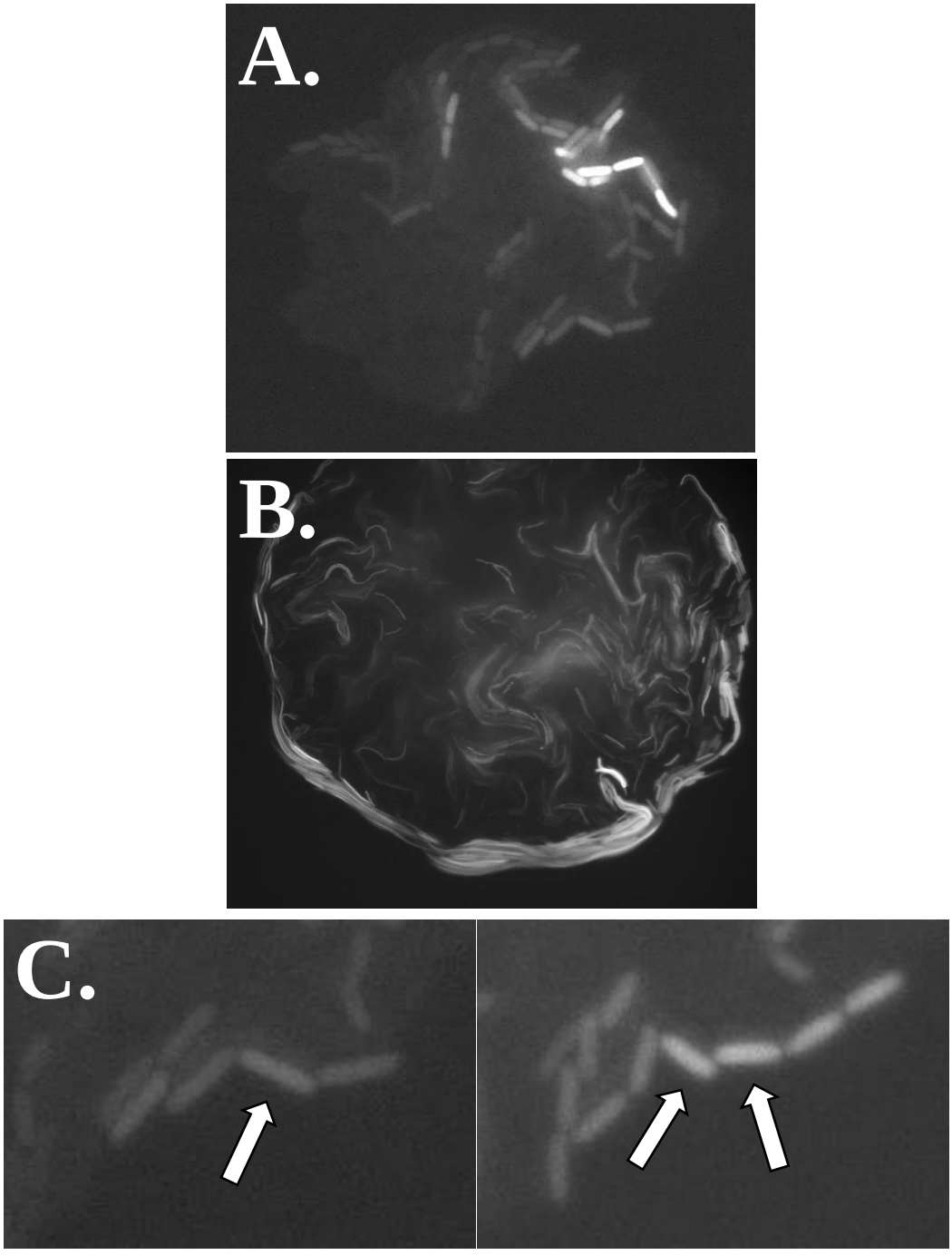

Figure 3

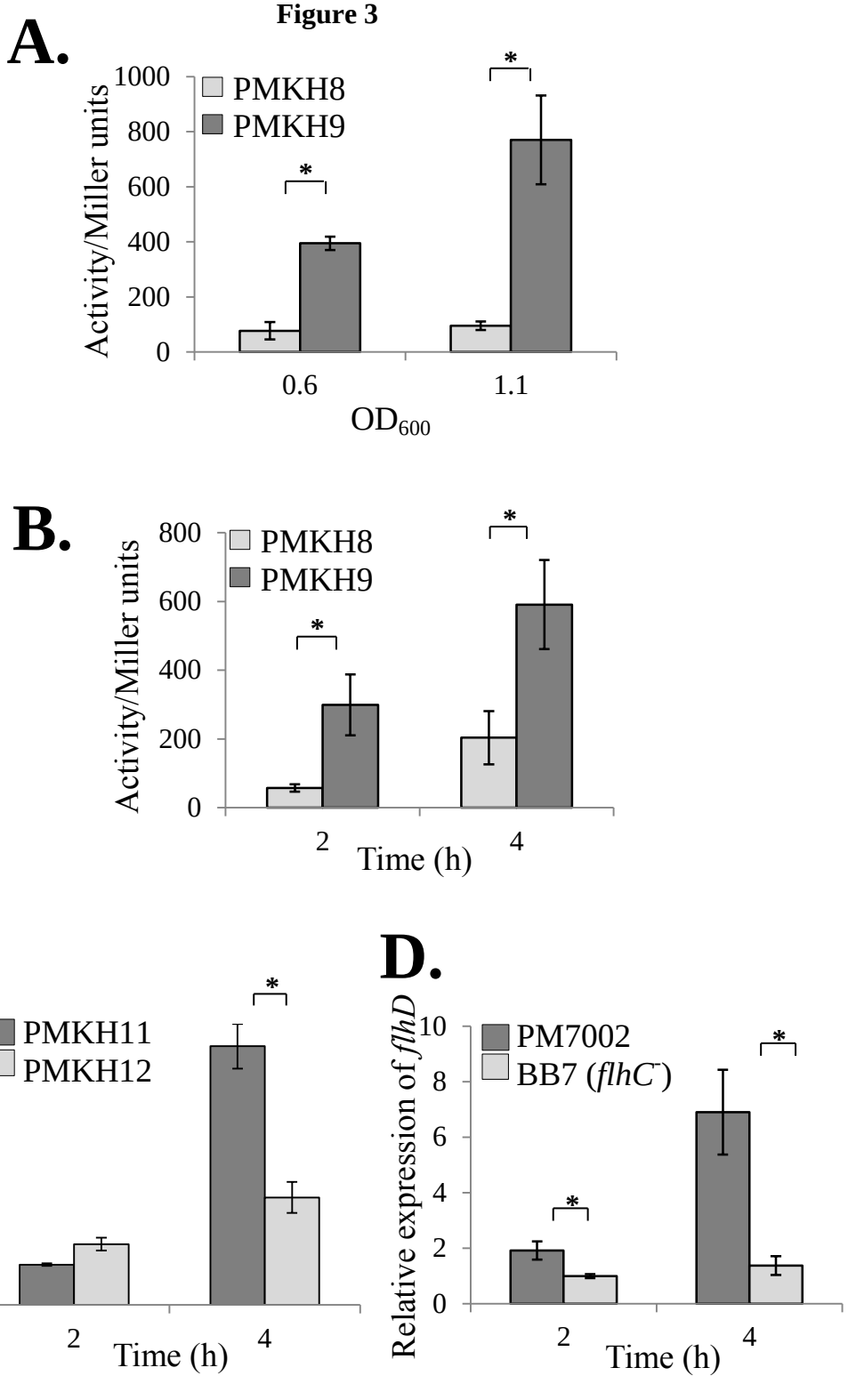
A.
Activity/Miller units
1000
800
600
400
200
0
PMKH8
PMKH9
*
*
0.6
1.1
OD600
B.
Activity/Miller units
800
600
400
200
0
PMKH8
PMKH9
*
*
2
4
Time (h)
C.
Activity/Miller units
60
50
40
30
20
10
0
PMKH11
PMKH12
*
2
4
Time (h)
D.
Relative expression of flhD
10
8
6
4
2
0
PM7002
BB7 (flhC-)
*
*
2
4
Time (h)

Figure 4

DNA: *flhDCp*	+	+	+	+
Protein: FlhC (pmol)	0	60	60	60
Competitor: *flhDCp*	0	0	+	0
abaI	0	0	0	+

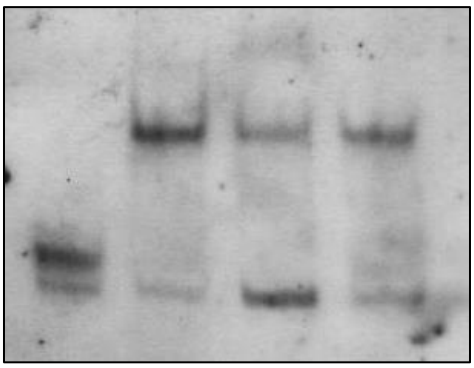

Figure 5

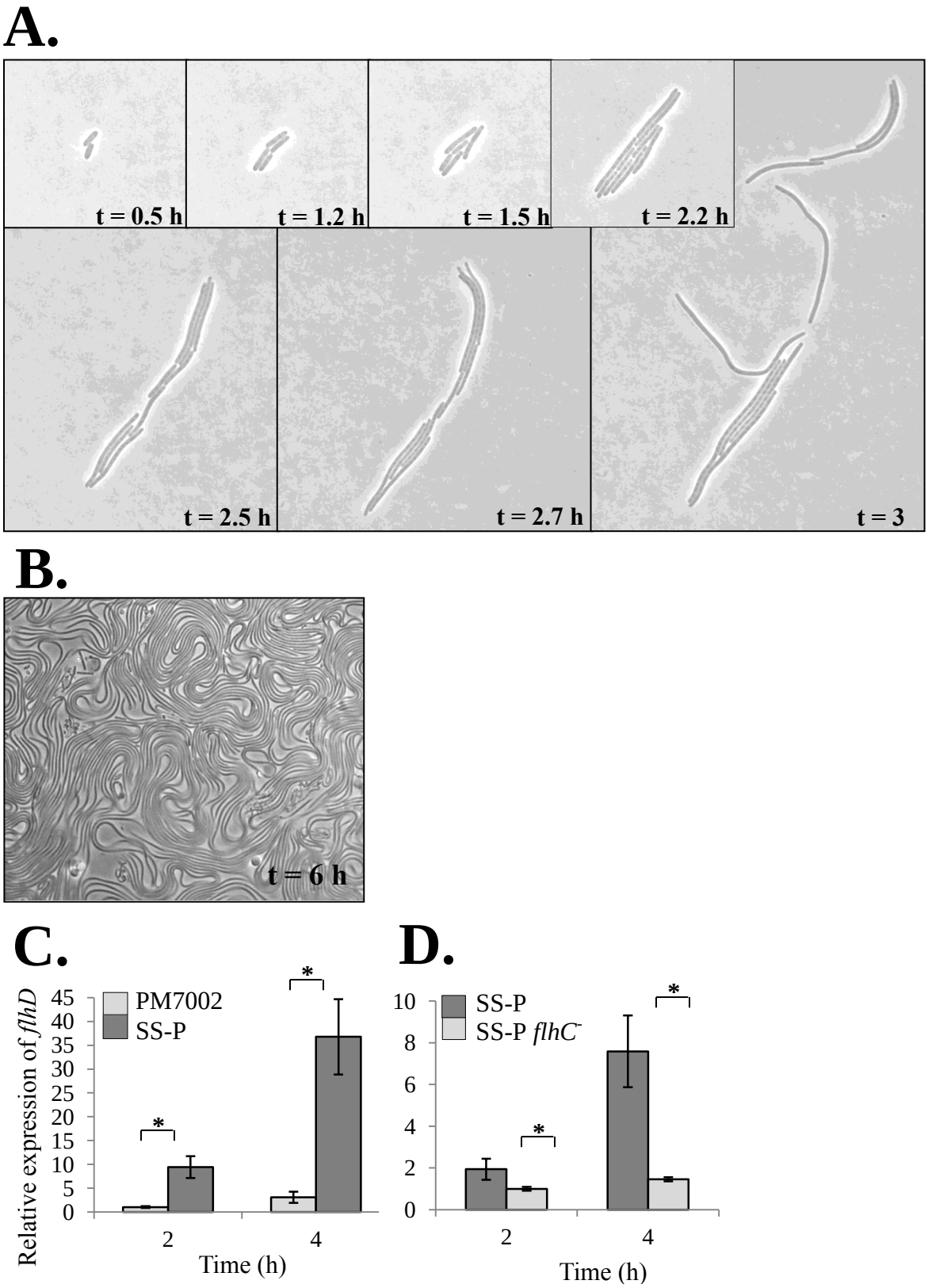
A.
t = 0.5 h
t = 1.2 h
t = 1.5 h
t = 2.2 h
t = 2.5 h
t = 2.7 h
t = 3
B.
t = 6 h
C.
Relative expression of flhD
PM7002
SS-P
Time (h)
D.
SS-P
SS-P flhC-
Time (h)

Figure 6

A.

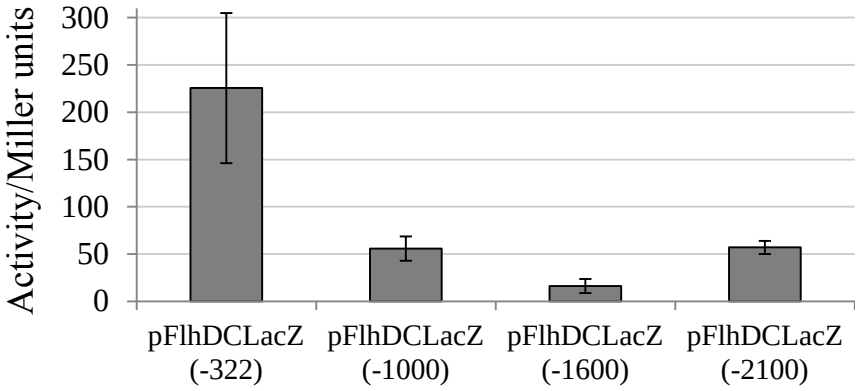
Activity/Miller units
300
250
200
150
100
50
0
pFlhDCLacZ (-322)
pFlhDCLacZ (-1000)
pFlhDCLacZ (-1600)
pFlhDCLacZ (-2100)

B.

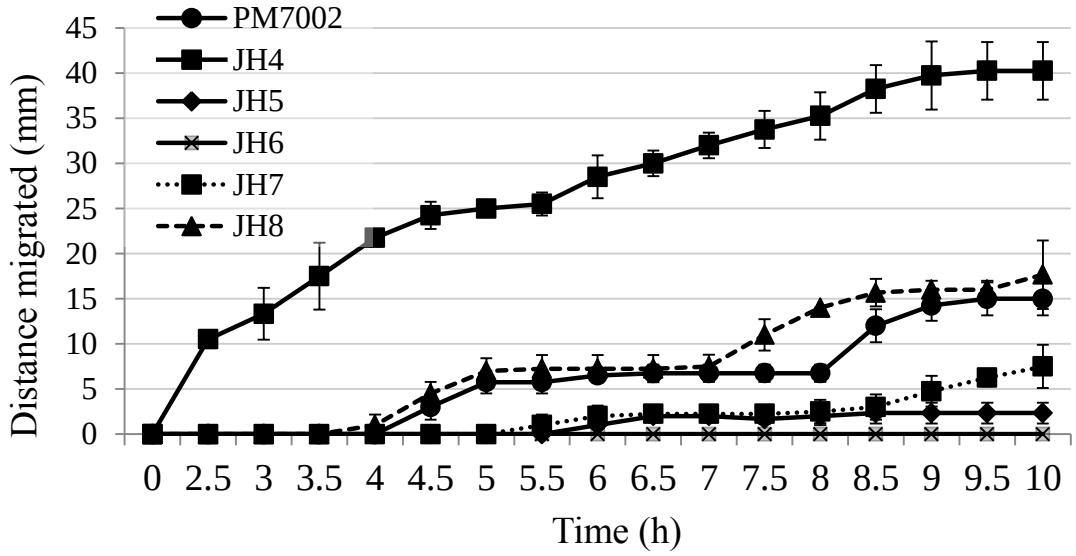
PM7002
JH4
JH5
JH6
JH7
JH8
Distance migrated (mm)
45
40
35
30
25
20
15
10
5
0
0 2.5 3 3.5 4 4.5 5 5.5 6 6.5 7 7.5 8 8.5 9 9.5 10
Time (h)

Figure 7

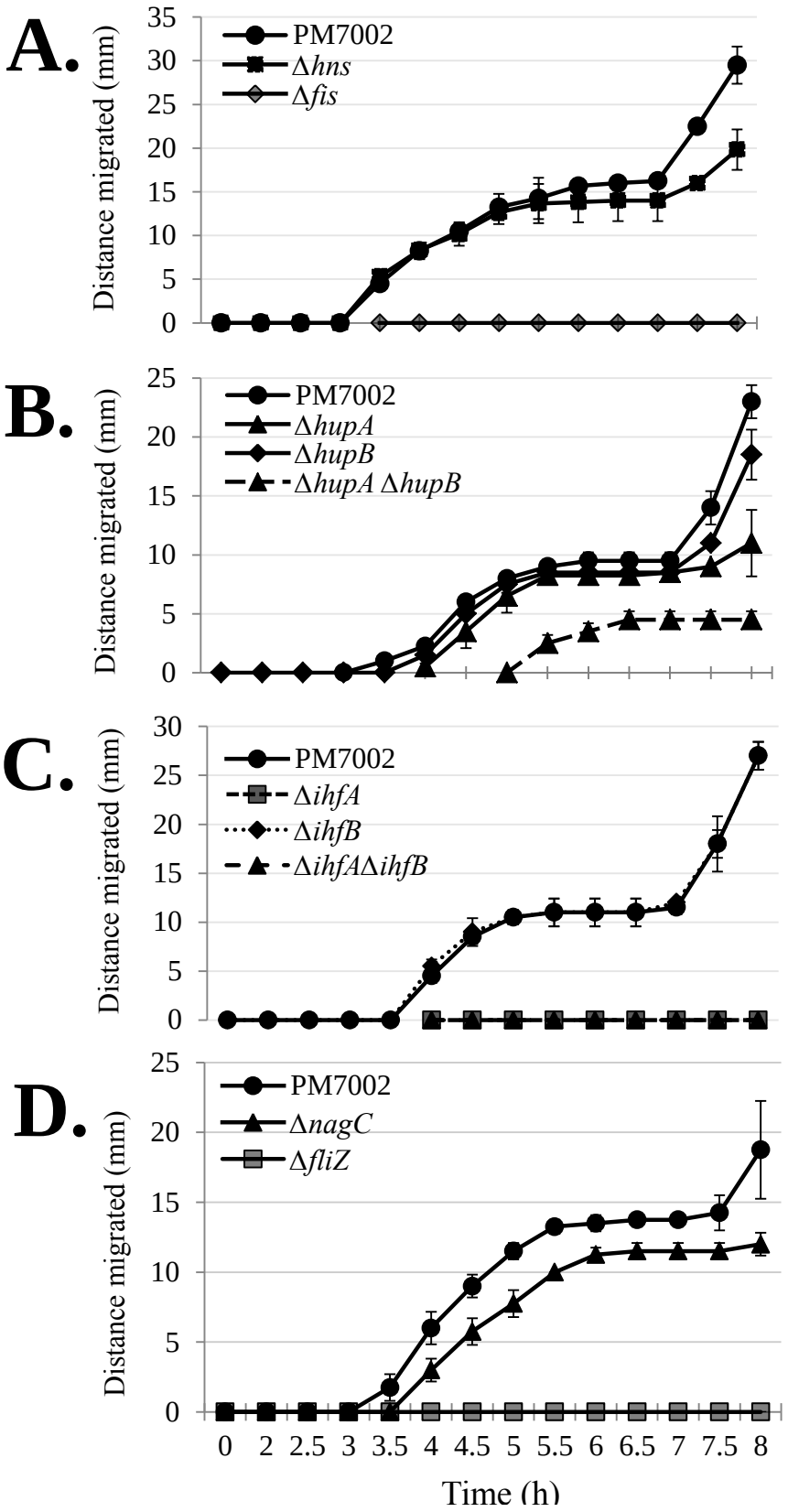
A.
Distance migrated (mm)
PM7002
Δhns
Δfis
B.
Distance migrated (mm)
PM7002
ΔhupA
ΔhupB
ΔhupA ΔhupB
C.
Distance migrated (mm)
PM7002
ΔihfA
ΔihfB
ΔihfAΔihfB
D.
Distance migrated (mm)
PM7002
ΔnagC
ΔfliZ
0 2 2.5 3 3.5 4 4.5 5 5.5 6 6.5 7 7.5 8
Time (h)

Supplementary Figure 1

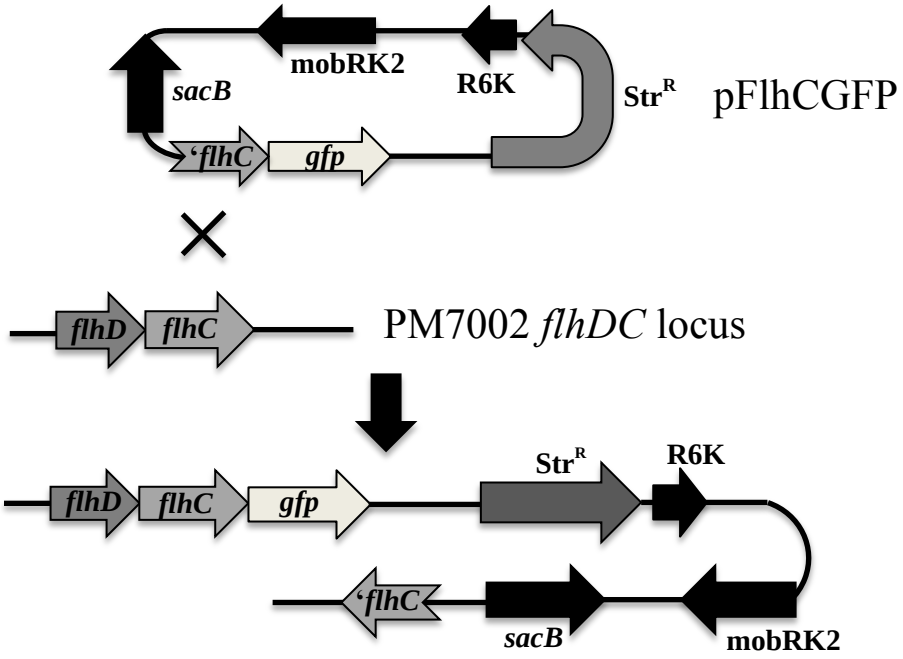

Chapter 5: Discussion

In this work, we further elucidated the multifaceted roles played by the Rcs phosphorelay and the master flagellar regulator $FlhD_4C_2$ in swarming motility of *P. mirabilis*. The contribution of the *flhDC* operon and its product $FlhD_4C_2$ to swarming motility has been established, as slight changes in *flhDC* expression affects swarming behavior drastically in *P. mirabilis* (1-3). The importance of *flhDC* to *P. mirabilis* swarming is compatible with its position at the top of the flagellar regulatory hierarchy (4). The importance of the Rcs phosphorelay to swarming is less studied and more elusive, as it was inherently thought to inhibit swarming through direct repression of *flhDC* (2, 5, 6). However, the elongation of Rcs mutants in liquid media led us to investigate the role of this system in swarmer cell differentiation (2, 6). Growth in liquid is a non-permissive condition for swarmer cell differentiation, and *P. mirabilis* strains artificially overexpressing *flhDC* do not differentiate under these conditions (2). While the hyperswarming phenotype of *rcs* mutants can be attributed to *flhDC* de-repression, it does not explain the elongation phenotype of *rcs* mutants in liquid. To identify Rcs-regulated genes that contribute to swarmer cell differentiation, the regulon of the RcsB response regulator was attained using RNA-Seq (7).

Within the RcsB regulon of *P. mirabilis* were two candidate genes hypothesized to contribute to differentiation: *minC* and *minD*. MinC and MinD are members of a cell division inhibition complex with another protein MinE. The oscillation of these three proteins from pole-to-pole keeps septum formation at the cell center and aids in cell elongation prior to division (8, 9). Increased Min concentrations at cell poles and the

oscillation period between poles affects cell length, and filamentous cells have multiple Min gradients (10, 11). Having more than one Min gradient results in the formation of numerous septa which could restore the short, rod-shaped morphology of *P. mirabilis* during consolidation (12).

The RNA-Seq data did not show *minE* within the RcsB regulon of *P. mirabilis*, but we confirmed it was RcsB-activated as well as its location in an operon with *minC* and *minD* (7). Furthermore, the introduction of a kanamycin cassette at the center of *minC*, the first gene in the *minCDE* operon, resulted in a delay in the onset of differentiation (7). This phenotype was recapitulated by introduction of this mutation into an *rcsB* mutant background. Additionally, swarmer cells of the *minC* mutant did not elongate properly; they were shorter and more bloated compared to the slender, highly elongated swarmer cells of the wild-type strain. The morphological defect of the swarmer cells could be rescued by reintroduction of the *minCDE* operon back into the *P. mirabilis* chromosome, but complementation neither restored the delay in differentiation nor the migration defect of the *minC* mutant. The swarming defect of the *minC* mutant and the complement strain was further attributed to less flagellin production in these strains.

The behavior of the *minC* complement strain raises additional questions. Perhaps the *minC* mutation was not polar or only affected the expression of the downstream gene, *minD*. The introduction of the entire *minCDE* operon back into the chromosome may have resulted in an artificial increase in other members of the Min system. This could be answered by complementation with *minC* alone or *minCD*. Moreover, how did the *minC* mutation affect flagellin production, and why was the defect not restored by complementation? The cells of the *minC* mutant were shorter which could result in less

flagellar production, but the complement strain exhibited the elongated morphology of wild-type. The roles played by Min in flagellar assembly remains a mystery in *P. mirabilis*, but studies in *E. coli* might help explain the results of this work. The Min proteins were recently shown to form reversible interactions with inner membrane associated proteins, many of which are involved in metabolism (11, 13). The construction of a *minC* mutant in one of these studies revealed alterations in metabolic status, illustrating the Min system impacts cell physiology (11). Another study showed the interaction of MinD with FliL, a stabilizer of the flagellar motor, and the chemotaxis protein CheW in *E. coli* which could influence surface expressed flagella (13).

The introduction of the *minC* mutation in the *rcsB* background resulted in a delay in the onset of differentiation and an overall decrease in migration, like wild-type. Despite this, the *rcsB minC* double mutant formed swarmer cells in liquid culture (data not shown). The RcsB regulon will require further examination in order to identify other gene candidates which lead to this phenotype. RcsB-activated genes that result in filamentous *E. coli* cells include *dmsA*/*B* and *tdcG*. DmsA/B forms a [4Fe-4S] cluster that is used by TdcG, an L-serine deaminase, to catalyze the formation of pyruvate from L-serine (14). Another candidate is GlpE, a co-chaperone induced during head shock, which causes elongation of *Streptococcus spp.* when mutated (15). Lastly, peptidoglycan (PG) remodeling is important for the maintenance of cell shape. MipA, a scaffolding protein important for PG synthesis, and PepD which is involved in PG degradation are both RcsB-activated (16). Though none of these genes were deleted in this work their expression would be decreased in the *rcsB* mutant which could contribute to the elongation of this mutant in liquid.

Rcs-repressed genes that may contribute to differentiation include *ccmA* (curved cell morphology), a gene hypothesized to affect delineation of swarming cells by mediating peptidoglycan assembly. Expression of *ccmA* is high during differentiation and during swarm phase (17, 18), and mutants of *ccmA* undergo differentiation but cannot swarm as a result of a curved cell morphology that prevents proper alignment of swarmer cell and subsequent migration (17). Another gene with increased expression in the *rcsB* mutant is PMI3378 which encodes a cell envelope opacity-associated protein. PMI3378 is a homolog of YtfB, a presently uncharacterized protein in *E. coli* but when overexpressed, results in filamentation (16). Overall, the differentiation of *rcs* mutants in liquid could result from a combination of metabolic defects, chaotic PG remodeling and membrane assembly, and cell division inhibition.

In addition to the importance of Rcs to differentiation, an examination of its contribution to other behaviors was undertaken. Genes highly downregulated in the *rcsB* mutant include fimbrial genes, which are important adhesins, and outer membrane proteins (*ompA*, *ompC*). These genes have been shown to be important to biofilm formation in *P. mirabilis* (19, 20) and other bacteria (21, 22). We showed RcsB is important for biofilm formation on catheters, a medically relevant substrate (23), which coincides with data that illustrating the importance of the relay protein RcsD to biofilm formation in *P. mirabilis* (24). The specific contributions of RcsB to biofilm formation may be due to activation of these important adhesins, as overexpression of flagella was not responsible for the biofilm defect in the *rcsB* mutant (23). Secondly, genes highly upregulated in the *rcsB* mutant include hemolysin and the immunoglobulin protease *zapA* (7, 23). Concurrent with the RNA-Seq data, the *rcsB* mutant was more effective at killing

Galleria mellonella waxworms than wild-type (23). Further studies should be undertaken to confirm which Rcs regulated genes specifically contribute to biofilm formation and virulence in *P. mirabilis*.

Chapters 2 and 3 illustrate the importance of the Rcs phosphorelay to biofilm formation, virulence, and swarmer cell differentiation. Interestingly, a system that is thought to inhibit swarming by direct repression of *flhDC* actually contributes to swarmer cell differentiation albeit indirectly. The Rcs phosphorelay is activated in response to cell stress, and stressed cells would not want to engage in an energy expensive process such as swarming. Sources of stress that induce the Rcs phosphorelay include outer membrane, LPS, and peptidoglycan defects; osmotic shock, interference with cytoskeletal integrity, and DNA replication (25-27).

Upon surface contact, membrane perturbations mediated by O-antigen lead to decreased Rcs activity resulting in de-repression of the *flhDC* operon, which is necessary for hyperflagellation (3, 28, 29). Cells divide at the point of inoculation to form a multilayered colony which is restricted by the agar surface. Osmotic shock may occur within the colony that leads to an increase in Rcs activity (30). Increased *minCDE* expression follows, which peaks 2 - 3 h following surface contact, inhibiting cell division and promoting cell elongation (31, 32). While the cell membrane and peptidoglycan are remodeled to facilitate increased length, the numerous flagella formed by increased *flhDC* expression following surface contact are incorporated into the cell body. RcsB-activated structures which facilitate the influx or efflux of solutes (Mcs, mechanosensing ion channels) (33, 34), promote membrane resilience (OsmB, OsmC) (25), and increase membrane fluidity (Cfa, cyclopropane fatty acyl phospholipid synthase) are incorporated

as well (35). Perhaps by undergoing morphological rearrangements, the activity of Rcs decreases as cells adapt to their new environment. However, as the Rcs is important for biofilm formation, why doesn't surface contact result in perpetual biofilm formation in *P. mirabilis*? Ultimately, multiple regulatory pathways govern surface-associated behaviors in bacteria which are influenced by the metabolic activity of the cell, the surface substrate, and the surrounding environment (36-38). Overall, the interplay between RcsB and $FlhD_4C_2$ following surface contact requires further investigation.

The regulation of the flagellar master operon *flhDC* was the focus of Chapter 4. Its product, $FlhD_4C_2$, is ultimately responsible for the transcription of flagellar genes (4) and flagellar-dependent motility (3, 39, 40). The expression of *flhDC* is essential for *P. mirabilis* swarming unlike other members of the *Enterobacteriaceae* which do not exhibit increases in *flhDC* expression following surface contact (41). However, unlike many bacteria, *P. mirabilis* is a robust swarmer and exhibits swarming behavior under a myriad of conditions. Cycling differentiation and consolidation phase to gauge intracellular resources necessary for intensive swarming phase may aid the vigorous swarming of *P. mirabilis*. Currently, it is unknown why cells enter consolidation phase. The goals of the work in Chapter 4 was to understand the spatial control of swarmer cell differentiation in subpopulations of vegetative cells on agar plates and the maintenance of immobile vegetative cells at the point of inoculation throughout the swarm cycle. What is ultimately responsible for triggering differentiation in some cells but not others is unknown, but high expression of the *flhDC* master operon is necessary for this process.

Vegetative populations in liquid constitutively express low levels of *flhDC*, but when placed onto agar surfaces, a drastic increase in *flhDC* transcription occurs ~ 2 h

following surface contact (2, 42). The expression of *flhDC* peaks prior to the onset of differentiation and remains at low levels until consolidation phase, where it begins to increase once more (18). The time-lapsed microscopy utilized in this study permitted the analysis of single-cells containing GFP reporter fusions, and our results mimic *flhDC* transcriptional patterns *in vitro*. The basal levels of *flhDC* expression in vegetative populations result from high *flhDC* expression in some individual cells but not others. Within the developing microcolony, cells expressing high *flhDC* expression are dispersed randomly throughout the population. As cell division occurs, daughter cells inherit high *flhDC* expression, which leads to an overall increase in *flhDC* transcript within the population. At the onset of differentiation, swarmer cells expressing high levels of *flhDC* were located at the edge of the microcolony where they migrated outward, leaving their immobile counterparts behind.

As *flhDC* expression was high in subpopulations of cells, but absent in others and inherited by daughter cells, we hypothesized the bifurcation of the initial population placed on solid surfaces resulted from bistable expression of *flhDC*. A form of epigenetic inheritance is one where daughter cells inherit active transcriptional regulators following division (43, 44). However, were these cells destined to swarm before placement on solid surfaces? Vegetative cells are capable of expressing high levels of *flhDC*, and yet they do not differentiate. Moreover, the short, rod shaped cells expressing high levels of *flhDC* during microcolony development were maintained hours prior to differentiation. What unknown factors influence differentiation? Known factors include the UcaJ and MrpJ fimbrial operon regulators and the Rcs phosphorelay which directly repress *flhDC*, while the cAMP-binding protein (CAP) has been shown to bind and activate the operon (45-

47). A transcriptomic analysis comparing *S. enterica* cells in lag phase to swarming cells may help identify unknown factors influencing differentiation when compared to our RcsB transcriptome analysis.

Swarming colonies of *S. enterica* have distinct metabolomic profiles. A proteomics analysis revealed proteins involved in glycolysis, pyruvate catabolism, protein folding, ribosome stabilization, DNA protection, and outer membrane composition are increased in interior, non-swarming cells. Swarmer cells exhibit increased amounts of proteins involved in the TCA cycle, energy production, nitrogen assimilation, and amino acid synthesis (48, 49). A transcriptome analysis of swarming *P. mirabilis* has been conducted, but compared vegetative cells, swarming cells, and consolidation phase cells rather than vegetative cells at the colony interior to swarmer cells (18). Interestingly, many of the proteins that are upregulated in *S. enterica* lag phase cells are also RcsB-activated genes in *P. mirabilis*. Out of the 36 proteins increased in *S. enterica* non-swarmers, 18 are Rcs-activated genes in *P. mirabilis*. These include stress-induced proteins and chaperones (*uspG*, *uspC*, *grpE*, *groS*, *groL*, *hybG*, *dnaK*), outer membrane proteins and porins (*ompA*, *ompC*, *osmB*, *tolQ*, PMI1017), proteins involved in glycolysis and pyruvate catabolism (*pgk*, *pepD*, *poxB*, *grcA*, *aspA*), and ribosome stabilization (HPF) (7, 48). Perhaps one factor preventing differentiation of vegetative cells at the colony interior is the Rcs phosphorelay.

We have shown that the bifurcation of *P. mirabilis* populations following surface contact is due, in part, to bistable regulation of $FlhD_4C_2$, which activates its own expression. However, what other factors are interfering with the ability of lag phase cells to initiate swarming? Perhaps one contributing element is RcsB which prevents *flhDC*

expression. Single cell analysis of cells harboring *rcsB* reporter fusions could help answer that question. However, *rcs* mutants still retain an immobile swarming lag population, albeit one much smaller than wild-type strains (2).

To understand the maintenance of vegetative rods at the colony interior, we studied the SS-P and SS-N mutants which do not retain the vegetative *P. mirabilis* morphotype following surface contact or undergo consolidation. These mutant phenotypes are conferred by transposon-mediated cassette insertions upstream of *flhDC*. The insertions result in constitutive high levels of *flhDC* following surface contact mediated, in part, by de-repression of the operon. As this phenotype cannot by complemented in *trans*, the cassette was not interrupting any open reading frames, and it did not create a new promoter, we hypothesized the cassette insertions were interrupting the binding site of a *trans*-acting repressor (2). Supporting this, if the *flhDC* upstream region is introduced in *trans* in a wild-type strain, differentiation occurs earlier and the cells exhibit increased motility (2). Moreover, the spatial regulation of the upstream region is multifaceted with certain segments promoting activation while others lead to complete *flhDC* repression. The interruption of the region using an integrative plasmid was also able to recapitulate the SS-P phenotype. Therefore, to identify proteins that bind and affect *flhDC* transcription, DNA affinity chromatography was utilized and in-frame deletion mutants were constructed in the genes corresponding to the bound proteins. The bound proteins identified included the transcription factors NagC, the *N*-acetyl-D-glucosamine operon repressor, and FliZ, a flagellar regulatory protein. The bacterial nucleoid associated proteins (NAPs) bound were H-NS, Fis, and both subunits of the HU-αβ, and IHF-αβ complexes.

To our surprise, none of the constructed mutants were identified as putative, direct *flhDC* repressors. Since, the probes used for the assay were incubated with lysates from cells grown to mid-logarithmic growth phase in LB broth, perhaps a repressor which confers the SS-P or SS-N phenotype was unavailable to bind to the probes as it was already bound to the native *flhDC* upstream region in vegetative cells, a state of *flhDC* repression. Many of the proteins identified were NAPs. Previous screens to identify swarming mutants were not optimized to identify NAPs, which have small open reading frames and are often found in heteromeric complexes (HU-αβ and IHF-αβ) which would require multiple disruptions to prevent intact complex formation. Though the deleted NAPs were not shown to repress swarming in *P. mirabilis*, the presence of NAP binding upstream of *flhDC* has implications for its regulation.

The *P. mirabilis flhDC* intergenic region is an attractive location for the binding of transcription factors and NAPs. It is large and AT rich with many poly(A) and poly(AT) tracts which promote DNA curvature. NAPs alter DNA trajectory by binding, bridging, or supercoiling it which could affect the promoter architecture of a stringently controlled gene. By altering DNA topology of the region upstream of *flhDC* by inserting either a kanamycin cassette that is comparatively GC rich (~60 %) or a large integrative plasmid, the tight regulation of the operon becomes destabilized. The resulting topology could be rearranged in such a way to promote the recruitment of transcriptional activators or negate repressor binding. Moreover, environmental signals can influence the expression and interaction of proteins like NAPs with DNA which would alter promoter architecture and subsequent gene expression (50). In the case of *P. mirabilis*, the

environmental signal could be surface contact which leads to a change in DNA topology and the subsequent expression of *flhDC* in subpopulations of cells.

The spatial control of the *flhDC* upstream region plays a large role the operon's expression and subsequently swarmer cell differentiation. While *flhDC* acts as the genetic element that governs swarming initiation, other factors must be involved in the maintenance of vegetative cells in the swarming population and the initiation of consolidation phase. Perhaps the Rcs phosphorelay plays a key role as it a system that responds to stress and has the ability to trigger both differentiation and consolidation. As waves of swarmer cells migrate from the lag phase colony, the swarm phase cells become multi-layered. This inhibits migration of the population and results in decreased water influx (51, 52). As membrane, osmolytic, and oxidative stress incur, the activity of the Rcs phosphorelay increases. RcsB activates the expression of the cell division genes FtsQAZ, septum formation occurs, and the cells enter consolidation phase where they can recuperate and prepare for another period of swarming migration. This phenomenon does not occur in SS-P as it constitutively expresses high levels of *flhDC* and does not form a multi-layered swarm front; thus Rcs activity is never increased. Further work to understand the expression and activity of the Rcs phosphorelay following surface contact and migration is required.

The interplay between the Rcs phosphorelay and $FlhD_4C_2$ in the control *of P. mirabilis* behavior is complex, as they have different regulons that serve different functions, and they are activated by different elements. In the end, the interaction between the two systems leads to the survival of *P. mirabilis* as it is able to initiate swarming when conditions are favorable, and repress swarming in undesirable

environments. Through this work, we further elucidate the complex regulatory network that dictates swarming behavior in *P. mirabilis*. We identified a new role played by the Rcs phosphorelay as an initiator of swarmer cell differentiation. We showed that the Min cell division inhibition system, an RcsB-activated operon, is important for swarmer cell elongation. Lastly, we describe $FlhD_4C_2$ auto-regulation, a novel mechanism of gene regulation which complements a bacterium that dedicates much of its physiology to motility.

References.

1. **Dufour A, Furness RB, Hughes C.** 1998. Novel genes that upregulate the Proteus mirabilis flhDC master operon controlling flagellar biogenesis and swarming. Molecular Microbiology **29:**741-751.
2. **Clemmer KM, Rather PN.** 2007. Regulation of flhDC expression in Proteus mirabilis. Research in Microbiology **158:**295-302.
3. **Furness RB, Fraser GM, Hay NA, Hughes C.** 1997. Negative feedback from a Proteus class II flagellum export defect to the flhDC master operon controlling cell division and flagellum assembly. J Bacteriol **179:**5585-5588.
4. **Chevance FFV, Hughes KT.** 2008. Coordinating assembly of a bacterial macromolecular machine. Nat Rev Micro **6:**455-465.
5. **Francez-Charlot A, Laugel B, Van Gemert A, Dubarry N, Wiorowski F, Castanie-Cornet MP, Gutierrez C, Cam K.** 2003. RcsCDB His-Asp phosphorelay system negatively regulates the flhDC operon in Escherichia coli. Mol Microbiol **49:**823-832.
6. **Belas R, Schneider R, Melch M.** 1998. Characterization of Proteus mirabilis precocious swarming mutants: identification of rsbA, encoding a regulator of swarming behavior. J Bacteriol **180:**6126-6139.
7. **Howery KE, Clemmer KM, Simsek E, Kim M, Rather PN.** 2015. Regulation of the Min Cell Division Inhibition Complex by the Rcs Phosphorelay in Proteus mirabilis. Journal of Bacteriology **197:**2499-2507.
8. **de Boer PA, Crossley RE, Rothfield LI.** 1990. Central role for the Escherichia coli minC gene product in two different cell division-inhibition systems. Proc Natl Acad Sci U S A **87:**1129-1133.

9. **Ward JE, Jr., Lutkenhaus J.** 1985. Overproduction of FtsZ induces minicell formation in E. coli. Cell **42:**941-949.

10. **Zieske K, Schwille P.** 2014. Reconstitution of self-organizing protein gradients as spatial cues in cell-free systems. eLife **3:**e03949.

11. **Lee HL, Chiang IC, Liang SY, Lee DY, Chang GD, Wang KY, Lin SY, Shih YL.** 2016. Quantitative Proteomics Analysis Reveals the Min System of Escherichia coli Modulates Reversible Protein Association with the Inner Membrane. Mol Cell Proteomics **15:**1572-1583.

12. **Zieske K, Schwille P.** 2015. Chapter 9 - Reconstituting geometry-modulated protein patterns in membrane compartments, p 149-163. *In* Jennifer R, Wallace FM (ed), Methods in Cell Biology, vol Volume 128. Academic Press.

13. **Arifuzzaman M, Maeda M, Itoh A, Nishikata K, Takita C, Saito R, Ara T, Nakahigashi K, Huang HC, Hirai A, Tsuzuki K, Nakamura S, Altaf-Ul-Amin M, Oshima T, Baba T, Yamamoto N, Kawamura T, Ioka-Nakamichi T, Kitagawa M, Tomita M, Kanaya S, Wada C, Mori H.** 2006. Large-scale identification of protein-protein interaction of Escherichia coli K-12. Genome Res **16:**686-691.

14. **Zhang X, El-Hajj ZW, Newman E.** 2010. Deficiency in L-serine deaminase interferes with one-carbon metabolism and cell wall synthesis in Escherichia coli K-12. J Bacteriol **192:**5515-5525.

15. **Murakami J, Terao Y, Morisaki I, Hamada S, Kawabata S.** 2012. Group A streptococcus adheres to pharyngeal epithelial cells with salivary proline-rich proteins via GrpE chaperone protein. J Biol Chem **287:**22266-22275.

16. **Burke C, Liu M, Britton W, Triccas JA, Thomas T, Smith AL, Allen S, Salomon R, Harry E.** 2013. Harnessing Single Cell Sorting to Identify Cell Division Genes and Regulators in Bacteria. PLoS One **8**.

17. **Hay NA, Tipper DJ, Gygi D, Hughes C.** 1999. A novel membrane protein influencing cell shape and multicellular swarming of Proteus mirabilis. J Bacteriol **181:**2008-2016.

18. **Pearson MM, Rasko DA, Smith SN, Mobley HL.** 2010. Transcriptome of swarming Proteus mirabilis. Infect Immun **78:**2834-2845.

19. **Scavone P, Iribarnegaray V, Caetano AL, Schlapp G, Härtel S, Zunino P.** 2016. Fimbriae have distinguishable roles in Proteus mirabilis biofilm formation. Pathogens and Disease doi:10.1093/femspd/ftw033.

20. **Jansen AM, Lockatell V, Johnson DE, Mobley HL.** 2004. Mannose-resistant Proteus-like fimbriae are produced by most Proteus mirabilis strains infecting the urinary tract, dictate the in vivo localization of bacteria, and contribute to biofilm formation. Infect Immun **72:**7294-7305.

21. **Smith SG, Mahon V, Lambert MA, Fagan RP.** 2007. A molecular Swiss army knife: OmpA structure, function and expression. FEMS Microbiol Lett **273:**1-11.

22. **Pantel A, Dunyach-Remy C, Ngba Essebe C, Mesureur J, Sotto A, Pages JM, Nicolas-Chanoine MH, Lavigne JP.** 2016. Modulation of Membrane Influx and Efflux in Escherichia coli Sequence Type 131 Has an Impact on Bacterial Motility, Biofilm Formation, and Virulence in a Caenorhabditis elegans Model. Antimicrob Agents Chemother **60:**2901-2911.

23. **Howery KE, Clemmer KM, Rather PN.** 2016. The Rcs regulon in Proteus mirabilis: implications for motility, biofilm formation, and virulence. Curr Genet doi:10.1007/s00294-016-0579-1.

24. **Liaw SJ, Lai HC, Ho SW, Luh KT, Wang WB.** 2001. Characterisation of p-nitrophenylglycerol-resistant Proteus mirabilis super-swarming mutants. J Med Microbiol **50:**1039-1048.

25. **Charoenwong D, Andrews S, Mackey B.** 2011. Role of rpoS in the development of cell envelope resilience and pressure resistance in stationary-phase Escherichia coli. Appl Environ Microbiol **77:**5220-5229.

26. **Hayashi K, Ohsawa T, Kobayashi K, Ogasawara N, Ogura M.** 2005. The H2O2 stress-responsive regulator PerR positively regulates srfA expression in Bacillus subtilis. J Bacteriol **187**.

27. **Huisman O, D'Ari R.** 1981. An inducible DNA replication-cell division coupling mechanism in E. coli. Nature **290:**797-799.

28. **Morgenstein RM, Clemmer KM, Rather PN.** 2010. Loss of the waaL O-antigen ligase prevents surface activation of the flagellar gene cascade in Proteus mirabilis. J Bacteriol **192:**3213-3221.

29. **Morgenstein RM, Rather PN.** 2012. Role of the Umo proteins and the Rcs phosphorelay in the swarming motility of the wild type and an O-antigen (waaL) mutant of Proteus mirabilis. J Bacteriol **194:**669-676.

30. **Ping L, Wu Y, Hosu BG, Tang JX, Berg HC.** 2014. Osmotic pressure in a bacterial swarm. Biophys J **107:**871-878.

31. **Li J, Overall CC, Johnson RC, Jones MB, McDermott JE, Heffron F, Adkins JN, Cambronne ED.** 2015. ChIP-Seq Analysis of the sigmaE Regulon of Salmonella enterica Serovar Typhimurium Reveals New Genes Implicated in Heat Shock and Oxidative Stress Response. PLoS One **10:**e0138466.

32. **Sun SX, Jiang H.** 2011. Physics of Bacterial Morphogenesis. Microbiol Mol Biol Rev **75:**543-565.

33. **Booth IR, Louis P.** 1999. Managing hypoosmotic stress: aquaporins and mechanosensitive channels in Escherichia coli. Curr Opin Microbiol **2:**166-169.

34. **Li J, Guo J, Ou X, Zhang M, Li Y, Liu Z.** 2015. Mechanical coupling of the multiple structural elements of the large-conductance mechanosensitive channel during expansion. Proc Natl Acad Sci U S A **112:**10726-10731.

35. **Moynihan PJ, Clarke AJ.** 2011. O-Acetylated peptidoglycan: controlling the activity of bacterial autolysins and lytic enzymes of innate immune systems. Int J Biochem Cell Biol **43:**1655-1659.

36. **Zhao K, Liu M, Burgess RR.** 2007. Adaptation in bacterial flagellar and motility systems: from regulon members to 'foraging'-like behavior in E. coli. Nucleic Acids Res **35:**4441-4452.

37. **Mangan MW, Lucchini S, T OC, Fitzgerald S, Hinton JC, Dorman CJ.** 2011. Nucleoid-associated protein HU controls three regulons that coordinate virulence, response to stress and general physiology in Salmonella enterica serovar Typhimurium. Microbiology **157:**1075-1087.

38. **Mangan MW, Lucchini S, Danino V, Croinin TO, Hinton JC, Dorman CJ.** 2006. The integration host factor (IHF) integrates stationary-phase and virulence gene expression in Salmonella enterica serovar Typhimurium. Mol Microbiol **59:**1831-1847.

39. **Young GM, Smith MJ, Minnich SA, Miller VL.** 1999. The Yersinia enterocolitica Motility Master Regulatory Operon, flhDC, Is Required for Flagellin Production, Swimming Motility, and Swarming Motility. Journal of Bacteriology **181:**2823-2833.

40. **Belas R, Suvanasuthi R.** 2005. The ability of Proteus mirabilis to sense surfaces and regulate virulence gene expression involves FliL, a flagellar basal body protein. J Bacteriol **187:**6789-6803.

41. **Harshey RM, Partridge JD.** 2015. Shelter in a Swarm. J Mol Biol **427:**3683-3694.

42. **Fraser GM, Claret L, Furness R, Gupta S, Hughes C.** 2002. Swarming-coupled expression of the Proteus mirabilis hpmBA haemolysin operon. Microbiology **148:**2191-2201.

43. **Dubnau D, Losick R.** 2006. Bistability in bacteria. Mol Microbiol **61:**564-572.

44. **Veening J-W, Smits WK, Kuipers OP.** 2008. Bistability, Epigenetics, and Bet-Hedging in Bacteria. Annual Review of Microbiology **62:**193-210.

45. **Pearson MM, Mobley HL.** 2008. Repression of motility during fimbrial expression: identification of 14 mrpJ gene paralogues in Proteus mirabilis. Mol Microbiol **69:**548-558.

46. **Bode NJ, Debnath I, Kuan L, Schulfer A, Ty M, Pearson MM.** 2015. Transcriptional analysis of the MrpJ network: modulation of diverse virulence-associated genes and direct regulation of mrp fimbrial and flhDC flagellar operons in Proteus mirabilis. Infect Immun **83:**2542-2556.

47. **Li X, Rasko DA, Lockatell CV, Johnson DE, Mobley HLT.** 2001. Repression of bacterial motility by a novel fimbrial gene product. The EMBO Journal **20:**4854-4862.

48. **Kim W, Surette MG.** 2004. Metabolic differentiation in actively swarming Salmonella. Molecular Microbiology **54:**702-714.

49. **White AP, Weljie AM, Apel D, Zhang P, Shaykhutdinov R, Vogel HJ, Surette MG.** 2010. A Global Metabolic Shift Is Linked to Salmonella Multicellular Development. PLoS One **5**.

50. **Travers A, Muskhelishvili G.** 2005. DNA supercoiling [mdash] a global transcriptional regulator for enterobacterial growth? Nat Rev Micro **3:**157-169.

51. **Lahaye E, Qin Y, Jamme F, Aubry T, Sire O.** 2014. A multi-scale approach of the mechanisms underlying exopolysaccharide auto-organization in the Proteus mirabilis extracellular matrix. Analyst **139:**4879-4886.

52. **Rauprich O, Matsushita M, Weijer CJ, Siegert F, Esipov SE, Shapiro JA.** 1996. Periodic phenomena in Proteus mirabilis swarm colony development. Journal of Bacteriology **178:**6525-6538.